

DEPARTMENT OF MINES AND RESOURCES  
CANADA

MINES, FORESTS, AND SCIENTIFIC SERVICES BRANCH

---

PUBLICATIONS

OF THE

**Dominion Astrophysical Observatory**

VICTORIA, B.C.

Volume VIII, No. 1

A STUDY OF LINE INTENSITIES IN THE SPECTRA  
OF FOUR SOLAR-TYPE STARS

BY

K. O. WRIGHT

A dissertation submitted in partial fulfillment of the requirements  
for the degree of Doctor of Philosophy in the University of Michigan.

Form 6184 8-44 3M

OTTAWA  
EDMOND CLOUTIER, C.M.G., B.A., L.Ph.,  
KING'S PRINTER AND CONTROLLER OF STATIONERY  
1948

*Price 25 Cents.*

DEPARTMENT OF MINES AND RESOURCES, CANADA  
MINES, FORESTS, AND SCIENTIFIC SERVICES BRANCH

---

---

PUBLICATIONS

OF THE

**Dominion Astrophysical Observatory**

VICTORIA, B.C.

Volume VIII, No. 1

---

---

A STUDY OF LINE INTENSITIES IN THE SPECTRA OF  
FOUR SOLAR-TYPE STARS\*

BY K. O. WRIGHT

**ABSTRACT.**—Equivalent widths of about 800 lines in the spectra of the sun, dG2,  $\gamma$  Cygni, cF7,  $\alpha$  Persei, cF4 and  $\alpha$  Canis Minoris, dF3 have been measured in the region  $\lambda\lambda$  3700-6750. The measured intensities have been corrected for blending effects and other possible systematic errors have been examined. For lines measured in common with other observers the adopted equivalent widths agree within the errors of measurement, though, for the weakest lines, it appears that an over-correction for blending effects may have been made. Measured profiles of the hydrogen and sodium D lines are also presented.

Menzel's theory of the curve of growth is summarized to show how turbulent velocities and damping constants may be derived from the fit of the observations on theoretical curves. Excitation temperatures may also be determined from the relative shift of  $\log X_0$ , the abscissa of the curve of growth, with excitation potential for lines of the same atom. Empirical curves of growth have been obtained by plotting  $\log W/\lambda$  against  $\log X_f$  where  $\log X_f$  was obtained for each line from an empirical curve of growth for the sun. It has been found that the observations require that different curves be used for neutral and ionized atoms for each star. Turbulent velocities are greater for ionized than for neutral atoms, and for giant than for dwarf stars. Damping factors may be less for ionized than for neutral atoms, and for giant than for dwarf stars, but, particularly for the giant stars, the damping portion of the curve is not well defined. Excitation temperatures do not show any great range from one atom to another and mean temperatures have been adopted for each star; they do not differ greatly from star to star and are considerably less than the effective temperatures.

The theory of the curve of growth and Saha's ionization equation have been used to determine the composition of these stellar atmospheres. Data obtained from high-dispersion spectra of the sun have been combined with theoretical intensities to determine the composition of the solar atmosphere for most elements having atomic lines in the spectral region studied and stellar line intensities have then been compared with the solar  $\log X_f$ -values to derive abundances in the stars relative to those in the sun. As the ionization temperatures of these stars are not known, both excitation temperatures and those computed for the level at which the absorption lines arise, which is taken as  $\tau = 0.3$ , have been used in the remaining calculations. By comparing the number of ionized and neutral atoms above the photosphere for the elements Mg, Si, Ca, Sc, Ti, Cr, V, Fe, Ni and Sr, electron pressures have been obtained. Results for different atoms give somewhat discordant results but since there is no direct evidence that there is stratification in the atmospheres, it has been assumed that there is no appreciable pressure gradient and mean electron pressures have been adopted in the further discussion. The level of ionization in these atmospheres is then readily determined and it seems that it increases with temperature and with luminosity if the stars studied in this paper may be taken as representative of their class.

The relative abundances of the twenty-one elements for which observations are available agree fairly well from star to star and confirm the general uniformity of stellar composition. There are about ten times as many atoms producing the absorption lines in the atmosphere of  $\gamma$  Cygni as in that of the sun and about five times the number in  $\alpha$  Persei; the numbers are almost equal in  $\alpha$  Canis Minoris and in the sun. Thus the number of atoms in giant atmospheres seems to be considerably greater than the number in dwarfs. Although it is difficult to draw positive conclusions, there may be small differences in the relative compositions of the giant and dwarf stars. No serious attempt to study the relative abundance of hydrogen has been made in this paper as it seems that results obtained from fitting profiles calculated according to Verweij's theory of the Stark effect to the wings of the hydrogen lines are not completely satisfactory.

\* The principal observational data and preliminary results of this paper were presented as a dissertation submitted in partial fulfilment of the requirements for the degree of Doctor of Philosophy in the University of Michigan in 1940. The results were revised and prepared for publication in December 1942 but printing was deferred until the end of the war. Recent advances in the methods of studying curve-of-growth phenomena have required a further complete revision of the analysis. Sections I and II have been changed only when additional information required such a revision but the remainder of the work was re-written in 1946 and 1947.

The following table lists the principal numerical results of the study:

	Sun <i>f</i> -values	Sun	$\gamma$ <i>Cygni</i>	$\alpha$ <i>Persei</i>	$\alpha$ <i>Canis Minoris</i>
Turbulent Velocity, $v_T$ km/sec.....	0.9	0.5	neutral atoms	3.7	1.2
			ionized atoms	5.7	3.0
Damping Constant, $\Gamma/\nu \times 10^6$ .....	2.6	1.6	neutral atoms	1.6	0.9
			ionized atoms	0.20	1.1
Excitation Temperature, $T_{exc}$ . ° K.....	4700	4875	4825	5100	5000
Temperature at Optical Depth 0.3, $T_{\tau=0.3}$ ° K.....	5275	5275	5075	5850	6200
Electron Pressure, $P_e$ dynes/cm. <sup>2</sup> .....	16	17	0.47	4.2	86
Mean Level of Ionization, $\bar{x}$ volts.....	8.0	7.9	9.2	9.6	8.7

## SECTION I.—INTRODUCTION

In recent theoretical discussions concerning the physics of stellar atmospheres, Menzel<sup>1</sup> and others have pointed out the great need for more observations of line intensities in stellar spectra. As a contribution toward this phase of the general problem the main portion of this paper is devoted to the measurement of line intensities in the spectra of the sun and the stars  $\gamma$  *Cygni*,  $\alpha$  *Persei*, and  $\alpha$  *Canis Minoris*. The final sections of the paper present certain applications of the results to the theory of stellar atmospheres and include a determination of excitation temperatures and estimates of the composition of these stars.

The study of stellar atmospheres has become an important section of astrophysics during the past twenty-five years. In the elementary theory, expressions were obtained for the absorption and scattering of radiation as it passed through a uniform layer of gas at a constant temperature. It predicted the relative shapes and intensities of spectral lines surprisingly well and is used in many calculations today. We know, however, that conditions in the reversing layer of the sun are very different from those postulated by this simple theory. Many refinements have been added to improve the results but for many years progress was impeded as much by the mathematical and physical complexities of the theory as by the observational difficulties which were encountered. The sun is the only star whose surface can be studied in detail, and deep-seated disturbances may be inferred from observations of sun-spots, granulations and prominences as they vary from day to day. Detailed studies of line intensities in solar spectra should also suggest these disturbances and the correlation should provide further information concerning the whole atmosphere. A detailed comparison of line intensities and shapes in the solar spectrum and in spectra of other stars, both giants and dwarfs, should then enable some quantitative estimates to be made concerning conditions in other stellar atmospheres.

<sup>1</sup> *Pop. A.*, 47, 6, 1939.

The transfer of radiation through the outer layers of a star was first studied by Schuster<sup>2</sup> in 1905 when he derived expressions for the intensity of monochromatic radiation, moving outward from a bright source, after it had been scattered by an intervening layer of gas. Schwarzschild,<sup>3</sup> in 1906, obtained formulae for the temperature of a similar layer of gas which absorbed radiation of a given intensity. Subsequently few important advances were made until 1924 when Stewart<sup>4</sup> combined these researches with the classical theory of radiation to evaluate the breadth and intensity of a spectral line in terms of the number of atoms above each square centimetre of the photosphere. During the next ten years many papers were written on the theory of stellar absorption lines. Milne<sup>5</sup> modified Saha's theory of ionization<sup>6</sup> and studied the opacity of an atmosphere as a function of the temperature and pressure at the base of a column of gas; Unsöld<sup>7</sup> discussed the theory of line profiles and applied it to his own observations of a few Fraunhofer lines in the solar spectrum; Eddington's paper on "The Formation of Stellar Absorption Lines"<sup>8</sup> has formed the basis for many later discussions on the subject; Woolley<sup>9</sup>, Pannekoek<sup>10</sup>, Rosseland<sup>11</sup>, Unsöld<sup>12</sup>, and Strömgen<sup>13</sup> attempted to explain the apparently real residual intensity at the centres of absorption lines; and Adams and Russell<sup>14</sup> applied atomic theory to the Rowland intensities of Fraunhofer lines and obtained a semi-quantitative estimate of the composition of the atmospheres of the sun and a few bright stars.

Until 1933 few observations were available to test the theories which had been developed. Schwarzschild<sup>15</sup> had measured the profiles of the *H* and *K* lines of Ca II in the sun in 1913; Unsöld<sup>7</sup> had made use of his own intensity measurements for a few solar lines; Minnaert<sup>16</sup> had begun a systematic study of the solar spectrum at Utrecht which has recently culminated in the "*Photometric Atlas of the Solar Spectrum*"<sup>17</sup>; and Miss Payne<sup>18</sup> and her co-workers had measured the intensities of many lines on objective-prism plates taken at Harvard Observatory. During the past thirteen years, extensive studies of the solar spectrum have been made by Woolley<sup>19</sup>, Mulders<sup>20</sup>, and Allen<sup>21</sup> and detailed investigations of a number of individual lines, such as the sodium *D* lines<sup>22</sup>, the magnesium *b* lines<sup>23</sup>, and a few neutral iron lines<sup>24</sup>, have been published. Observations of individual

<sup>2</sup> *Ap. J.*, **21**, 1, 1905.

<sup>3</sup> *Göttinger Nach.*, p. 41, 1906.

<sup>4</sup> *Ap. J.*, **59**, 30, 1924.

<sup>5</sup> *Phil. Tr., A.*, **228**, 421, 1929; *M.N.*, **92**, 150, 1932 (with S. Chandrasekhar).

<sup>6</sup> *Phil. Mag.*, **40**, 472, 1920.

<sup>7</sup> *Z. Phys.*, **44**, 793, 1927; *Z. Phys.*, **46**, 765, 1928.

<sup>8</sup> *M.N.*, **89**, 620, 1929.

<sup>9</sup> *M.N.*, **90**, 170, 1929.

<sup>10</sup> *Pr. K. Ac.*, Amsterdam, **34**, 1352, 1931.

<sup>11</sup> *Theoretical Astrophysics*, p. 140, Oxford Univ. Press, 1936.

<sup>12</sup> *Z. f. Ap.*, **4**, 319, 1932; *Physik der Sternatmosphären*, p. 301, Springer, Berlin, 1938.

<sup>13</sup> *Z. f. Ap.*, **10**, 237, 1935.

<sup>14</sup> *Ap. J.*, **68**, 9, 1928.

<sup>15</sup> *Sber. Preuss. Ak.*, p. 1183, Berlin, 1914.

<sup>16</sup> *Z. Phys.*, **45**, 610, 1927.

<sup>17</sup> Minnaert, M., G. F. W. Mulders and J. Houtgast, Schnabel, Kampert and Helm, Amsterdam, 1940.

<sup>18</sup> *Stars of High Luminosity*, *Harv. O. Mon.* No. 3, 1930.

<sup>19</sup> *An. Sol. Phys. O.*, Cambridge, **3**, Pt. 2, 1933.

<sup>20</sup> *Diss. Utrecht*, 1934; *Z. f. Ap.*, **10**, 297, 1935.

<sup>21</sup> *Mem. Comm. Sol. O.*, Canberra, **1**, No. 5, 1934; **2**, No. 6, 1938.

<sup>22</sup> Unsöld, A., *Z. Phys.* **46**, 765, 1928; Korff, S., *Ap. J.*, **76**, 291, 1932; Thackeray, A. D., *M. N.*, **94**, 99, 1933; Shane, C. D., *Lick O. B.*, **19**, 119, 1941.

<sup>23</sup> Minnaert, M. and G. F. W. Mulders, *Z. f. Ap.*, **1**, 192, 1930; d'Azambuja, L., *Ann. O. Paris-Meudon*, **8**, Pt. 2, 1930; Righini, G., *Oss. Mem. Arcetri*, No. 48, 29, 1931; Plaskett, H. H., *M. N.* **91**, 870, 1931; Korff, S., *Ap. J.*, **76**, 291, 1932; Cherrington, E., *Lick O. B.*, **17**, 161, 1935; ten Bruggencate, P., *Z. f. Ap.*, **18**, 330, 1939;

<sup>24</sup> Shane, C. D., *Lick O. B.*, **16**, 76, 1932; Thackeray, A. D., *M. N.* **94**, 99, 1933; ten Bruggencate, P. and H. von Klüber, *Z. f. Ap.*, **18**, 284, 1939; Redman, R. O., *M. N.*, **97**, 552, 1937.

late-type stellar spectra include  $\theta$  *Cygni*,  $\pi$  *Cephei* and  $\delta$  *Equulei* by Pannekoek and van Albada<sup>25</sup>,  $\alpha$  *Carinae* by Greenstein<sup>26</sup>,  $\gamma$  *Cygni* by Mrs. Bailey<sup>27</sup> and Sahade and Cesco<sup>28</sup> and  $\alpha$  *Persei*<sup>29</sup> and  $\delta$  *Canis Majoris*<sup>30</sup> by Miss Steel; the variable stars: *R Coronae Borealis* by Berman<sup>31</sup>,  $\delta$  *Cephei* by Krieger<sup>32</sup> and by Pannekoek and van Albada<sup>25</sup>; the eclipsing binaries,  $\zeta$  *Aurigae* by Christie and Wilson<sup>33</sup> and *VV Cephei* by Goedicke<sup>34</sup>, and the Cepheid variables,  $\delta$  *Cephei* and  $\eta$  *Aquilae* by Whipple<sup>34a</sup> and by Melnikov<sup>35</sup>. In addition, a comparison of the spectra of the K-type giant,  $\alpha$  *Bootis*, with the dwarf, 70 *Ophiuchi A*, has recently been completed by Miss van Dijke<sup>36</sup> which gives useful information concerning the atmospheres of these stars. Intensity measurements of the hydrogen lines have been made, for solar-type stars, by Elvey and Struve<sup>37</sup>, Williams<sup>38</sup>, Günther<sup>39</sup>, and Jensen<sup>40</sup>, but since many of these observations were obtained with instruments of low dispersion their accuracy may not be high. Other intensity measurements which have been published for solar-type stars include data on a few iron and titanium multiplets by Struve and Elvey<sup>41</sup> and on a number of lines from  $\lambda\lambda$  5000-6000 by Thackeray<sup>42</sup>. Of the above papers, those dealing with the sun,  $\gamma$  *Cygni*,  $\alpha$  *Persei* and  $\alpha$  *Canis Minoris* form the basis for comparison of the present work with that of other observers.

Early discussions linked the theory of stellar atmospheres with the profiles of absorption lines but observations of line profiles with different dispersions showed that, except for broad lines such as those of hydrogen in the A-type stars, the shape of a line was determined very largely by the spectrograph. Methods have been developed<sup>42a</sup> to allow for this instrumental profile but Unsöld<sup>43</sup> has pointed out the difficulty of obtaining the true shape of solar lines weaker than Rowland intensity 5. As already mentioned, true profiles of strong solar Fraunhofer lines have been derived for a few lines<sup>22, 23, 24</sup>. Numerous attempts<sup>44</sup> have been made to trace the course of radiation through a stellar atmosphere and to compare observed profiles of absorption lines with those calculated for certain specified conditions. For many years the mathematical complexities of the theory discouraged further studies of this nature, but recently Chandrasekhar<sup>45</sup> has developed methods by which the equation of transfer can be solved directly. In addition,

<sup>25</sup> *P. A. Inst.*, Amsterdam, No. 6, Pt. 1, 1939; No. 6, Pt. 2, 1946 was received after the manuscript had been largely completed.

<sup>26</sup> *Ap. J.*, **95**, 161, 1942.

<sup>27</sup> *Thesis*, Univ. of Arizona, 1942.

<sup>28</sup> *Ap. J.*, **104**, 133, 1946.

<sup>29</sup> *Ap. J.*, **102**, 43, 1945.

<sup>30</sup> *Ap. J.*, **102**, 429, 1945.

<sup>31</sup> *Ap. J.*, **81**, 369, 1935.

<sup>32</sup> *Ap. J.*, **85**, 304, 1937.

<sup>33</sup> *Ap. J.*, **81**, 426, 1935.

<sup>34</sup> *P. O. Univ. Mich.*, **8**, 1, 1939.

<sup>34a</sup> *Lick O. B.*, **16**, 1, 1932.

<sup>35</sup> *A. Cir. Ac. Sc., U.S.S.R.*, No. 45, 6, 1945.

<sup>36</sup> *Ap. J.*, **104**, 27, 1946.

<sup>37</sup> *Ap. J.*, **71**, 191, 1930; *Ap. J.*, **72**, 277, 1930.

<sup>38</sup> *An. Sol. Phys. O.*, Cambridge, **2**, Pt. 2, 1932.

<sup>39</sup> *Z. f. Ap.*, **7**, 106, 1933.

<sup>40</sup> *A. N.*, **266**, 269, 1938.

<sup>41</sup> *Ap. J.*, **79**, 263, 1934; *Ap. J.*, **79**, 409, 1934.

<sup>42</sup> *M. N.* **94**, 99, 1933; *M. N.*, **94**, 538, 1934.

<sup>42a</sup> See e.g. Unsöld, *A. Physik der Sternatmosphären*, p. 208; Redman, R. O., *M. N.*, **98**, 311, 1938.

<sup>43</sup> *Ap. J.*, **69**, 326, 1929.

<sup>44</sup> See Unsöld, A., op. cit., p. 226.

<sup>45</sup> *Ap. J.*, **99**, 180, 1944 et. seq.

Strömgren<sup>46</sup> obtained expressions for the profile of a line in terms of the abundance of the atom producing it and, for certain resonance lines, was able to make an estimate of the abundance of a given element relative to that of all metals, and to hydrogen. His theory can be applied to stars other than the sun and can be used for total intensities of lines, but the method has not yet been thoroughly applied.

Although the true line shapes can be obtained for only a few of the strongest lines in the spectra of a few bright stars, where the lines are sharp as in the sun, the total absorption or equivalent width of an absorption line is a quantity which is independent of the spectrographic resolving power and, for a given line, the same value should be obtained with any instrument. This is the observational datum which has been found most useful in the past few years and with which this paper is primarily concerned. In 1931, Minnaert, Mulders and Slob<sup>47</sup> were able to relate the equivalent width of any line to the number of active atoms involved in the transition which produced the line. The course of the curve relating these two quantities is called a curve of growth and will be fully considered in Section III. Struve and Elvey<sup>41b</sup> formed curves of growth for a number of stars by applying their equivalent-width observations of lines in a few multiplets and thereby discovered the "turbulence effect", namely, that the velocities of the atoms in the atmospheres of many stars appear to be much greater than those which can be ascribed to thermal motion alone. Later, Menzel<sup>48</sup> and his co-workers at Harvard Observatory extended the theory of equivalent widths, applied it to Allen's solar data and obtained an excitation temperature for the sun which was somewhat lower than the usually accepted value for the reversing layer.

At the outset of this investigation the only published measurements of line intensities which covered a considerable range of spectrum, were homogeneous and included both strong and weak lines, were those of Allen<sup>21</sup> and of Mulders<sup>20</sup> for the sun. In order partially to remedy this obvious lack of observational data the present program was undertaken at Victoria in the spring of 1937. Previously, a number of spectrograms of fifteen representative stars had been obtained with the two-prism spectrograph attached to the 37½-inch telescope of the Observatory of the University of Michigan in an effort to obtain a relation between the central intensities of spectral lines and the heights of the corresponding elements in stellar atmospheres. When the writer moved to Victoria, however, the availability of much more powerful equipment presented an opportunity to make a detailed study of line intensities in the spectra of a few stars and the earlier investigation has been superseded.

It is well known that many errors are inherent in the spectrophotometric measurement of line intensities and although Dunham<sup>49</sup> is extending Adams and Russell's empirical work on line intensities to determine the number and distribution of atoms in stellar atmospheres, it is felt that additional data on the spectra of a few typical stars will be of considerable value. This paper presents observations of the equivalent widths of eight hundred lines in the region  $\lambda\lambda$  3700-6750 for the four solar-type stars, the sun,  $\gamma$  Cygni,  $\alpha$  Persei and  $\alpha$  Canis Minoris. These intensities have been combined with solar  $\log X_r$

<sup>46</sup> *Ap. J.*, **86**, 1, 1937; *Festschrift für Elis Strömgren*, p. 218, Munksgaard, Copenhagen, 1940; *P. Med. Kobenhavns O.*, No. 138, 1944.

<sup>47</sup> *Z. f. Ap.*, **2**, 165, 1931; *Pr. K. Ac.*, Amsterdam, **34**, 542, 1931.

<sup>48</sup> *Ap. J.*, **84**, 462, 1936; *Ap. J.*, **87**, 81, 1938; *Pop. A.*, **47**, 6, 66, and 124, 1939.

<sup>49</sup> *Mt. Wilson Ann. Rep.*, 1933-38.

values, which are derived from an empirical curve of growth for the sun, to obtain curves of growth and excitation temperatures for the four stars. They have also been compared with solar data obtained from spectrograms taken with instruments of very high resolving power to provide preliminary information concerning the pressures and ionizations in these stellar atmospheres and approximate values for the abundances of the elements observable in the spectral region studied in this paper.

During the past year improved observational data have permitted a more detailed comparison of empirical curves of growth with those given by theory. A solar curve of growth derived by the writer<sup>50</sup> from intensities given by Allen and in the *Utrecht Photometric Atlas*, and from laboratory  $g_i f$ - values measured in absorption by R. B. King and A. S. King<sup>51</sup> showed deviations from the theoretical curve of best fit which have not yet been explained; similar deviations are also present in the curve of growth for *Arcturus* which was constructed by Miss van Dijke<sup>52</sup>. In addition, when measures of lines in the spectrum of  $\alpha$  *Persei* were plotted against solar  $\log X_r$  values<sup>50</sup>, it seemed clear that different curves of growth were required not only for neutral and ionized atoms in this star<sup>52</sup>, but also for lines arising from different levels in the same element (neutral iron)<sup>53</sup>.

These observations indicate that accurate measures will demonstrate the need for considerable extensions of the present theory of the curve of growth. However, it must be remembered that Struve<sup>54</sup> has pointed out that curve-of-growth phenomena provide one method for securing some information concerning the structure of stellar atmospheres but it is only a substitute for the study of true line profiles undistorted by the spectrograph. As an example of the value of the latter, he cites the study by Spitzer<sup>55</sup> of the spectra of M-type super-giants. Very recently, Struve<sup>56</sup> has also shown that there is a serious discrepancy in the value for the turbulent velocity derived from line profiles and from the curve of growth for  $\delta$  *Canis Majoris* which also suggests the need for a further modification of the theory.

In view of these remarks, it appears that there is a fruitful field in the study of stellar line intensities, both from the standpoint of the curve of growth and from that of line profiles. It will be many years before it will be possible to develop instruments capable of giving true line profiles for faint stars. Therefore it seems desirable that the two methods should be studied concurrently and that all possible information be derived from each in the hope that our knowledge of stellar atmospheres will be further advanced.

<sup>50</sup> *Ap. J.*, **99**, 249, 1944.

<sup>51</sup> *Ap. J.*, **87**, 24, 1938.

<sup>52</sup> *J. R. A. S. Can.*, **40**, 183, 1946.

<sup>53</sup> *J. R. A. S. Can.*, **41**, 49, 1947.

<sup>54</sup> *Ap. J.*, **98**, 134, 1943.

<sup>55</sup> *Ap. J.*, **90**, 494, 1939.

<sup>56</sup> *Ap. J.*, **104**, 138, 1946.

## SECTION II.—OBSERVATIONAL MATERIAL AND MEASUREMENTS

### THE SPECTROGRAMS

The three stars,  $\gamma$  *Cygni*,  $\alpha$  *Persei*, and  $\alpha$  *Canis Minoris*, were selected for detailed study because they are representative bright stars, similar to the sun in spectral type, yet covering a large range in absolute magnitude. Observations of the sun were included in the program in order to compare the Victoria spectrograph and experimental procedures with those of other observers. In the case of the sun, plates of the sky and also of the moon were taken as they represent the integrated light from the whole solar surface and are directly comparable to the light from the stars. Observations of the sky and moon were studied separately at first but, as no systematic difference was apparent, the results have been grouped together. Table 1 lists the relevant data concerning the stars as given by Moore<sup>57</sup> and Kuiper.<sup>58</sup>

TABLE 1. STARS OBSERVED FOR SPECTRAL LINE INTENSITIES

—	Sun	$\gamma$ <i>Cygni</i>	$\alpha$ <i>Persei</i>	$\alpha$ <i>Canis Minoris</i>
<i>H. D.</i> No.....		194093	20902	61421
$\alpha$ (1900).....		20 <sup>h</sup> 18 <sup>m</sup> 6	3 <sup>h</sup> 17 <sup>m</sup> 2	7 <sup>h</sup> 34 <sup>m</sup> 1
$\delta$ (1900).....		39° 56'	49° 30'	5° 29'
Spectrum, <i>H. D.</i> .....	G0	F8p	F5	F5
Revised.....	dG2	cF7	cF4	dF3
$m_{pv}$ .....	-26.84	+2.29	+1.90	+0.45
$M_{pv}$ .....	+4.73	-5	-4.4	+2.77
$T_{eff}$ ° K.....	5725	5500	6325	6725

In order to cover the desired spectral range, four series of spectrograms were obtained at the Cassegrain focus of the 72-inch telescope of the Dominion Astrophysical Observatory. The "blue" region from  $\lambda$  4028 to  $\lambda$  4603 was studied first with the three-prism spectrograph which gave dispersions of 4.8 A/mm. at  $\lambda$  4028 and 10.1 A/mm. at  $\lambda$  4603. After the intensities of available lines in this region had been measured and preliminary results had been obtained, it was decided to extend the investigation to cover the green and red regions of the spectrum. For the "green" region from  $\lambda$  4571 to  $\lambda$  5701, the same spectrographic combination was used but the deviation was changed and the dispersions were 7.6 A/mm. at  $\lambda$  4571 and 20.8 A/mm. at  $\lambda$  5701. As the dispersion of the prisms was decreasing rapidly at this point, the Wood aluminum-on-glass grating, which has a strong

<sup>57</sup> *P. Lick O.*, 18, 1932.

<sup>58</sup> *Ap. J.*, 88, 429, 1938; *Ap. J.*, 88, 472, 1938.

first order, was used for the "red" region from  $\lambda$  5435 to  $\lambda$  6752. The grating acts against the usual single-prism arrangement of the spectrograph as described by Beals and McKellar<sup>59</sup> and the dispersion increases from 18.1 A/mm. at  $\lambda$  5435 to 13.2 A/mm. at  $\lambda$  6752. In the blue and green regions the field was very flat and excellent definition was obtained over the entire plate; in the red region, because the lens had been made for use with a single prism, the field was not absolutely flat, although good definition was obtained over a range extending from  $\lambda$  5600 to  $\lambda$  6750. In 1943 the stellar spectrograph was re-designed to permit the use of prisms and gratings in a Littrow form<sup>60</sup>. It was found that the Wood grating which gave a strong red spectrum in the second order was suitable for use in the third order in the ultraviolet region from  $\lambda\lambda$  3700-4000 where a reasonably flat field was given by the collimator lens. As this region contains numerous strong lines of neutral iron, many of which are on the damping portion of the curve of growth for the sun, it was decided to obtain a fourth series of plates for the stars studied in this paper and to measure the intensities of all lines which seemed to be suitable for this purpose.

Details of the spectrograms are given in Table 2. The date, the emulsion, the exposure time, the region actually measured on each plate, its density, the instrument and the observing conditions are listed in successive columns. Photographs of selected regions of the spectrum, together with microphotometer tracings of the same regions, are shown in Plates I to III. Intensitometer traces, showing the observed intensity of the spectrum from  $\lambda\lambda$  3835-3875 relative to the adopted position of the continuous background (taken as 100 per cent) are shown in Folding Plate IV. A number of different emulsions were used; the choice of a particular emulsion depended on the spectral region, observing conditions and the time available at the telescope. The Ilford Astra II plates are very satisfactory when great speed is required but somewhat coarse-grained and, in the blue region, Eastman 33 or Eastman 40 plates were used whenever possible. The Ilford Special Rapid Panchromatic plates have a suitable grain and are moderately fast over the region to which they are sensitive, but in order to study  $H\alpha$  and the lines to the red of  $\lambda$  6500 many Ilford Astra VIII plates were used. However, as shown by the microphotometer tracings, the weak absorption lines in the red region are particularly difficult to distinguish from the grain of the plate and for that region lower weights have been assigned to the results obtained for these lines. More recently, Eastman 103a 0, II 0, III 0 and Lantern Slide emulsions were used for the ultraviolet region.

#### CALIBRATION OF THE PLATES

All plates were exposed in the single-prism calibrating spectrograph, which gives a dispersion of 53 A/mm. at  $\lambda$  4350, for from ten to thirty minutes immediately before the stellar exposure. The latter varied from a few minutes for plates of the sky and  $\alpha$  *Canis Minoris* to nearly two hours for some plates of  $\gamma$  *Cygni* but, as Jones and his collaborators<sup>61</sup> have shown, this exposure factor does not introduce an appreciable error due to failure of the reciprocity law. Immediately after exposure the plates were brush-developed for four minutes at 20° C.; the blue and ultraviolet plates were developed in D-11 and the green and red plates were developed in Rodinal which had been diluted with water in a

<sup>59</sup> *J. R. A. S., Can.* 32, 369, 1938.

<sup>60</sup> Beals, C. S., R. M. Petrie and A. McKellar, *J. R. A. S. Can.*, 40, 349, 1946.

<sup>61</sup> *J. O. S. A.*, 11, 319, 1925; *J. O. S. A.*, 12, 321, 1926; *J. O. S. A.*, 14, 223, 1927.

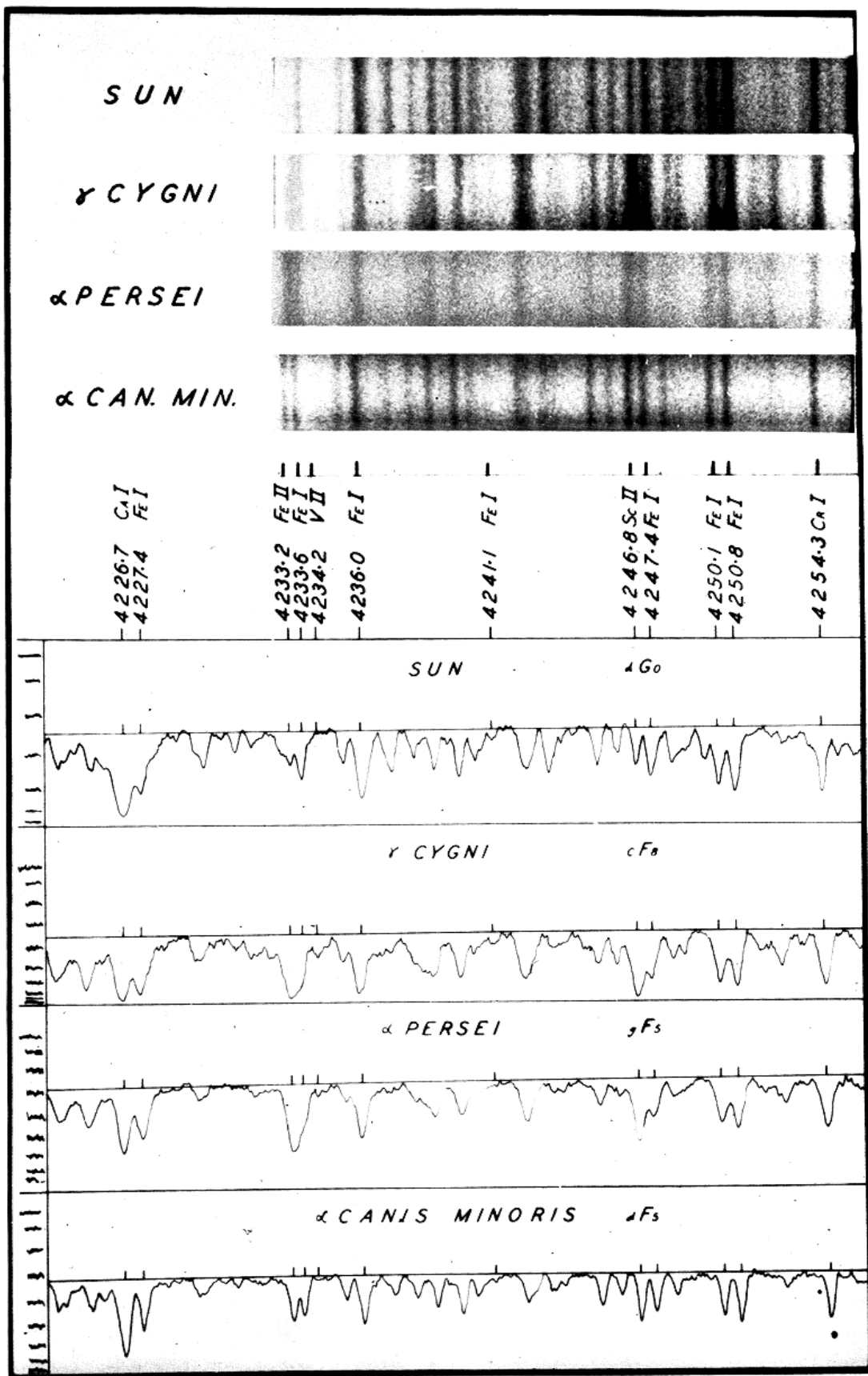


PLATE I. Spectra and Microphotometer Tracings of the Sun,  $\gamma$  Cygni,  $\alpha$  Persei and  $\alpha$  Canis Minoris in the Region  $\lambda\lambda$  4225-4255. Wave-lengths and identifications have been marked and the lines measured for each star are indicated by vertical strokes on the appropriate tracing. The magnification is  $25 \times$  the original spectrograms.

A line representing the position of the continuous spectrum has been drawn on each tracing. The density of the original plate is shown by the calibration steps which have been drawn at the left of the tracings; the intensity ratio between steps is 2.00 for the sun and 1.58 for the other stars.

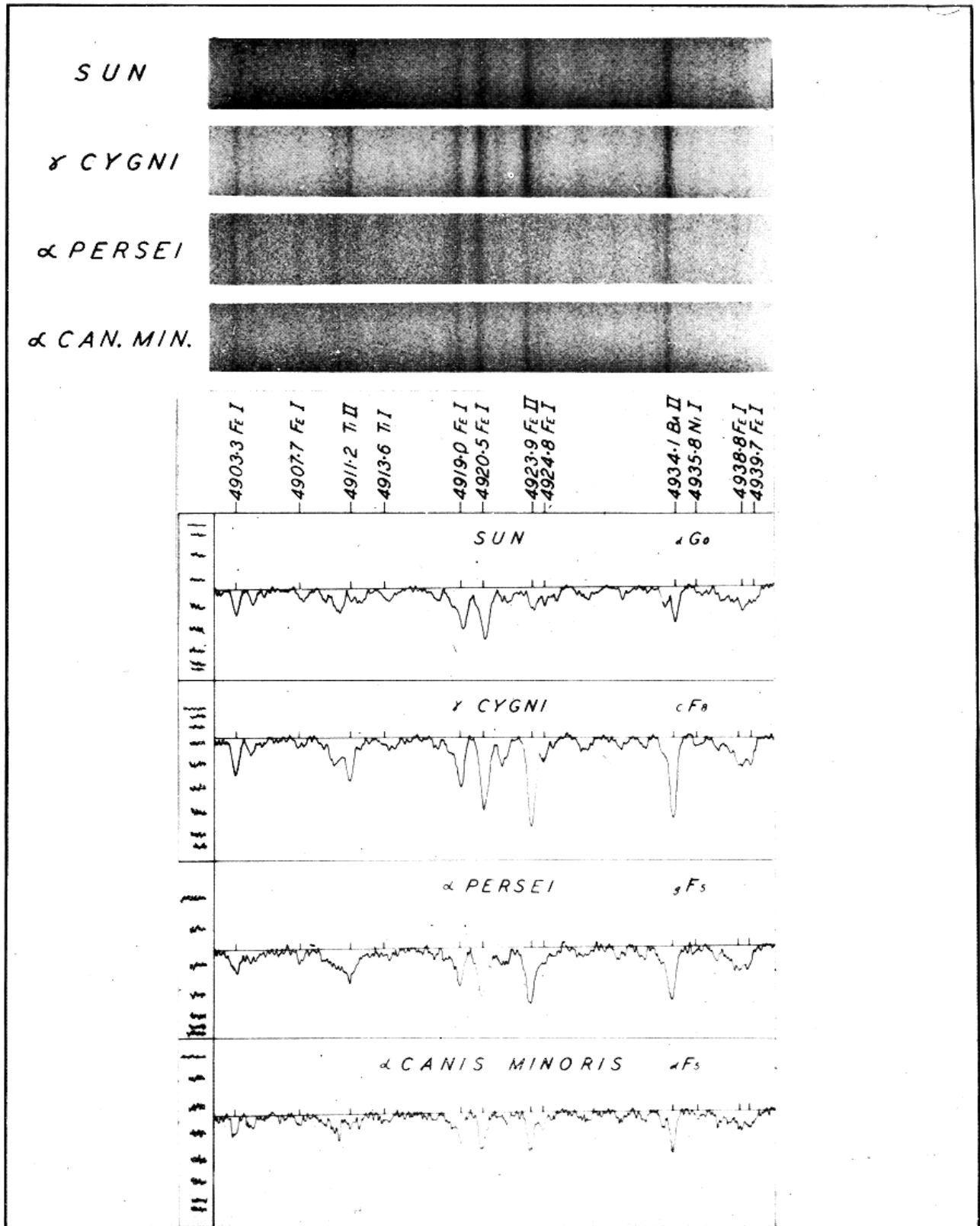


PLATE II. Spectra and Microphotometer Tracings of the Sun,  $\gamma$  Cygni,  $\alpha$  Persei and  $\alpha$  Canis Minoris in the Region  $\lambda\lambda$  4900-4940. Wave-lengths and identifications of the lines have been marked and the lines measured for each star are indicated by vertical strokes on the corresponding tracing. The magnification is  $24 \times$  the original spectrograms.

A line representing the position of the continuous spectrum has been drawn on each tracing. The density of the original plate is shown by the calibration steps which are shown at the left; the intensity ratio between each step is 1.58.

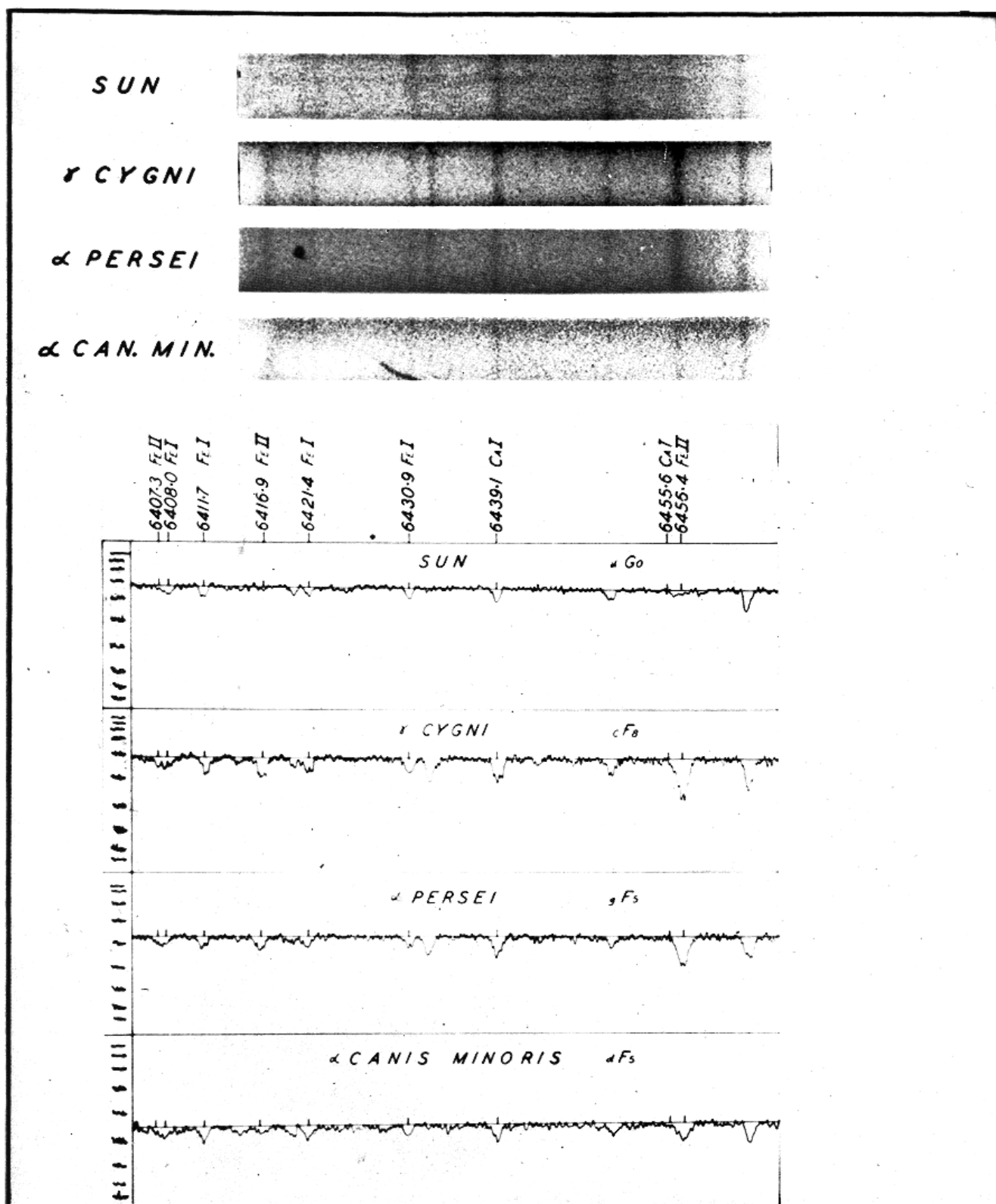


PLATE III. Spectra and Microphotometer Tracings of the Sun,  $\gamma$  Cygni,  $\alpha$  Persei and  $\alpha$  Canis Minoris in the Region  $\lambda\lambda$  6410-6460. Wave-lengths and identifications of the lines are indicated on each tracing. Note that the lines are considerably weaker than those shown in Plates I and II. The magnification is  $22 \times$  the original spectrograms.

A line representing the position of the continuous spectrum has been drawn midway through the deflections produced by grains of the plate. The calibration steps are shown at the left; the intensity ratio between each step is 1.58.

TABLE 2. LIST OF OBSERVATIONS

Date U.T.	Emulsion	Exposure min.	Region $\lambda\lambda$	Instrument	Density	Remarks
Sky and Moon						
1937 Feb. 19-947.....	A II	6	4028-4603	III Prisms	Good	
Mar. 18-981.....	E 33	5	4028-4603		Good	
Sept. 9-041.....	E 33	25	4028-4590		Sl. strong	
Sept. 9-056.....	E 33	14	4028-4603		Sl. strong	
Sept. 22-326.....	E 40	60	4028-4590		Good	Clouds
Sept. 22-360.....	E 40	32	4028-4603		Weak in violet	
Sept. 22-385.....	E 40	42	4333-4603		Weak in violet	Clouds
1938 Nov. 19-833.....	S.R.P.	6	4571-5625	III Prisms	Cal. strong	
Dec. 12-803.....	A IX	5	4634-5690		Compn. strong	
Dec. 12-866.....	S.R.P.	22	4602-5683		Good	Clouds
1938 Sept. 13-374.....	A VIII	46	5688-6753	Prism and Grating	Good	
Dec. 13-625.....	A IX	40	5638-6142		Weak in red	
1939 Mar. 27-820.....	A VIII	5	6081-6753		Green weak	
May 9-821.....	A VIII	15	5555-6661		Sl. weak	
May 9-846.....	A VIII	20	5522-6233		Good	
May 9-864.....	A VIII	24	6142-6753		Good	
1943 Aug. 18-097.....	II 0	12	3690-4010	Grating	Sl. weak	
1944 June 8-994.....	L.S.	12	3690-4010		Good	
June 22-955.....	L.S.	14	3690-4010		Good	

$\gamma$  Cygni

1937 May 27-427.....	A II	61	4028-4584	III Prisms	Cal. strong	Clouds
June 5-462.....	A II	50	4028-4603		Good	
Sept. 9-152.....	E 40	50	4080-4603		Weak in violet	
Sept. 9-201.....	E 40	90	4056-4603		Good	
Sept. 9-284.....	E 40	115	4134-4603		Weak in violet	Clouds
Sept. 22-158.....	E 40	104	4028-4603		Good	
Sept. 22-257.....	E 40	120	4028-4603		Weak in violet	Clouds
1938 Feb. 25-556.....	E 33	30	4028-4603		Weak in violet	
1938 Oct. 4-131.....	A II	42	4584-5156	III Prisms	Weak in green	
Dec. 13-047.....	A IX	22	4716-5690		Sl. strong	
Dec. 13-063.....	A IX	26	4571-4872		Good	
Dec. 13-081.....	A IX	22	4914-5701		Sl. weak	
Dec. 13-099.....	A IX	30	4576-4940		Good	
Dec. 13-137.....	S.R.P.	80	4583-5690		Good	
1938 Sept. 13-299.....	A VIII	56	5683-6753	Prism and Grating	Sl. strong	
Nov. 22-075.....	S.R.P.	84	5445-6152		Compn. strong	
Nov. 22-135.....	A VIII	88	6216-6753		Sl. weak	
Nov. 22-198.....	S.R.P.	90	5497-6312		Fair	
1939 May 9-442.....	A VIII	68	5555-6753		Good	
May 9-482.....	A VIII	106	5576-6753		Good	
1943 Aug. 18-285.....	103a 0	210	3705-4010	Grating	Sl. weak	Haze
1944 June 9-397.....	Cr.H.S.	120	3690-4010		Good	
June 10-446.....	Cr.H.S.	50	3690-4010		Sl. weak	

TABLE 2. LIST OF OBSERVATIONS—*Concluded*

Date U.T.	Emulsion	Exposure min.	Region $\lambda\lambda$	Instrument	Density	Remarks
<i><math>\alpha</math> Persei</i>						
1937 Feb. 20·111.....	A II	51	4028-4590	III Prisms	Good	Clouds
Mar. 28·162.....	A II	20	4028-4590		Weak in violet	
Sept. 9·403.....	E 40	70	4028-4603		Weak in violet	
1938 Jan. 19·064.....	A II	30	4028-4590		Strong in blue	
Feb. 25·136.....	A II	14	4028-4576		Sl. strong	
Feb. 25·144.....	A II	8	4028-4603		Good	
1938 Sept. 16·449.....	S.R.P.	60	4576-5683	III Prisms	Strong in green	
Nov. 15·301.....	A IX	14	4588-5701		Good	
Dec. 13·225.....	S.R.P.	46	4588-5701		Good	
1938 Sept. 13·411.....	S.R.P.	50	5688-6417	Prism and Grating	Fair	
Sept. 13·488.....	A VIII	50	5703-6753		Good	
Nov. 22·264.....	A VIII	80	5471-6753		Good	
Nov. 22·326.....	S.R.P.	80	5435-5775		Good	
1939 Mar. 14·157.....	A VIII	36	5498-6753		Sl. weak	
1944 Mar. 12·169.....	Cr.H.S.	82	3690-4010	Grating	Good	
Mar. 12·251.....	Cr.H.S.	90	3690-3905		Good	
Oct. 6·382.....	III 0	94	3690-4010		Sl. weak	
Oct. 6·461.....	III 0	130	3690-4010		Good	
Oct. 11·433.....	II 0	108	3690-4010		Sl. strong	
1945 Feb. 20·196.....	II 0	76	3690-4010		Good	
<i><math>\alpha</math> Canis Minoris</i>						
1937 Feb. 20·250.....	A II	15	4049-4590	III Prisms	Good	
Mar. 28·145.....	A II	17	4028-4603		Good	
Mar. 28·176.....	A II	5	4028-4603		Good	
1938 Feb. 25·217.....	E 33	6	4028-4603		Sl. strong	
Feb. 25·228.....	E 33	2	4028-4603		Good	
Feb. 25·231.....	E 33	1	4028-4603		Good	
1938 Nov. 15·500.....	S.R.P.	50	5172-5619	III Prisms	Weak	
Dec. 13·321.....	A IX	12	4572-5185		Good	
Dec. 13·364.....	S.R.P.	40	4583-5174		Sl. strong	
Dec. 13·408.....	S.R.P.	25	4572-5690		Good	
Dec. 13·430.....	S.R.P.	36	5166-5701		Good	
1938 Nov. 22·460.....	A VIII	40	5512-6753	Prism and Grating	Compn. strong	
Nov. 22·510.....	A VIII	40	5615-6753		Sl. weak	
Nov. 22·543.....	A VIII	56	5490-6753		Good	
1939 Mar. 28·162.....	A VIII	70	6355-6696		Sl. strong	
1944 Mar. 10·228.....	Cr.H.S.	30	3690-3906	Grating	Good	
Mar. 10·263.....	Cr.H.S.	26	3690-4005		Good	
Mar. 10·292.....	Cr.H.S.	36	3690-3895		Good	
Oct. 11·558.....	III 0	44	3800-3922		Good	
1945 Feb. 20·238.....	II 0	34	3690-4010		Good	
Feb. 20·300.....	II 0	40	3690-3865		Good	

ratio of 1 : 20. Before this observing program was begun, tests were made on a number of developers, including borax D-76 and paraphenylene-diamene, to test the relative graininess of the plates and the presence of any Eberhard developer effect. Since the size of the grains did not decrease greatly, since the necessary exposure time was lengthened considerably by the use of a fine grain developer, and since no Eberhard effect was apparent for any of the developers, the use of those employed at the Observatory was continued.

Intensity steps were impressed on the plates by means of a rapidly rotating step-sector placed immediately in front of the slit of the calibrating spectrograph. Until March, 1937, a sector with nine steps which had a uniform intensity ratio such that  $\Delta (\log_{10} I) = 0.301$  was used. The sector was then replaced by one of similar construction but which had twelve steps with a uniform ratio of  $\Delta (\log_{10} I) = 0.200$  between each step. The calibrations obtained with this arrangement have been compared with (a) a step-slit; (b) a number of step-weakeners made of sputtered platinum by McKellar at the Massachusetts Institute of Technology; and (c) a step-weakener sent by Minnaert from Utrecht with which calibrating devices in use at several observatories have been compared. The calibration curves obtained with the sectors were shown to be identical, within the errors of observation, with curves obtained by means of step-slit and step-weakeners. All comparisons, which covered almost the entire range observed in the present investigation,  $\lambda\lambda$  4000-6700, were made by Petrie and McKellar<sup>62</sup> and by Beals and McKellar<sup>63</sup>.

#### MICROPHOTOMETRY OF THE PLATES

The plates were analysed with the photo-electric recording microphotometer of the Observatory designed by Beals<sup>64</sup>. To obtain the full resolving power, narrow slits were used on the microphotometer and the speed was regulated so that one centimetre on the plate was covered in about five minutes. In order to allow for any change in the lamp or in the amplification system, calibrations were placed on the tracings both before and after each run along the spectrum. In most cases the maximum deflection of the galvanometer remained sensibly constant but for the few times where a change was noted, all deflections, both for the calibrations and throughout the spectrum, were reduced to average values.

In the green, red, and ultraviolet regions, all tracings were made with a 100-fold wave-length magnification. In the blue region, for identification purposes and for measuring profiles, the same magnification was used but for lines where the intensity at the centre of the line and its width at the continuous spectrum were the measured data, a 20-fold magnification was employed. In all cases the sensitivity of the microphotometer was such that the amplitude of the galvanometer deflection between clear glass and total darkness was between 10 and 11 cm.

Much has been written concerning the variation with wave-length of the slope of the calibration curve relating galvanometer deflection and  $\log$  (intensity). While no detailed examination of this problem is attempted in this paper, it may be noted that, for the plates used, there was little appreciable change in the slope of the straight-line portion of the curve from  $\lambda$  3700 to  $\lambda$  4600; that an increase in slope occurred between  $\lambda$  4800

<sup>62</sup> *J. R. A. S., Can.* **31**, 130, 1937.

<sup>63</sup> Unpublished.

<sup>64</sup> *M. N.*, **96**, 730, 1936.

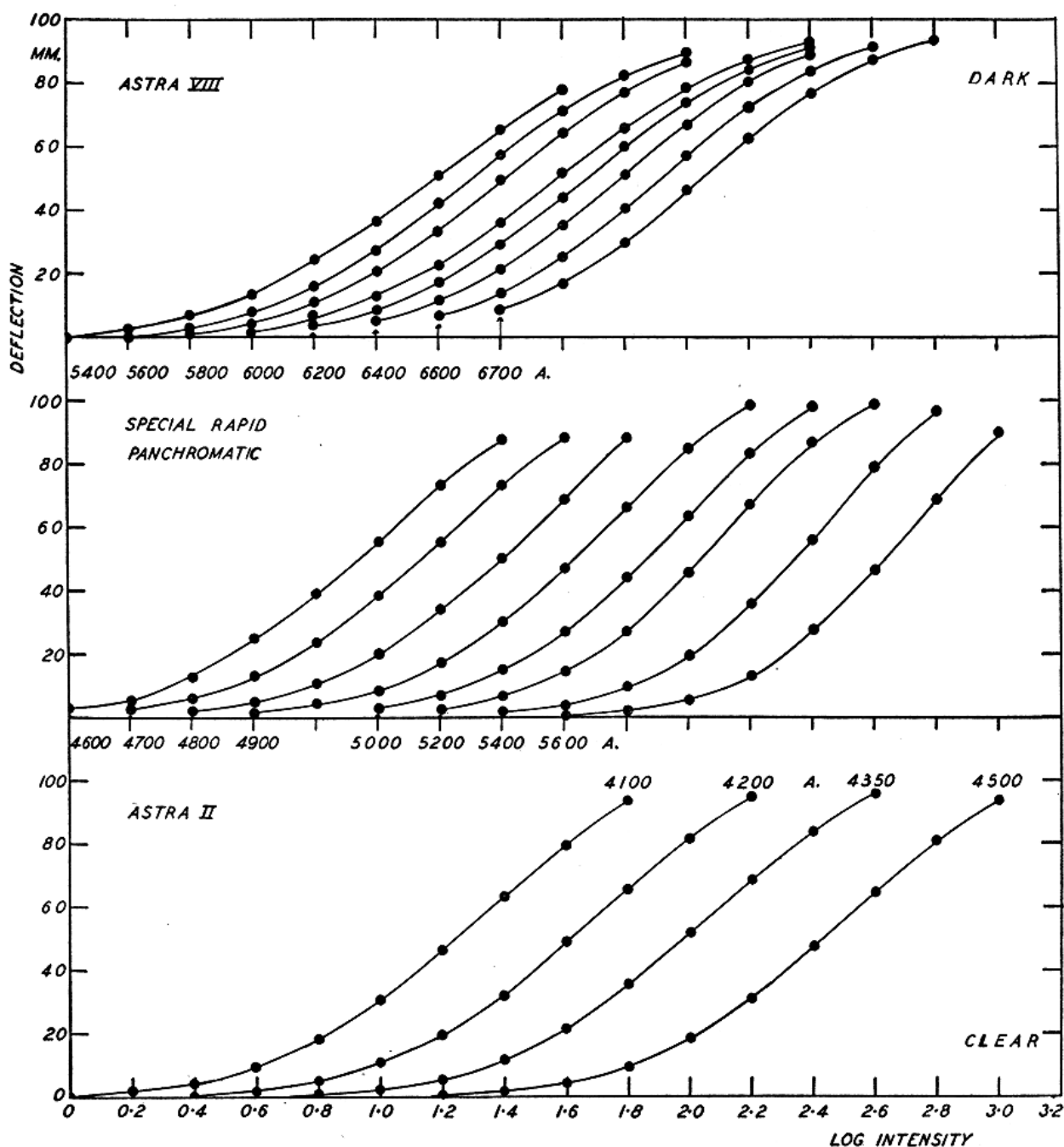


FIG. 1. Typical Calibration Curves. Clear glass is at the bottom of each diagram and total darkness is near the top; the scales vary slightly. Note that the points fit a very well-defined curve and that there is a gradual change of slope with wave-length.

and  $\lambda$  5000; and that there was a gradual increase in the slope of the curve from  $\lambda$  5500 to  $\lambda$  6700. The calibration curves shown in Fig. 1 were selected from the tracings almost at random and indicate these changes. To eliminate possible errors from this effect, calibration curves were placed on each tracing every 150 angstroms in the blue region and every 200 angstroms throughout the remainder of the range except from  $\lambda$  4800 to  $\lambda$  5200, where they were impressed every 100 angstroms.

## SELECTION AND MEASUREMENT OF LINES

As so few measurements of line intensities in these stars have been published, all measurable lines in the blue region were studied. When the investigation was extended to include the green and red regions of the spectrum, only lines for which theoretical intensities were available were measured. In the ultraviolet region, the high resolving power combined with the large scale of the intensitometer tracings permitted measurement of numerous lines in spite of the congestion of the spectrum; the intensity of a line was measured whenever it was felt that a reasonable estimate of its strength could be obtained. In the blue region many lines are so hopelessly blended together that even a rough estimate of their intensity is difficult and, except for a few important lines, no measurement was attempted if another line of comparable intensity lay within 0.8 angstroms. For lines in the green and red regions, the limit of proximity for selection of a line was usually set at one angstrom.

Identification of the lines in the spectrum of each star was made by comparison with the published wave-length tables: *Revision of Rowland's Table of Solar Wave-lengths* by St. John, *et al.*<sup>65</sup>, and the *Utrecht Photometric Atlas of the Solar Spectrum*<sup>66</sup>, when it became available; notes on  $\gamma$  Cygni by Adams and Joy<sup>67</sup> and Roach's study of "The Spectrum of  $\gamma$  Cygni"<sup>68</sup> in the region  $\lambda\lambda$  3977-4405; "The Spectrum of *Alpha Persei*" by Dunham<sup>69</sup>; and "The Spectrum of *alpha Canis Minoris*" by Albrecht<sup>70</sup>. Swensson's paper on "The Spectrum of *Procyon*"<sup>71</sup> was received after the tables had been typed for publication; a comparison of his wave-length identifications with those adopted suggests very few changes. It appears that molecular lines of CN and CH are faintly present and a few lines in the ultraviolet which were attributed to rare earths should be considered molecular lines.

Hartmann formulae were used to compute dispersion tables in the blue and green regions. For the red region, where prism and grating are combined, a first approximation was obtained by means of a linear formula; the computed positions were then improved by drawing a correction curve through the measured positions of the iron and neon comparison lines. The dispersion of the grating spectra in the ultraviolet region was almost linear. It changed from 4.81 A/mm. at  $\lambda$  3700 to 4.67 A/mm at  $\lambda$  4000. Allowance for this variation was made both for line identifications and in calculation of equivalent widths. In all cases a final approximation to the true position of a line was obtained by measuring the positions of known lines on the tracings and making a correction curve from these. All lines listed in Tables 3 and 4 were found to lie very close to the position calculated for the corresponding Rowland solar wave-length.

Before the tracings were measured, the estimated position of the continuous background was sketched, as discussed later in the paper, along the upper edge of the small variations in the microphotometer curve which seemed to be caused mainly by grains of the plate. The profiles of all lines to be measured were also drawn on the tracings; suitable allowance was made for the wings and for the blending of other lines as well as for any obvious irregularities produced by the grains of the plate.

<sup>65</sup> *P. Carnegie Inst., Washington*, No. 396, 1928.

<sup>66</sup> Minnaert, M., G. F. W. Mulders and J. Houtgast, Schnabel, Kampert and Helm, Amsterdam, 1940.

<sup>67</sup> *P. A. S. P.*, 38, 322, 1926; *Pr. Ac. S.*, Washington, 13, 393, 1927.

<sup>68</sup> *Ap. J.*, 96, 272, 1942.

<sup>69</sup> *Cont. Princ. O.*, No. 9, 1929.

<sup>70</sup> *Ap. J.*, 80, 86, 1934.

<sup>71</sup> *Ap. J.*, 103, 207, 1946.

All tracings in the region  $\lambda\lambda$  4028-6750 were measured on a special machine designed for the purpose by Beals<sup>72</sup>. It consists essentially of an illuminated millimetre reseau with rollers at each end on which the tracing is wound and which keep the paper firmly in position during measurement. For most tracings the line-width at the continuous spectrum and the deflection at the centre of each line and at the continuous background were measured. Where profiles were determined, the deflection at each millimetre from the centre of the line was measured for narrow lines, though larger intervals were permitted in the wings of broad lines such as those of hydrogen. By means of the appropriate calibration curve obtained from the same tracing, the galvanometer deflections were reduced to log (intensity) and intensity which, in accordance with Allen's notation, is designated  $r_m$ , the measured residual intensity at the centre of the line expressed as a percentage of the continuous background.

The equivalent width of a line is defined as the width in angstrom units of a rectangular line which completely absorbs the background intensity and which is equal in area to the given line. In this investigation equivalent widths were determined in three ways:

(1) *Profiles*: For many lines whose profiles were not seriously affected by blending the observed shape of the line was reduced to intensity units and, after the profile had been plotted on graph paper, the area was measured with a planimeter. For strong, unblended lines this method undoubtedly gives the most accurate measure of the equivalent width but, in these stars, many lines are too badly blended to permit the sketching of an accurate profile on the tracing. Profiles of about 75 lines were determined as a control on the total absorptions obtained by other methods.

(2) *Triangles*: For most lines of weak and moderate intensity, Elvey<sup>73</sup> has shown that the line may be assumed to be triangular in shape and the equivalent width may be determined by a measurement of the intensity at the centre and the width at the continuous background. This method may be considered a first approximation valid in many-lined stars where it is difficult to estimate the profile on account of blending. For this reason all lines in the region  $\lambda\lambda$  4028-6750 have been measured in this way. A comparison of equivalent widths shows that profile determinations give values about ten per cent greater than the triangle measurement. The difference, for which allowance has been made in the final results, is not considered serious because the blending of neighbouring lines tends to make the lines appear too strong.

(3) *Central Intensities*: Since, in the blue region, many of the tracings were made with only a 20-fold magnification, the writer felt that the results should be checked in some way. Accordingly the central intensity,  $r_m$ , was plotted against equivalent width,  $W$ . Since the central intensity increases with decreasing dispersion as a result of the averaging effect when points on the wings are superimposed on the centre of a line, and since the dispersion decreases with increasing wave-length, a direct correlation had not been expected. However, after several functions had been considered, a good correlation was found between  $r_m$  and  $W/\lambda^4$ . In order to test the reality of this correlation over a greater range, these functions were again plotted for the four stars after the green region had been measured. In Fig. 2, the mean curves for the four stars have been superposed on the individual observations and it is seen that the agreement remained excellent. As this

<sup>72</sup> Unpublished.

<sup>73</sup> *Ap. J.*, **79**, 263, 1934.

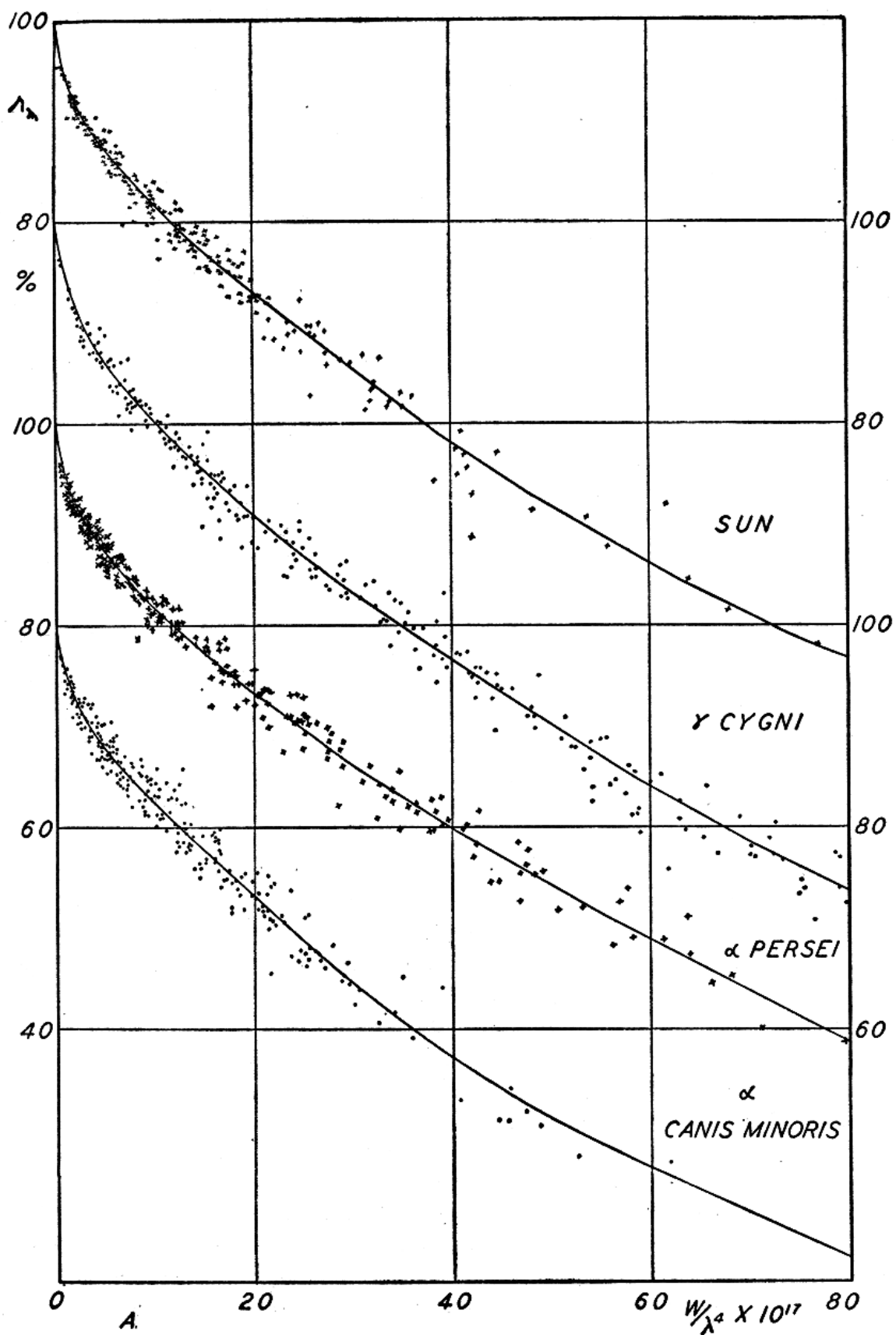


FIG. 2. The Relation Between Measured Central Intensity,  $r_m$ , and Equivalent Width,  $W/\lambda^4$ , for Solar-Type Stars in the Green Region,  $\lambda\lambda$  4600-5700.

relation gives a semi-independent determination of the equivalent width, and as Woolley<sup>74</sup>, Allen<sup>75</sup>, Merrill, Sanford, Wilson and Burwell<sup>76</sup>, and others have discovered similar correlations, the mean value from profile, triangle and curve was accepted as the preliminary equivalent width. When the red region was studied, a correlation was found between  $r_m$  and  $W$  which proved satisfactory.

A comparison of the results for the sun with those obtained by Allen showed that the Victoria values, for weak and moderate lines, were appreciably greater than Allen's. This had been expected because, in the preliminary study, full allowance for the blending effect of neighbouring lines had not been made. Even Allen, with his greater dispersion, found a blending effect in his central intensities for which it was necessary to apply a correction before the true equivalent width could be determined.

With the dispersion used in the present investigation the lines are crowded together on the plate and the blending effect is more serious but, on account of the many lines, it cannot be readily determined. For a few lines, most of which were in the blue region where the effect is most serious, the central intensities which would give Allen's equivalent width were read from the curve relating  $r_m$  and  $W/\lambda^4$ . The difference between these adjusted central intensities and those obtained from the tracings was taken to be the necessary correction for blending. As they seemed to be of the right order of magnitude and as the results were consistent, corrections were applied to the central intensities of all lines. This correction for blending was estimated from the observed effect of the neighbouring lines; the closest approach of the line wing to the continuous background on each side of the line was taken as the criterion. Series of corrections for lines of different intensities were made up but, after some practice, the estimate, to the nearest one per cent, was made by inspection. All lines in the region  $\lambda\lambda$  4028-6750 were corrected in this manner though, in the green and red regions, the corrections were often small or negligible. Allowance was also made for the difference in the width of average lines in the sun and in the other stars.

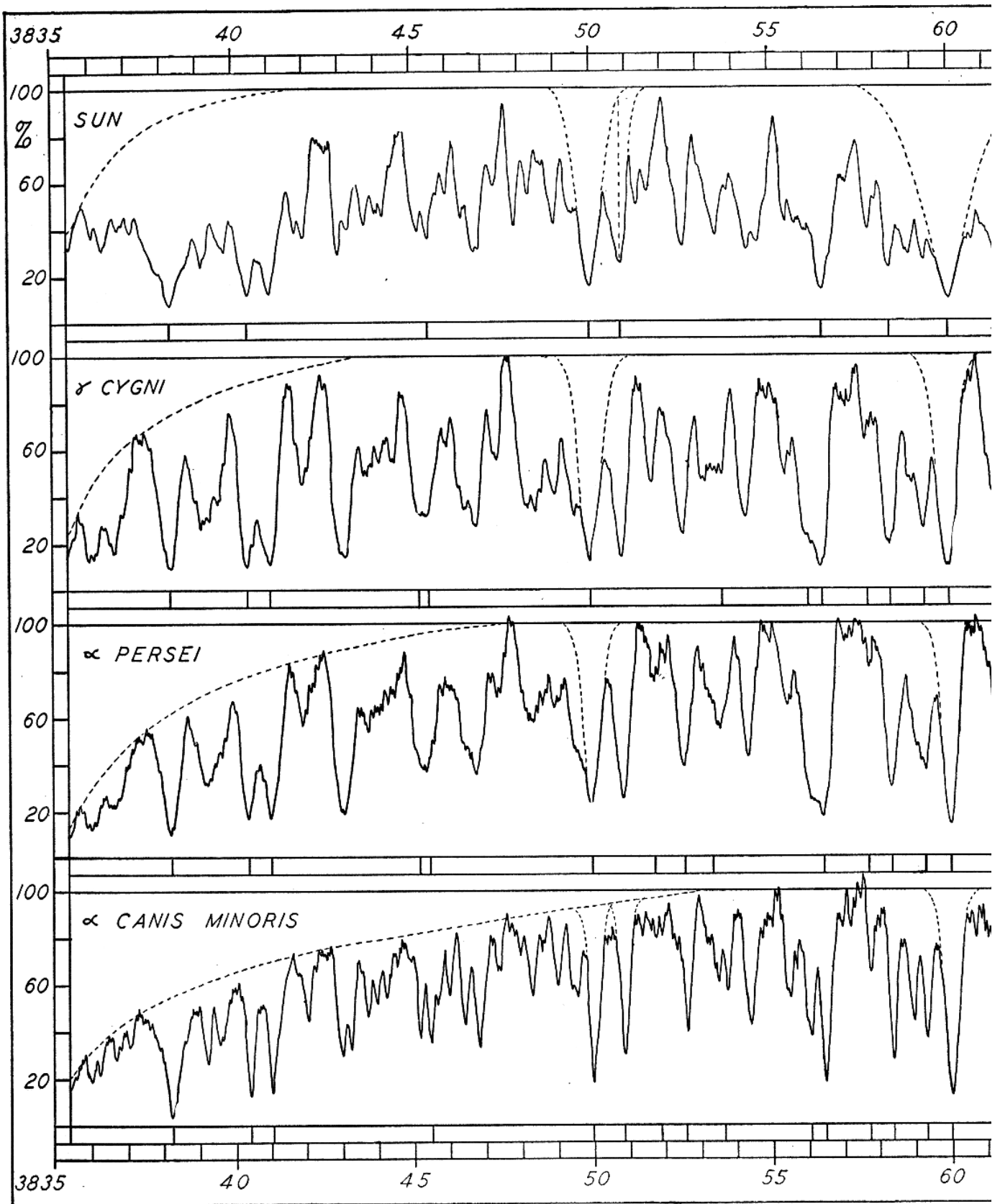
Throughout the spectrum the profiles gave slightly higher values than the equivalent widths obtained from the triangles. As the triangle measurements frequently agreed more closely with measures of the same lines by other observers, especially in the red region, and as the profiles were not completely corrected for blending effects, triangle and profile measures were given equal weight when the final mean curve relating central intensity and equivalent width was drawn. After  $r_b$ , the central intensity of a given line corrected for blending, had been used to obtain a value of the equivalent width from one of these curves, a small additional correction was added to the latter. This correction was positive if the original triangle measurement was above the curve and negative if it was below. This final value is the equivalent width listed in Table 3. For extremely strong lines, such as those in the iron multiplet,  $a^3F-y^3F^o$ , the hydrogen lines, the magnesium  $b$  triplet, the sodium  $D$  lines, calcium  $\lambda$  4227, and a few others, values of the equivalent width obtained from profile measurements have been used. For the few lines in the extensive wings of the hydrogen lines, the equivalent widths have been increased in accordance with the result found by Thackeray<sup>77</sup> that "the observed intensity of a blended

<sup>74</sup> *An. Sol. Phys. O.*, Cambridge, 3, Pt. 2, 1933.

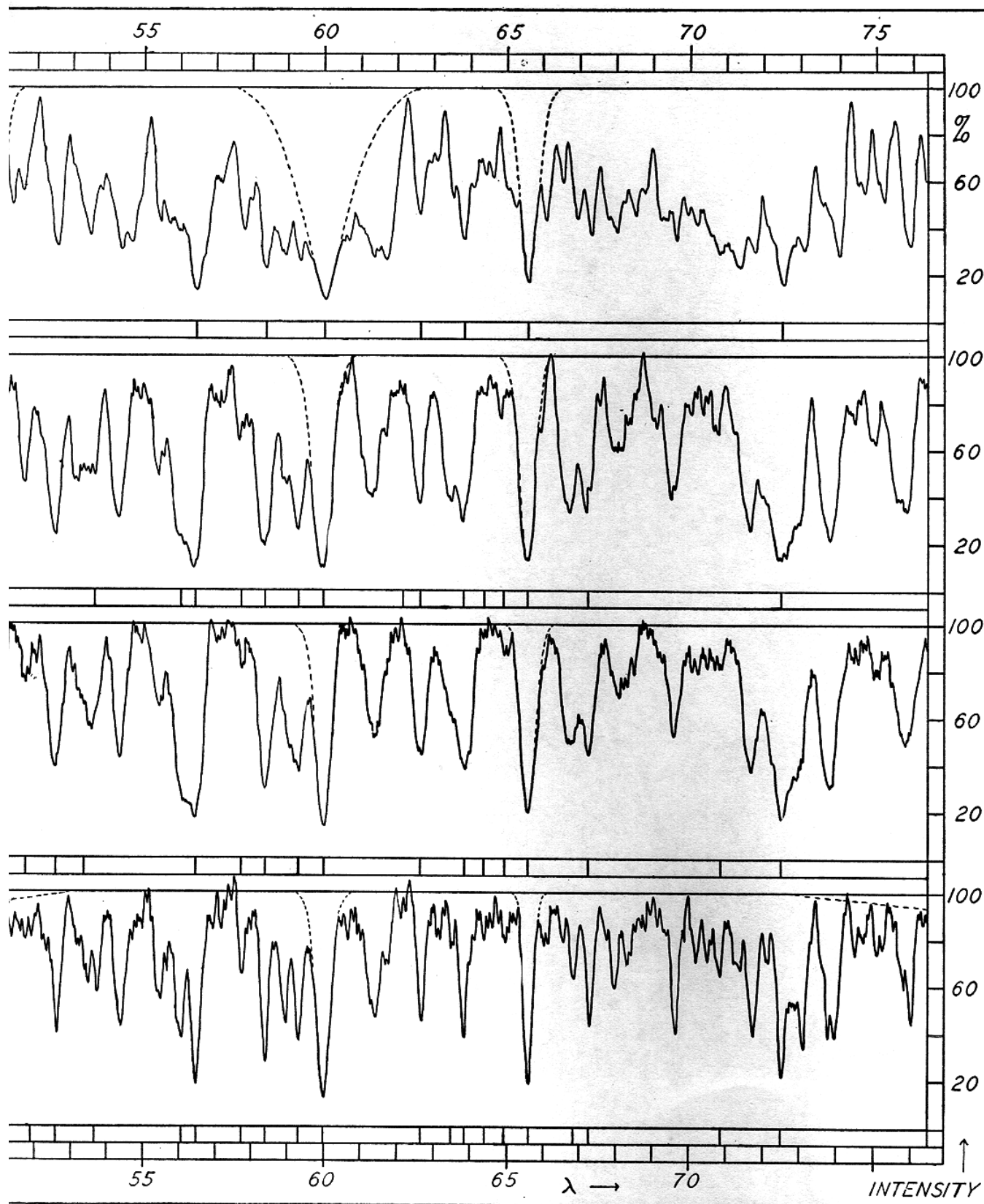
<sup>75</sup> *Mem. Comm. Sol. O.*, Canberra, 1, No. 5, 1934; 2, No. 6, 1938.

<sup>76</sup> *Ap. J.*, 86, 274, 1937.

<sup>77</sup> *Ap. J.*, 84, 433, 1936.



FOLDING PLATE IV. Intensitometer Tracings of the Sun,  $\gamma$  Cygni,  $\alpha$  Persei and  $\alpha$  Canis Minoris in the Region  $\lambda\lambda$  3835-3875. T on each tracing. The positions of lines measured and listed in Table 4 have been indicated at the bottom of each tracing but profiles have been smoothed. The profiles of  $\lambda$  3835, H $\eta$  down the sequence; the wings of  $\lambda$  3860, Fe I, in the sun and their absence in  $\gamma$  Cygni and  $\alpha$  Persei; and the great difficulty in  $\alpha$  Canis Minoris is  $34 \times$  the original spectrograms.



$\alpha$  *Canis Minoris* in the Region  $\lambda\lambda$  3835-3875. The estimated position of the continuous spectrum has been rectified to read 100 per cent at the bottom of each tracing but profiles have been drawn for only a few representative lines. Note the increasing breadth of the wings in  $\gamma$  *Cygni* and  $\alpha$  *Persei*; and the great difficulty in estimating the shapes of the lines, particularly in the case of the sun. The magnification

line is reduced in proportion to the intensity within the blending line." If  $W_b$  is the measured equivalent width of a line in the wing of a hydrogen line, referred to the wing as the continuous spectrum; if  $W$  is the true equivalent width the line would have if no blending occurred; and if  $r_w$  is the intensity of the wing of the hydrogen line at the centre of the line being studied, then

$$W = \frac{W_b}{r_w}.$$

This relation is not exact and therefore lines deep in the wings of the hydrogen lines have not been used in deriving curves of growth. However, it seems to be the best means available for correcting the intensities of blended lines and the equivalent widths calculated according to this formula have been used for lines of atoms which could not be studied otherwise in this region of the spectrum. It has been found particularly useful in the ultraviolet region where the hydrogen lines tend to overlap near  $\lambda$  3700.

#### INTENSITOMETER MEASURES

Before the ultraviolet set of plates was measured, an intensitometer, by means of which the observed intensity of spectral lines relative to the continuous spectrum can be drawn, was designed by Dr. C. S. Beals<sup>78</sup> and constructed for the Observatory by S. S. Girling. In its original form, as used for the plates studied in this paper, galvanometer deflections on the microphotometer tracings were transformed directly to intensities by means of a single calibration curve; in this form, the continuous spectrum is drawn on the intensitometer tracing by joining portions of the spectrum where no appreciable line absorption occurs or, if only weak lines are present, where it is estimated that the continuous spectrum should be. Under these circumstances, the position of the continuum changes continuously and it is sometimes difficult to estimate the true equivalent width of a line, particularly if it lies within the wings of a hydrogen line. The intensitometer was altered in 1945 to permit motion of the microphotometer tracing both perpendicular to and along the direction of the dispersion. By first making a logarithmic tracing on which the position of the continuous background and the wings of the hydrogen lines may be drawn and then transforming it into a direct intensity tracing, the position of the continuum may be obtained as a straight line along the direction of the dispersion; this method simplifies somewhat the procedure of measuring the intensities of lines deep in the wings of other strong lines. In addition, tracings drawn with the revised instrument can be superposed and thus plate grain and differences due to other causes can be averaged before the mean profile is drawn. The tracings shown in Folding Plate IV were made following this modification of the intensitometer.

#### *Grating Ghosts*

In grating spectra, the presence of Rowland ghost lines is always a source of error as, in absorption-line spectra, the ghost lines on either side of the main line tend effectively to decrease the intensity of the continuous spectrum. Minnaert<sup>79</sup> studied this effect and showed that the position of zero intensity should be raised relative to the continuum by an amount equal to the sum of the ghost lines, referred to the main line. This method is easily applied on intensitometer tracings where the intensity at any point is referred directly to the continuous spectrum.

<sup>78</sup> *J. R. A. S., Can.*, 38, 65, 1944.

<sup>79</sup> *Z. Phys.*, 45, 610, 1927.

The intensities of the ghost lines were determined by photographing a mercury arc with a rotating sector placed in front of the slit of the spectrograph. As the maximum intensity of a satellite line is only 1.4 per cent of the main line, it was necessary to compare the ghost satellites of  $\lambda$  4358.34 with the line at  $\lambda$  4347.50 and then determine the relative intensities of the two mercury lines. It was found that intensities of seven satellite lines to the violet of  $\lambda$  4358 could be measured and six to the red. The weakest line measured was 0.12 per cent and the strongest satellite was 1.37 per cent of the main line; the sum of these intensities was 8.1 per cent of  $\lambda$  4358. In the ultraviolet region of the spectra of the stars studied in this paper, the intensity of the observed spectrum rarely reaches that of the estimated continuous spectrum and, to allow for this, the intensity of the zero line was raised only 5 per cent instead of the calculated 8 per cent. Thus, in practice, the calibration curve was drawn on a scale of 10.5 inches between zero and 100 per cent, but all measurements were made (or reduced) on the basis of 10.0 inches between zero intensity and the continuous spectrum.

#### STUDIES OF INDIVIDUAL LINES

During the early stages of this investigation, the writer was interested in comparing the central intensities of solar lines obtained with the Victoria spectrograph with those obtained by Redman<sup>80</sup> and Allen<sup>75</sup> with instruments of considerably higher dispersion. A number of lines were studied and correction was made for the distortion by the spectrograph caused by the finite slit-width and the diffraction pattern formed by the slit. It was found that the central intensities of the hydrogen lines were very nearly as low as those obtained with spectrographs of higher resolving power, though the correction for instrumental distortion improved the results. For all other lines, the rectified central intensities were still much greater than those obtained by Redman and Allen, and it seems probable that the stellar spectrograph in the form used for this work has insufficient resolving power for the determination of the true profiles of narrow lines.

#### *The Hydrogen Lines*

Profiles of the first four members of the Balmer hydrogen series are shown in Fig. 3. A comparison of the equivalent widths with those of other observers shows a considerable scatter but, as most other measures were obtained with lower dispersion, it is believed that the present values merit considerable weight. Of the profiles shown in Fig. 3, it is possible that the wings of  $H\gamma$  in the sun and in  $\gamma$  *Cygni* have been sketched in too sharply. The profile as it has been drawn is, however, the mean of all observations and a re-examination of the tracings did not suggest a change in the original sketch of the line profile. In this region many other strong lines are present and the extent of the wings is particularly difficult to estimate.

A first measurement of the wings of the hydrogen lines in  $\alpha$  *Canis Minoris* tended to confirm Albrecht's suggestion<sup>70</sup> that they vary from time to time. A closer examination of the tracings indicated, however, that this apparent result was due to differences in density of the several plates and it is now believed that the variation from night to night is no more than might be expected from the accidental errors of measurement.

<sup>80</sup> *M. N.*, 95, 742, 1935; *M. N.*, 97, 552, 1937.

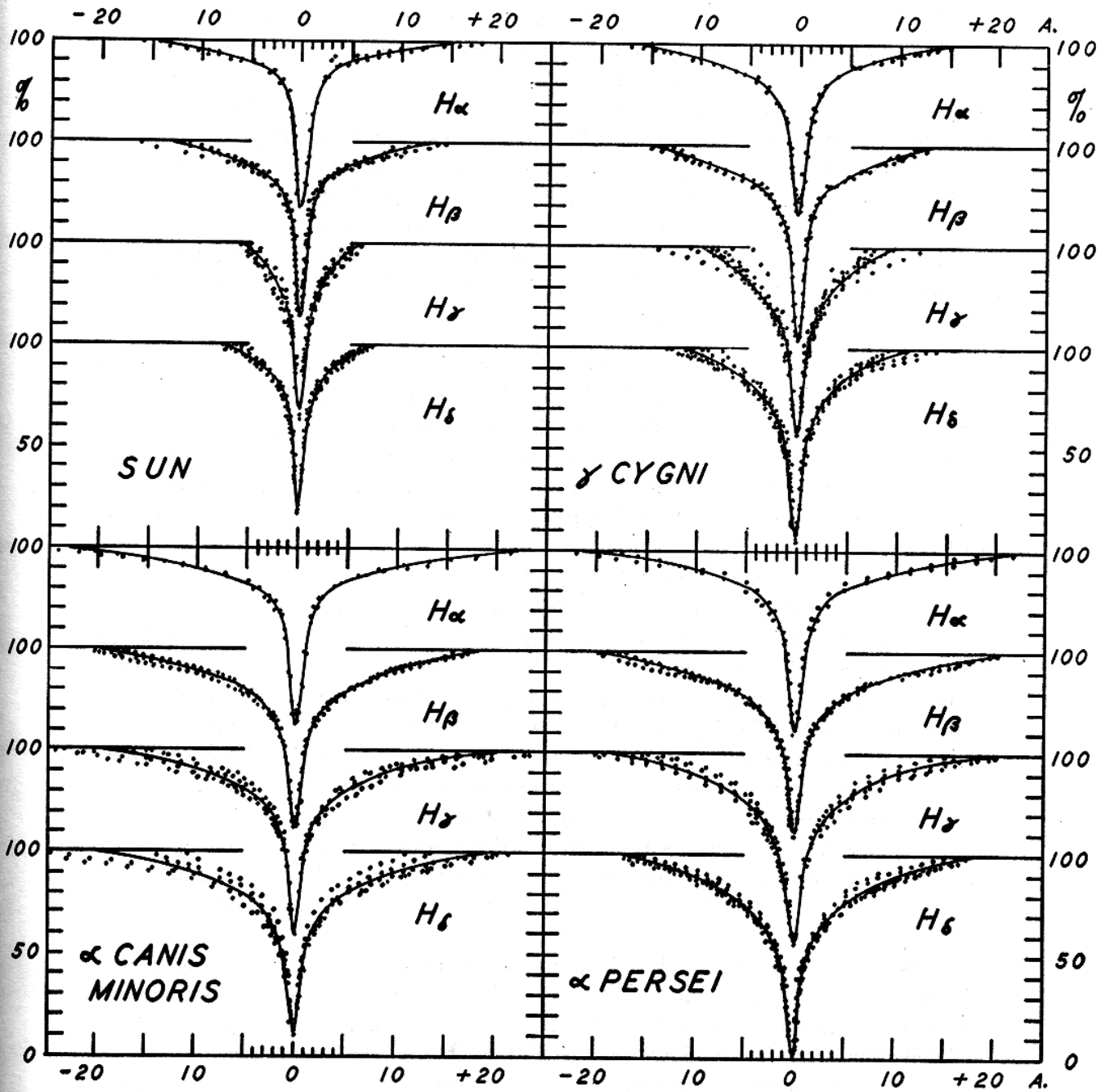


FIG. 3. Profiles of the Hydrogen Lines  $H\alpha$  to  $H\delta$  in the Spectra of the Sun,  $\gamma$  Cygni,  $\alpha$  Persei and  $\alpha$  Canis Minoris. Each plotted point represents a measure on a single plate. In the Sun and  $\gamma$  Cygni the narrower wings of  $H\gamma$ , relative to  $H\beta$  and  $H\delta$ , would indicate that the position of the continuous background may have been drawn too low.

*The Sodium D Lines*

The sodium *D* lines in these four stars have been the subject of a separate note.<sup>81</sup> The observed profiles are shown in Fig. 4. The lines in three stars remain sensibly constant on all plates but there is an apparently real change in the strength of the lines in  $\gamma$  *Cygni*. On November 22, 1938, three plates gave central intensities for  $D_1$  and  $D_2$  of 49 and 43 per cent, respectively; measures of eight other plates on four nights gave values of 30 and 21 per cent, respectively, with probable errors of less than three per cent per night. On these eleven plates, the  $H\alpha$  line remains constant within the errors of measurement, but other lines in the red region are so weak that it is uncertain whether they show a real variation or not. The *D* lines of the other stars show no variation from night to night though several plates were taken on November 22, 1938. This result tends to confirm the real variation of the *D* lines in  $\gamma$  *Cygni*.

*Other Lines*

Profiles of three typical absorption lines of Fe I, Sr II, and Ti II, respectively, are shown in Fig. 5. They indicate that, for a line of given central intensity, the breadth increases in the order  $\alpha$  *Canis Minoris*, the sun,  $\alpha$  *Persei* and  $\gamma$  *Cygni*. The increase in strength of lines arising from ionized atoms in the giant stars and the greater strength of neutral iron in stars of later spectral type, regardless of absolute magnitude, are also clearly shown.

## TABLES OF EQUIVALENT-WIDTH MEASURES

As the equivalent-width measurements are used in the formation of curves of growth and in the determination of excitation temperatures of the stars, which require a knowledge of the atomic transition to which each line corresponds, the table of observations, Table 3, is listed in multiplet form. For some purposes this arrangement is not as convenient as the usual tabulation of the data in order of wave-length but, for the present investigation, it is believed that this form will prove useful. Table 3 contains also the information which is used throughout the remainder of the paper for lines in the region  $\lambda\lambda$  4028-6750.

The arrangement of Table 3 follows that of Miss Moore's *Multiplet Table of Astrophysical Interest*<sup>82</sup>. The elements are listed in order of atomic weight and the lines of an ionized atom follow immediately after those of the neutral atom. Within an element, the lines are grouped according to multiplet and multiplets are listed in order of increasing wave-length.

In the table, column 1 gives the tabular number of the line in the present investigation. Column 2 lists the multiplet number in Miss Moore's *Multiplet Table of Astrophysical Interest, Revised Edition* (denoted by *R. M. T.*)<sup>83</sup>. In the manuscript copy of Table 3, the designation in the first edition<sup>82</sup> was followed but the number only is given here both for ease in printing and to indicate certain improvements in the identifications. Wherever the multiplet designation is different in the *R. M. T.*, the number is placed in brackets. In nearly all cases the excitation potential of the lower level remains the same but the theoretical intensity may be changed. However, the calculations were made before the new table was received and, for that reason, these values are retained in the table. Columns 3-5 are taken directly from the *Multiplet Table*<sup>82</sup> and give:

<sup>81</sup> *P. A. S. P.*, 52, 405, 1940.

<sup>82</sup> Princeton, 1933.

<sup>83</sup> *Cont. Princ. O.*, No. 20, 1945.

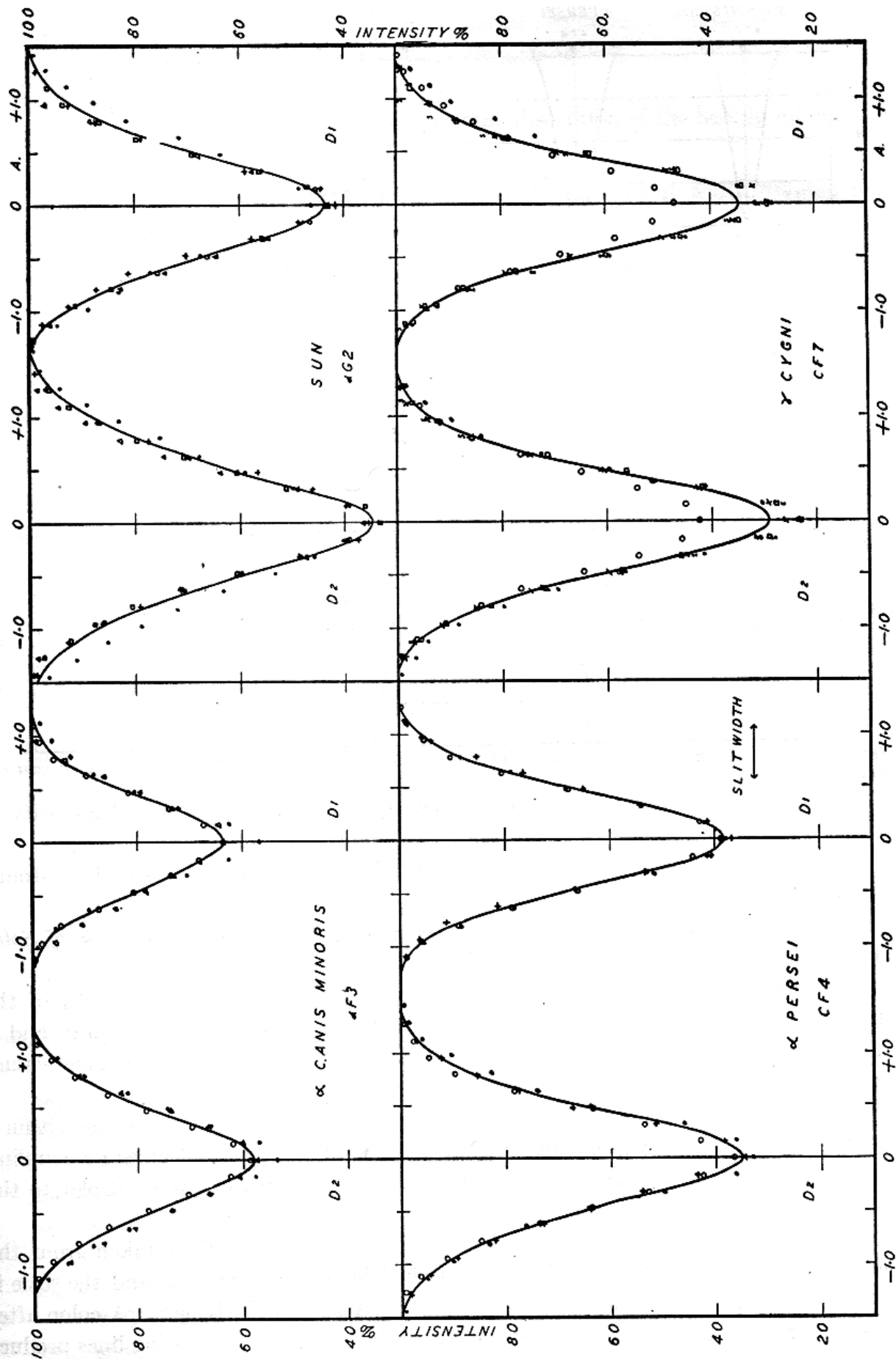


FIG. 4. Observed Profiles of the Sodium *D* Lines in Solar-Type Stars. Open circles (o) represent plates taken on November 22, 1938; they show an apparently real change in the strength of the *D* lines in the spectrum of  $\gamma$  Cygni.

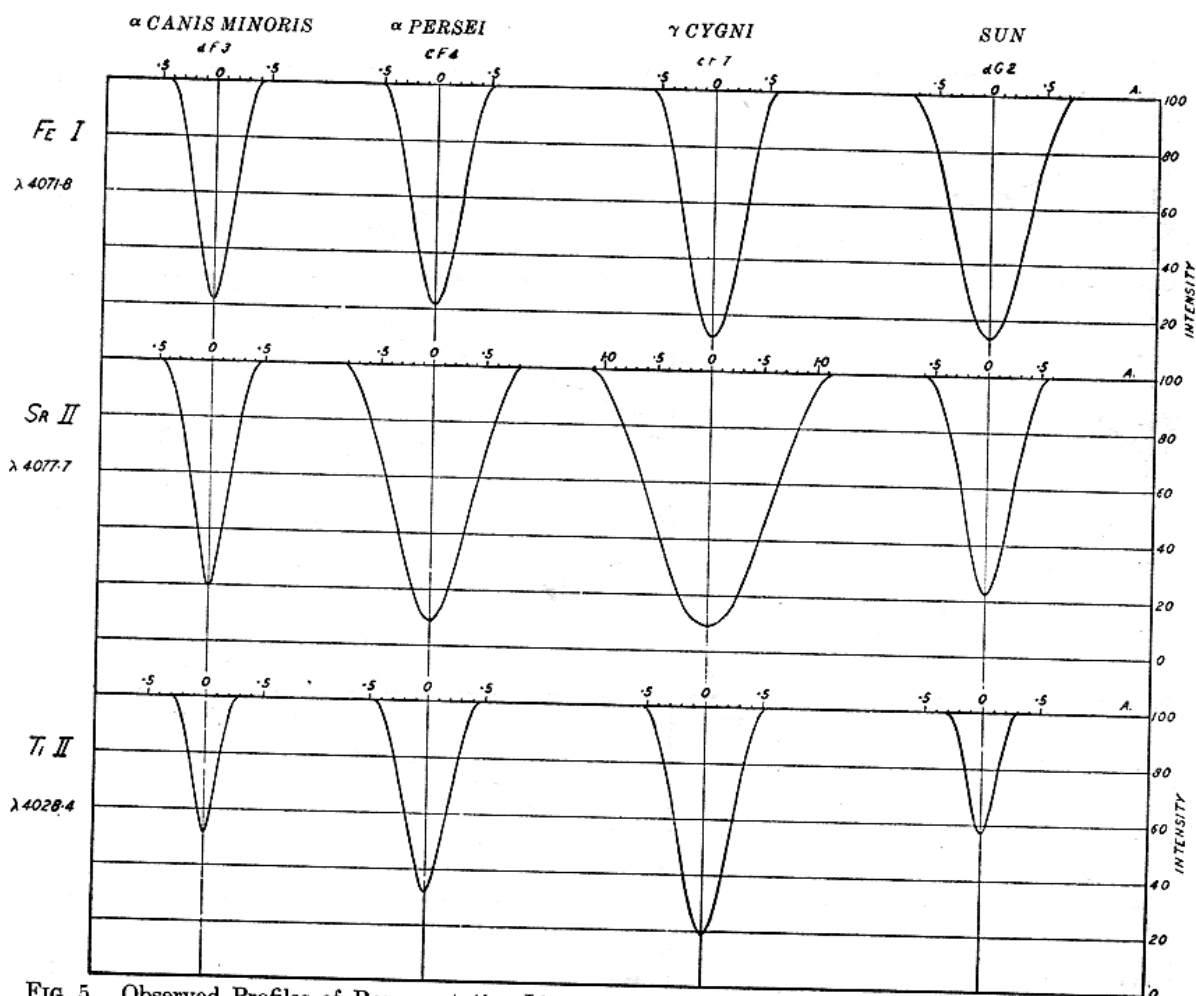


FIG. 5. Observed Profiles of Representative Lines in the Spectra of  $\alpha$  Canis Minoris,  $\alpha$  Persei,  $\gamma$  Cygni and the Sun.

Column 3, the inner quantum numbers upon which the theoretical intensity of the line is based;

Column 4, the excitation potential, in volts, of the lower level of the atomic transition;

Column 5, the solar wave-length given in the *Revised Rowland Table of Solar Wave-lengths*<sup>84</sup>.

Column 6 gives the common logarithm of the spectroscopic strength of the multiplet relative to other multiplets in the same electron transition array and is taken from a compilation of multiplet strengths by Goldberg<sup>84</sup>; most of these values are also given by Menzel, Baker, and Goldberg<sup>85</sup>.

Column 7 represents the logarithm of the theoretical intensity of a line within a multiplet. Entries in this column are taken from Russell<sup>86</sup>, who assumes LS coupling for the transitions, and give the ratio of the total strength of the multiplet to the strength of the individual line.

Column 8 gives the solar  $\log X_f$ -value for each line. It is taken from the empirical curve of growth for the sun described below (*see* page 76) and the scale is based on the absolute  $f$ -values of neutral iron given by R. B. King<sup>87</sup>. A colon after a number indicates that it is somewhat uncertain because neighbouring lines produce serious blending effects.

<sup>84</sup> *Ap. J.*, 82, 1, 1935.

<sup>85</sup> *Ap. J.*, 87, 81, 1938.

<sup>86</sup> *Ap. J.*, 83, 129, 1936.

<sup>87</sup> *Ap. J.*, 95, 78, 1942.

The remainder of the table, except for the last two columns, contains the observational data used throughout this study. The stars are arranged in order of spectral class and three items are listed for each star:

(a)  $W$ , the equivalent width, or the total absorption of the line, in milliangstrom units;

(b)  $\log_{10}\left(\frac{W}{\lambda}\right)$ , the common logarithm of the equivalent width divided by the wave-length, in units of  $10^{-6}$ .

(c) the weight of the intensity measurements of the line, which is arbitrary but depends on the general appearance of the line on the tracings, the amount of blending with other lines, etc. The most trustworthy lines are given weight 4.

The values of  $\log(g_i f)$  as given by R. B. King and A. S. King<sup>88</sup> are tabulated in the second to last column. These are laboratory measures of the relative intensities of lines in neutral titanium and neutral iron, and should be preferable to the theoretical intensities given in column 7.

The numbers in the final column relate multiplets belonging to the same electron transition array. Details of the arrays are included in Table 19.

Table 4 contains the data derived from the ultraviolet series of plates in the region  $\lambda\lambda$  3689-4010 and has been printed in order of wave-length.

Column 1 gives the laboratory wave-length listed in Miss Moore's *Revised Multiplet Table*;

Column 2 gives the atom producing the line;

Column 3 is the number of the multiplet, taken from the *Revised Multiplet Table*, from which the multiplet designation and inner quantum numbers may be obtained;

Column 4 gives the excitation potential of the lower level of the atomic transition;

Column 5 gives the solar  $\log X_r$ -value derived from the solar curve of growth which is described more fully on page 76.

Column 6 gives the weight assigned to the solar  $\log X_r$ -value and depends on the quality of the line in the *Utrecht Atlas*. Lines almost free from blends are given weight 3; average lines are given weight 2 or 1; and lines which are badly blended or for which the measurement is otherwise uncertain are listed as 1-.

The remaining sixteen columns give the observational data for the four stars. The order for the stars follows that of Table 3 and four columns are given for each star:

(a)  $r_w$ , the intensity of the blending wing at the centre of the line if there is any blending with a hydrogen (or other) line; this number is omitted if there is no such blending.

(b) The observed equivalent width,  $W$ , referred to the continuous spectrum if there is no blending; if there is a blending wing, this value is referred to the wing as if it were the continuum.

(c)  $\log(W/\lambda)$ , in units of  $10^{-6}$ . Thackeray's relation<sup>77</sup> has been used here for the  $W$  of blended lines.

(d) The weight of the line as it appears in the stellar spectrum; it varies from 3 for a good line, relatively free from blends, to 1 for lines badly blended with other lines, and for which the measurement is uncertain.

<sup>88</sup> *Ap. J.*, 87, 24, 1938.



Al I

23	5	1/2-3/2	3-129	6696-041	0-778	0-176	-2-16	41	0-79	2	40	0-78	3	19	0-45	3	28	0-62	3	(13)
24		1/2-1/2	3-129	6698-678		0-477	-2-33	10	0-17	2	17	0-40	2	9	0-13	2	14	0-32	3	

Si I

25	10	1-2	4-908	5645-621	0-954	0-857	-1-99	32	0-75	3	38	0-83	3	26	0-66	3	16	0-45	2	(14)
26		0-1	4-899	5665-566		0-954	-1-92	24	0-63	4	34	0-78	2	43	0-88	3	26	0-66	2	
27		1-1	4-908	5690-435		1-079	-1-71	54	0-98	3	55	0-98	3	36	0-80	3	35	0-79	2	
28		2-2	4-932	5708-408		0-380	-1-46	79	1-14	2	115	1-30	1	74	1-11	2	58	1-01	2	
29	(17)	0-1	4-899	5772-152	1-176	0-954	-1-80	66	1-06	3	59	1-01	3	46	0-90	3	64	1-04	2	(14)
30	9	1-2	4-908	5793-083		0-602	-1-93	54	0-97	3	64	1-04	2	62	1-03	3	54	0-97	3	
31	(16)	1-0	5-040	5948-552	0-000	0-000	-1-36	111	1-27	2	142	1-38	3	104	1-24	3	115	1-29	2	(14)

Si II

32	2	1/2-3/2	8-085	6347-104	0-778	0-176	-1-84	50	0-90	3	343	1-73	3	331	1-72	3	131	1-31	3	(15)
33		1/2-1/2	8-085	6371-362		0-477	-2-21	35	0-74	3	224	1-55	2	249	1-59	3	89	1-14	3	

Ca I

34	25	2-2	2-512	4094-942	2-498	1-431	-0-27	74	1-26	2	63	1-19	2	21	0-71	2	39	0-98	2	(23)
35	39	2-3	2-697	4108-536	2-021	0-000	-1-53	53	1-11	2	37	0-95	2	16	0-59	2	30	0-86	2	(24)
36	2	0-1	0-000	4226-742	0-778	0-000	+2-23	1476	2-64	2	884	2-32	2	509	2-08	4	505	2-08	3	(16)
37	5	1-2	1-878	4283-016	1-255	0-857	+0-35	168	1-59	4	210	1-69	4	127	1-47	3	137	1-50	4	(17)
38	4	0-1	1-871	4425-446	1-954	0-954	+0-34	166	1-57	4	239	1-73	4	152	1-54	4	135	1-48	3	(19)
39		1-1	1-878	4435-690		1-079	+0-20	134	1-48	3	267	1-78	2	142	1-50	3	100	1-35	3	
40	23	1-2	2-510	4578-562	2-498	0-669	-0-93	73	1-20	4	97	1-33	2	88	0-92	2	61	1-12	3	(22)
41		3-2	2-515	4585-876		2-976	-0-45	138	1-48	3	143	1-49	3	91	1-30	2	95	1-32	2	
42	51	1-2	2-920	4685-277	1-477	0-000	-1-55	56	1-08	3	73	1-19	3	23	0-69	2	33	0-85	3	(26)
43	22	1-2	2-510	5260-395	0-954	2-265	-2-05	22	0-62	3	18	0-53	3	24	0-66	3	21	0-60	2	(20)
44	48	1-0	2-920	5512-991	0-477	0-000	-1-19	104	1-28	2	105	1-28	2	72	1-12	2	54	0-99	2	(25)
45	21	2-3	2-512	5581-981	1-176	1-285	-1-01	97	1-24	3	163	1-46	3	72	1-11	3	80	1-16	3	(20)
46		3-3	2-515	5588-766		0-382	+0-08	175	1-50	3	277	1-70	3	193	1-54	3	123	1-34	3	
47		1-2	2-510	5590-128		1-301	-1-16	98	1-24	3	112	1-30	2	43	0-89	2	56	1-00	3	
48		2-2	2-512	5694-473		0-635	-0-25	135	1-38	2	271	1-68	2	141	1-40	2	146	1-42	2	
49		3-2	2-515	5601-288		1-285	-0-53	90	1-21	3	112	1-30	2	92	1-22	3	89	1-20	2	

TABLE 3. OBSERVATIONS OF LINE INTENSITIES IN THE SPECTRA OF SOLAR-TYPE STARS—Continued

No.	Multiplet R.M.T.	I.Q. No.	Low E.P.	Wave- length	log S	log $\lambda s/s$	log $X_j$	Sun		$\gamma$ Cygni		$\alpha$ Persei		$\alpha$ Canis Minoris		Array log $\sigma_f$				
								W	log W/ $\lambda$	W	log W/ $\lambda$	W	log W/ $\lambda$	W	log W/ $\lambda$		W	log W/ $\lambda$	W	log W/ $\lambda$
Ca I—Continued																				
50	46	1-0	2.920	5867.573	0.301	0.000	-2.22	24	0.61	3	16	0.44	2	18	0.49	2	25	0.63	3	(17)
51	3	1-1	1.878	6123.231	0.954	0.477	+0.45	261	1.63	4	272	1.65	3	273	1.65	3	179	1.47	3	(18)
52		2-1	1.891	6162.185		0.255	+0.58	267	1.64	3	303	1.69	3	276	1.65	2	139	1.35	3	
53	20	1-0	2.510	6166.446	1.954	0.954	-1.65	81	1.12	2	63	1.01	2	41	0.82	3	41	0.82	2	(21)
54	18	3-4	2.515	6439.090	1.322	0.368	-0.01	224	1.54	4	320	1.70	3	273	1.63	3	191	1.47	3	(20)
55		3-3	2.515	6471.676		1.431	-1.37	116	1.25	3	97	1.18	3	95	1.17	3	102	1.20	3	
56		1-2	2.510	6493.796		0.699	-0.47	161	1.40	3	214	1.52	2	198	1.48	3	158	1.39	2	
57		2-2	2.512	6499.663		1.431	-1.41	72	1.04	2	106	1.21	2	73	1.05	2	94	1.16	3	
58	32	2-1	2.697	6717.697	0.477	0.000	-0.74	168	1.40	3	188	1.45	3	127	1.28	3	102	1.18	3	(20)
Sc I																				
59	12	9/2-11/2	1.442	5671.835	1.556	0.477	-2.46	15	0.42	2	21	0.57	2	14	0.39	2	10	0.25	2	(27)
Sc II																				
60	7	2-2	0.314	4246.838	0.699	0.000	+0.57	162	1.58	4	478	2.05	4	359	1.93	4	215	1.70	4	(28)
61	15	4-3	0.616	4314.093	2.225	0.368	-0.51	165	1.58	3	497	2.06	3	414	1.98	3	196	1.66	3	(29)
62		2-1	0.593	4325.000		0.699	+0.22	181	1.62	3	396	1.96	3	296	1.84	4	167	1.59	3	
63	14	3-4	0.603	4354.617	1.924	1.572	-1.34	48	1.04	2	301	1.84	3	146	1.52	2	37	0.93	2	(29)
64		3-3	0.603	4400.399		0.553	-0.47	94	1.33	3	414	1.97	2	251	1.76	2	111	1.40	2	
65		2-2	0.593	4415.565		0.674	-0.28	103	1.37	1	356	1.91	1	243	1.74	1	99	1.35	2	
66		4-3	0.616	4420.673		1.572	-2.34	10	0.36	2	177	1.60	3	65	1.17	3	12	0.43	2	
67		3-2	0.603	4431.366		1.578	-1.97	27	0.78	2	142	1.51	2	64	1.16	2	18	0.61	2	
68	23	2-1	1.351	5031.026	1.322	0.000	-1.36	60	1.08	3	422	1.92	3	284	1.75	3	94	1.27	3	(28)
69	26	0-1	1.449	5239.825	.....	0.000	-1.69	36	0.84	3	302	1.76	3	163	1.49	3	72	1.14	3	
70	31	4-3	1.761	5526.823	2.033	0.000	-1.32	69	1.10	3	428	1.89	3	295	1.73	3	86	1.19	3	(29)
71	29	1-1	1.494	5667.157	1.908	1.079	-2.07	23	0.61	2	245	1.64	2	116	1.31	2	42	0.87	2	(29)
72		1-0	1.494	5669.043		0.954	-2.01	30	0.72	3	307	1.73	3	141	1.40	2	54	0.98	2	
73	28	1-1	1.494	6320.863	1.431	1.079	-2.85	7	0.04	2	89	1.15	2	60	0.98	3	37	0.77	3	(29)
74	19	2-2	1.351	6604.609	1.544	0.000	-2.02	40	0.78	3	231	1.54	3	134	1.31	3	60	0.96	3	(29)

Ti I

75	80	1-2	1-048	4060-271	1-079	0-857	-1-74	18	0-65	2	13	0-50	1	5	0-09	1	7	0-24	2	2-57 (30)
76	44	4-4	0-832	4287-414	1-398	1-368	-1-21	42	0-99	3	51	1-08	1	21	0-69	1	19	0-65	2	2-892 (31)
77	43	3-2	0-822	4326-359	.....	.....	-1-87	.....	.....	.....	.....	.....	.....	8	0-27	1	4	1-97	1	2-15
78	160	5-5	1-879	4449-152	1-431	0-408	-1-38	57	1-11	2	93	1-32	1	26	0-77	1	23	0-71	2	(31)
79	160	4-4	1-871	4450-903	.....	0-522	-1-55	34	0-88	1	.....	.....	.....	.....	.....	.....	14	0-50	2	.....
80	80	3-3	1-865	4453-712	.....	0-615	-1-72	34	0-88	2	24	0-73	1	16	0-56	1	17	0-58	1	.....
81	146	2-3	1-732	4465-816	1-176	0-808	-1-79	23	0-71	2	33	0-87	1	18	0-60	2	16	0-55	2	3-15 (31)
82	42	4-5	0-832	4512-746	1-544	1-502	-1-37	50	1-04	3	60	1-12	2	32	0-85	2	19	0-62	2	2-740 (31)
83	88	3-4	0-822	4518-034	.....	1-350	-1-21	54	1-08	1	64	1-15	1	40	0-95	1	30	0-82	1	2-875
84	84	5-5	0-845	4533-251	.....	0-548	-0-35	114	1-40	2	162	1-56	2	96	1-33	2	65	1-16	2	3-708
85	85	4-4	0-832	4534-789	.....	0-742	-0-49	70	1-19	2	101	1-35	2	54	1-08	1	52	1-06	2	3-544
86	86	3-3	0-822	4535-578	.....	0-948	-0-71	106	1-37	1	112	1-39	1	50	1-04	2	68	1-18	2	3-279
87	87	3-2	0-822	4548-775	.....	1-368	-1-28	60	1-12	2	40	0-94	1	31	0-83	1	27	0-77	2	2-866
88	88	5-4	0-845	4555-494	.....	1-502	-1-34	40	0-94	2	.....	.....	.....	.....	.....	.....	22	0-68	2	2-740
89	7	3-2	0-020	4562-639	.....	.....	-2-53	9	0-30	1	23	0-70	1	9	0-30	1	.....	.....	.....	0-556
90	145	3-4	1-741	4617-280	1-398	0-444	-1-49	47	1-01	3	46	1-00	3	18	0-59	3	14	0-48	3	3-531 (31)
91	91	2-3	1-732	4623-103	.....	0-729	-1-62	49	1-02	3	27	0-77	3	14	0-48	2	15	0-51	2	3-23
92	92	1-1	1-726	4639-948	.....	1-046	-1-84	16	0-54	2	26	0-75	3	17	0-56	2	9	0-29	2	.....
93	93	1-0	1-726	4645-196	.....	1-398	-2-17	16	0-54	2	26	0-75	2	12	0-41	2	9	0-29	3	.....
94	94	2-1	1-732	4650-023	.....	1-523	-2-31	10	0-33	2	11	0-37	2	8	0-24	2	8	0-24	2	.....
95	95	3-2	1-741	4656-056	.....	1-875	-2-42	11	0-37	2	27	0-76	2	17	0-56	2	8	0-24	2	.....
96	6	2-3	0-000	4656-474	1-255	0-623	-1-30	64	1-14	3	65	1-14	2	41	0-94	2	32	0-84	3	1-845 (30)
97	97	3-3	0-020	4693-679	.....	1-681	-2-42	11	0-37	2	13	0-44	3	10	0-33	3	12	0-41	2	0-415
98	98	4-4	0-048	4715-298	.....	1-681	-2-56	11	0-37	2	.....	.....	.....	8	0-23	3	.....	.....	.....	0-380
99	77	2-3	1-062	4675-114	.....	.....	-1-93	25	0-73	2	14	0-48	2	5	0-03	3	4	1-93	2	1-85
100	233	4-4	2-237	4742-800	1-519	0-582	-2-00	23	0-69	2	14	0-47	2	16	0-53	3	10	0-32	3	(31)
101	101	5-5	2-239	4758-126	.....	0-507	-1-77	25	0-72	2	26	0-74	3	18	0-58	3	14	0-47	2	.....
102	102	6-6	2-246	4759-278	.....	0-417	-1-76	38	0-90	3	39	0-91	3	18	0-58	3	23	0-68	3	.....
103	126	4-3	1-496	4820-416	.....	0-000	-1-75	31	0-81	3	42	0-94	3	18	0-57	3	16	0-52	3	.....
104	250	3-4	2-295	4827-623	.....	0-669	-2-35	11	0-36	2	15	0-49	2	7	0-16	3	15	0-49	2	(34)
105	53	2-2	0-896	4840-886	1-000	0-000	-1-47	65	1-13	3	48	1-00	3	17	0-54	3	19	0-59	3	2-663 (30)
106	231	4-5	2-227	4868-265	1-591	0-564	-1-97	23	0-68	2	23	0-68	3	11	0-35	3	13	0-43	2	(31)
107	107	5-6	2-239	4870-138	.....	0-489	-1-85	34	0-84	3	37	0-88	3	17	0-54	3	15	0-49	3	.....
108	157	5-6	1-879	4885-090	1-519	0-405	-1-57	54	1-04	2	74	1-18	2	.....	.....	.....	30	0-79	2	3-53 (31)
109	109	3-4	1-865	4913-624	.....	0-587	-1-65	39	0-90	2	35	0-85	3	19	0-59	3	23	0-67	3	3-40

TABLE 3. OBSERVATIONS OF LINE INTENSITIES IN THE SPECTRA OF SOLAR-TYPE STARS—Continued

No.	Multiplet R.M.F.	I.Q. No.	Low E.P.	Wave- length	log S	log $\lambda/s$	log $X_f$	Sun		$\gamma$ Cygni		$\alpha$ Persei		$\alpha$ Canis Minoris		Array log $\theta_i$	
								W	log W/ $\lambda$	W	log W/ $\lambda$	W	log W/ $\lambda$	W	log W/ $\lambda$		W
Ti I—Continued																	
110	173	4-4	1.988	4973.06	1.653	1.451	.....	96	1.28	128	1.41	38	0.88	69	1.14	1	(33)
111		4-3	1.988	5000.992		0.786	-1.88	19	0.58	31	0.79	17	0.53	12	0.38	2	
112		6-5	2.032	5025.568		0.539	-1.69	24	0.68	19	0.58	7	0.14	10	0.30	3	
113	5	3-2	0.020	5039.966	1.000	0.528	-1.28	56	1.05	73	1.16	14	0.44	29	0.76	3	2.130 (30)
114		4-3	0.048	5064.660		0.868	-1.04	75	1.17	75	1.17	36	0.85	39	0.89	1	2.255
115	38	5-6	0.845	4981.742	1.653	0.539	-0.25	127	1.41	198	1.60	115	1.36	103	1.32	3	3.716 (31)
116		5-5	0.845	5016.170		1.612	-1.47	43	0.93	31	0.79	20	0.60	18	0.56	2	2.663
117		3-3	0.822	5022.876		1.459	-1.33	32	0.80	73	1.16	16	0.50	23	0.66	2	2.771
118		2-2	0.815	5024.852		1.623	-1.50	46	0.96	61	1.08	24	0.68	28	0.75	3	2.613
119	199	3-2	2.165	5052.882	.....	0.331	-2.26	24	0.68	19	0.58	16	0.50	8	0.20	3	
120	110	4-4	1.454	5071.493	.....	1.681	-2.11	18	0.55	17	0.52	16	0.50	5	1.99	2	
121	109	3-2	1.437	5113.449	.....	0.528	-2.12	14	0.44	19	0.57	6	0.07	9	0.24	3	2.623
122	288	5-6	2.567	5120.425	1.114	0.000	-1.97	27	0.72	.....	.....	37	0.86	21	0.61	2	(31)
123	4	2-3	0.000	5147.484	1.146	1.578	-1.91	20	0.59	37	0.86	9	0.24	6	0.07	2	1.167 (30)
124		2-2	0.000	5173.751		0.674	-1.29	92	1.25	66	1.11	19	0.56	48	0.97	2	2.130
125		4-4	0.048	5210.394		0.396	-0.91	74	1.15	91	1.24	31	0.77	46	0.95	3	2.380
126		3-2	0.020	5219.708		1.578	-2.12	21	0.60	12	0.36	7	0.13	7	0.13	3	0.886
127	3	3-3	0.020	5426.260	.....	.....	-2.84	9	0.22	7	0.11	7	0.11	4	1.87	2	0.407
128	259	2-2	2.335	5429.152	0.954	0.380	-2.50	.....	.....	19	0.54	11	0.31	.....	.....	.....	(31)
129	107	4-3	1.454	5490.161	.....	.....	-2.30	30	0.74	34	0.79	17	0.49	25	0.66	2	2.477
130	287	5-4	2.567	5503.906	.....	0.000	-2.41	24	0.64	26	0.67	16	0.46	9	0.21	2	
131	240	4-4	2.258	5644.149	0.954	0.000	-2.10	31	0.74	36	0.80	25	0.65	8	0.15	2	3.519 (31)
132	249	3-4	2.295	5675.437	1.398	0.669	-1.78	73	1.11	47	0.92	48	0.93	42	0.87	2	(33)
133	228	5-5	2.239	5739.486	.....	0.507	-2.86	10	0.24	10	0.24	11	0.28	.....	.....	.....	
134		4-4	2.227	5739.988	.....	0.582	-2.99	13	0.36	15	0.42	11	0.28	.....	.....	.....	
135	309	3-4	3.279	5766.337	2.519	0.854	-2.73	9	0.19	14	0.38	13	0.35	10	0.24	2	(35)
136		4-5	3.291	5774.039	.....	0.753	-2.63	12	0.32	16	0.44	14	0.38	14	0.38	2	
137	72	2-3	1.062	5866.464	1.301	0.331	-1.88	49	0.92	31	0.72	33	0.75	33	0.75	3	2.423 (30)



TABLE 3. OBSERVATIONS OF LINE INTENSITIES IN THE SPECTRA OF SOLAR-TYPE STARS—Continued.

No.	Multiplet R.M.T.	I.Q. No.	Low E.P.	Wave- length	log S	log $\Sigma s/s$	log $X_f$	Sun		$\gamma$ Cygni		$\alpha$ Persei		$\alpha$ Canis Minoris		Array log $\theta_i f$				
								W	log W/ $\lambda$	W	log W/ $\lambda$	W	log W/ $\lambda$	W	log W/ $\lambda$		W	log W/ $\lambda$	Wt.	Wt.
167	31	9/2-7/2	1.126	4468.502		0.255	+0.20	141	1.50	4	541	2.08	4	379	1.93	4	186	1.62	4	(36)
168		7/2-5/2	1.111	4501.280		0.368	+0.07	128	1.45	4	539	2.08	4	372	1.92	4	199	1.65	4	
169	18	3/2-5/2	1.075	4493.532		.....	-1.96	22	0.69	2	208	1.66	3	73	1.21	2	24	0.73	2	
170	60	1/2-3/2	1.219	4568.330		.....	-2.08	16	0.54	3	182	1.60	2	110	1.38	2	16	0.54	2	
171	82	9/2-9/2	1.565	4529.491	2.297	1.995	-1.44:	87	1.28	1	359	1.90	3	241	1.73	3	132	1.46	2	(36)
172		9/2-7/2	1.565	4571.982		0.352	+0.14	170	1.57	4	620	2.13	4	449	1.99	4	205	1.65	4	
173	50	1/2-3/2	1.216	4563.768	1.459	0.474	+0.04	117	1.41	2	544	2.08	3	421	1.96	4	190	1.62	4	(36)
174		3/2-3/2	1.232	4589.955		1.176	-0.93	70	1.18	3	443	1.98	4	306	1.82	3	105	1.36	3	
175	38	3/2-5/2	1.160	4636.328		.....	-2.26	11	0.38	3	169	1.56	3	65	1.15	3	16	0.54	3	
176	49	3/2-5/2	1.232	4708.674		.....	-1.69	35	0.87	2	318	1.83	3	207	1.64	3	52	1.04	3	
177	92	1/2-1/2	2.039	4779.986	0.301	0.477	-1.70	49	1.01	3	413	1.94	3	229	1.68	3	68	1.15	3	(37)
178		3/2-1/2	2.052	4805.102		0.176	-0.60	98	1.31	2	427	1.95	3	302	1.80	3	124	1.41	3	
179	(114)	3/2-1/2	3.081	4874.016		0.474	-1.91	24	0.69	2	307	1.80	3	100	1.31	3	41	0.92	2	
180		5/2-3/2	3.110	4911.201		0.222	-1.63	37	0.88	2	333	1.83	3	205	1.62	3	61	1.09	2	
181	113	3/2-3/2	3.081	5010.221		0.444	-2.19	16	0.50	1	180	1.56	3	61	1.08	2	26	0.72	2	
182	86	7/2-7/2	1.885	5185.910		0.364	-1.47	60	1.06	2	411	1.90	3	256	1.69	3	117	1.35	3	(36)
183	70	3/2-5/2	1.559	5154.077		1.398	-1.39	68	1.12	2	459	1.95	3	292	1.75	3	95	1.27	3	
184	69	5/2-7/2	1.575	5336.796		0.243	-1.54	54	1.00	3	398	1.87	3	217	1.61	3	95	1.25	3	(36)
185		3/2-5/2	1.559	5381.030		0.398	-1.81	54	1.00	3	351	1.81	3	186	1.54	3	71	1.12	3	
186		5/2-5/2	1.575	5418.777		1.544	-1.86	26	0.68	3	353	1.81	3	155	1.46	3	61	1.05	3	
187	91	3/2-5/2	2.082	6491.590		0.222	-2.04	27	0.62	2	276	1.63	3	216	1.52	3	74	1.06	3	
188		1/2-3/2	2.039	6559.588		0.474	-2.38:	20	0.48	2	186	1.45	2	142	1.34	2	45	0.84	2	
189		3/2-3/2	2.052	6606.988		1.176	-2.85	10	0.18	2	82	1.09	2	44	0.82	2	29	0.64	3	

Ti II—Continued

V I

100	27	5/2-7/2	0.274	4099-790	1.477	1.067	-0.85	33	0.91	2	17	0.62	2	21	0.71	2	16	0.59	2	(38)
191		3/2-3/2	0.266	4116-708		2.829	-1.92	14	0.53	1	17	0.62	1	13	0.50	2	5	0.08	2	(38)
192		5/2-3/2	0.274	4128-101		1.097	-0.58	94	1.36	2	253	1.79	2	158	1.58	2	83	1.30	3	(38)
193	22	9/2-11/2	0.299	4379-240	1.623	0.544	-0.07	112	1.41	4	69	1.20	2	24	0.74	3	43	0.99	2	(38)
194		5/2-7/2	0.274	4389-990		0.912	-0.36	116	1.42	2	38	0.94	1	16	0.56	1	20	0.66	2	(38)
195		9/2-9/2	0.299	4406-654		1.356	-0.76	76	1.24	3	30	0.83	3	11	0.40	2	14	0.50	2	(38)
196	87	13/2-15/2	1.860	4452-009	1.716	0.512	-2.07	19	0.63	2	46	1.01	1	15	0.53	1	11	0.39	1	(38)
197		9/2-11/2	1.846	4469-713		0.664	-2.16	20	0.65	1				24	0.73	1				(38)
198	35	3/2-5/2	1.046	5703-590	1.447	0.796	-2.08	17	0.47	3	22	0.59	2	20	0.54	2	16	0.45	3	(38)
199		5/2-5/2	1.059	5737-077		1.282	-2.54	5	1.94	2	13	0.36	2	8	0.14	2				(38)
200	34	5/2-5/2	1.059	6039-745	1.079	1.046	-2.60	13	0.33	2	17	0.45	3	13	0.33	2	9	0.17	3	(38)
201		3/2-3/2	1.046	6081-458		0.972	-2.50	10	0.22	2	16	0.42	2	16	0.42	2	14	0.36	2	(38)
202		7/2-5/2	1.076	6090-222		0.398	-2.02	31	0.71	2	25	0.61	2	24	0.60	2	19	0.49	2	(38)
203		1/2-1/2	1.039	6111-668		1.079	-2.58	13	0.33	2	17	0.44	3	11	0.26	2	7	0.06	2	(38)
204	20	9/2-11/2	0.299	6150-158		0.544	-2.61	12	0.29	2	23	0.57	2	12	0.29	2	12	0.29	2	(38)
205	19	7/2-9/2	0.285	6199-195		1.210	-2.73	14	0.35	2	18	0.46	2	19	0.49	3	13	0.32	2	(38)
206		5/2-7/2	0.274	6216-366		1.067	-2.04	21	0.53	2	21	0.53	3	11	0.25	2	12	0.28	2	(38)
207		9/2-9/2	0.299	6243-120		0.566	-2.14	18	0.46	2	20	0.51	2	14	0.35	2	10	0.20	2	(38)

V II

208	37	5-4	2.041	4183-461		0.390	-1.53	86	1.31	3	232	1.74	3	132	1.50	2	48	1.06	3	(39)
209	(24)	2-3	1.678	4234-229			-2.41	6	0.15	2	99	1.37	3	25	0.77	2	9	0.33	2	(39)

Cr I

210	35	6-6	2.532	4126-523		0.569	-1.61	27	0.82	3	28	0.83	1	14	0.53	2	15	0.56	2	(40)
211		5-6	2.534	4127-276		1.715	-2.14	14	0.53	1							14	0.53	2	(40)
212		6-5	2.532	4153-065		1.715	-2.59	7	0.23	1	16	0.59	1				7	0.23	2	(40)
213	1	3-4	0.000	4254-348	1.322	0.368	+1.22	303	1.85	4	426	2.00	4	326	1.88	4	214	1.70	4	(40)
214		3-3	0.000	4274-808		0.477	+1.03	309	1.86	3	391	1.96	4	288	1.83	4	199	1.67	4	(40)
215		3-2	0.000	4289-731		0.623	+0.92	270	1.80	2							155	1.56	3	(40)
216	96	2-1	2.877	4319-640		1.067	-2.26	10	0.36	1	6	0.14	2	7	0.21	2	6	0.14	2	(40)
217	197	2-1	3.361	4492-313		0.255	-2.09	16	0.55	2	17	0.58	2	16	0.55	2	12	0.43	2	(40)
218	10	2-2	0.937	4545-964		0.477	-0.76	63	1.14	3	72	1.20	3	48	1.02	2	44	0.99	2	(40)

TABLE 3. OBSERVATIONS OF LINE INTENSITIES IN THE SPECTRA OF SOLAR-TYPE STARS—Continued

No.	Multiplet R.M.T.	I.Q. No.	Low E.P.	Wave- length	log S	log $\lambda_s/s$	log $X_f$	Sun		$\gamma$ Cygni		$\alpha$ Persei		$\alpha$ Canis Minoris		Array log $\sigma_f$				
								W	log W/ $\lambda$	W	log W/ $\lambda$	W	log W/ $\lambda$	W	log W/ $\lambda$		W	log W/ $\lambda$	W	log W/ $\lambda$
Cr I—Continued																				
219	33	4-3	2.534	4541.071	.....	1.560	-2.04	23	0.70	2	35	0.89	4	18	0.60	4	16	0.55	2	(41)
220	21	2-2	0.979	4616.134	.....	0.933	-0.83	94	1.31	3	94	1.31	2	53	1.06	2	59	1.11	3	
221		1-1	0.964	4626.184	.....	1.046	-1.02	94	1.31	3	136	1.47	3	76	1.22	3	74	1.20	3	
222		4-3	1.026	4646.171	.....	0.444	-0.51	133	1.46	3	235	1.70	2	53	1.06	3	97	1.32	3	
223		2-1	0.979	4651.292	.....	1.156	-1.52	93	1.30	3	107	1.36	3	50	1.03	3	56	1.08	3	
224		3-2	0.999	4652.169	.....	0.729	-0.51	129	1.44	3	172	1.57	3	70	1.18	3	79	1.23	3	
225	186	4-5	3.131	4628.464	1.690	2.339	-2.74	8	0.24	2	.....	.....	.....	18	0.59	1	.....	.....	.....	(44)
226		3-2	3.112	4689.363	.....	1.213	-1.89	43	0.96	2	33	0.85	2	11	0.37	2	14	0.48	2	
227		5-4	3.154	4708.021	.....	0.745	-1.58	41	0.94	3	40	0.93	3	22	0.67	2	19	0.61	2	
228		6-5	3.181	4718.425	.....	0.576	-1.40	48	1.01	3	68	1.16	3	18	0.58	3	31	0.82	3	
229	62	3-2	2.696	4697.060	.....	0.331	-1.89	32	0.83	2	22	0.67	3	12	0.41	3	10	0.33	3	
230	7	2-2	0.937	5206.046	1.176	0.477	+0.58	262	1.70	3	.....	.....	.....	.....	.....	.....	221	1.63	3	(40)
231	18	0-1	0.957	5247.576	.....	1.398	-1.20	64	1.09	2	53	1.00	2	38	0.86	3	35	0.82	2	
232		2-1	0.979	5296.704	.....	1.156	-0.74	100	1.28	3	89	1.22	3	36	0.83	3	47	0.95	3	
233		2-3	0.979	5300.755	.....	1.875	-1.54	62	1.07	3	43	0.91	3	20	0.58	2	24	0.66	3	
234		3-3	0.999	5348.327	.....	1.030	-0.76	77	1.16	3	139	1.42	3	27	0.70	2	71	1.12	3	
235		4-3	1.026	5409.739	.....	0.444	-0.04	150	1.44	2	234	1.64	3	86	1.20	2	100	1.27	3	
236	225	4-4	3.449	5304.183	1.322	1.016	-2.39	22	0.62	3	6	0.05	2	12	0.35	2	8	0.18	3	(44)
237		3-3	3.434	5312.857	.....	0.903	-2.27	20	0.58	2	17	0.50	2	16	0.48	3	13	0.39	2	
238	94	3-4	2.887	5397.387	2.322	0.794	-1.10	58	1.04	2	65	1.09	2	34	0.81	2	39	0.87	2	(42)
239	119	4-4	2.998	5712.782	.....	0.523	-2.40	9	0.20	2	22	0.58	2	14	0.39	2	9	0.20	2	(43)
240		2-3	3.000	5787.024	.....	1.097	-2.85	5	1.94	1	9	0.19	2	.....	.....	.....	.....	.....	.....	
241	(282)	4-4	4.175	6661.090	1.398	0.523	-2.64	9	0.13	2	16	0.38	2	7	0.02	2	6	1.95	2	(44)
Cr II																				
242	31	7/2-5/2	3.848	4261.935	.....	0.611	-1.43	68	1.20	1	312	1.86	4	211	1.69	4	79	1.27	3	
243	16	3/2-3/2	3.092	4572.871	.....	.....	-2.48	16	0.54	2	22	0.68	3	19	0.62	3	9	0.29	3	
244	44	7/2-7/2	4.054	4554.994	.....	1.389	-1.73	41	0.96	2	195	1.63	2	143	1.50	2	50	1.04	2	(45)
245		9/2-7/2	4.056	4558.652	.....	0.447	-0.98	74	1.21	3	456	2.00	4	322	1.85	2	117	1.41	3	
246		7/2-5/2	4.054	4568.206	.....	0.611	-1.28	54	1.07	3	379	1.92	4	283	1.79	4	103	1.35	3	

Cr II—Continued

247	44	3/2-3/2	4-055	4616-630		1-398	-1-71	21	0-66	2	268	1-76	3	154	1-52	3	52	1-05	3	(45)
248		3/2-1/2	4-055	4634-081		1-000	-1-57	47	1-01	2	323	1-84	3	219	1-67	3	92	1-30	3	(45)
249	30	7/2-9/2	3-848	4812-357		1-826	-1-84	18	0-57	2	175	1-56	3	96	1-30	3	28	0-76	3	(45)
250		5/2-3/2	3-842	4884-600		1-544	-2-20	18	0-57	2	186	1-58	2	81	1-22	2	38	0-89	2	(45)
251	(24)	5/2-5/2	3-810	5305-868		0-456	-2-11	14	0-42	4	175	1-52	3	112	1-32	3	44	0-92	3	(45)
252	43	9/2-9/2	4-056	5237-327		0-485	-1-62	19	0-56	3	308	1-77	3	223	1-63	3	89	1-23	3	(45)
253		7/2-5/2	4-054	5308-426		1-417	-2-09	21	0-60	3	184	1-54	3	91	1-23	3	37	0-84	3	(45)
254		3/2-5/2	4-055	5310-693		1-544	-2-47	21	0-60	3	114	1-33	3	63	1-07	3	17	0-50	3	(45)
255		5/2-5/2	4-057	5313-587		0-831	-2-00	30	0-75	3	233	1-64	3	146	1-44	3	42	0-90	3	(45)
256		3/2-3/2	4-055	5334-872		0-942	-2-01	21	0-60	3	216	1-61	3	93	1-24	3	52	0-99	3	(45)
257	(23)	1/2-3/2	3-698	5246-783		0-857	-2-34	9	0-23	1	106	1-30	2	57	1-04	3	46	0-94	2	(45)
258	50	5/2-3/2	4-126	5503-239		0-845	-2-79				143	1-41	2	63	1-06	2				(45)
259		7/2-5/2	4-138	5508-635		0-718	-2-36	18	0-51	2	135	1-39	2	65	1-07	2				(45)

Mn I

260	5	7/2-7/2	2-133	4055-553	1-477	0-924	+0-26	146	1-56	4	174	1-63	3	83	1-31	3	106	1-42	3	(47)
261	2	5/2-5/2	0-000	4033-077		0-477	+1-08	276	1-84	3	361	1-95	3	314	1-89	3	215	1-73	4	(46)
262		5/2-3/2	0-000	4034-494		0-653	+0-95	240	1-77	3	329	1-91	3	228	1-75	3	186	1-66	4	(46)
263	29	5/2-5/2	3-060	4059-390		0-477	-1-56	42	1-02	2	18	0-65	3	6	0-17	2	14	0-54	2	(47)
264		7/2-5/2	3-062	4061-735		0-352	-1-24	43	1-02	1	30	0-87	1	17	0-62	1	19	0-67	2	(47)
265	23	3/2-3/2	2-928	4265-927	1-079	0-972	-1-35	32	0-88	3	28	0-82	3	12	0-45	3	31	0-86	3	(47)
266	22	5/2-3/2	2-907	4436-358	1-301	1-155	-1-20	55	1-09	2	42	0-98	2	30	0-83	2	10	0-35	1	(47)
267		3/2-1/2	2-928	4453-008		1-301	-1-54							26	0-77	1	17	0-58	1	(47)
268		3/2-3/2	2-928	4470-140		1-097	-1-50	39	0-94	1				24	0-73	1	14	0-50	1	(47)
269		3/2-5/2	2-928	4498-902		1-155	-1-52				57	1-10	2	33	0-87	1	21	0-67	1	(47)
270		5/2-7/2	2-907	4502-226		1-243	-1-45	39	0-94	2	27	0-78	2	22	0-69	2	18	0-60	2	(47)
271	21	7/2-7/2	2-876	4709-720	1-447	1-389	-1-31	40	0-93	2	62	1-12	3	15	0-50	3	24	0-71	2	(47)
272		3/2-3/2	2-928	4739-115		1-398	-1-56	75	1-20	3	34	0-86	3	22	0-67	3	21	0-65	3	(47)
273		1/2-3/2	2-940	4761-530		1-000	-1-16	73	1-18	3	74	1-19	3	28	0-77	3	44	0-96	3	(47)
274		7/2-9/2	2-876	4762-377		0-447	-0-30	157	1-52	3	290	1-77	1	207	1-64	2	126	1-42	3	(47)
275		3/2-5/2	2-928	4765-866		0-796	-1-08	74	1-19	2	72	1-18	2	43	0-96	3	43	0-96	2	(47)
276		5/2-7/2	2-907	4766-425		0-611	-0-64	120	1-40	2	116	1-39	3	57	1-08	3	71	1-17	2	(47)
277	16	5/2-7/2	2-272	4754-041	1-380	0-602	+0-05	161	1-53	3	211	1-65	3	115	1-38	3	112	1-37	3	(48)
278		7/2-7/2	2-288	4783-426		0-477	+0-33	208	1-64	3	240	1-70	3	115	1-38	3	121	1-40	3	(48)

TABLE 3. OBSERVATIONS OF LINE INTENSITIES IN THE SPECTRA OF SOLAR-TYPE STARS—Continued

No.	Multiplet R.M.T.	I.Q. No.	Low E.P.	Wave- length	log S	log $\Sigma s/s$	log X <sub>f</sub>	Sun		$\gamma$ Cygni		$\alpha$ Persei		$\alpha$ Canis Minoris		Array log $g_f$		
								W	log W/ $\lambda$	W	log W/ $\lambda$	W	log W/ $\lambda$	W	log W/ $\lambda$		W	log W/ $\lambda$
Mn I—Continued																		
279	4	5/2-5/2	2-154	5470-640	.....	0-914	-1-78	48	0-94	2	51	0-97	23	0-62	2	11	0-30	2
280		3/2-3/2	2-169	5516-785		1-030	-1-86	38	0-84	2	33	0-78	24	0-64	2	16	0-46	2
281	42	5/2-3/2	3-827	5377-616	1-079	0-301	-1-89	41	0-88	3	60	1-05	21	0-59	2	31	0-76	3
282		3/2-5/2	3-059	6013-503	1-255	0-653	-1-36	101	1-22	3	93	1-19	78	1-11	3	95	1-20	3
283	27	5/2-5/2	3-060	6016-653		0-477	-1-07	110	1-26	3	89	1-17	77	1-11	3	80	1-12	3
284		7/2-5/2	3-062	6021-808		0-352	-1-02	114	1-28	3	89	1-17	68	1-05	3	83	1-14	3
Fe I																		
285	43	4-4	1-478	4045-827	1-322	0-396	+2-18	1174	2-46	3	1008	2-40	698	2-24	4	532	2-12	3
286		3-2	1-551	4063-607		0-553	+1-92	924	2-36	3	745	2-26	530	2-12	4	362	1-95	4
287		2-2	1-601	4071-751	0-477	0-674	+1-82	721	2-25	3	579	2-15	421	2-01	4	315	1-89	4
288		2-3	1-601	4132-069	0-954	1-578	+1-34	375	1-96	3	426	2-01	352	1-93	3	249	1-78	4
289		3-4	1-551	4143-880		1-572	+1-45	415	2-00	3	422	2-01	346	1-92	3	245	1-77	4
290	218	3-3	2-577	4049-338	.....	1-681	-1-16	39	0-98	2	81	1-30	26	0-81	1	35	0-94	3
291	(359)	2-1	2-819	4044-619	0-477	0-255	+0-20:	131	1-51	3	182	1-65	92	1-36	2	121	1-48	4
292		1-1	2-833	4062-451		0-477	-0-01	108	1-42	3	185	1-66	123	1-48	1	112	1-44	3
293		0-1	2-846	4079-848		0-954	-0-38	74	1-26	4	95	1-37	34	0-92	1	64	1-20	2
294	(559)	3-3	3-227	4085-319	.....	.....	+0-22	141	1-54	2	182	1-65	69	1-23	1	84	1-31	3
295	(698)	1-0	3-415	4065-390	.....	1-398	-0-85	54	1-12	2	80	1-29	28	0-84	1	43	1-02	3
296		1-1	3-415	4072-514		1-398	-0-78:	65	1-20	2	117	1-46	61	1-18	1	59	1-16	3
297		2-2	3-402	4082-117		1-243	-0-75	43	1-02	2	35	0-93	34	0-92	1	31	0-88	1
298		5-4	3-318	4084-503		0-503	+0-25	148	1-56	3	196	1-68	87	1-33	2	111	1-43	3
299		4-4	3-354	4133-861		1-368	-0-46	114	1-44	3	218	1-72	104	1-40	1	83	1-30	2
300	(559)	4-5	3-197	4067-990	.....	.....	+0-37	170	1-62	4	215	1-72	143	1-55	3	132	1-51	4
301	(558)	3-3	3-227	4070-779	.....	.....	-0-09	98	1-38	3	155	1-58	83	1-31	2	105	1-41	4
302	(694)	5-4	3-318	4087-103	.....	.....	-0-67	72	1-25	3	100	1-39	44	1-03	1	54	1-12	3
303		4-4	3-354	4136-530	.....	.....	-0-87	59	1-15	4	40	0-98	30	0-86	2	42	1-01	3
304	357	2-1	2-819	4091-562	1-176	2-255	-1-27	54	1-12	3	52	1-10	10	0-39	1	16	0-59	2
305		2-2	2-819	4114-453		1-079	-0-26	91	1-34	3	122	1-47	67	1-21	1	80	1-29	2
306		1-2	2-833	4132-910		0-602	0-00	110	1-42	2	179	1-64	99	1-38	2	89	1-33	2

Fe I—Continued

307	18	5-4	0-855	4100-749	.....	.....	+0-01:	99	1-38	2	173	1-62	2	94	1-36	1	62	1-18	2	(49)
308	(354)	2-2	0-986	4139-939	.....	.....	-0-68	69	1-22	4	71	1-23	2	24	0-76	1	41	1-00	2	
309	(354)	2-1	2-819	4107-496	.....	.....	+0-12	137	1-52	3	301	1-86	4	141	1-54	2	131	1-50	3	
310	(354)	1-0	2-833	4126-857	0-954	.....	-1-84	15	0-56	1	23	0-75	1	8	0-29	2	10	0-38	2	
311	355	2-1	2-819	4154-507	0-857	.....	+0-22	129	1-49	2	.....	.....	.....	.....	.....	.....	97	1-37	3	
312		0-1	2-846	4191-685	0-954	.....	-0-34	71	1-23	1	140	1-52	1	37	0-95	1	68	1-21	1	
313	3	3-3	0-051	4206-704	.....	.....	-0-08	154	1-56	3	193	1-06	2	64	1-18	1	76	1-26	3	I-778
314		4-4	0-000	4216-193	.....	.....	+0-28	133	1-50	2	.....	.....	.....	119	1-45	2	116	1-44	3	0-330
315		3-4	0-051	4291-475	.....	.....	-0-43	72	1-22	1	123	1-46	1	55	1-11	2	49	1-06	3	I-653
316	(422)	3-3	3-005	4141-873	.....	.....	-1-13	51	1-09	2	122	1-47	3	41	1-00	2	37	0-95	2	
317	42	4-3	1-478	4147-677	1-431	.....	+0-11	138	1-52	2	234	1-75	3	139	1-52	2	107	1-41	3	(49)
318		4-4	1-478	4202-042	.....	.....	+1-32	377	1-95	3	464	2-04	3	432	2-01	3	245	1-76	3	2-949
319		3-3	1-551	4250-799	1-681	.....	+1-28	295	1-84	4	364	1-93	4	269	1-80	4	211	1-70	4	2-944
320		4-5	1-478	4271-776	0-390	.....	+1-78	604	2-15	4	488	2-06	4	398	1-97	4	316	1-87	4	3-389
321		2-3	1-601	4325-777	0-623	.....	+1-69	564	2-12	3	471	2-04	3	392	1-96	4	319	1-87	4	3-580
322	(354)	2-2	2-819	4156-808	.....	.....	+0-24	186	1-65	3	263	1-80	2	183	1-64	2	167	1-60	3	
323		1-2	2-833	4175-645	.....	.....	+0-08	119	1-46	4	255	1-78	4	177	1-63	4	121	1-46	4	
324	(695)	2-3	3-402	4157-790	.....	.....	+0-21	140	1-53	4	216	1-72	4	146	1-54	4	132	1-50	4	
325	(689)	3-3	3-382	4208-612	.....	.....	-0-36:	79	1-27	3	141	1-52	1	54	1-11	1	71	1-23	3	
326	19	4-3	0-911	4174-919	.....	.....	+0-69	148	1-55	3	191	1-66	4	102	1-39	3	113	1-43	3	
327	(476a)	2-2	3-004	4182-389	.....	.....	-0-54	93	1-35	4	141	1-53	3	63	1-18	2	75	1-25	4	
328	152	3-2	2-439	4187-049	1-067	.....	+0-98	238	1-76	4	295	1-85	2	235	1-75	2	174	1-62	4	
329		2-1	2-458	4191-439	1-243	.....	+0-84	243	1-76	2	332	1-90	2	276	1-82	3	168	1-60	3	
330		3-3	2-439	4222-223	1-602	.....	+0-69	174	1-62	4	315	1-87	2	215	1-71	3	123	1-46	4	
331		1-2	2-471	4233-613	1-243	.....	+0-94	212	1-70	3	278	1-82	1	234	1-74	1	139	1-52	3	
332		4-4	2-415	4235-951	0-979	.....	+1-18	339	1-90	4	418	1-99	4	342	1-91	3	280	1-82	4	
333		2-3	2-458	4250-132	1-067	.....	+1-18	279	1-82	4	354	1-92	4	244	1-76	4	189	1-65	4	
334		5-5	2-389	4260-488	0-600	.....	+1-60	535	2-10	3	518	2-08	2	405	1-98	3	278	1-82	4	
335		3-4	2-439	4271-166	1-050	.....	+1-19:	330	1-89	3	353	1-92	3	218	1-71	3	205	1-68	4	
336	(693)	4-5	3-354	4247-434	.....	.....	+0-43	187	1-64	4	252	1-77	3	153	1-56	3	143	1-53	4	
337	(693)	5-6	3-318	4227-442	.....	.....	+1-06:	165	1-59	1	202	1-84	1	272	1-81	3	189	1-65	4	
338	41	3-3	1-551	4337-057	.....	.....	+0-28:	185	1-63	2	310	1-85	2	215	1-70	1	117	1-43	1	2-114
339		4-5	1-478	4383-559	.....	.....	+2-01	960	2-34	3	567	2-11	4	393	1-95	4	385	1-94	4	3-763
340		3-4	1-551	4404-763	.....	.....	+1-81	745	2-23	4	563	2-11	4	414	1-97	4	322	1-86	4	3-477
341		2-3	1-601	4415-137	.....	.....	+1-30	353	1-90	3	434	1-99	2	325	1-87	2	207	1-67	3	3-000

TABLE 3. OBSERVATIONS OF LINE INTENSITIES IN THE SPECTRA OF SOLAR-TYPE STARS—Continued

No.	Multiplet R.M.T.	I.Q. No.	Low E.P.	Wave- length	log S	log $\epsilon$ /s	log X <sub>γ</sub>	Sun		γ Cygni		α Persei		α Canis Minoris		Array log g/f				
								W	log W/λ	W	log W/λ	W	log W/λ	W	log W/λ		W	log W/λ		
342	351	2-1	2.819	4241-122	.....	.....	-1.60	37	0.94	3	33	0.89	3	14	0.52	3	19	0.65	4	
343	(976)	4-3	3.865	4276-683	.....	0.368	-1.39	43	1.00	3	51	1.08	3	27	0.80	3	27	0.80	3	
344	71	3-2	2.167	4282-413	0.699	0.331	+0.48	169	1.60	4	346	1.91	3	254	1.77	3	151	1.55	4	(49)
345		1-2	2.213	4352-745	.....	0.699	+0.05	181	1.62	4	233	1.73	3	155	1.55	3	128	1.47	4	
346	2	4-4	0.000	4347-244	.....	.....	-1.73	29	0.82	2	27	0.79	1	.....	.....	.....	6	0.14	1	1.36
347		4-5	0.000	4375-946	.....	.....	+0.31	176	1.60	3	303	1.84	4	199	1.66	4	128	1.47	4	0.643
348		3-2	0.051	4389-256	.....	.....	-1.14	60	1.14	2	51	1.07	2	31	0.85	2	18	0.61	2	1.38
349		3-4	0.051	4427-319	.....	.....	+0.52	211	1.68	3	342	1.89	3	236	1.73	3	140	1.50	2	0.653
350		0-1	0.121	4489-750	.....	.....	-0.51	78	1.24	2	147	1.52	2	69	1.19	2	55	1.09	2	1.799
351	415	4-3	2.977	4365-906	.....	.....	-1.60	28	0.81	3	20	0.66	2	19	0.64	2	16	0.56	2	
352	68	1-0	2.213	4430-624	.....	1.398	-0.06	143	1.51	2	159	1.56	2	97	1.34	1	85	1.28	1	
353		2-2	2.188	4442-351	.....	0.983	+0.63	182	1.61	4	292	1.82	2	150	1.53	1	120	1.43	4	
354		1-1	2.213	4447-730	.....	1.046	+0.47	163	1.56	4	272	1.79	4	149	1.52	3	139	1.50	4	
355		2-3	2.188	4494-575	.....	0.729	+0.58	188	1.62	4	356	1.90	3	248	1.74	3	115	1.41	2	
356		3-4	2.167	4528-629	.....	0.444	+0.99	256	1.75	1	429	1.98	2	325	1.86	3	191	1.62	3	
357	116	2-2	2.269	4439-891	.....	.....	-1.62	30	0.83	2	28	0.80	2	18	0.61	2	18	0.61	2	
358	39	2-1	1.601	4602-011	.....	.....	-1.13	52	1.05	3	82	1.25	3	34	0.87	3	32	0.84	3	
359		4-5	1.478	4602-951	.....	.....	-0.18	131	1.45	3	269	1.77	3	193	1.62	3	103	1.35	3	
360	555	2-3	3.252	4504-840	.....	.....	-1.74	35	0.89	3	28	0.79	2	32	0.85	2	21	0.67	3	
361	(472)	2-1	3.058	4517-537	.....	.....	-1.10	54	1.08	3	51	1.05	2	21	0.67	2	37	0.91	2	
362	554	2-2	3.252	4607-655	.....	1.243	-0.80:	92	1.30	3	119	1.41	3	42	0.96	3	49	1.03	3	
363		3-3	3.227	4625-054	.....	1.222	-0.71	115	1.40	3	182	1.60	3	90	1.29	3	86	1.27	3	
364		1-2	3.269	4637-512	.....	1.097	-0.70	90	1.29	3	159	1.54	3	44	0.98	3	62	1.13	3	
365		4-5	3.197	4736-783	.....	0.503	+0.22	194	1.61	3	264	1.75	3	163	1.54	3	124	1.42	3	
366	409	5-5	2.936	4647-445	.....	0.408	-0.65	107	1.36	3	194	1.62	3	99	1.33	3	103	1.35	3	
367		4-3	2.977	4661-981	.....	1.791	-1.73	35	0.88	2	34	0.86	2	16	0.54	3	25	0.73	3	
368		4-4	2.977	4691-429	.....	0.522	-0.58	113	1.38	3	150	1.50	3	72	1.19	3	84	1.25	3	
369		3-3	3.005	4710-292	.....	0.615	-0.74	91	1.29	3	122	1.41	3	37	0.90	3	58	1.09	3	
370	687	1-1	3.415	4863-652	.....	1.243	-1.40:	56	1.06	2	83	1.23	3	36	0.87	2	20	0.61	2	
371		5-4	3.318	4875-883	.....	1.502	-1.56	44	0.96	2	86	1.25	2	26	0.73	2	42	0.94	2	

Fe I—Continued

Fe I—Continued

372	2-2	3-402	4882-150	1-146	-1.33	70	1-16	2	100	1-31	2	41	0-92	3	42	0-93	2	(50)
373	1-2	3-415	4907-737	1-544	-1.52	64	1-12	3	55	1-05	3	33	0-83	3	84	0-71	2	(50)
374	4-4	3-354	4946-397	0-742	-0.37	109	1-34	3	155	1-50	3	74	1-18	3	85	1-23	3	(50)
375	2-3	3-402	4950-113	1-368	-0.14	77	1-19	3	80	1-21	3	53	1-03	3	74	1-17	3	(50)
376	5-5	3-318	4966-097	0-548	-0.28	160	1-51	3	251	1-70	3	133	1-43	3	115	1-36	3	(50)
377	3-4	3-382	5002-799	1-350	-1.16	66	1-12	2	113	1-35	3	29	0-76	3	31	0-79	3	(50)
378	2-2	2-269	4924-779	1-079	-0.54	78	1-20	3	161	1-52	3	64	1-11	3	69	1-15	3	(50)
379	2-3	2-269	5049-829	0-331	+0.04	182	1-56	3	306	1-78	3	185	1-56	3	141	1-45	3	(50)
380	1-1	2-414	5141-748	1-079	-0.80	69	1-13	3	94	1-26	3	18	0-54	3	44	0-93	3	(50)
381	2-1	2-863	4859-749	1-611	+0.27	170	1-54	2	320	1-82	2	167	1-54	3	109	1-35	3	(50)
382	3-2	2-853	4871-327	1-213	+0.77	264	1-73	2	379	1-89	3	254	1-72	3	170	1-54	2	(50)
383	1-1	2-870	4872-146	1-389	+0.52	235	1-68	2	355	1-86	3	216	1-65	3	134	1-44	2	(50)
384	2-2	2-863	4890-765	1-213	+0.78	280	1-76	3	367	1-88	3	252	1-71	3	151	1-49	3	(50)
385	4-3	2-839	4891-504	0-950	+1.07	368	1-88	3	375	1-88	3	270	1-74	3	174	1-55	3	(50)
386	1-2	2-870	4903-325	1-690	+0.06	154	1-50	3	288	1-77	3	130	1-42	3	105	1-33	3	(50)
387	3-3	2-853	4919-000	1-146	+0.93	298	1-78	3	352	1-86	3	264	1-73	3	172	1-54	3	(50)
388	5-4	2-820	4920-516	0-745	+1.31	468	1-98	4	568	2-06	3	348	1-85	3	246	1-70	3	(50)
389	2-3	2-863	4938-822	1-787	+0.26	112	1-36	3	178	1-56	3	94	1-28	3	94	1-28	3	(50)
390	4-5	2-839	5044-220	2-389	-1.54	57	1-05	3	88	1-24	3	38	0-88	3	24	0-68	3	(50)
391	3-2	3-867	4896-444	1-285	-1.98	28	0-76	3	28	0-76	3	17	0-54	3	15	0-49	3	(50)
392	1-1	3-943	4973-106	0-824	-1.60	96	1-28	1	128	1-41	1	38	0-88	1	69	1-14	1	(50)
393	5-4	0-855	4939-695	1-502	-0.52	89	1-26	3	208	1-62	3	109	1-34	3	69	1-14	3	(50)
394	4-3	0-911	4994-139	1-350	-0.50	97	1-29	3	229	1-66	3	93	1-27	3	95	1-28	3	(50)
395	3-3	0-954	5083-347	0-948	-0.52	109	1-33	3	247	1-69	3	119	1-37	3	82	1-21	3	(50)
396	4-5	0-911	5127-370	1-042	-0.64	89	1-24	3	275	1-73	3	77	1-18	3	64	1-10	3	(50)
397	2-3	0-986	5150-854	1-368	-0.49	120	1-37	3	239	1-67	3	119	1-36	3	115	1-35	3	(50)
398	1-2	1-007	5151-919	1-544	-0.50	86	1-22	3	167	1-51	3	59	1-06	3	61	1-07	3	(50)
399	4-3	3-865	5001-872	0-368	+0.02	139	1-44	3	281	1-75	3	226	1-66	3	126	1-40	3	(50)
400	3-2	3-926	5014-951	0-528	-0.35	106	1-32	3	159	1-50	3	113	1-35	3	93	1-27	3	(50)
401	2-1	3-967	5022-243	0-699	-0.50	85	1-23	1	181	1-56	2	70	1-14	2	82	1-21	2	(50)
402	4-4	1-478	5171-612	0-396	+0.23	166	1-51	1	319	1-79	3	206	1-60	3	151	1-46	3	2-000
403	2-2	1-601	5216-285	0-674	-0.34	136	1-42	3	265	1-71	3	136	1-42	3	145	1-44	3	(50)
404	2-3	1-601	5307-371	1-578	-0.83	79	1-17	3	146	1-44	3	83	1-19	3	86	1-21	3	(50)
405	3-4	1-551	5332-910	1-572	-0.86	108	1-31	3	190	1-55	3	68	1-11	3	80	1-18	3	(50)
406	4-4	0-000	5110-409	.....	-0.04	164	1-51	3	295	1-76	3	172	1-53	3	119	1-37	3	(50)
407	4-5	0-000	5166-286	.....	-0.38	119	1-36	2	111	1-33	2	52	1-00	2	61	1-07	2	(50)
408	2-1	3-025	5191-467	1-067	+0.15	170	1-52	3	301	1-76	3	172	1-52	2	151	1-46	3	(50)
409	3-3	2-985	5192-355	0-903	+0.61	263	1-69	3	327	1-80	3	203	1-59	3	154	1-47	2	(50)
410	4-5	2-927	5232-954	0-503	+1.02	338	1-81	4	438	1-92	4	301	1-76	3	240	1-66	4	(50)
411	3-4	2-985	5266-565	0-794	+0.77	228	1-64	3	353	1-83	3	219	1-62	3	171	1-51	3	(50)
412	2-3	3-025	5281-800	1-244	+0.09	151	1-46	3	226	1-63	3	123	1-37	3	139	1-42	3	(50)

TABLE 3. OBSERVATIONS OF LINE INTENSITIES IN THE SPECTRA OF SOLAR-TYPE STARS—Continued

No.	Multiplet R.M.T.	I.Q. No.	Low E.P.	Wave- length	log S	log $\lambda$ s/s	log X <sub>f</sub>	Sun		$\gamma$ Cygni		$\alpha$ Persei		$\alpha$ Canis Minoris		Array log $g_f$	
								W	log W/ $\lambda$	W	log W/ $\lambda$	W	log W/ $\lambda$	W	log W/ $\lambda$		W
413	66	2-2	2-188	5145.104	.....	1-556	-1.79	29	0.75	29	0.75	13	0.40	13	0.40	3	(50)
414		1-2	2-213	5198.718	.....	0-824	-0.68	70	1.13	138	1.42	59	1.06	66	1.10	3	
415		2-3	2-188	5250.656	.....	0-808	-0.58	93	1.25	170	1.51	66	1.10	86	1.22	3	
416	553	2-1	3-252	5215.190	1-398	1-155	-0.17	122	1.37	161	1.49	87	1.22	119	1.36	3	
417		4-3	3-197	5217.398	.....	1-222	-0.40	123	1.37	135	1.41	55	1.02	103	1.30	3	
418		1-0	3-269	5229.862	.....	1-398	-0.25	121	1.36	222	1.63	104	1.30	125	1.38	3	
419		1-1	3-269	5253.470	.....	2-000	-1.18	50	0.98	81	1.19	32	0.78	68	1.11	2	
420		2-2	3-252	5263.316	.....	1-301	-0.24	101	1.28	168	1.50	67	1.10	101	1.28	2	
421		1-2	3-269	5302.309	.....	1-155	+0.14	141	1.42	283	1.73	160	1.48	137	1.41	3	
422		4-4	3-197	5324.193	.....	0-523	+0.94	298	1.75	347	1.81	228	1.63	220	1.62	4	
423		2-3	3-252	5339.939	.....	1-097	+0.01	159	1.47	216	1.61	118	1.34	133	1.40	3	
424		3-4	3-227	5393.173	.....	1-222	-0.04	137	1.40	307	1.76	158	1.47	100	1.27	3	
425	15	5-4	0-855	5269.552	.....	0-503	+1.21	442	1.92	444	1.92	300	1.76	250	1.68	3	
426		3-2	0-954	5371.503	.....	0-863	+0.86	299	1.75	495	1.96	326	1.78	185	1.54	3	
427		4-4	0-911	5397.143	.....	1-368	+0.63	219	1.61	481	1.95	324	1.78	169	1.50	3	
428		2-1	0-986	5405.787	.....	1-097	+0.70	213	1.60	481	1.95	287	1.72	176	1.51	3	
429		3-3	0-954	5429.708	.....	1-222	+0.60	306	1.75	466	1.93	300	1.74	201	1.57	3	
430		1-0	1-007	5434.536	.....	1-398	+0.40	181	1.52	403	1.87	226	1.62	144	1.42	3	
431		2-2	0-986	5446.926	.....	1-243	+0.70	281	1.71	470	1.94	313	1.76	217	1.60	3	
432		1-2	1-007	5497.528	.....	2-243	-0.21	133	1.38	377	1.84	214	1.59	137	1.40	3	
433		2-3	0-986	5506.793	.....	2-243	-0.25	130	1.37	305	1.74	182	1.52	112	1.31	2	
434	1163	5-5	4-368	5445.055	.....	0-408	-0.26	134	1.39	188	1.54	96	1.25	94	1.24	3	
435		4-5	4-416	5562.718	.....	1-788	-1.66	60	1.03	64	1.06	35	0.80	26	0.67	3	
436	(1062)	1-2	4-199	5543.946	.....	1-155	-1.54	65	1.07	73	1.12	48	0.94	39	0.85	2	
437	1107	2-2	4-191	5618.645	0-954	1-079	-1.79	35	0.79	44	0.89	15	0.43	17	0.48	2	
438		1-1	4-242	5655.502	.....	1-079	-1.47	77	1.13	84	1.17	53	0.97	62	1.04	2	
439		0-1	4-266	5717.844	.....	0-954	-1.58	58	1.01	60	1.02	49	0.93	50	0.94	3	
440		1-2	4-242	5753.135	.....	0-602	-1.29	98	1.23	97	1.23	70	1.08	91	1.20	2	
441		2-3	4-191	5763.005	.....	0-331	-0.94	118	1.31	155	1.43	112	1.29	110	1.28	2	
442	(1183)	4-3	4-529	5554.902	.....	0-368	-1.25	91	1.21	134	1.38	80	1.16	54	0.99	3	
443		3-2	4-588	5565.715	.....	0-528	-1.06	87	1.19	133	1.38	73	1.12	36	0.81	2	
444		2-2	4-632	5679.034	.....	1-431	-1.65	61	1.03	53	0.97	33	0.76	35	0.79	3	
445	209	2-1	2-597	5567.402	.....	0-699	-1.64	62	1.05	71	1.10	41	0.87	24	0.63	3	
446		4-3	2-548	5701.559	.....	0-368	-1.16	90	1.20	121	1.33	61	1.03	48	0.92	2	
447		3-3	2-577	5778.466	.....	1-431	-2.33	14	0.38	21	0.56	19	0.52	16	0.44	3	
448		2-3	2-597	5834.040	.....	2-976	-2.47	14	0.38	15	0.41	15	0.41	13	0.35	2	

Fe I—Continued

Fe I—Continued

449	686	2-1	3-402	5569.633	1.544	1.097	+0.11	174	1.49	3	279	1.70	3	165	1.47	3	113	1.31	3	(50)
450		3-2	3-382	5572.853		0.863	+0.51	211	1.58	3	336	1.78	3	228	1.78	3	158	1.45	2	
451		1-0	3-415	5576.101		1.398	-0.37	112	1.30	3	214	1.58	3	115	1.32	3	104	1.27	3	
452		4-3	3-354	5586.773		0.669	+0.64	238	1.63	3	369	1.82	3	247	1.65	3	164	1.47	3	
453		5-4	3-318	5615.661		0.503	+0.91	254	1.66	1	362	1.81	2	233	1.62	2	169	1.48	2	
454		2-2	3-402	5624.559		1.243	-0.23	147	1.42	2	235	1.62	2	126	1.35	2	133	1.37	2	
455		3-4	3-382	5784.670		2.544	-2.23	26	0.65	2	23	0.60	2	12	0.32	2	25	0.64	2	
456	(1087)	4-3	4-202	5638.274		0.669	-1.37	75	1.12	3	98	1.24	2	41	0.86	2	33	0.77	2	
457		3-3	4-238	5731.775		1.222	-1.66	53	0.97	3	62	1.03	2	46	0.90	2	52	0.96	2	
458		1-2	4-283	5759.550		2.243	-2.66:	14	0.39	2	19	0.52	2	17	0.47	3	19	0.52	2	
459		4-4	4-202	5775.091		1.368	-1.70	70	1.08	3	54	0.97	3	38	0.82	3	61	1.02	3	
460		3-4	4-238	5873.222		2.544	-2.40	25	0.63	2	13	0.34	2	19	0.51	2	22	0.57	3	
461	1180	4-4	4-529	5752.043		1.681	-1.72	63	1.04	2	56	0.99	2	44	0.88	2	55	0.98	3	
462		3-3	4-588	5806.736		1.681	-1.76	68	1.07	3	48	0.92	3	53	0.96	3	64	1.04	2	
463		4-5	4-529	5862.371		0.390	-1.18	95	1.21	3	107	1.26	3	83	1.15	3	102	1.24	3	
464		2-3	4-632	5930.194		0.623	-1.24	141	1.38	3	131	1.34	3	93	1.20	3	98	1.22	2	
465	982	3-3	3-867	5809.228		1.431	-1.80	52	0.95	3	42	0.86	3	46	0.90	3	66	1.06	3	
466		2-3	3-912	5934.669		0.528	-1.47	94	1.20	3	97	1.21	3	78	1.12	3	78	1.12	3	
467	170	4-4	2-443	5916.262			-1.75	42	0.85	2	40	0.83	3	42	0.85	2	32	0.73	2	
468	959	3-3	3-926	5976.791		0.553	-1.58	75	1.10	2	66	1.04	2	47	0.90	2	46	0.89	2	
469		4-4	3-865	6003.027		1.578	-1.95	109	1.26	3	86	1.16	3	74	1.09	3	108	1.26	3	
470		2-3	3-967	6096.675		1.572	-1.92	32	0.72	3	28	0.66	2	34	0.75	3	37	0.78	2	
471		3-4	3-926	6188.002			-1.47	48	0.89	2	63	1.01	2	39	0.80	3	40	0.81	3	
472	(1259)	3-3	4-713	6056.018		1.431	-1.44	88	1.16	3	83	1.14	2	99	1.21	3	86	1.15	3	
473		2-2	4-775	6078.504		1.431	-1.44	95	1.19	3	89	1.16	3	112	1.26	3	92	1.18	2	
474	1260	3-2	4-713	5984.830		0.331	-1.31	106	1.25	3	113	1.28	3	63	1.02	3	90	1.18	3	
475		2-1	4-775	5987.075		0.602	-1.54	87	1.16	3	92	1.19	3	44	0.87	3	82	1.14	3	
476		2-2	4-775	6170.522		1.079	-1.72	99	1.21	2	75	1.08	2	52	0.93	2	58	0.97	2	
477	207	3-2	2-577	6005.556		1.578	-2.31:	17	0.45	2	16	0.42	2	17	0.45	2	15	0.40	3	
478		2-2	2-597	6065.499		0.674	-0.43	121	1.30	3	176	1.46	3	159	1.42	3	105	1.24	3	
479		3-3	2-577	6137.709		0.553	-0.32	157	1.41	3	184	1.48	2	166	1.43	3	98	1.20	2	
480		2-3	2-597	6200.327		1.578	-1.67	92	1.17	3	85	1.14	3	48	0.89	3	54	0.94	3	
481		4-4	2-548	6230.742		0.396	-0.53	185	1.47	3	239	1.58	3	183	1.47	3	106	1.23	3	
482		3-4	2-577	6322.701		1.572	-1.52	67	1.02	2	66	1.02	2	48	0.88	3	44	0.84	3	
483	169	4-3	2-443	6136.631		0.587	-0.27	199	1.51	3	232	1.58	2	204	1.52	3	132	1.33	3	
484		6-5	2-394	6252.572		1.405	-0.69	128	1.31	3	172	1.44	3	134	1.33	3	105	1.22	3	
485		5-5	2-422	6344.162		1.876	-1.70	87	1.14	3	72	1.06	2	49	0.89	2	43	0.83	3	
486	62	3-2	2-167	6151.630		1.875	-1.85	52	0.93	3	47	0.88	2	26	0.63	2	42	0.83	2	
487		1-0	2-213	6173.348		1.398	-1.67	82	1.12	3	83	1.13	3	59	0.98	3	46	0.87	3	

TABLE 3. OBSERVATIONS OF LINE INTENSITIES IN THE SPECTRA OF SOLAR-TYPE STARS—Continued

No.	Multiplet R.M.T.	I.Q. No.	Low E.P.	Wave- length	log S	log $\lambda_s/s$	log $X_f$	Sun		$\gamma$ Cygni		$\alpha$ Persei		$\alpha$ Canis Minoris		Array log $g_f$			
								W	log W/ $\lambda$	W	log W/ $\lambda$	W	log W/ $\lambda$	W	log W/ $\lambda$		W	log W/ $\lambda$	W
488	62	1-1	2.213	6213.443	1.046	-1.56	98	1.20	3	107	1.24	3	80	1.11	3	60	0.98	3	
489		2-2	2.188	6219.294	0.933	-1.32	91	1.16	3	134	1.33	2	85	1.14	2	73	1.07	3	
490		3-3	2.167	6265.148	1.030	-1.49	113	1.26	3	104	1.22	3	72	1.06	2	59	0.97	2	
491		1-2	2.213	6297.808	1.156	-1.58	79	1.10	3	80	1.10	3	80	1.10	3	58	0.96	2	
492		2-3	2.188	6335.345	0.729	-1.06	93	1.17	3	154	1.39	3	103	1.21	3	71	1.05	3	
493		3-4	2.167	6430.863	0.444	-0.81	130	1.31	3	204	1.50	3	139	1.34	3	104	1.21	3	
494	816	2-1	3.638	6232.655	1.523	-1.45	60	0.98	3	73	1.07	2	37	0.77	3	41	0.82	2	(50)
495		1-1	3.671	6336.837	1.046	-0.88	136	1.33	3	162	1.41	3	122	1.28	3	88	1.14	3	
496		3-4	3.587	6400.018	0.444	-0.01	252	1.60	2	234	1.56	2	189	1.47	3	147	1.36	3	
497		1-2	3.671	6408.033	1.156	-1.18	101	1.20	3	122	1.28	2	102	1.20	3	87	1.13	3	
498		2-3	3.638	6411.665	0.729	-0.46	167	1.42	3	213	1.52	3	153	1.38	3	169	1.42	3	
499	342	1-1	2.833	6229.240	1.079	-2.07	21	0.53	3	37	0.77	2	15	0.38	2	23	0.57	2	
500		0-1	2.846	6270.237	0.954	-1.81	44	0.85	3	95	1.18	3	49	0.89	3	43	0.84	3	
501		2-2	2.819	6311.511	1.079	-2.21	23	0.56	2	21	0.52	2	20	0.50	2	14	0.35	2	
502		1-2	2.833	6355.043	0.602	-1.59	86	1.13	3	63	1.00	3	44	0.84	3	61	0.98	3	
503		2-3	2.819	6518.384	0.331	-1.73	75	1.06	2	59	0.96	2	45	0.84	2	38	0.77	2	
504	111	2-1	2.269	6254.253	0.857	-0.89	104	1.22	3	122	1.29	2	115	1.26	3	88	1.15	3	
505		2-2	2.269	6421.367	0.380	-1.17	142	1.34	3	199	1.49	3	130	1.31	3	144	1.35	3	
506		1-1	2.414	6750.173	1.079	-1.58	64	0.98	3	98	1.16	3	28	0.62	3	33	0.69	3	
507	206	4-3	2.548	6475.640	3.481	-1.79	56	0.94	2	46	0.85	2	38	0.77	1	45	0.84	2	
508		3-3	2.577	6575.045	1.681	-1.74	54	0.91	1	32	0.69	2	25	0.58	2	31	0.67	2	
509		4-4	2.548	6609.126	1.681	-1.63	77	1.07	3	79	1.08	3	45	0.83	2	44	0.82	3	
510		2-3	2.597	6646.975	0.623	-2.82	8	0.08	2	16	0.38	2	16	0.38	2	8	0.08	2	
511	268	3-2	2.747	6546.260	0.623	-1.70	172	1.42	3	203	1.49	3	115	1.24	3	114	1.24	3	
512		4-3	2.716	6592.934	0.505	-0.67	188	1.46	3	202	1.49	3	161	1.39	3	115	1.24	3	
513		5-4	2.681	6678.007	0.390	-0.66	172	1.41	3	271	1.61	3	150	1.35	3	124	1.27	3	
514		3-3	2.747	6703.585	1.681	-2.04	31	0.66	3	34	0.70	3	21	0.50	3	18	0.43	3	
515	(1195)	2-1	4.587	6639.726	1.523	-2.39	15	0.35	2	17	0.41	2	17	0.41	2	15	0.35	2	
516		2-2	4.587	6713.053	0.933	-2.24	23	0.54	3	25	0.57	3	22	0.52	3	12	0.25	2	
517		1-0	4.618	6733.162	1.398	-2.20	22	0.51	3	25	0.57	2	29	0.63	3	15	0.35	2	
518		1-1	4.618	6752.725	1.046	-2.02	25	0.57	3	29	0.63	2	15	0.35	2	15	0.35	3	

Fe I—Concluded

Fe II

519	28	5/2-7/2	2-572	4178-863	.....	-0.63	65	1.19	4	449	2.03	3	335	1.90	3	146	1.54	4
520		3/2-5/2	2-693	4296-580	.....	-0.79	146	1.53	2	417	1.99	3	309	1.86	2	108	1.40	2
521		1/2-3/2	2-766	4369-408	.....	-1.78	26	0.78	2	.....	.....	.....	.....	.....	.....	47	1.03	3
522	27	5/2-3/2	2-572	4128-744	.....	-1.62	27	0.82	3	242	1.77	2	91	1.34	1	40	0.99	1
523		5/2-7/2	2-572	4233-171	.....	+0.20	97	1.36	1	481	2.06	1	383	1.96	2	193	1.66	3
524		3/2-3/2	2-693	4303-181	.....	-0.45	.....	.....	.....	345	1.90	1	241	1.75	1	117	1.43	3
525		1/2-1/2	2-766	4385-389	.....	-0.55	47	1.03	1	398	1.96	2	273	1.79	3	106	1.38	2
526		1/2-3/2	2-766	4416-829	.....	-0.82	64	1.16	3	412	1.97	4	301	1.83	4	112	1.40	3
527	37	5/2-3/2	2-832	4472-934	.....	-1.61	.....	.....	.....	313	1.84	2	225	1.70	3	.....	.....	.....
528		7/2-5/2	2-816	4489-189	.....	-1.34	81	1.26	2	357	1.90	3	258	1.76	3	89	1.30	3
529		3/2-3/2	2-843	4491-410	.....	-1.04	45	1.00	4	387	1.94	4	272	1.78	4	96	1.33	4
530		5/2-5/2	2-832	4515-345	.....	-0.87	79	1.24	3	461	2.01	4	337	1.87	4	118	1.42	2
531		9/2-7/2	2-795	4520-231	.....	-0.90	69	1.18	2	441	1.99	3	310	1.84	4	125	1.44	3
532		5/2-7/2	2-832	4582-835	.....	-1.62	44	0.98	3	367	1.90	3	229	1.70	2	74	1.21	3
533		7/2-9/2	2-816	4666-756	.....	-1.64	47	1.00	1	373	1.90	3	264	1.75	3	89	1.28	1
534	38	3/2-1/2	2-843	4508-293	.....	-0.81	62	1.14	3	464	2.01	4	350	1.89	4	126	1.45	3
535		5/2-3/2	2-832	4522-640	.....	-0.26	.....	.....	.....	493	2.04	1	407	1.96	3	171	1.58	3
536		3/2-3/2	2-843	4541-525	.....	-1.58	58	1.11	2	372	1.91	4	279	1.79	4	76	1.22	2
537		5/2-5/2	2-832	4576-342	.....	-1.46	45	0.99	3	398	1.92	4	277	1.78	3	93	1.31	3
538		9/2-7/2	2-795	4583-841	.....	-0.22	126	1.44	3	556	2.08	3	396	1.94	3	180	1.59	3
539		7/2-7/2	2-816	4620-522	.....	-1.62	37	0.90	3	337	1.86	3	219	1.68	3	74	1.20	3
540	42	5/2-3/2	2-879	4923-932	.....	+0.28	162	1.52	3	664	2.13	3	439	1.95	3	278	1.75	3
541		5/2-5/2	2-879	5018-452	.....	+0.37	242	1.68	3	640	2.10	3	473	1.97	3	327	1.81	3
542	49	5/2-3/2	3-217	5197-578	.....	-1.12	70	1.13	2	458	1.94	3	311	1.78	3	161	1.49	3
543		7/2-5/2	3-207	5234-632	.....	-1.11	55	1.02	3	533	2.01	3	325	1.79	3	133	1.40	3
544		9/2-7/2	3-186	5276-001	.....	-0.75	138	1.42	1	481	1.96	2	331	1.80	2	204	1.59	2
545		7/2-7/2	3-207	5325-562	.....	-1.81	37	0.84	3	297	1.75	3	174	1.52	3	62	1.07	3
546		9/2-9/2	3-186	5425-261	.....	-1.83	25	0.66	3	282	1.73	3	123	1.36	3	59	1.04	3
547	74	1/2-1/2	3-873	6149-255	.....	-1.94	38	0.79	3	211	1.54	3	183	1.47	2	55	0.95	2
548		3/2-3/2	3-872	6238-396	.....	-1.87	31	0.70	2	249	1.60	3	194	1.49	3	67	1.03	3
549		1/2-3/2	3-873	6239-962	.....	-2.54	8	0.11	2	149	1.38	3	97	1.19	2	28	0.65	3
550		5/2-3/2	3-875	6247-569	.....	-1.76	39	0.80	2	283	1.66	3	301	1.68	3	66	1.02	3
551		3/2-5/2	3-872	6407-310	.....	-2.17	15	0.37	2	103	1.21	2	88	1.14	3	31	0.68	3
552		5/2-5/2	3-875	6416-935	.....	-1.88	33	0.71	3	259	1.61	3	228	1.55	3	59	0.96	3
553		7/2-5/2	3-887	6456-396	.....	-1.68	61	0.98	3	514	1.90	3	423	1.82	3	171	1.42	2

Co I

554	28	7/2-9/2	0-919	4121-327	.....	+0.18	126	1.48	4	160	1.59	2	60	1.16	2	120	1.46	4	(51)
555	158	9/2-7/2	3-202	4813-481	1.732	-1.87	19	0.60	2	18	0.57	3	16	0.52	3	13	0.43	2	(52)
556		13/2-11/2	3-103	4867-876	.....	-1.57	43	0.95	2	47	0.98	2	18	0.57	3	16	0.52	2	
557	174	7/2-9/2	3-616	6455-024	.....	-2.54	26	0.60	2	23	0.55	2	22	0.53	2	14	0.34	2	
558	111	3/2-5/2	2-270	6632-481	.....	-2.85	4	1.78	2	11	0.22	2	11	0.22	2	6	1.96	2	

TABLE 3. OBSERVATIONS OF LINE INTENSITIES IN THE SPECTRA OF SOLAR-TYPE STARS—Continued

No.	Multiplet R.M.T.	I.Q. No.	Low E.P.	Wave- length	log S	log $\lambda s/s$	log $X_f$	Sun		$\gamma$ Cygni		$\alpha$ Persei		$\alpha$ Canis Minoris		Array log $\lambda f$		
								W	log W/ $\lambda$	W	log W/ $\lambda$	W	log W/ $\lambda$	W	log W/ $\lambda$		W	log W/ $\lambda$
Ni I																		
559	86	1-2	3.450	4462.463	1.398	1.097	-1.14	60	1.13	1	61	1.14	31	0.84	2	34	0.88	(54)
560	168	3-3	3.663	4437.570	1.176	0.382	-2.02	21	0.68	2	24	0.73	11	0.39	2	15	0.53	(56)
561	235	3-4	4.088	4732.468	1.322	1.572	-1.70	33	0.84	3	33	0.84	15	0.50	3	13	0.44	(54)
562	163	3-4	3.663	4806.996	.....	0.368	-1.37	57	1.07	3	73	1.18	35	0.86	3	30	0.80	
563	51	2-3	1.669	4519.993	.....	0.000	-1.87	15	0.52	1	38	0.92	27	0.78	2	17	0.58	(53)
564	98	4-3	3.465	4604.998	1.653	0.786	-1.09	74	1.21	2	105	1.36	50	1.04	3	57	1.09	(54)
565		5-4	3.405	4648.659	.....	0.657	-1.07	84	1.26	3	226	1.69	93	1.30	2	99	1.33	
566		2-2	3.582	4686.223	.....	1.623	-1.47	66	1.15	3	52	1.04	14	0.48	3	45	0.98	
567		6-5	3.365	4714.424	.....	0.539	-0.12	207	1.64	3	257	1.74	122	1.41	3	139	1.47	
568		3-3	3.528	4715.769	.....	1.459	-1.18	80	1.23	3	90	1.28	25	0.72	3	52	1.04	
569		4-4	3.465	4756.523	.....	1.451	-1.05	105	1.34	3	105	1.34	35	0.87	3	20	0.62	
570		2-3	3.582	4814.595	.....	2.799	-2.20	13	0.43	2	11	0.36	14	0.46	2	10	0.32	
571		3-4	3.528	4874.795	.....	2.748	-2.14	18	0.57	1	27	0.74	11	0.35	2	11	0.35	
572	145	3-3	3.620	5000.351	1.623	0.553	-1.32	70	1.15	3	116	1.36	43	0.93	2	53	1.02	(55)
573	162	3-4	3.663	5084.107	1.924	0.368	-0.82	76	1.18	3	118	1.37	62	1.09	3	62	1.09	(55)
574	130	1-1	3.642	5082.351	1.607	1.079	-1.54	41	0.91	3	29	0.76	14	0.44	2	32	0.80	(55)
575	111	2-1	3.724	4857.397	1.544	1.544	-1.61	44	0.96	3	26	0.73	19	0.59	3	35	0.86	(54)
576		5-4	3.524	4866.279	.....	1.502	-1.14	79	1.21	3	93	1.28	22	0.66	2	48	0.99	
577		3-2	3.683	4873.448	.....	1.368	-1.50	54	1.04	2	61	1.10	17	0.54	2	39	0.90	
578		2-2	3.724	4953.214	.....	1.146	-1.58	33	0.82	3	35	0.85	20	0.61	3	34	0.84	
579		4-4	3.590	4998.232	.....	0.742	-1.60	33	0.82	3	49	0.99	17	0.53	3	24	0.68	
580		5-5	3.524	5017.586	.....	0.548	-0.67	78	1.19	2	124	1.39	51	1.01	3	65	1.11	
581	177	3-2	3.924	4935.836	.....	0.623	-1.47	32	0.81	3	34	0.84	18	0.56	3	31	0.80	(55)
582		5-4	3.817	5115.400	.....	0.390	-1.34	53	1.02	3	91	1.25	32	0.80	3	52	1.01	(55)
583		4-4	3.824	5130.376	.....	1.681	-2.12	15	0.47	2	.....	.....	.....	.....	.....	11	0.33	
584	144	3-3	3.620	5010.945	0.778	1.431	-1.90	25	0.70	3	27	0.73	13	0.41	3	22	0.64	(55)
585	(161)	1-1	3.816	5048.066	.....	.....	-2.02	19	0.58	1	22	0.64	22	0.64	3	23	0.66	(55)
586	210	2-3	3.881	5155.773	1.447	0.000	-1.28	77	1.17	2	88	1.23	29	0.75	3	52	1.00	(55)
587	209	2-2	3.881	5176.567	1.243	0.000	-1.64	52	1.00	3	51	0.99	22	0.63	3	50	0.98	(55)

Ni I—Continued																				
588	231	3-4	4-088	5760-843	.....	1-872	-2-04	32	0-74	2	45	0-89	2	18	0-50	2	39	0-83	3	(53)
589	70	0-1	1-977	5435-868	.....	0-854	-1-73	41	0-88	3	51	0-97	3	9	0-22	2	22	0-61	2	(53)
590	250	3-3	4-136	5614-784	.....	1-431	-1-86	.....	.....	.....	45	0-90	2	26	0-67	2	22	0-59	2	(53)
591	591	1-2	4-248	5669-951	.....	0-689	-2-37	15	0-42	2	.....	.....	.....	.....	.....	.....	17	0-48	2	(53)
592	47	2-2	1-669	5578-731	.....	0-000	-1-71	40	0-86	3	46	0-92	2	20	0-56	2	15	0-43	2	(55)
593	221	1-2	4-072	5625-331	1-021	0-000	-1-96	38	0-83	2	52	0-97	2	24	0-63	2	22	0-59	2	(55)
594	230	4-4	4-071	6111-085	.....	0-396	-2-01	28	0-66	3	23	0-58	2	22	0-56	3	24	0-59	3	(55)
595	595	2-3	4-149	6366-498	.....	1-578	-2-20	19	0-48	2	15	0-37	2	13	0-31	2	25	0-59	2	(55)
596	228	4-5	4-071	6176-822	.....	0-390	-1-76	72	1-07	3	68	1-04	3	60	0-99	3	56	0-96	3	(55)
597	597	3-4	4-088	6223-996	.....	0-505	-2-16	14	0-35	2	12	0-28	2	18	0-46	3	11	0-25	2	(55)
598	68	0-1	1-977	5892-885	.....	.....	-1-48	122	1-32	2	68	1-06	2	42	0-85	2	69	1-07	2	(55)
599	249	2-2	4-217	5996-745	.....	1-431	-2-34	14	0-37	3	25	0-62	2	17	0-45	2	16	0-43	2	(55)
600	600	1-2	4-248	6086-294	.....	0-689	-1-90	22	0-56	2	35	0-76	3	26	0-63	2	23	0-58	3	(55)
601	601	3-3	4-136	6322-173	.....	1-431	-2-41	14	0-34	2	25	0-60	2	15	0-38	2	9	0-15	2	(55)
602	602	2-3	4-217	6598-621	.....	0-528	-2-21	18	0-44	3	18	0-44	2	24	0-56	3	16	0-38	2	(55)
603	248	1-1	4-248	6130-147	.....	0-824	-2-27	17	0-44	2	38	0-79	2	18	0-47	2	13	0-33	2	(55)
604	229	4-3	4-071	6133-973	.....	0-368	-2-97	5	1-91	1	12	0-29	2	9	0-17	2	10	0-21	1	(55)
605	605	3-3	4-088	6186-725	.....	1-431	-2-18	32	0-71	2	28	0-66	3	15	0-38	3	20	0-51	2	(55)
606	606	2-2	4-149	6360-828	.....	1-431	-2-42	29	0-66	3	26	0-61	2	20	0-50	2	22	0-54	3	(55)
607	64	2-1	1-927	6532-890	.....	2-255	-2-48	22	0-53	2	33	0-70	2	26	0-60	2	24	0-56	2	(55)
608	264	3-4	4-400	6635-146	.....	0-000	-2-26	16	0-38	2	24	0-56	2	15	0-35	2	18	0-43	2	(55)
Ni II																				
609	9	9/2-7/2	4-012	4362-104	.....	.....	-2-14	21	0-68	2	112	1-41	3	55	1-10	2	15	0-54	2	(55)
Cu I																				
610	2	5/2-3/2	1-383	5105-547	.....	0-222	-1-63	92	1-26	3	83	1-21	3	28	0-74	3	49	0-98	3	(55)

TABLE 3. OBSERVATIONS OF LINE INTENSITIES IN THE SPECTRA OF SOLAR-TYPE STARS—Concluded

No.	Multiplet R.M.T.	I.Q. No.	Low E.P.	Wave- length	log S	log $\lambda s/\epsilon$	log $X_f$	Sun		$\gamma$ Cygni		$\alpha$ Persei		$\alpha$ Canis Minoris		Array log $g_f$	
								W	log W/ $\lambda$	W	log W/ $\lambda$	W	log W/ $\lambda$	W	log W/ $\lambda$		W
Zn I																	
611	2	1-1	4.012	4722.165	0.954	0.477	-1.30	68	1.16	98	1.32	43	0.96	76	1.21	3	(57)
612		2-1	4.060	4810.539		0.255	-1.09	71	1.17	114	1.38	46	0.98	71	1.17	3	
613	6	1-2	5.771	6362.357	1.477	0.000	-2.30	39	0.79	53	0.92	46	0.86	32	0.70	2	(58)
Sr I																	
614	2	0-1	0.000	4607.340	0.778	0.000	-1.75	22	0.68	40	0.94	17	0.57	20	0.64	3	(59)
Sr II																	
615	1	1/2-3/2	0.000	4077.726	0.778	0.176	+1.26	332	1.01	608	2.17	679	2.22	340	1.92	4	(60)
616		1/2-1/2	0.000	4215.545		0.477	+1.08	250	1.77	536	2.10	485	2.06	287	1.83	4	
Y II																	
617	22	4-3	1.079	4883.692	2.225	0.368	-1.60	61	1.10	440	1.95	294	1.78	114	1.37	3	(61)
618	20	4-4	1.079	5087.428	1.924	0.396	-1.77	27	0.72	385	1.88	237	1.67	61	1.08	3	(61)
619		2-2	0.988	5200.417		0.674	-1.92	22	0.63	317	1.78	132	1.40	50	0.98	3	
620	27	1-1	1.731	5521.591	1.908	1.079	-2.96	11	0.30	80	1.16	47	0.93	9	0.21	2	(61)
621		1-0	1.731	5544.618		0.954	-3.13	.....	.....	75	1.13	52	0.97	10	0.26	2	
622		2-1	1.740	5546.035		0.857	-2.83	.....	.....	107	1.28	43	0.89	8	0.16	2	
Zr II																	
623	41	5/2-5/2	0.710	4208.987	1.146	0.389	-1.62	23	0.74	264	1.80	115	1.44	44	1.02	2	(62)
624	15	3/2-5/2	0.524	4211.891	.....	.....	-1.33	61	1.16	291	1.84	167	1.60	33	0.90	3	
625	67	7/2-5/2	0.968	4613.923	2.005	0.368	-2.14	22	0.68	90	1.29	25	0.73	9	0.29	3	(63)
626	95	3/2-3/2	1.658	5112.291	.....	0.444	-2.66	.....	.....	99	1.29	38	0.87	8	0.19	2	(63)

Ba II

627	1	1/2-3/2	0.000	4554.088	0.778	0.176	+0.55	191	1.62	4	549	2.08	4	410	1.96	4	208	1.66	4	(64)
628		1/2-1/2	0.000	4924.072		0.477	+0.69	254	1.71	3	583	2.07	3	409	1.92	3	231	1.67	3	
629	2	3/2-3/2	0.602	5853.691	1.778	1.176	-1.67	47	0.90	3	380	1.81	3	305	1.72	3	103	1.25	3	(65)
630		5/2-3/2	0.701	6141.733		0.222	-1.26	157	1.41	3	504	1.91	3	419	1.83	3	156	1.40	3	
631		3/2-1/2	0.602	6496.916		0.474	-1.16	116	1.25	1	581	1.95	2	432	1.82	3	191	1.47	2	

La II

632	25	2-3	0.172	4322.511	.....	0.000	-2.47	9	0.32	3	76	1.24	3	19	0.64	2	4	1.97	2	(67)
633	24	2-2	0.172	4333.765	0.699	0.000	-1.84	39	0.95	3	286	1.82	4	105	1.38	3	24	0.74	3	
634	8	2-1	0.000	4662.522	1.623	0.699	-2.71	8	0.23	2	122	1.42	2	48	1.01	3	.....	.....	.....	(66)
635	65	4-5	0.923	4748.739	2.297	0.000	-3.02	.....	.....	.....	51	1.03	3	14	0.47	3	.....	.....	.....	(66)
636	37	1-1	0.234	4804.035	.....	1.079	-2.69	4	1.92	2	37	0.89	3	13	0.43	3	5	0.02	2	
637	36	1-1	0.234	5114.516	.....	0.824	-2.42	.....	.....	.....	102	1.30	3	17	0.52	2	.....	.....	.....	
638	4	3-3	0.125	5805.77	2.565	0.553	-2.67	9	0.19	2	51	0.94	2	33	0.76	2	22	0.58	2	(66)

TABLE 4. INTENSITIES OF SPECTRAL LINES IN SOLAR-TYPE STARS IN THE REGION  $\lambda$  3690-4010

$\lambda$ R.M.T.	Atom	Multiplet R.M.T.	Low E.P.	$\log X_r$ Wt.	Sun		$\gamma$ Cygni		$\alpha$ Persei		$\alpha$ Canis Minoris	
					$r_s$	$W \log W/\lambda$ Wt.	$r_s$	$W \log W/\lambda$ Wt.	$r_s$	$W \log W/\lambda$ Wt.	$r_s$	$W \log W/\lambda$ Wt.
3689.916	Ti I	18	0.05	-0.58	73	1.30	2	78	26	0.95	1	
91.557	H	4	10.15	-2.43	10	0.43	1		1540	2.62	2	
92.652	Fe I	.....	.....	-1.31	54	1.16	2	72	80	1.48	2	
97.154	H	3	10.15	+0.96	81	1.34	1		2000	2.73	2	1890
98.17	Zr II	71	1.01	.....	.....	.....	.....	54	147	1.87	2	
99.147	Fe I	490	3.00	-0.83	67	1.26	3	81	61	1.31	2	77
3700.337	V II	116	2.50	-1.75	28	0.88	2	92	265	1.90	1	82
01.086	Fe I	385	2.99	+0.92	184	1.70	3	91	330	1.99	2	82
02.033	Fe I	369	2.83	-0.66	80	1.34	2	80	140	1.68	1	79
3703.855	H	3	10.15	+1.08	196	1.72	1		1640	2.65	2	2250
09.246	Fe I	21	0.91	+1.65	640	2.24	2	90	350	2.02	1	80
10.30	Y II	7	0.18	-0.68	102	1.45	2	78	350	2.08	2	73
11.973	H	3	10.15	+1.16	240	1.81	1		1820	2.69	2	2720
14.77	Zr II	18	0.52	-1.84	19	0.71	3	93	225	1.82	1	83
15.19	Cr II	20	3.09	-1.10	50	1.13	2	97	380	2.03	1	85
15.476	V II	15	1.57	-0.35	98	1.42	1		295	1.92	1	
15.911	Fe I	124	2.27	-0.46	95	1.41	2	99	189	1.61	1	86
17.393	Ti I	17	0.00	-1.34	50	1.15	3		15	0.62	1	84
3719.935	Fe I	5	0.00	+2.52	1690	2.69	2	82	540	2.25	2	65
21.940	H	3	10.15	+1.62	680	2.26	1		1740	2.67	2	3700
23.631	Ti II	72	1.56	-1.26	.....	.....	.....	80	260	1.94	2	60
24.106	Ti II	73	1.57	-1.46	.....	.....	.....	86	205	1.80	1	65
24.380	Fe I	124	2.27	-0.75	129	1.55	2	93	260	1.88	1	68
24.94	Eu II	2	0.00	-1.95	.....	.....	.....	93	210	1.79	1	73
25.498	Fe I	534	3.03	-0.53	.....	.....	.....	96	184	1.71	1	
32.760	V II	15	1.56	-0.20	54	1.31	2	66	250	2.01	1	58
3733.319	Fe I	5	0.11	+1.69	295	2.10	2	58	320	2.17	2	50
34.370	H	3	10.15	+1.94	910	2.39	2		2700	2.86	2	4200
34.867	Fe I	21	0.86	+2.99	.....	.....	.....	49	620	2.53	1	48
37.133	Fe I	5	0.05	+2.36	.....	.....	.....	79	780	2.42	2	70
41.059	Ti I	17	0.02	-0.26	82	1.34	3		167	1.65	1	89
41.633	Ti II	72	1.57	+0.43	189	1.70	2		470	2.10	2	88
44.105	Fe I	385	3.03	+0.36	153	1.61	2	97	194	1.73	1	86



TABLE 4. INTENSITIES OF SPECTRAL LINES IN SOLAR-TYPE STARS IN THE REGION  $\lambda$  3690-4010—Continued

$\lambda$ R.M.T.	Atom	Multiplet R.M.T.	Low E.P.	$\log X_r$	Wt.	Sun		$\gamma$ Cygni		$\alpha$ Persei		$\alpha$ Canis Minoris				
						$r_w$	$W \log W/\lambda$ Wt.	$r_w$	$W \log W/\lambda$ Wt.	$r_w$	$W \log W/\lambda$ Wt.	$r_w$	$W \log W/\lambda$ Wt.			
3787.164	Fe I	916	3.62	-1.31	1-	133	1.55	240	1.80	98	127	1.53	96	89	1.38	3
87.883	Fe I	21	1.01	+1.56	2	410	2.04	410	2.04	96	360	1.99	95	210	1.77	3
88.70	Y II	7	0.10	-0.65	1	135	1.55	440	2.06	93	310	1.94	93	127	1.56	2
89.178	Fe I	289	2.72	0.00	1-			195	1.71	94	162	1.66	92	108	1.49	1
90.095	Fe I	22	0.99	+0.93	1			450	2.07	88	320	1.98	89	188	1.74	2
94.340	Fe I	177	2.44	+0.58	1	92	1.61	82	1.91	64	390	2.21	75	98	1.54	2
95.004	Fe I	21	0.99	+1.66	1-	89	2.11			70	5600	3.17	70	215	1.91	2
97.900	H	2	10.15	+2.63	1-	1980	2.72	3200	2.93	32	200	2.22	37	5100	3.13	3
98.513	Fe I	21	0.91	+1.74	1-	54	2.01	43	2.24	56	350	2.23	57	225	2.02	2
99.549	Fe I	21	0.95	+1.76	1-	73	2.29									
3802.283	Fe I	666	3.29	-0.30	1	96	1.46	88	1.62	81	46	1.18	79	62	1.32	1
03.097	Ce II	37	(0.36)	-0.84	1-			93	1.56				82	21	0.83	1
03.474	V I	28	0.29	-1.42	1			95	1.37				83	14	0.65	1
04.013	Fe I	702	3.32	+0.03	1			98	1.66	84	107	1.52	86	80	1.39	2
05.345	Fe I	608	3.29	+0.85	1					89	250	1.87	90	134	1.59	3
07.144	Ni I	33	0.42	+0.90	2								94	159	1.65	2
07.534	Fe I	73	2.21	+0.89	2			340	1.95	99	210	1.75	95	135	1.57	2
08.731	Fe I	222	2.55	+0.17	3			225	1.77				98	106	1.46	2
09.043	Fe I	367	2.85	-0.58	1			80	1.32				98	46	1.09	1
3810.759	Fe I	665	3.29	+0.20	1			245	1.81							
12.964	Fe I	22	0.95	+1.33	2			470	2.10					114	1.48	2
13.390	Ti II	12	0.60	-0.42	1-			500	2.12					235	1.79	3
15.842	Fe I	45	1.48	+2.17	2			620	2.21							
18.34	Y II	7	0.13	-1.52	1-			320	1.92					380	2.00	2
19.67	Eu II	1	0.00	.....	..											
20.428	Fe I	20	0.86	+2.47	3			690	2.26					171	1.65	2
21.181	Fe I	608	3.25	+0.71	2			280	1.87					460	2.09	3
3822.474	Nd II	.....	.....	-2.63	1-									166	1.65	3
22.888	V I	28	0.29	-0.58	1-			55	1.16	99	29	0.88	91	46	1.12	1
24.444	Fe I	4	0.00	+1.70	1	76	2.14	45	1.07	98	38	1.01	94	41	1.06	1
25.884	Fe I	20	0.91	+2.34	1			620	2.21	95	650	2.25	92	360	2.00	3
27.825	Fe I	45	1.55	+1.35	1-			660	2.24	91	440	2.10	89	390	2.06	3
29.355	Mg I	3	2.70	+2.09	1-			640	2.22	85	500	2.19	84	340	2.02	2
								620	2.23	80	510	2.23	79	450	2.17	2

3831.690	Ni I	31	0.42	+1.38	1	93	1660	2.67	1	78	265	1.95	1	65	186	1.87	1	69	166	1.80	1	
32.302	Mg I	3	2.70	+2.56	1-	72	770	2.44	1	72	510	2.26	2	61	360	2.19	1	65	420	2.22	2	
34.225	Fe I	20	0.95	+2.12	1-	47	1930	2.70	1	47	400	2.34	2	41	330	2.32	2	45	255	2.17	2	
35.386	H	2	10.15	+2.68	1-						4000	3.02	2		6700	3.24	2		7300	3.28	3	
38.293	Mg I	3	2.70	+2.84	1-	71				71	560	2.32	2	61	420	2.26	2	64	570	2.37	2	
40.439	Fe I	20	0.99	+1.84	1-	88				88	450	2.12	2	74	370	2.11	2	76	260	1.95	2	
41.051	Fe I	45	1.60	+1.59	1-	92				92	500	2.15	2	77	370	2.10	2	78	295	1.99	2	
45.170	Fe I	124	2.41	+0.10	1		179	1.67	1		280	1.86	1	93	240	1.83	1					
45.468	Co I	34	0.92	+0.23	1-		310	1.90	1		280	1.86	1	93	215	1.77	1	92	169	1.68	1	
49.969	Fe I	20	1.01	+1.66	1		600	2.19	2		590	2.18	2		480	2.10	3		260	1.83	3	
3850.820	Fe I	22	0.99	+1.09	1		340	1.94	1										193	1.70	3	
51.748	Nd II	35	0.18	.....	..										78	1.30	2		23	0.77	1	
52.574	Fe I	73	2.17	+0.41	1						182	1.67	1		260	1.83	2		154	1.60	3	
53.657	Si II	1	6.83	.....	..						350	1.95	1		157	1.61	2		104	1.43	1	
56.021	Si II	1	6.83	-0.06	1-						450	2.06	2		430	2.05	2		192	1.70	1	
56.373	Fe I	4	0.05	+1.62	1		840	2.34	1		86	1.35	1		42	1.04	2		265	1.84	2	
57.631	Cr I	69	2.70	+0.43	1-	96	187	1.71	1		400	2.02	2		320	1.91	3		66	1.23	3	
58.301	Ni I	32	0.42	+1.04	1	80	290	1.87	1										205	1.72	3	
3859.214	Fe I	175	2.39	+0.76	1						255	1.82	1		260	1.83	2		173	1.65	2	
59.913	Fe I	4	0.00	+2.46	2		1760	2.66	2		580	2.18	3		450	2.06	3		370	1.98	3	
62.223	V I	8	0.02	-2.71	1-						18	0.66	1						2	1.59	1	
62.592	Si II	1	6.83	-1.40	1-		98	1.40	1		230	1.78	3		205	1.72	3		120	1.49	3	
63.409	Nd II	26	0.00	-0.74	1														37	0.98	2	
63.745	Fe I	280	2.68	+0.59	1		270	1.85	2		330	1.93	2		260	1.82	2		165	1.43	3	
64.49	La II	141	3.53	-1.04	1						24	0.79	1		12	0.47	1		28	0.86	1	
64.862	V I	7	0.02	-0.61	2						56	1.16	2		13	0.53	2		36	0.97	2	
3865.526	Fe I	20	1.01	+1.39	2		460	2.08	2		430	2.05	2		320	1.92	2		240	1.80	3	
66.796	Nd II	.....	.....	.....	..															75	1.29	1
67.219	Fe I	488	3.00	+0.20	1						255	1.82	2		199	1.71	2		128	1.52	3	
70.866	Ce II	.....	.....	.....	..										39	1.00	2		75	1.29	1	
72.504	Fe I	20	0.99	+1.64	1-		600	2.19	1		600	2.19	1		490	2.11	2		250	1.82	2	
78.021	Fe I	20	0.95	+1.59	1		520	2.13	1		480	2.09	2		450	2.08	2		260	1.85	1	
87.051	Fe I	20	0.91	+1.39	1	77	245	1.91	1	70	285	2.02	2	64	270	2.03	2	62	192	1.90	2	
3889.051	H	2	10.15	+2.79	2		2350	2.78	2		3300	2.93	2		5300	3.14	2		5500	3.15	3	
95.658	Fe I	4	0.11	+1.34	2	99	430	2.04	2		590	2.19	2	86	380	2.06	2	85	255	1.89	2	
97.449	Fe I	429	2.94	-0.18	2		126	1.51	2		440	2.05	2		320	1.94	3	90	88	1.40	2	
99.709	Fe I	4	0.09	+1.47	2		430	2.05	2		460	2.07	2		400	2.02	2	93	197	1.74	3	
3900.546	Ti II	34	1.13	+0.59	1																	



THE ACCURACY OF THE RESULTS

In spectrophotometric work, where a quantitative measure of the intensity of a stellar absorption line relative to the continuous background of the spectrum is derived from a photographic plate, there are many possible sources of error. Some of these errors may be small and unimportant; others are large and often difficult to determine. A number of investigators<sup>89</sup> have studied the problem during the course of their own researches and have listed sources of error in such measurements but a summary of possible errors and their effect upon the present results may well be outlined. Such errors, together with the estimated uncertainties, are given in Table 5. As most of these effects have been considered elsewhere, they will be discussed here only briefly.

TABLE 5. SOURCES OF ERROR IN SPECTROPHOTOMETRY

Source	Estimated Error (Per cent)	Source	Estimated Error (Per cent)
<b>SPECTROGRAPH</b>		<b>DEVELOPMENT—Concluded</b>	
(1) Focus.....	—	(2) Gelatin Contraction.....	—
(2) Temperature Changes.....	—	(3) Plate Irregularities.....	—
(3) Scattered Light.....	3	<b>MICROPHOTOMETER</b>	
(4) Poor Guiding.....	—	(1) Focus.....	(3)
<b>CALIBRATIONS</b>		(2) Resolving Power.....	—
(1) Exposure Effect.....	2	<b>REDUCTION OF TRACINGS</b>	
(2) Intermittency Effect.....	—	(1) Calibration Curve.....	3
(3) Latent Image.....	—	(2) Grain Effect.....	5
(4) Method of Calibration.....	3	(3) Continuous Background.....	5
<b>DEVELOPMENT</b>		(4) Blending Effect.....	10
(1) Eberhard Effect.....	3		

THE SPECTROGRAPH:

(1) *The Focus* was excellent for all plates in the ultraviolet, blue, and green regions. In the red region, the focus was not uniformly good over the whole plate, and the equivalent widths might be less than average in regions of poorer focus where higher central intensities are the result of the broader lines. This result was not apparent, however, when the triangle measurements were compared with the profiles.

(2) A *Temperature Change* in the spectrograph during the exposure would tend to broaden the lines just as in the case of poor focus. No temperature change greater than 0.2° C. was recorded for any plate which has been studied, and this would not cause any appreciable error.

(3) *The Effect of Scattered Light* in the prisms and lenses has not been investigated thoroughly but it is usually considered to be small. Scattered light is usually less in prism spectrographs than in gratings. *Rowland Ghosts* in the grating spectra produce a systematic error which has already been discussed (page 17). It should not amount to

<sup>89</sup> Harrison, G. R., *J. O. S. A.*, 19, 267, 1929; Thackeray, A. D., *M. N.*, 94, 99, 1933; Allen, C. W., *Mem. Comm. Sol. O.*, Canberra, 1, No. 5, 1934; Minnaert, M., *Observatory*, 57, 328, 1934.

more than one per cent for the grating used in the red region and a systematic correction of 5 per cent has been adopted for the ultraviolet plates. For highest accuracy this effect should be studied for each line individually and allowance made for the satellites of all neighbouring lines which might affect it, but it is unlikely that an error of as much as 3 per cent can be attributed to this cause. For the Littrow mounting of the spectrograph an occulting device was inserted to cut off the light of the slit image formed by reflections from the collimator-camera lens.

(4) *Poor Guiding* sometimes produces a non-uniform density across the width of the spectrum. Although these irregularities are averaged out by the microphotometer slit, the resulting deflection does not necessarily represent the corresponding point on the calibration curve. As all plates in this series were very nearly uniform, this effect must be small.

#### THE CALIBRATIONS:

(1) *The Exposure Effect*: Jones and his collaborators<sup>61</sup> have shown that the expression for a catenary best represents the relation between  $I \cdot t$  and  $t$ , the intensity,  $I$ , and time,  $t$ , factors in photographic photometry. For moderate intensities, considerable latitude is allowed and the factor of five to one in exposure time between calibration and stellar spectrum, which has sometimes been necessary, should not affect the results. Recently Pannekoek and van Albada<sup>90</sup> in their study of the instrumental profile for plates taken with the Victoria spectrograph, showed that the shape of the characteristic curve depends on the exposure time. In their case, however, the exposure ratios were quite large, as the calibrations were exposed for a few minutes while the comparison spectra were exposed for seconds and the stellar spectra sometimes for hours. Therefore their conclusions are not applicable to the present investigation.

(2) *The Intermittency Effect*: Both calibration and stellar spectra are intermittent; the sector rotates very rapidly but the stellar image drifts very slowly across the slit. Webb<sup>91</sup> has found that no appreciable errors result when the sector rotates 600 times per minute; the speed in this case is about 6,000 times per minute.

(3) *The Latent Image*: The calibration was placed on the plate as much as two hours before development and the stellar spectrum was developed immediately after exposure. The calibration would, then, have had more time to form a latent image than the stellar spectrum and the former might be relatively too dense. Thackeray<sup>89b</sup> found a slight change in the calibration curve due to this cause but Harrison<sup>89a</sup> states that other observers have found no such effect. As the time between mid-exposure of calibration and stellar spectra was usually less than an hour and since the middle, straight-line portion of the characteristic curve has been used for most plates, no correction has been made for this effect.

(4) *The Method of Calibration*: Although the sector has been standardized against step-slit and various step-weakensers, the calibrations might still remain a source of error. As a check, Beals<sup>92</sup> has compared the profiles of  $H\gamma$  in  $\gamma$  *Ursae Majoris* with those from plates taken at the University of Michigan, the Mount Wilson, and the Cambridge Solar

<sup>90</sup> *P. A. Inst.*, Amsterdam, No. 6, Pt. 2, 1946.

<sup>91</sup> *J. O. S. A.*, 23, 157, 1933.

<sup>92</sup> Unpublished.

Physics Observatories. The agreement of the Victoria results with those of Michigan and Mount Wilson were well within the errors of measurement; the difference between the Victoria and Cambridge profiles was very little greater than the computed probable errors. Accordingly, unless these Observatories have a common systematic error in their methods of calibration, it is probable that the Victoria calibrating spectrograph does not introduce any serious error into the results.

R. M. Petrie and W. Petrie<sup>93</sup> have published intensity measurements of four lines in the spectrum of  $\iota$  *Herculis* determined from spectrograms obtained at Victoria. Williams<sup>94</sup> at Mount Wilson Observatory, and Rudnick<sup>95</sup> at the Yerkes Observatory included  $\iota$  *Herculis* in studies of line intensities in many O- and B-type stellar spectra and the comparison is made in Table 6. The percentage differences between the Victoria results and the mean values are listed in the final column and they may also be considered to give confidence in the methods of calibration used at this Observatory.

TABLE 6. EQUIVALENT WIDTHS OF LINES IN  $\iota$  *Herculis*

Line	Atom	Petrie	Williams	Rudnick	Mean	Difference Victoria—Mean	
						A.	Per cent
4340	H $\gamma$	5.77	5.41	....	5.59	+0.18	+ 3
4388	He I	0.72	0.91	0.82	0.82	-0.10	-12
4471	He I	1.17	1.34	1.18	1.23	-0.06	- 5
4481	Mg II	0.24	0.39	0.26	0.30	-0.06	-20

#### DEVELOPMENT

(1) *The Eberhard Effect* seems to be the most serious error produced by the developer. Elvey and Miss Westgate<sup>96</sup> have studied the effect of this phenomenon on the profiles of absorption lines and it seems generally agreed that, when plates are developed in D-11 or in weak Rodinal, and when the developer is kept in constant motion during development by brushing lightly over the surface of the plate, it should not be important. On the plates, this effect should occur most pronouncedly at the far edge of the strongest calibration step; although it has been observed on a few plates taken by the writer, no such effect was observed on any used for this study and it may be assumed to be small.

(2) *Contraction of the Gelatin*, if uniform over the plate, would change the dispersion slightly; if irregular it might cause certain lines to appear too broad or too narrow. This effect is sometimes present in films but is negligible for glass plates.

(3) *Irregularities in the Plates* have been noted in a few cases. It is sometimes found that small sections of the plate are either lighter or darker than surrounding regions. These areas occur most frequently on plates which have been sensitized, as was the case for the green and red regions, and where the ammonia has, perhaps, evaporated unevenly. Allowance for such non-uniformity was made when the tracings were reduced.

<sup>93</sup> *These Publications*, 7, 189, 1940.

<sup>94</sup> *Ap. J.*, 83, 279, 1936.

<sup>95</sup> *Ap. J.*, 83, 439, 1936.

<sup>96</sup> *J. O. S. A.*, 24, 43, 1934.

## THE MICROPHOTOMETER

(1) *Errors in Focusing* appear to be small as Thackeray<sup>89b</sup> has shown that a relatively large error in focusing the microphotometer will introduce little or no error into the final intensity of a line. Nevertheless, the focus was tested immediately before the tracings were made, over the entire length of each plate and it was always found to be uniformly good.

(2) *The Resolving Power* of the microphotometer, particularly with the narrow slits which were used, is much greater than that of the spectrogram and no errors should be introduced from this source.

## REDUCTION OF THE TRACINGS

(1) *The Calibration Steps*, shown in Plates I to III and in Fig. 1 were placed on the tracings for each range of 150-200 angstroms in order that each section of the spectrum might be reduced with the appropriate curve. Each step, put on with the 20-fold magnification, was one-half inch in width, which permitted an adequate averaging of the grain effect; the calibrations were repeated both before and after the spectrum was recorded in order to allow for any change in sensitivity of the microphotometer. As all points lay on a smooth curve (though the straight-line portion was usually very short), the accidental errors in intensity caused by the calibration curve were much smaller than most other effects discussed here.

(2) *The Grain Effect* is present to an appreciable extent on all plates. Since a line is drawn along the estimated position of the continuous background, this error may be averaged for each tracing but, in the measurement of the width of a line or its central intensity, the grain effect may only be eliminated by the use of a number of plates for each star. In the blue region, at least five measures of each line were available, as shown in Table 2; in the ultraviolet, green and red regions, at least three measures were averaged for each line. The grain effect should, therefore, be minimized in the final results.

(3) *The Position of the Continuous Background*, in F- and G-type stars, is very difficult to estimate on the tracing. In the ultraviolet and blue regions the lines are crowded together so closely that the galvanometer deflection rarely represents the position of the continuous background. A comparison of the tracings with Rowland's *Map of the Solar Spectrum*<sup>97</sup> indicated places where the lines are very weak or absent and for such gaps in the spectrum it was assumed that the upper edge of the grain was just above the position of the continuous background.

The Utrecht *Photometric Atlas of the Solar Spectrum* was used as an aid to determine the position of the continuous spectrum for the region  $\lambda\lambda$  3700-4000. In this region the *H* and *K* lines of ionized calcium and the numerous hydrogen lines which approach the Balmer limit at  $\lambda$  3646 make this determination extremely difficult, but it is hoped that the continuum has been drawn at approximately the correct height on the tracings. The error due to misjudgment in drawing the continuous spectrum should not be more than 5 per cent\* but it is possible that it could be considerably more since this effect on the equivalent widths is magnified greatly for lines with appreciable wings. Straight lines were drawn across the tracings between the points at the continuum and joined to form

<sup>97</sup> Johns Hopkins Univ., 1888.

\* The comparisons with other observers shown in Table 8 indicate that this estimate of the error may be unduly low.

a curve with a slowly changing slope such as might be expected from the sensitivity of the plate and the energy distribution of the incident light. In regions of longer wave-length the number of absorption lines in the spectrum decreases and the position of the continuous background becomes less difficult to determine. For the red region the background was drawn through the average of the grains wherever lines were not present.

(4) *The Blending Effect* has already been discussed on page 16 and it is hoped that an estimate of the true intensity of each line, independent of all neighbouring lines, has been obtained by means of the blending correction. More recent measurements of lines in  $\alpha$  Persei<sup>98</sup> suggest that an over-correction for the blending of weak lines was made for this star, which might amount to about 10 per cent. A comparison of the results with those of other observers suggests that the measurements for the other stars may have been over-corrected similarly (see below).

#### ACCIDENTAL ERRORS

The many possible systematic errors present in the measurement of line intensities may explain why the results of different observers sometimes vary by as much as 100 per cent. But there are also accidental errors inherent in all measures and some estimate of these may be made from the internal agreement of the different sets of measurements.

The probable error of  $r_m$  was determined for each line according to the formula

$$P. E. = \pm 0.67 \sqrt{\frac{\sum v^2}{n(n-1)}}.$$

where  $v$  is the deviation of any measure from the mean and  $n$  is the number of measures. For each star it was found that the error in  $r_m$  was greatest for lines with central intensities from 55-88 per cent of the continuous background and the error decreased for both stronger and weaker lines. The computed errors were about one per cent and were approximately the same for all stars.

The probable error of  $r_b$ , the central intensity corrected for blending, includes the error in  $r_m$  plus the error made in estimating the effect of blends. For large corrections, the latter may be as much as 5 per cent but for most lines the error in this estimate may be about one per cent. Most lines in the blue region are affected by blending more or less seriously and it is estimated that the total probable error of  $r_b$  is 2.5 per cent. In the green and red regions, blends are less important and the total probable error of  $r_b$  is then about 2.0 per cent.

Tabulated values of  $W$ , the equivalent width, were determined directly from the curves relating  $r_b$  and  $W/\lambda^4$  and the probable errors have been estimated by substituting upper and lower limits for given values of  $r_b$  in each curve. As probable errors for a given  $W$  were very nearly the same for each star, the values listed in Table 7 are the means for the four stars. The percentage probable errors are much greater for weak lines than for strong lines and are somewhat greater in the red, than in the green, region. The curves of Fig. 2 indicate that the scatter of individual observations from the mean curve is greater for strong lines than for weak lines and allowance for this effect has been made in Table 7.

<sup>98</sup> Unpublished.

TABLE 7. PERCENTAGE PROBABLE ERRORS OF EQUIVALENT-WIDTH MEASUREMENTS

$W$ (A.)	0.01	0.02	0.05	0.10	0.20	0.25	0.50
Blue region.....	30	24	16	12	10	9	10
Green region.....	35	30	25	15	12	10	12
Red region.....	50	45	35	20	15	12	15
Allen.....	20	10	6	6	8	11	15

The probable errors that Allen determined for  $W$  in his study of the solar spectrum are given in the last line of this table. The increase in his errors for equivalent widths greater than 0.10 A. may mean that his curves are relatively flatter than those obtained at Victoria and, for strong lines, there is a greater change in  $W$  for a given change in  $r_b$ . The direct method of measuring equivalent widths for the ultraviolet region of the spectrum makes an estimate of the errors more difficult. Although each measure should be more accurate than one which is based on related quantities, such as the central intensity and the width at the base of the line, the difficulty of making full allowance for the effect of neighbouring lines in this region of the spectrum makes it appear probable that the accuracy of the results is about the same as that for the blue region.

These probable errors may be compared with those estimated for the sources of error listed earlier in this section and which are tabulated in Table 5. Estimates are given only when the errors are one per cent or more. The errors in the determination of the continuous spectrum, the grain effect and the blending effect of neighbouring lines appear to be the largest sources of error. Assuming that they are independent, the total probable error for a single measurement is about 14 per cent, which is somewhat less than the values listed in Table 7 for the probable errors which were determined directly from the equivalent-width measurements.

#### COMPARISON OF EQUIVALENT-WIDTH MEASUREMENTS WITH THOSE OF OTHER OBSERVERS

Although relatively few detailed studies of line intensities have been published, it has been noted that there are usually systematic differences between intensities of the same line measured at different observatories. While it is not the purpose of the present paper to make a detailed study of these differences, Table 8 has been compiled to show the variation between Victoria measures ( $V$ ) and those made by other observers ( $O$ ) from star to star and for lines of different intensity. Two sets of differences were obtained for each range of intensity,  $O - V$ , taking regard for sign, which is, then, a measure of the systematic difference between the observations, and  $|O - V|$ , without regard for sign, which gives some indication of the total scatter of the observations but, as it includes the systematic difference, is not a true measure of the probable error. These columns were obtained by summing the differences for all lines within the given intensity range, dividing by the mean of the Victoria intensities and expressing the result as a percentage; the number of lines on which the results are based is given in the third column for each intensity range. At the end of the table, for comparison purposes, the approximate probable error of the Victoria observations is listed for each intensity.

As Table 8 presents a quantitative estimate of the observed percentage differences in equivalent-width measurements for the stars studied in this paper, it is necessary only to mention the results very briefly:

TABLE 8. COMPARISON OF VICTORIA OBSERVATIONS WITH THOSE OF OTHER OBSERVERS

Observer	Star	Region $\lambda\lambda$	0 - 50 mA.		51 - 100 mA.		101 - 200 mA.		201 - 400 mA.		401 - 600 mA.		601 - 1000 mA.				
			$\frac{O-V}{V}$	$\frac{ O-V }{V}$   No.													
Utrecht.....	Sun	3700 - 4000	+18	21	9	18	25	32	23	32	-7	24	11	15	20	4	
		4028 - 4603	+39	40	58	19	50	16	54	16	54	+3	13	20	7	10	2
		4570 - 5701	+27	37	106	16	81	15	55	15	55	-11	14	27	17	17	2
		5521 - 6752	+7	29	96	17	52	22	38	22	38	-7	19	7	16	16	2
		4028 - 4603	+35	37	58	18	50	15	54	15	54	+2	8	20	10	10	2
		4570 - 5701	+21	32	102	14	81	14	55	14	55	-10	15	27	10	18	2
		5521 - 6752	+11	30	83	17	52	21	38	21	38	+2	21	7	14	14	2
		3897 - 3956			0	19	4	5	2	5	2	-15	15	2	3	10	2
		4383 - 4603	+44	44	5	22	7	9	8	9	8	+9	9	2	16	1	2
		5154 - 5269	+59	59	2	16	10	18	8	18	8	-1	6	5	11	10	2
		5565 - 6022	+48	53	25	6	13	23	14	18	14	+21	21	2	2	17	2
		6592 - 6718	+27	28	9	3	2	3	3	27	3						
ten Bruggencate and von Klüber.....		4885 - 5456	+39	39	8	18	10	9	15	-14	14	13					
Thackeray.....		5172 - 5896						0	30	-5	5	5		-9	9	4	
Bailey.....	$\gamma$ Cygni	4028 - 6592	+94	94	1	67	8	32	23	0	13	37	7	25	5	1	
		4028 - 4755	+260	260	121	126	16	74	29	+48	48	52	29	22	22		
		5172 - 5896									-5	10	10	10	10		



1. *The Utrecht Photometric Atlas of the Solar Spectrum*<sup>99</sup> gives a graphical representation of the line spectrum relative to the continuum from  $\lambda\lambda$  3332-8771 and is the first complete publication of this kind. The intensity of any line can be determined directly from the *Atlas* by sketching the profile, after making any necessary allowance for blends, and measuring its area. The plates were taken with the grating spectrograph of the 150-foot tower telescope of the Mount Wilson Observatory and were made with dispersions of 3.0 mm/A. in the second order and 1.5 mm/A. in the first. The photometry appears to be excellent and the results should be accurate to within about 10 per cent. The differences between Victoria and Utrecht measures listed in Table 8 may be considered as due almost entirely to errors in the Victoria measurements as a result of the considerably lower dispersion employed. However, they are within the probable errors of these observations, though the differences are largely systematic in character and vary somewhat with the strength of the line. It appears that an over-correction was made for the effect of blends on very weak lines ( $< 50$  mA.) but for lines from 100 to 400 mA. in intensity this correction was not made sufficiently large.

2. *Allen*<sup>100</sup> obtained his observations with the sun telescope of the Commonwealth Solar Observatory. His spectra were made using the equivalent of five 60° glass prisms and gave a dispersion which varied from 0.5A/mm. at  $\lambda$  4300 to 2.2 A/mm. at  $\lambda$  6600. He calibrated his equivalent widths in terms of the central intensity of the line, found that a small correction for blending was necessary for most lines and listed the true equivalent width derived from the corrected central intensity. A direct comparison of Allen's data with those of the Utrecht *Atlas* indicates that systematic differences, if any, are small. This is also seen from Table 8 where the trend is much the same for these two series of observations. As Allen's intensities were taken as a standard when this work was first undertaken, a detailed comparison of the results has been made and, in addition, the intensities for all lines listed in Table 3 have been plotted in Fig. 6. In three sections of this figure, lines of intensity less than 300 mA. have been compared for the blue, green and red regions of the spectrum and in the fourth section the intensities of strong lines over the entire spectral range have been compared. The general trend of the correlation between Canberra and Victoria results is very similar for the blue and green regions; for weak lines the Victoria measures are somewhat smaller than those obtained by Allen; for lines of moderate intensity the trend is reversed; but for strong lines the measurements represent very well the one-to-one correspondence that should be expected if no systematic errors are present. In the red region the correspondence is very good for weak lines; for lines of moderate intensity the Victoria results appear to be somewhat stronger than those derived at Canberra; but the few strong lines agree well with measures in other regions.

3. *Mulders*<sup>101</sup> obtained solar spectra having a dispersion of 2 A/mm. with the second order of the Rowland grating at Utrecht and made a study of 462 lines in selected regions of the spectrum. Except for very weak lines, there is sufficiently close agreement with the Victoria measures, and in some cases the scatter is less than that for the comparison with the Utrecht *Atlas*.

<sup>99</sup> Minnaert, M., G. F. W. Mulders and J. Houtgast, Schnabel, Kampert, and Helm, Amsterdam, 1940.

<sup>100</sup> *Mem. Comm. Sol. O.*, Canberra, 1, No. 5, 1934; 2, No. 6, 1938.

<sup>101</sup> *Diss.*, Utrecht, 1934; *Z. f. Ap.*, 10, 297, 1935.

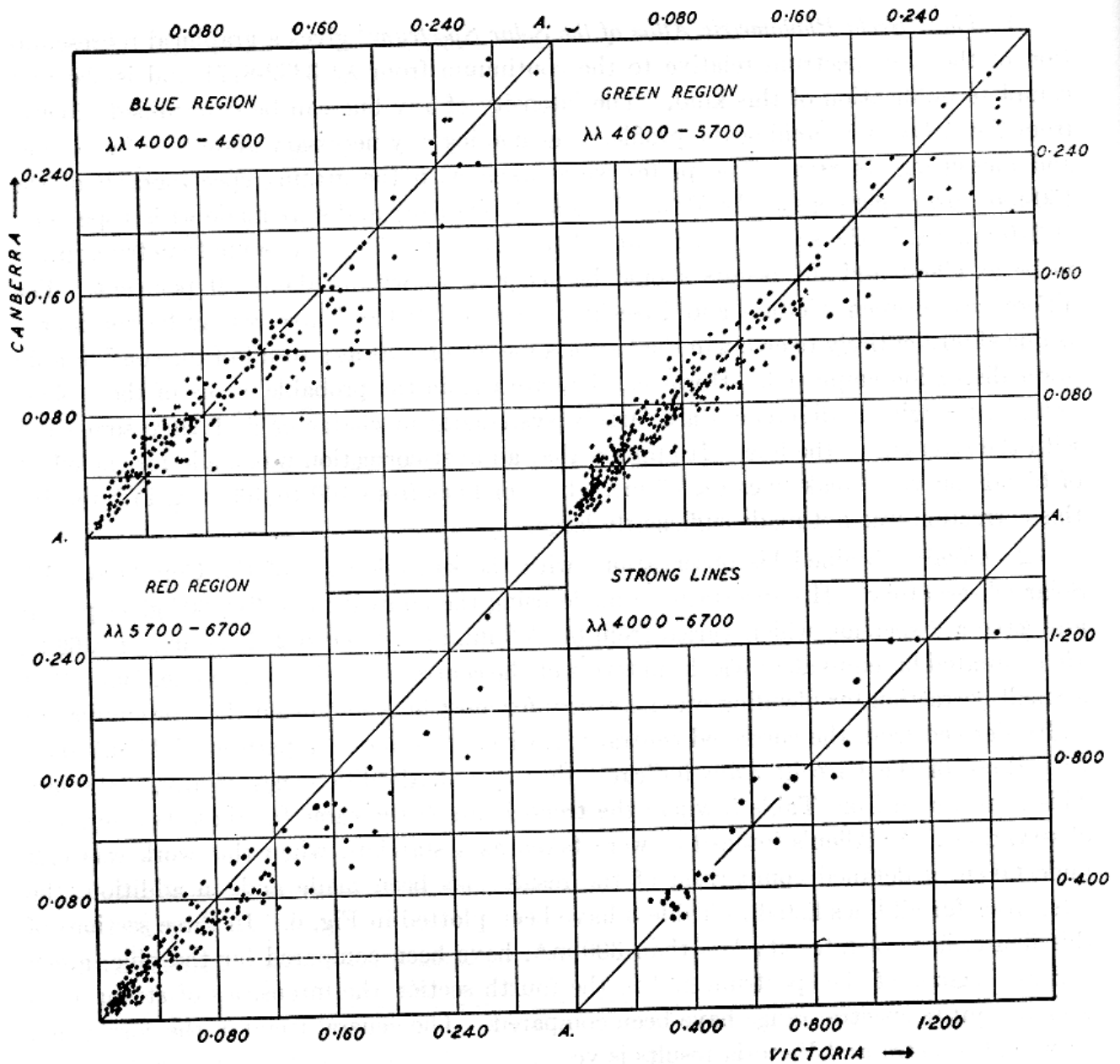


FIG. 6. Comparison of Solar Equivalent Widths Measured at Canberra and at Victoria.

4. Woolley<sup>102</sup> studied the solar spectrum from  $\lambda$  4040 to  $\lambda$  4390 using spectra obtained by Evershed at Ewhurst, which had a dispersion of about 0.5 A/mm. at  $\lambda$  4200. Mulders found that it was necessary to multiply Woolley's values for the line intensities, which were obtained with a prism train which included a liquid prism, by a factor of 1.3 in order to bring the results into agreement; Allen found that a similar factor was necessary. Woolley's intensities are almost always lower than the Victoria measures and, although a detailed comparison is not given in Table 8, the value for the factor mentioned above is about 1.25.

5. Ten Bruggencate and von Klüber<sup>103</sup> obtained spectra of the centre of the sun's disk with the grating spectrograph of the Potsdam Institut der Sonnenphysik which gives a dispersion of 1.4 A/mm. in the first order. They made a comparative study of neutral iron and titanium lines over disk and over sun-spots in the region  $\lambda\lambda$  4885-5455. A

<sup>102</sup> *An. Sol. Phys. O.*, Cambridge, 3, Pt. 2, 1933.

<sup>103</sup> *Z. f. Ap.*, 18, 284, 1939.

comparison with the disk intensities shows that for thirteen weak titanium lines the Potsdam measures are greater than the corresponding Victoria values, but for 53 iron lines the result is reversed. The average differences are approximately the same as for other comparisons.

6. *Thackeray*<sup>104</sup> included the four stars of this paper in a study of line intensities in thirty late-type stars in the region  $\lambda\lambda$  5150-5900. He obtained spectra with the Huggins 15-inch refractor of the Cambridge Solar Physics Observatory, which had a dispersion of 50 A/mm. at  $\lambda$  5183. The general agreement of the measurements made at Cambridge and at Victoria is very good; the mean differences, regardless of sign, is 12 per cent for the sun, 10 per cent for  $\gamma$  *Cygni*, 19 per cent for  $\alpha$  *Persei* and 17 per cent for  $\alpha$  *Canis Minoris*.

7. *Mrs. Frances S. Bailey*<sup>105</sup> studied intensities of neutral iron and ionized titanium lines in the spectrum of  $\gamma$  *Cygni* in the region  $\lambda\lambda$  4000-6700 determined from plates obtained with the Coudé spectrograph of the McDonald Observatory. Sixty-four neutral iron lines and 35 ionized titanium lines were measured in common with those presented in this paper, and, in general, good agreement was noted between the two sets of measures. For lines having equivalent widths greater than 250 mÅ. there is a one-to-one correspondence, with a maximum scatter of 20 per cent. For weaker lines, Mrs. Bailey's measures become progressively greater; they are 40 per cent larger than the Victoria lines with  $W = 100$  mÅ. and the scatter also increases greatly. For weak lines the McDonald plates, with their higher resolving power, should give better results but it may be that the blending correction has been under-estimated by Mrs. Bailey and over-estimated by the writer.

8. *Sahade and Cesco*<sup>106</sup> obtained intensities of lines in the spectrum of  $\gamma$  *Cygni* from a plate taken with the Coudé spectrograph of the McDonald Observatory which had been run through the direct-intensity microphotometer developed by Williams and Hiltner<sup>106a</sup>. Over the region for which a comparison is possible,  $\lambda\lambda$  4028-4755, the intensities measured by Sahade and Cesco are all greater than those measured on the Victoria plates and, for weak lines, the difference is several-fold. The apparent explanation for most of this difference seems to be that the level of the continuous spectrum on the McDonald plate was drawn considerably higher than that determined by the writer. This explanation was confirmed when Hiltner and Williams' *Photometric Atlas of Stellar Spectra*<sup>107</sup> was received at this Observatory and a comparison was made for  $\alpha$  *Persei*. Further studies of this difference are not made at this time, but it seems that the determination of the position of the continuous spectrum of these stars may offer greater difficulties than had been expected.

9. *Miss Helen R. Steel*<sup>108</sup> measured intensities in the spectrum of  $\alpha$  *Persei* on two McDonald Coudé plates in the regions  $\lambda\lambda$  4000-4727 and  $\lambda\lambda$  4440-6700. A comparison of the measures shows that the McDonald intensities are considerably greater for very weak lines—though the difference is not as great as that for the measures of Sahade and

<sup>104</sup> *M. N.*, 94, 99 and 538, 1934.

<sup>105</sup> *Thesis*, Univ. of Arizona, 1942. The writer wishes to express his thanks to the Librarian of the University of Arizona for making this manuscript available to him.

<sup>106</sup> *Ap. J.*, 104, 133, 1946.

<sup>106a</sup> *P. O. Univ. Mich.*, 8, 45, 1940.

<sup>107</sup> Univ. of Michigan Press, Ann Arbor, 1946.

<sup>108</sup> *Ap. J.*, 102, 429, 1945.

Cesco—but the effect decreases rapidly and for strong lines the Victoria measures are greater; hence the difference in this case is probably due to the greater correction for the blending effect on weak lines of the Victoria plates, though errors in calibration could produce such an effect. Fortunately these systematic differences are of the same order as the probable errors, but they could affect the interpretation of the results if they were not understood. They serve to emphasize the systematic differences which arise from measures made at the various observatories.

10. *Struve and Elvey*<sup>109</sup>: In order to study the “turbulence effect,” Struve and Elvey measured Yerkes three-prism spectrograms of  $\alpha$  *Persei* and a number of other stars. In the region  $\lambda\lambda$  4350–4780 common to both measures, the scatter of individual observations is large but it would appear that, on the average, the Yerkes equivalent widths are about 50 mÅ. greater than the Victoria values for all lines.

11. *Elvey*<sup>110</sup> measured the total absorptions of a few multiplets of ionized iron and titanium in  $\alpha$  *Persei*,  $\alpha$  *Canis Minoris* and other F5 stars. The 13 lines in  $\alpha$  *Persei* for which a comparison is possible are about 17 per cent stronger, and the 12 lines in  $\alpha$  *Canis Minoris* are about 28 per cent stronger, than the corresponding Victoria values.

A general comparison of the Victoria equivalent widths of solar-type stars with those published elsewhere shows that the Victoria results are usually somewhat less than other values. This could arise from systematic differences such as the determination of the continuous background, the blending effect of neighbouring lines or a systematic error in the calibrations. It is probable that at least the first two causes are present and that, although Allen also corrected his intensities for blending effects, the Victoria central intensities may have been over-corrected in the case of weak lines; as noted above, any systematic errors in the calibrations seem to be small. On the whole, except for a few comparisons of weak lines, the agreement with other observers is sufficiently good; the differences are not greater than the probable errors of the Victoria measures and the results of this comparison may be considered satisfactory. However, with the development of direct intensity traces of the spectrum it will be possible to obtain more accurate intensities and it will be necessary to find the cause of any systematic differences. A program of inter-comparison of intensities measured at the several observatories seems highly desirable. For the present paper, however, it seems that the results should not be affected seriously by the differences shown in Table 8 and no further corrections have been made to the results.

<sup>109</sup> *Ap. J.*, 79, 409, 1934.

<sup>110</sup> *Ap. J.*, 79, 263, 1934.

### SECTION III. STELLAR CURVES OF GROWTH

#### THEORETICAL DISCUSSION

All theories of absorption lines which were applicable to stellar atmospheres and which were available for the present analysis used only first approximations to the conditions existing in these atmospheres. However, whether the exponential function for the shape of a line, which represents a purely absorbing atmosphere and which has been used by Struve, or the Schuster-Schwarzschild model, which assumes a purely scattering atmosphere, is used, the principal results and the general form of the curve of growth remain the same.

Absorption lines in laboratory spectra are produced when light from a source emitting a continuous spectrum is passed through a chamber containing the gas under investigation. If  $I_0$  is the intensity of the continuous spectrum at frequency  $\nu_0$ , and  $I_\nu$  is the intensity at any point on a spectral line centred at  $\nu_0$ , then

$$I_\nu = I_0 e^{-k_\nu x}$$

where  $k_\nu$  is the absorption coefficient of the gas and  $x$  is the thickness of the absorbing layer.

The principal agents which cause a line to be broadened and which therefore determine the form of the absorption coefficient are:

- (1) Natural, radiation damping due to the finite lifetime of an electron in the excited state, i.e. the finite breadth of the energy levels within the atom;
- (2) Doppler broadening produced by the random, thermal motions of the atoms;
- (3) Pressure broadening which is the result of collisions between the atoms and which includes:
  - (a) Lorentz broadening produced by collisions with foreign gases;
  - (b) Holtzmark broadening resulting from collisions with absorbing atoms of the same kind;
  - (c) Stark broadening due to collisions with electrons and ions.

The theory applicable to laboratory spectra and the results obtained up to 1934 are well-presented in the monograph by Mitchell and Zemansky<sup>111</sup>. They show that under laboratory conditions when the pressure of the absorbing gas is less than 0.01 dynes/cm.<sup>2</sup> and the thickness of the absorbing layer is small, the wings of the line may be neglected and only Doppler motions need be considered in determining the intensity of a line, but when the pressure increases to 10 dynes/cm.<sup>2</sup>, then the intensity of the line is determined almost entirely by the broad wings which are due to natural damping. Voigt<sup>112</sup> derived an expression for the absorption coefficient of a gas affected by Doppler and natural broadening and van der Held<sup>113</sup> made a series of calculations based on similar expressions for different values of the damping constant which, when related to the observed intensity of a line as the number of atoms increases, is the original basis for the theory of the curve of growth.

<sup>111</sup> *Resonance Radiation and Excited Atoms*, p. 92, Cambridge Univ. Press, 1934.

<sup>112</sup> *Münch. Ber.*, p. 603, 1912.

<sup>113</sup> *Z. Phys.*, **70**, 508, 1931.

Unsold<sup>114</sup> has summarized the theory of the classical harmonic oscillator and has shown how Minnaert, Mulders, and Slob<sup>115</sup> applied it to the theory of stellar absorption lines in 1931. This theory applies strictly only to resonance lines and assumes that the centres of the lines are completely black—which we know is not the case—but it has been applied by Struve to discover the “turbulence effect” in stellar atmospheres<sup>116</sup> and, very recently, to show that turbulent velocities determined from the curve of growth do not agree with those derived from line profiles in  $\delta$  *Canis Majoris*<sup>117</sup>.

In this paper, the theory of the curve of growth follows that developed by Menzel<sup>118</sup>. The Schuster-Schwarzschild model of a stellar atmosphere assumes that the photosphere is a definite radiating surface and above it lies the reversing layer in which the lines are produced by scattering. In this case, which Milne calls monochromatic radiative equilibrium, for each light quantum absorbed in a given frequency, a quantum of exactly the same frequency is emitted, though without restriction as to direction. Thus we see that some re-emission may occur in the centre of the line, though it is not as great according to theory as some observations seem to indicate. The theory applies specifically to resonance lines, such as the sodium *D* lines, but Weisskopf and Wigner<sup>119</sup> have suggested that for subordinate lines the present theory may apply without too severe a modification.

The observations are expressed in terms of the equivalent width,  $W$ , in angstrom units, and  $\lambda$ , the wave-length, but it is found more convenient to express the elementary theory in terms of  $\nu$ , the frequency, where

$$\lambda = \frac{c}{\nu} ; W = \Delta \lambda = \frac{c}{\nu^2} \Delta \nu . \quad (1, 2)$$

$\Delta \nu$  is the equivalent width in frequency units.

According to the Schuster-Schwarzschild approximation, the intensity,  $r_\nu$ , at any point,  $\nu$ , on the line profile relative to the continuous spectrum is given by

$$r_\nu = \frac{1}{1 + N \alpha_\nu} . \quad (3)$$

By definition,

$$\Delta \nu = \int_0^\infty (1 - r_\nu) d \nu \quad (4)$$

and hence

$$\Delta \nu = \int_0^\infty \frac{N \alpha_\nu}{1 + N \alpha_\nu} d \nu \quad (5)$$

where  $N$  is the number of active atoms (i.e. atoms in the lower level of the electron transition) per square centimetre in the column above the photosphere;

and  $\alpha_\nu$  is the atomic absorption coefficient, which has been considered by many writers and, in the form given by Menzel, is

$$\alpha_\nu = \frac{\pi \epsilon^2}{m c} f \left[ \frac{1}{\sqrt{\pi}} \frac{c}{\nu \nu_0} e^{-\frac{(\nu - \nu_0)^2 c^2}{\nu_0^2 \nu^2}} + \frac{\Gamma}{4 \pi^2} \frac{1}{(\nu - \nu_0)^2} \right] . \quad (6)$$

<sup>114</sup> *Physik der Sternatmosphären*, p. 159, Springer, Berlin, 1938.

<sup>115</sup> *Pr. K. Ac.*, Amsterdam, **34**, 542, 1931; *Z. f. Ap.*, **2**, 165, 1931.

<sup>116</sup> *Ap. J.*, **79**, 409, 1934.

<sup>117</sup> *Ap. J.*, **104**, 138, 1946.

<sup>118</sup> *Ap. J.*, **84**, 462, 1936; *Pop. A.*, **47**, 6, 66 and 124, 1939.

<sup>119</sup> *Z. Phys.*, **63**, 54, 1930.

Here  $\epsilon$  and  $m$  are the charge and mass of an electron, respectively;

$c$  is the velocity of light;

$f$  is the oscillator strength;

$\nu_0$  is the frequency at the centre of the line;

$\Gamma$  is the damping constant which is defined as the sum of the reciprocal mean lifetimes of electrons in the upper and lower states involved in the transition;

and  $v$  is the most probable velocity of the atoms according to the kinetic theory of gases.

The first term within the brackets in equation (6) represents the form of the absorption coefficient near the centre of the line if a Maxwellian distribution of velocities among the atoms is assumed. This gives the broadening of the line due to the Doppler motions of the atoms and determines the shape of all but strong lines. As the radiation damping portion of the absorption coefficient becomes important only in the wings of the absorption line, the second term in (6) may be disregarded until its value becomes appreciable compared with the first term.  $\Gamma$  has been calculated from the classical theory of a simple harmonic oscillator but may not have the same value when calculated by the quantum mechanics.

In order to study the integral (5), set

$$X_0 = N \frac{\pi \epsilon^2}{m c} f \frac{1}{\sqrt{\pi}} \frac{c}{v \nu_0} \quad (7)$$

which, from (6) is the value of  $N\alpha_\nu$  when  $\nu = \nu_0$  and is termed the optical depth at the centre of the absorption line. It has been found that  $\frac{W}{\lambda}$  can be conveniently related to the value of  $X_0$  and this relation is called the "curve of growth." As equation (5) cannot be integrated directly, Menzel obtained asymptotic expressions for different values of  $X_0$ :

(i)  $X_0 \ll 1$  near the centre of the line and the second term in (6) may be disregarded.

Then

$$\Delta \nu = X_0 \sqrt{\pi} \frac{v \nu_0}{c} \left[ 1 - \frac{X_0}{\sqrt{2}} + \frac{X_0^2}{\sqrt{3}} - \dots \right] \quad (8)$$

or, approximately,

$$\frac{W}{\lambda} \approx \sqrt{\pi} \frac{v}{c} X_0. \quad (9)$$

This asymptotic expression for the Doppler portion of the function holds until  $X_0 \approx 0.1$ .

(ii) When  $X_0 > 1$  but the damping portion of the coefficient is not yet important, Menzel derived the expression

$$\Delta \nu = \frac{2 v \nu_0}{c} (\log_e X_0)^{\frac{1}{2}} \left[ 1 - \frac{\pi^2}{24} \frac{1}{(\log_e X_0)^2} - \frac{7 \pi^4}{384} \frac{1}{(\log_e X_0)^4} \dots \right] \quad (10)$$

or

$$\frac{W}{\lambda} \approx \frac{2 v}{c} (\log_e X_0)^{\frac{1}{2}}. \quad (11)$$

(iii) When  $X_0 \gg 1$ , the second term in equation (6) becomes important and the Doppler term may be neglected. The expression for the asymptote is

$$\Delta \nu = \frac{\pi^2}{2} \left[ X_0 \Gamma \frac{v \nu_0}{c} \right]^2 \quad (12)$$

or

$$\frac{W}{\lambda} = \frac{\pi^2}{2} \left[ X_0 \frac{\Gamma}{\nu_0} \frac{v}{c} \right]^2. \quad (13)$$

For intermediate values of  $X_0$ , Baker<sup>120</sup> derived the expression

$$\log \frac{W}{\lambda} = \log X_0 \frac{v}{c} \sqrt{\pi} - \frac{1}{2} \log (1 + X_0) - \frac{\frac{1}{2} \log 4 \sqrt{\pi} \frac{v}{c} \Gamma}{1 + 15 e^{-2 \log X_0}}. \quad (14)$$

This formula, which is semi-empirical, was deduced to fit the observed curve of growth for the sun and, therefore, holds only for the sun and for stars existing under conditions very similar to it. If  $v$  or  $\Gamma$  change by a factor of ten, the flat transition portion of the curve becomes  $\sim$ -shaped.

When observational data are used to determine curves of growth,  $\log W/\lambda$  is plotted against either theoretical or laboratory intensities, which are proportional to  $X_0$  (see below). Each plot is then fitted on to one of a family of theoretical curves from which the empirical constants of the curve of growth,  $v$  and  $\Gamma/\nu$  may be determined. In order to obtain these values more easily, Menzel<sup>118b</sup> has modified the above equations as follows:

$$\text{Set } Z = \frac{\Gamma c}{\nu v}. \quad (15)$$

$$\text{Then (9) becomes } \frac{W}{\lambda} \frac{c}{v} \approx \sqrt{\pi} X_0; \quad (16)$$

$$(11) \text{ becomes } \frac{W}{\lambda} \frac{c}{v} \approx 2 (\log_e X_0)^2; \quad (17)$$

$$\text{and (13) becomes } \frac{W}{\lambda} \frac{c}{v} = \frac{\pi^2}{2} \left[ X_0 Z \right]^2. \quad (18)$$

Thus  $W/\lambda \cdot c/v$  may be plotted as a function of  $X_0$  for suitable values of  $Z$ . Such curves have been published by Menzel and by Unsöld<sup>121</sup>, and have also been reproduced in Fig. 7. The curves in this figure are based primarily on those given by Unsöld, but the theoretical data were recalculated where possible and were re-drawn on the scale used for the observational curves of growth throughout this paper.

These curves illustrate the change in the strength of an absorption line as the number of absorbing atoms increases. In a laboratory investigation, the actual amount of material producing a given line can be varied and its increase in absorption studied—the name, “curve of growth,” is derived from this consideration. Under stellar conditions, it is necessary to measure numerous lines arising from different levels within the same atom and compare their intensities. Assuming a Boltzmann distribution of atoms among the energy states, an excitation temperature may be derived and from it the relative number of atoms populating any given level may be calculated.

<sup>120</sup> *Ap. J.*, **84**, 474, 1936.

<sup>121</sup> *Op. cit.*, p. 268.

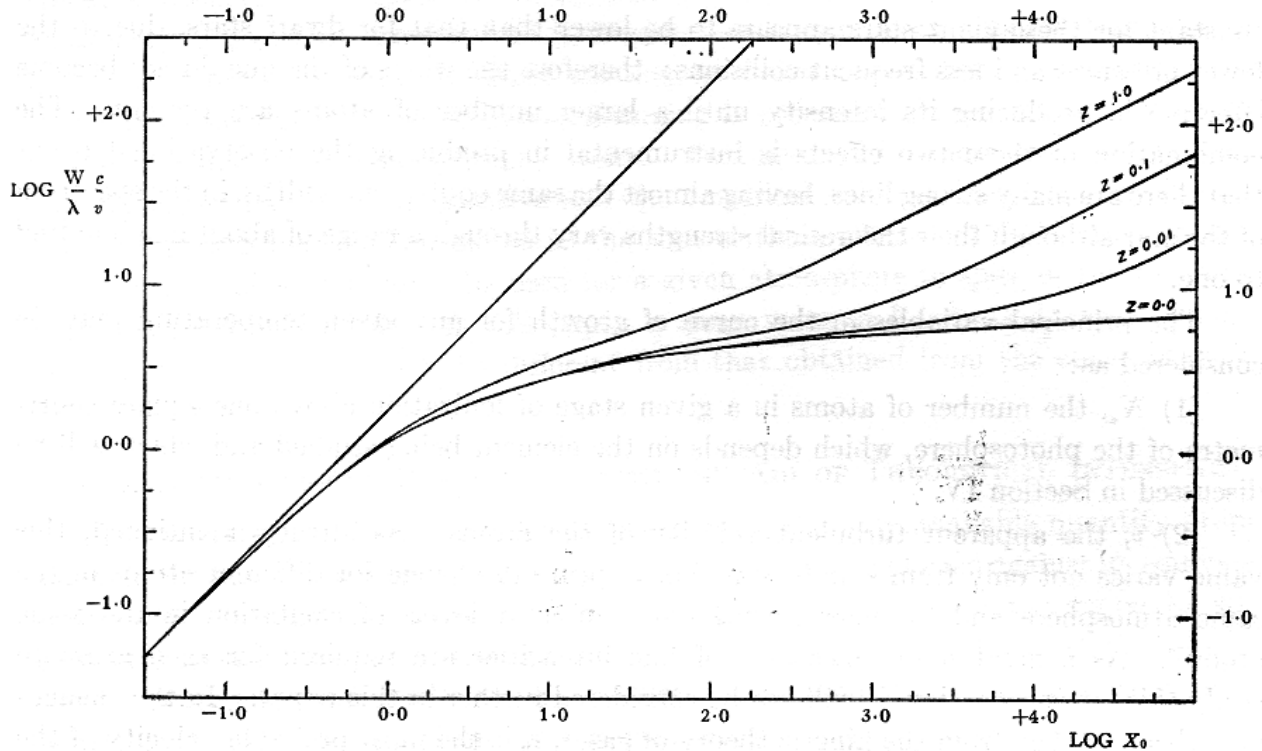


FIG. 7. Theoretical Curves of Growth (after Menzel and Unsöld).

It is seen that for very weak lines ( $W < 0.03 \text{ \AA}$ . in the case of the sun), the curve is a straight line at an angle of  $45^\circ$  as given by the Doppler formula that  $W/\lambda \propto N$ . The random motions of the atoms produce a zone of absorption near the centre of the line, and the absorption increases with the number of atoms until almost all the background radiation at that wave-length has been removed; then a considerable increase in the number of atoms does not change the strength of the line very greatly. For motions corresponding to thermal velocities of the atoms, the centre of the line becomes saturated quickly and a departure from the straight-line relation becomes perceptible for relatively weak lines; this departure from the  $45$ -degree line becomes increasingly marked until the curve may become almost horizontal and the intensity does not increase appreciably as the number of atoms producing the line becomes greater. Eventually, however, the wings of the line, which are produced by radiation or collisional damping, become effective and the intensity of the line again increases with the number of atoms producing it until this agency is the sole factor in the increase of line strength and the curve becomes a straight line with  $\log \frac{W}{\lambda} \propto \frac{1}{2} \log N$ , i.e.  $W/\lambda$  increases as the square root of  $N$ .

Under different conditions the shape of the curve may vary considerably. Struve and Elvey<sup>116</sup> could not explain their observations of line intensities, which indicated that the transition portion of the curve of growth for giant stars was almost flat and occurred over the range from moderately strong to strong lines, until they postulated that the random motions of the atoms must be much greater than those produced by thermal motions alone, and they suggested that these additional motions might be produced by turbulence in the atmosphere. These large velocities increase the zone of absorption at the centre of the line; the Doppler portion of the curve is extended; and the transition portion is not reached until the lines become moderately strong. In addition, the damping

constant for these giant stars appears to be lower than that for dwarf stars, due to the lower pressures and less frequent collisions; therefore the wings of the line do not become effective in producing its intensity until a larger number of atoms are present. The combination of these two effects is instrumental in producing the observational result that there are many strong lines, having almost the same equivalent widths, in the spectrum of the star although their theoretical strengths vary through a range of about one hundred to one.

The principal variables in the curve of growth for any given temperature may be considered as:

(1)  $N_a$ , the number of atoms in a given stage of ionization above one square centimetre of the photosphere, which depends on the element being studied and which will be discussed in Section IV.

(2)  $v$ , the apparent turbulent velocity of the atoms. As already mentioned, this value varies not only from star to star, but appears to change for different atoms in the same atmosphere and for lines arising from different levels of excitation in the same atom<sup>122</sup>. As a great many measures of line intensities are required for each atom to study this latter variation, it will not be considered further in this paper. In the elementary theory, taken from the kinetic theory of gases,  $v_0$  is the most probable velocity of the atoms of a given element, and is given by the formula

$$v_0 = \sqrt{\frac{2 k T_e}{m_1 \mu}} \quad (19)$$

where  $T_e$  is the effective temperature of the star;

$k$  is the Boltzmann gas constant;

$m_1$  is the mass corresponding to unit atomic weight;

and  $\mu$  is the atomic weight of the element being studied. When average values for the velocity are being determined,  $\mu$  is usually taken as 50, since iron and titanium lines are given greatest weight in its determination.

If  $v$  is the velocity obtained from a study of the curve of growth, and

$v_T$  is the velocity produced by the turbulent motions of the atoms, then Goldberg<sup>123</sup> has noted that

$$v^2 = v_0^2 + v_T^2. \quad (20)$$

(3)  $\Gamma$  or, in the present theory,  $\Gamma/v$ , which is assumed to be constant for a given curve although it is known that it changes somewhat from line to line. A summary of the values obtained for the ratio of the observed damping constant,  $\Gamma$  to the classical value,  $\gamma$ , has been given by Minnaert<sup>124</sup>. The observational result that this ratio is about ten led early observers to consider  $\Gamma$  as a variable from star to star and later results have confirmed this procedure. Minkowski and King<sup>125</sup> have discussed values of the damping constant which have been determined for individual multiplets and have suggested that the variation may be partially a result of pressure broadening although other effects must also be present—there is a great need for further laboratory investigations of the damping constant. Unsöld<sup>126</sup> studied the effect of pressure broadening in

<sup>122</sup> *J. R. A. S., Can.*, **41**, 49, 1947.

<sup>123</sup> *Ap. J.*, **89**, 636, 1939.

<sup>124</sup> *Observatory*, **57**, 339, 1934.

<sup>125</sup> *Ap. J.*, **95**, 86, 1942.

<sup>126</sup> *Op. cit.*, p. 273.

stellar atmospheres and came to the conclusion that collisions between the atom under consideration and ions, electrons or hydrogen atoms may be as important as radiation damping at pressures equal to those existing in stellar atmospheres; Strömberg<sup>127</sup> has found that, for the sun, the collisional damping is produced almost entirely by Lorentz broadening due to neutral hydrogen atoms. Fortunately, for most purposes, radiation and collisional damping are additive and the empirical value of  $\Gamma$  determined from the curve of growth may be considered as the sum of these effects. Unsöld also concluded that a mean value of  $\Gamma$  could be used for a given atmosphere in spite of the theoretical variation from line to line. In this paper, a mean value of  $\Gamma/\nu$  is used; that found for neutral atoms may, however, be different from that obtained from the curve of growth for ionized atoms.

#### CURVES OF GROWTH DETERMINED WITH THE AID OF THEORETICAL INTENSITIES

In early studies of curve-of-growth phenomena, the only available quantity proportional to the number of atoms producing a line which could be plotted against its equivalent width was the theoretical intensity. As the observational data for the region  $\lambda\lambda$  4028-6750 presented in this paper were studied by this method until 1942, a brief résumé of the theory, procedures and results are given below. The preliminary results were presented before meetings of the American Astronomical Society from 1939 to 1942.<sup>128</sup>

In many-lined spectra a large range in theoretical intensities may be obtained through the use of supermultiplets, or, better, of all the multiplets in a given transition array. For this purpose it is necessary to know the electron configuration of both upper and lower levels for each line, as a transition array consists of all permitted transitions between the terms of two configurations. For most atoms these are given in the compilation of Bacher and Goudsmit<sup>129</sup>; for atoms which have been analyzed since 1932, additional references have been given by Miss Moore in her *Revised Multiplet Table*<sup>130</sup>. Relative multiplet strengths can be calculated for many transition arrays where one electron changes its state by one unit in azimuthal quantum number,  $l$ . If the jump involves equivalent electrons, the origin, or parentage, of the level may not be obvious; for many transition arrays of astrophysical importance the parentages have been given by Menzel and Goldberg<sup>131</sup>. Relative multiplet strengths have been calculated by Goldberg<sup>132</sup> and relative line strengths within a multiplet, calculated according to the original sum rules, have been presented in convenient form by Russell<sup>133</sup>.

The optical depth at the centre of a line,  $X_0$ , has been defined in terms of atomic and universal constants by equation (7). In logarithms this may be expressed as

$$\log X_0 = \log \left( \frac{N_a}{b(T)} \frac{\sqrt{\pi} \epsilon^2}{m c} \right) - \log \nu + \log g_i f \lambda - \frac{5040}{T} \chi_i \quad (21)$$

by expressing  $N$ , the number of atoms producing the line, in terms of

$N_a$ , the total number of atoms in the given stage of ionization;

$$b(T) = \sum_i g_i e^{-\chi_i/kT} \quad (22)$$

<sup>127</sup> *Festschrift für Elis Strömberg*, p. 218, Munksgaard, Copenhagen, 1940.

<sup>128</sup> *P. Am. A. S.*, **9**, 276, 1939; *P. Am. A. S.*, **10**, 34, 1940; *P. Am. A. S.*, **10**, 323, 1943.

<sup>129</sup> *Atomic Energy States*, McGraw-Hill, New York, 1932.

<sup>130</sup> *Cont. Princ. O.*, No. 20, 1945.

<sup>131</sup> *Ap. J.*, **84**, 1, 1936.

<sup>132</sup> *Ap. J.*, **82**, 1, 1935.

<sup>133</sup> *Ap. J.*, **83**, 129, 1936.

which is the partition function, being the weighted sum of all levels within the atom; this value changes slowly with temperature and is usually considered a constant for each atom after a preliminary temperature has been adopted;

$g_i$ , the statistical weight of the given spectroscopic level,  $= 2J + 1$ ;

$f$ , the oscillator strength,

and  $\chi_i$ , the excitation potential in electron volts, of the lower level of the transition.

As few  $f$ -values are known for the most important atoms used in the study of curves of growth, equation (21) is re-written in terms of theoretical line strengths:

$$\log X_0 = \log \left( \frac{N_a}{b(T)} \frac{\sqrt{\pi} \epsilon^2}{3 m c R} \right) + \log \frac{c}{v} + \log \varphi S \frac{s}{\Sigma s} - \frac{5040}{T} \chi_i \quad (23)$$

where  $R$  is the spectroscopic Rydberg constant;

$\varphi = \frac{1}{4 l^2 - 1} \rho$  is a dimensionless constant peculiar to the transition array; it

has usually been taken as unity, but Goldberg<sup>134</sup> has obtained an approximate formula which can be used to calculate  $\rho$ , the radial quantum function and this has been used in the determination of relative abundances (see page 95).

$S$  is the strength of a multiplet relative to others in the same transition array; and

$s$  is the strength of an individual line relative to  $\Sigma s$ , the sum of all line strengths in the multiplet.

A preliminary curve of growth is obtained for a given star by plotting  $\log (W/\lambda)$  against

$$\log (S.s/\Sigma s) - \frac{5040}{T} \chi_i. \quad (24)$$

For each transition array where sufficient data are available to define some portion of the curve of growth, some preliminary temperature,  $T$ , is assumed; it is an excitation temperature, and has always been found to be considerably below the effective temperature adopted for stars of the same spectral class. An improved temperature is determined later in the analysis and may be inserted in equation (24) to obtain a better fit of the observations on a curve of growth if the temperature is appreciably different from that used at the beginning.

Plots of the several transition arrays are superposed by sliding them horizontally along the abscissa until the best fit is obtained, and the mean curve obtained from all the plots is compared with the family of curves shown in Fig. 7. The vertical shift of the observed curve relative to the theoretical curve is a measure of  $\log (c/v)$ , and hence of apparent turbulent velocity,  $v$ ; the differences in the horizontal shift are used later to determine the relative abundances of the atoms. On the damping portion, a value of  $Z$  can usually be found to define a curve which fits the observations reasonably well.

This mean curve of growth may be used to determine the final excitation temperature. For a given curve,  $v$  may be considered constant and equation (23) may be rewritten as

$$Y = \log X_0 - \log S \frac{s}{\Sigma s} = L - \frac{5040}{T} \chi_i \quad (25)$$

where the first part of the equation defines  $Y$  and

$$L = \log \left( \frac{1}{3 \sqrt{\pi} R} \frac{\pi \epsilon^2}{m c} \cdot \frac{c}{v} \cdot \frac{N_a}{b(T)} \cdot \varphi \right) \quad (26)$$

may be considered a constant for a given transition array.

<sup>134</sup> Unpublished.

As the multiplet and line strengths have already been tabulated,  $Y$  may be found for each multiplet and a mean value of  $\chi_i$  may be used. Then in equation (25)  $L$  and  $T$  are, theoretically, the only unknowns and there should be a straight-line relation between  $Y$  and  $\chi_i$ . By plotting these values for all available multiplets in a given transition array, and by making a least-squares solution for the straight line, values for  $L$  and  $T$  may readily be found. If the original assumed temperature differs from that found in the analysis by more than a few hundred degrees, it is probable that a second determination of the curve of growth should be made.

A more accurate value of  $T$  for the same number of lines should be obtained if laboratory rather than theoretical intensities are available, as the uncertainties introduced by any departures from LS-coupling would be removed. Temperatures have been derived from laboratory  $g_i f$ -values of neutral iron and titanium in this way and have been found to be of the same order of magnitude as those obtained with the aid of theoretical intensities.

Curves of growth for the stars studied in this paper have been determined using the equivalent-width and theoretical line-intensity data given in Table 3. Numerous curves were obtained for each star using the excitation temperature calculated from the previous approximation. In the final analysis in which this method was used, the preliminary temperatures were adopted as:

Sun: 4800° K;  $\gamma$  Cygni: 5050° K;  $\alpha$  Persei: 6225° K; and  $\alpha$  Canis Minoris: 5750° K.

The plot for each transition array was fitted on the curves of Fig. 7 to obtain values for the unknowns,  $\log c/v$  and  $Z$ . These values were listed and given weights which depended on the number of lines, the scatter of the points about the theoretical curve and the precision of the determination. The latter depended a great deal on the portion of the curve covered by a given transition array; for example, array No. 31 of Ti I contains many lines but they are not strong enough to determine either the height of the transition portion of the curve ( $\log c/v$ ) or the damping constant ( $\log Z$ ) and hence the array was given low weight, except in the case of the sun, where  $\log c/v$  could be determined; on the other hand the lines of transition array No. 36 of Ti II, though few in number, lie directly on the transition portion of the curve and were important in the final determination of the unknowns. Mean values of these constants of the curve of growth for the four stars, as determined in this way, are shown in Table 9, and the curves of growth calculated for these values are shown as solid lines in Fig. 8. The plotted points show the observations

TABLE 9. EMPIRICAL CONSTANTS FOR CURVES OF GROWTH  
(1942 DATA)

	Sun	$\gamma$ Cygni	$\alpha$ Persei	$\alpha$ Canis Minoris
$\log c/v$ .....	5.16	4.65	4.70	5.05
$v$ km/sec.....	2.1	6.7	6.0	2.6
$v_0$ km/sec.....	1.4	1.4	1.5	1.5
$v_T$ km/sec.....	1.6	6.6	5.8	2.2
$\log Z$ .....	-0.30	-0.81	-0.58	-0.47
$\log \Gamma/v$ .....	-5.46	-5.46	-5.28	-5.52
$\Gamma/v \times 10^6$ .....	3.5	3.5	5.2	3.0
$\Gamma \times 10^{-9}$ sec. <sup>-1</sup> .....	2.1	2.1	3.1	1.8

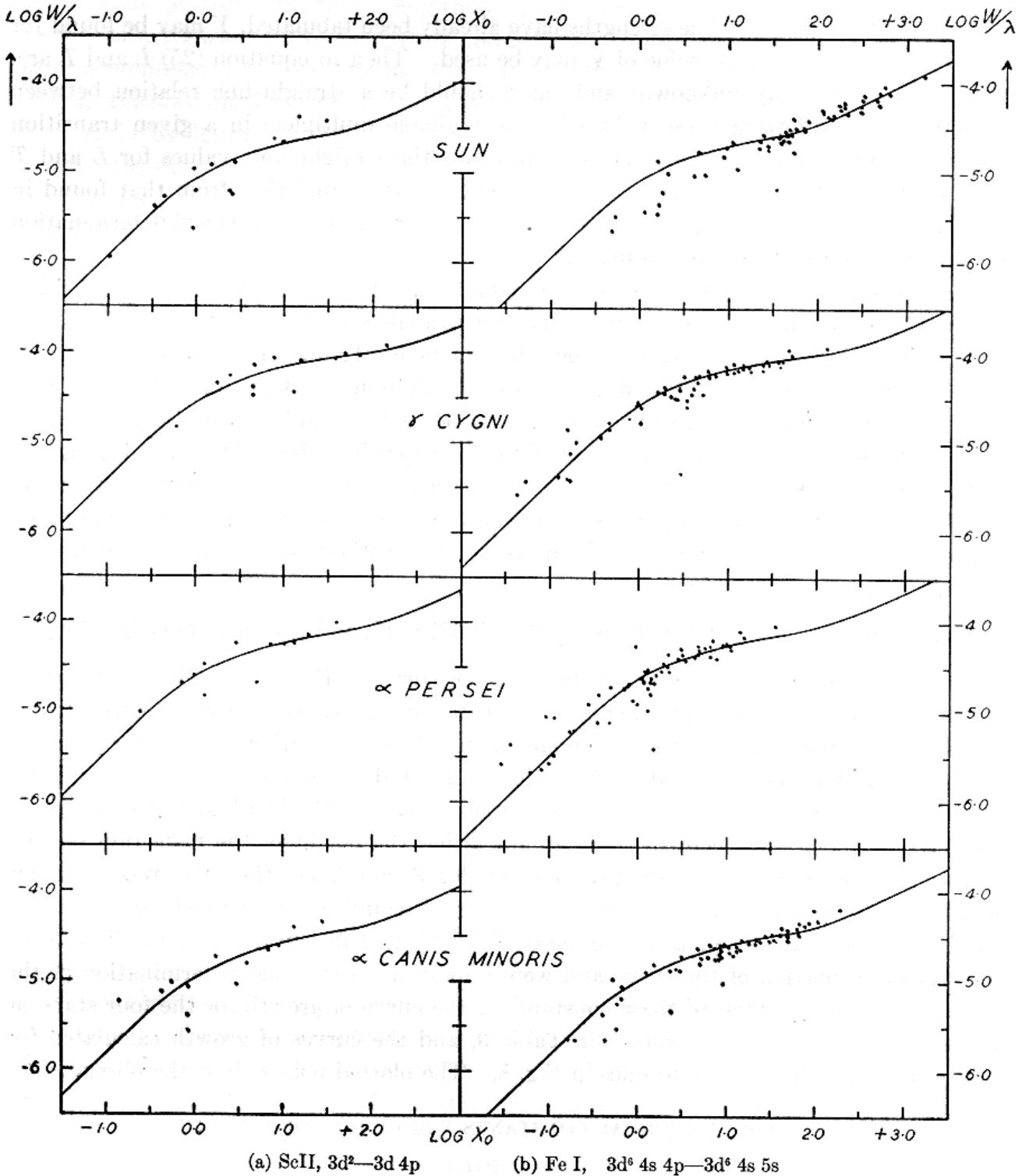


FIG. 8. Curves of Growth for the Sun,  $\gamma$  Cygni,  $\alpha$  Persei and  $\alpha$  Canis Minoris Determined from Theoretical Intensities. The theoretical curves, shown as solid lines, represent the turbulent velocities and damping factors adopted in Tables 9 and 10. The several multiplets in each transition array have been shifted along the  $X_0$ -axis to agree with the adopted excitation temperature. The  $\log W/\lambda$ -scale has been reduced to absolute units by adding  $-6.0$  to the values given in Tables 3 and 4.

for the transition arrays No. 29, ScII,  $3d^2-3d 4p$  and No. 50, Fe I,  $3d^6 4s 4p-3d^6 4s 5s$  for each of the four stars. These transition arrays contain more observations than the average and also cover a greater range in intensity, but may be considered representative of the fit obtained when equivalent widths are combined with theoretical intensity data. These curves, which were calculated with the temperatures adopted in 1942 for these stars, may be considered among the best that can be obtained when supermultiplet

intensities are used. It was believed that when errors in the equivalent-width measurements and in the theoretical intensities and the fact that the curve is made up of many superposed segments were considered, a reasonable estimate for the uncertainty in the turbulent velocity was 0.5 km/sec, and in the value of  $\Gamma/\nu$  was a factor of 2.

From these curves of growth, excitation temperatures were determined in three ways:—

(1) *Theoretical Intensities*: For each multiplet,  $\log W/\lambda$  was plotted against  $\log S \frac{s}{\Sigma s}$  and these observations were fitted on to the adopted curve of growth. The shift of the plot relative to the curve gave a value of

$$Y = \log X_0 - \log S.s/\Sigma s$$

for each multiplet and these values were plotted against the corresponding mean excitation potential,  $\chi_i$ , as shown in Fig. 9. The slope of the straight line drawn through these points is inversely proportional to the excitation temperature which can thus be found. Least-squares solutions were made for the transition arrays most satisfactory for this purpose (i.e. containing many lines and covering a large range in excitation potential) and the results for a few of these, together with the probable errors of the temperatures are given in Table 10, section 1.

(2) *Laboratory Intensities*: For neutral iron and titanium lines, King's  $f$ -values were available and for each multiplet  $\log W/\lambda$  was plotted against  $\log g.f . \lambda$ . The shift of the plot relative to the adopted curve gave a value of

$$V = \log X_0 - \log g.f . \lambda$$

for each multiplet, and the several values of  $V$  were plotted against the corresponding mean excitation potential,  $\chi_i$ . According to the theory (equation 21), these points should fall on a straight line, the slope of which is inversely proportional to the excitation temperature. Excitation temperatures for Fe I and Ti I derived from  $f$ -values are given in the second section of Table 10.

(3) *Theoretical Intensities Improved by Means of Laboratory  $g.f$ -Values*. This method has been applied for the transition arrays No. 30, Ti I,  $3d^2 4s^2 - 3d^2 4s 4p$ ; No. 31, Ti I,  $3d^3 4s - 3d^3 4p$  and No. 49, Fe I,  $3d^7 4s - 3d^7 4p$ . It has been shown by the writer<sup>135</sup> that there is not a one-to-one correspondence between theoretical intensities and the laboratory  $g.f . \lambda$ -values, and it is believed that the principal errors lie in the calculation of the theoretical intensities. In order to utilize the observational material to its fullest extent, corrections were applied to the theoretical intensities of neutral iron and titanium lines to bring them into closer agreement with the laboratory  $f$ -values. The method is described in the Appendix, where a brief discussion of theoretical intensities is also given. Plots between  $\log W/\lambda$  and the corrected theoretical intensities were made as in subsection (1), above, and the derived excitation temperatures are given in the third section of Table 10.

In the 1942 determination of excitation temperatures for the four stars, only six sets of data were included in the final analysis and these were the ones which gave the lowest probable errors for the temperatures: those derived for transition array No. 50, Fe I,  $3d^6 4s 4p - 3d^6 4s 5s$ , for which uncorrected theoretical intensities were used, gave good

<sup>135</sup> *Ap. J.*, 99, 249, 1944.

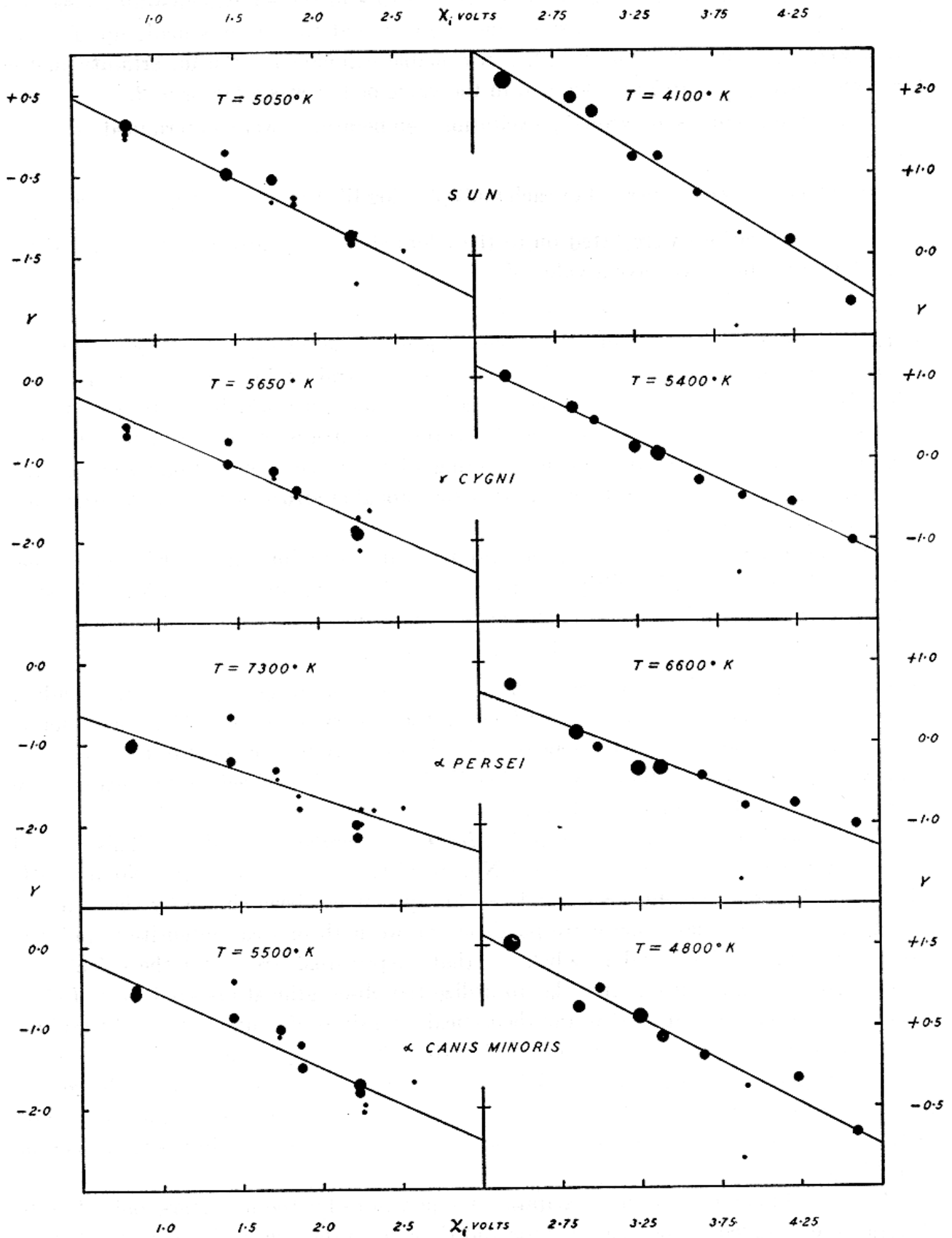


FIG. 9. Excitation Temperatures Determined from Theoretical Line Intensities.

(a) Transition Array No. 31  
Ti I  $3d^3 4s-3d^3 4p$ (b) Transition Array No. 50  
Fe I  $3d^6 4s 4p-3d^6 4s 5s$

TABLE 10. EXCITATION TEMPERATURES OF SOLAR-TYPE STARS  
(1942 DATA)

Atom	Array No.	Intensities	Sun		$\gamma$ Cygni		$\alpha$ Persei		$\alpha$ Canis Minoris	
			T ° K.	Wt.	T ° K.	Wt.	T ° K.	Wt.	T ° K.	Wt.
Sc II.....	29	LS	3500 ± 550	—	6100 ± 1200	—	5000 ± 1500	—	4400 ± 1100	—
Ti I.....	30		10500 ± 2000	—	11500 ± 2500	—	12000 ± 5000	—	13000 ± 5000	—
Ti I.....	31		5800 ± 850	—	6900 ± 1000	—	7600 ± 800	—	6350 ± 600	—
Ti II.....	36		7500 ± 5000	—	8500 ± 6000	—	7500 ± 4500	—	5500 ± 1400	—
Fe I.....	49		4150 ± 1000	—	3800 ± 1000	—	3050 ± 900	—	4000 ± 1200	—
Fe I.....	50		4100 ± 150	6	5400 ± 150	10	6600 ± 500	6	4800 ± 250	6
Ti I.....	30	LS + <i>gf</i>	4700 ± 750	2	4650 ± 850	1	4550 ± 1250	1	4950 ± 1150	1
Ti I.....	31		5050 ± 300	4	5650 ± 350	4	7300 ± 750	3	5500 ± 350	5
Fe I.....	49		5350 ± 450	1	3850 ± 350	1	3550 ± 300	1	4950 ± 450	1
Ti I.....	—	<i>gf</i>	4700 ± 200	8	5250 ± 300	6	5700 ± 550	3	5850 ± 450	5
Fe I.....	—		4700 ± 300	6	5800 ± 500	3	6100 ± 550	3	6150 ± 400	7
Adopted Temperature.....			4600		5350		6000		5500	

agreement between individual multiplets and no valid reason could be advanced why it should not be used; the three transition arrays for which corrected theoretical intensities were used—Nos. 30 and 31 of Ti I and No. 49 of Fe—should be satisfactory for this purpose though for a few lines there was no way of correcting the intensities by means of the  $f$ -values; and one would expect that the temperatures determined from the  $f$ -values alone should be reliable. The weights assigned to each determination of an excitation temperature are listed in the column following the probable error for each star in Table 10. These weights depend on: (1) the sum of the weights of individual lines in the multiplet; (2) a factor governed by the fit of the observations of each multiplet on the curve of growth; (3) the square of the range in excitation potential covered by the transition array; and (4) the probable error of the temperature factor,  $\theta = (5040/T)$  in the least-squares solution of equation (25). The adopted excitation temperatures given at the end of Table 10 have been determined from  $\theta$  rather than from the temperatures which are listed in the Table because it is the temperature factor which is determined directly from the least-squares solution; (the results, however, are not greatly altered by this procedure). No probable errors have been given for the adopted temperatures in Table 10 although they have been calculated for each individual determination. The possibility of systematic errors in the combination of the results obtained for different elements by the use of different methods is large and the mathematical probable errors would have little significance. However, at the time these results were obtained, it was thought that an estimate of 200° as the uncertainty in the excitation temperatures of these solar-type stars seemed to be reasonable.

#### THE SOLAR CURVE OF GROWTH

The use of theoretical intensities for lines in a given transition array made it possible to draw curves of growth for many atoms and this method was used by Menzel, Baker, and Goldberg<sup>136</sup> (combined with Allen's equivalent-width measurements for the sun) to derive a solar curve of growth. These workers and others at Harvard Observatory adopted this solar curve of growth as a standard and showed how solar  $\log X_0^1$ -values could be obtained for any line, the equivalent width of which had been measured on spectra taken at the centre of the solar disk.

However, supermultiplet intensities depend on the accuracy with which the energy levels within an atom follow LS (Russell-Saunders) coupling—see Appendix. For simple atoms, the spin-orbit interaction is small compared with the Coulomb interaction, and there is very little interaction between configurations; but for complex atoms, such as neutral iron and titanium, there are many intercombination lines and it is to be expected that LS coupling would break down with the result that the calculated theoretical intensities would depart from observed values. Thus it would seem that laboratory data are to be preferred to theoretical intensities if they are obtained under sufficiently controlled conditions. Unfortunately laboratory intensities, measured in emission, require particularly rigid observing conditions to determine the temperature and to correct for self-reversal effects. Measurements of laboratory intensities which were published to the end of 1938 are summarized by Unsöld<sup>137</sup>.

<sup>136</sup> *Ap. J.*, 87, 81, 1938.

<sup>137</sup> *Physik der Sternatmosphären*, p. 207.

The most extensive series of laboratory intensities, given in terms of oscillator strengths, are those for neutral iron and titanium published by R. B. King and A. S. King<sup>138</sup>—as already mentioned. These measures were made on photographs of spectra taken through an absorption furnace where the number of atoms was such that the intensities of all lines lay on the Doppler portion of the curve of growth; it is believed that individual measurements are accurate within about ten per cent. The writer<sup>135</sup> compared these measurements with theoretical intensities—see also Appendix—and showed that serious discrepancies existed; it appears that the intensity rules hold fairly well within multiplets, but the multiplet strengths ( $S$ ) are frequently in error.

Therefore a curve of growth for the sun was constructed by the writer<sup>135</sup> with the aid of equivalent widths measured by Allen<sup>139</sup> and by himself from the Utrecht *Photometric Atlas of the Solar Spectrum*<sup>140</sup>, combined with the Kings' laboratory  $g,f \cdot \lambda$ -values. Equivalent widths of about one thousand lines in the *Atlas* in the region  $\lambda\lambda$  3500-6750 have been measured either by counting squares or with the planimeter, after corrections for blending with other lines and for the position of the continuous spectrum had been made. The agreement between Allen's data and the Utrecht values is very satisfactory. The probable error of any given equivalent width is about 7 per cent for very weak lines ( $W < 0.050$  A.) and slightly less than 6 per cent for all stronger lines. As no systematic differences have been detected, average values have been used whenever a line was available in each publication.

King and King's measures of Fe I lines give values of  $g,f$  for 115 lines ranging in excitation potential from 0.0 to 1.6 volts; and their measures of Ti I lines give  $g,f$ -values for 227 lines in the range 0.0 to 2.5 volts. Of these lines, 75 iron lines and 137 titanium lines were sufficiently free from blending effects in the solar spectrum to be used in determining a solar curve of growth.

In this determination, lines of iron and titanium were considered separately, and were divided into groups according to excitation potential. For each small range in excitation potential,  $\log W/\lambda$  was plotted against  $\log g,f \cdot \lambda$ . We can write equation (21) as

$$\log X_0 = C + \log g,f \cdot \lambda - \frac{5040}{T} \chi_i \quad (27)$$

where the first term in the right member is a constant for a given atom and a given curve of growth. As already noted, each plot must be shifted horizontally relative to the others in order to form a single curve of growth for the sun. When the mean curve has been formed, the abscissa of which is termed  $\log X_f$ , then the shift of each plot,  $\log X_f - \log g,f \cdot \lambda$  is proportional to  $\chi_i$ ; and when these values are plotted, the slope of the straight line drawn through the points is given by  $5040/T$ . Numerous determinations of the excitation temperature of the sun have been made for these atoms, using variations of the above method, and it has been found that the best values are  $4550 \pm 125^\circ$  K. for Ti I, and  $4850 \pm 125^\circ$  K. for Fe I. It would seem that until  $f$ -values become available for additional atoms, a mean value of  $4700^\circ$  K. for the sun should be used when lines of atoms other than Ti I or Fe I are used to derive stellar curves of growth.

<sup>138</sup> *Ap. J.*, 87, 24, 1938.

<sup>139</sup> *Mem. Comm. Sol. O.*, Canberra, 1, No. 5, 1934; 2, No. 6, 1938.

<sup>140</sup> Minnaert, M., G. F. W. Mulders, and J. Houtgast, Schnabel, Kampert, and Helm, Amsterdam, 1940.

The mean solar curve of growth shown in Fig. 10 is an empirical curve obtained by combining the two curves for Ti I and Fe I. The titanium lines cover the region shown by the closed circles in Fig. 10 from the Doppler straight line to the transition portion; the iron lines, shown as crosses, include the transition and damping portions of the curve. When the two sets of observations were brought together, there was sufficient overlap to determine the shift necessary to fit one on the other quite accurately: it is necessary to add 3.01 to the relative  $f$ -values of iron to form a single mean curve covering the observations for both neutral titanium and neutral iron lines. As already noted<sup>135</sup>, the empirical curve does not fit any possible theoretical curve precisely, since the values of  $\log W/\lambda$  for the shoulder between the Doppler and transition portions of the empirical curve are above those for any theoretical curve which is made to fit the lower Doppler and the flat transition region. Similarly at the point where the transition portion changes to

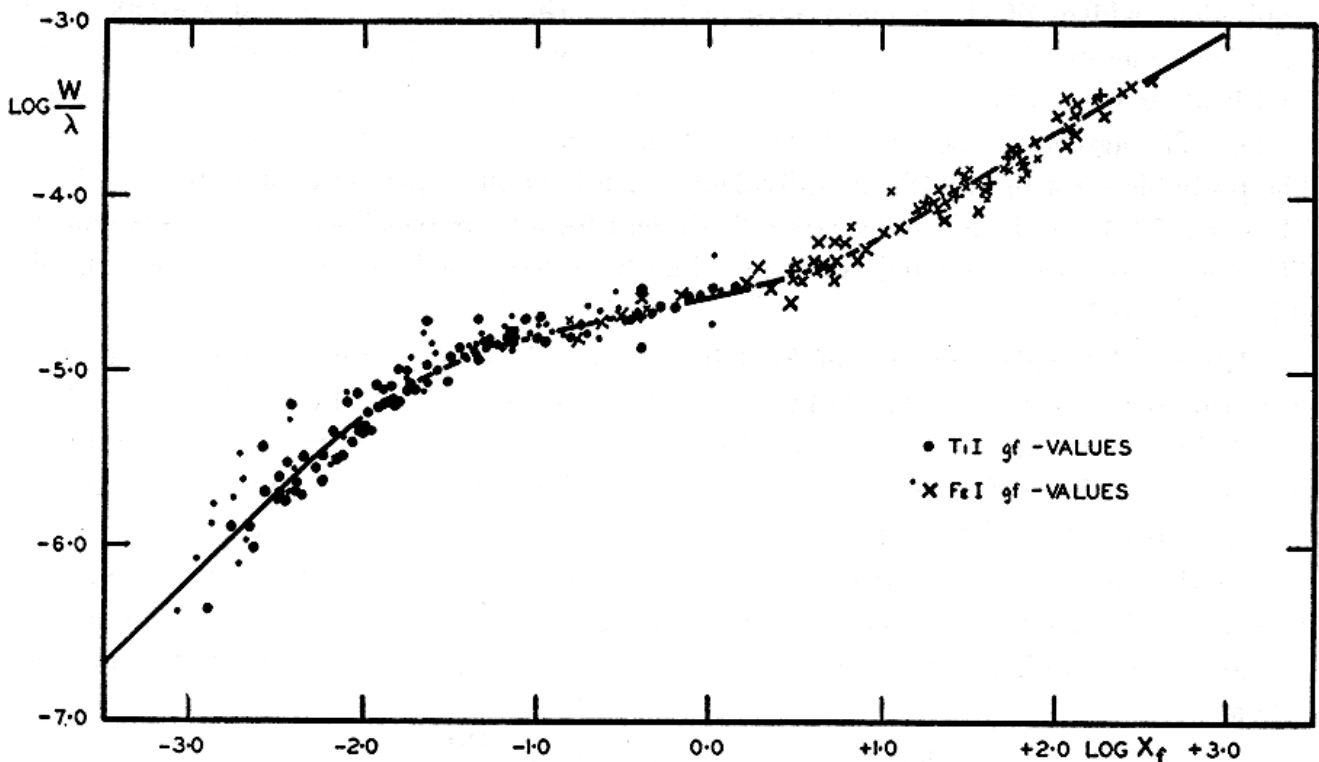


FIG. 10. Solar Curve of Growth Determined from Laboratory  $g,f$ -Values.

The origin of the  $\log X_f$ -scale is based on King's absolute  $f$ -values for Fe I. The size of each point is approximately proportional to the weight assigned to the line. The relative shift of each multiplet has been calculated for an excitation temperature of 4550° K. for Ti I and 4850° K. for Fe I.

the damping region of the curve the  $\log W/\lambda$ -value for the empirical curve is below that for the theoretical curve. In addition, the slope of the straight line which fits the points on the damping portion of the curve is nearly 0.60, which has been adopted in this paper, rather than the theoretical value of 0.50. The best theoretical curve which could be fitted to the observations corresponded to a velocity,  $v$ , of 1.6 km/sec. and a damping factor,  $\Gamma/\nu$ , of  $2.61 \times 10^{-6}$ .

The origin of abscissae adopted for the solar curve shown in Fig. 10 is based on the absolute  $f$ -values of neutral iron lines determined by R. B. King<sup>141</sup>.

He found that

$$\log f_{\text{abs.}} = \log f_{\text{rel.}} - 3.73.$$

<sup>141</sup> *Ap. J.*, 95, 78, 1942.

Therefore the solar  $\log X_f$ -values are based on the equation

$$\log X_f = \log g,f \cdot \lambda - 3.73 - 5040 \chi_i/T \quad (28)$$

where  $g,f$  is the relative  $f$ -value given by King and King.

The solar  $\log X_f$ -values listed in Table 4 are taken directly from this curve by reading off the value of  $\log X_f$  corresponding to a given value of  $\log W/\lambda$ , where  $W$  is the mean of the equivalent widths of a given line as published by Allen and as measured by the writer in the Utrecht *Photometric Atlas of the Solar Spectrum*. The curve from which the  $\log X_f$ -values listed in Table 3 were read is slightly different from that which was used in this investigation. It follows the observations even more closely than that of Fig. 10, but is not sufficiently different to warrant further discussion.

In the calculation of the composition of the solar atmosphere the relation between  $\log X_f$  and  $\log X_0$  is found useful:

$$\log X_0 = \log X_f + 1.86 . \quad (29)$$

#### STELLAR CURVES OF GROWTH OBTAINED WITH THE AID OF SOLAR LOG $X_f$ -VALUES

The observational result that excitation temperatures obtained for dwarfs seemed to be lower than those for giant stars when theoretical intensities were used to study curve-of-growth phenomena indicated the necessity for further analysis of the observations. As already mentioned, one of the most serious sources of error lay in the theoretical intensities themselves and therefore it was decided to derive a new curve of growth for the sun which could be used as a basis for comparison with stellar line intensities. It is believed that the solar  $\log X_f$ -values are the best data available at present for most lines although this cannot be said without some reservation as Struve has pointed out in a letter to the writer: "the continuous absorption coefficient is probably different from that in a supergiant star; as this coefficient . . . [varies] with wave-length, if it is materially different in the two stars the solar  $\log X_f$ -value would not give accurate results for the star." No suggestion that such a condition exists has been detected as yet in studies of line intensities and it is believed that the method is satisfactory for the study of intensities in the spectra of solar-type stars.

In the final study of curves of growth presented in this paper, all lines in Tables 3 and 4 were separated according to element and stage of ionization; they were then divided into groups according to excitation potential, each group having a range of about half a volt. For each line in such a group,  $\log W/\lambda$  was plotted against  $\log X_f$  to form a portion of the curve of growth. The several plots for each atom were superposed and shifted horizontally along the abscissa until the best empirical curve was formed. Representative curves for a few atoms are shown in Figs. 11, 12, 13, and 14; lines of different excitation potential are distinguished by different symbols. It is seen immediately that the curves for neutral and ionized atoms are different in shape for the stars—those for the sun should all be the same, of course, since it has been necessary to assume that the ionized atoms follow the same curve of growth as that derived for neutral atoms in obtaining the  $\log X_f$ -values. Further it is unlikely that there is any large difference between the curve obtained from observations of the centre of the disk, from which the  $\log X_f$ -

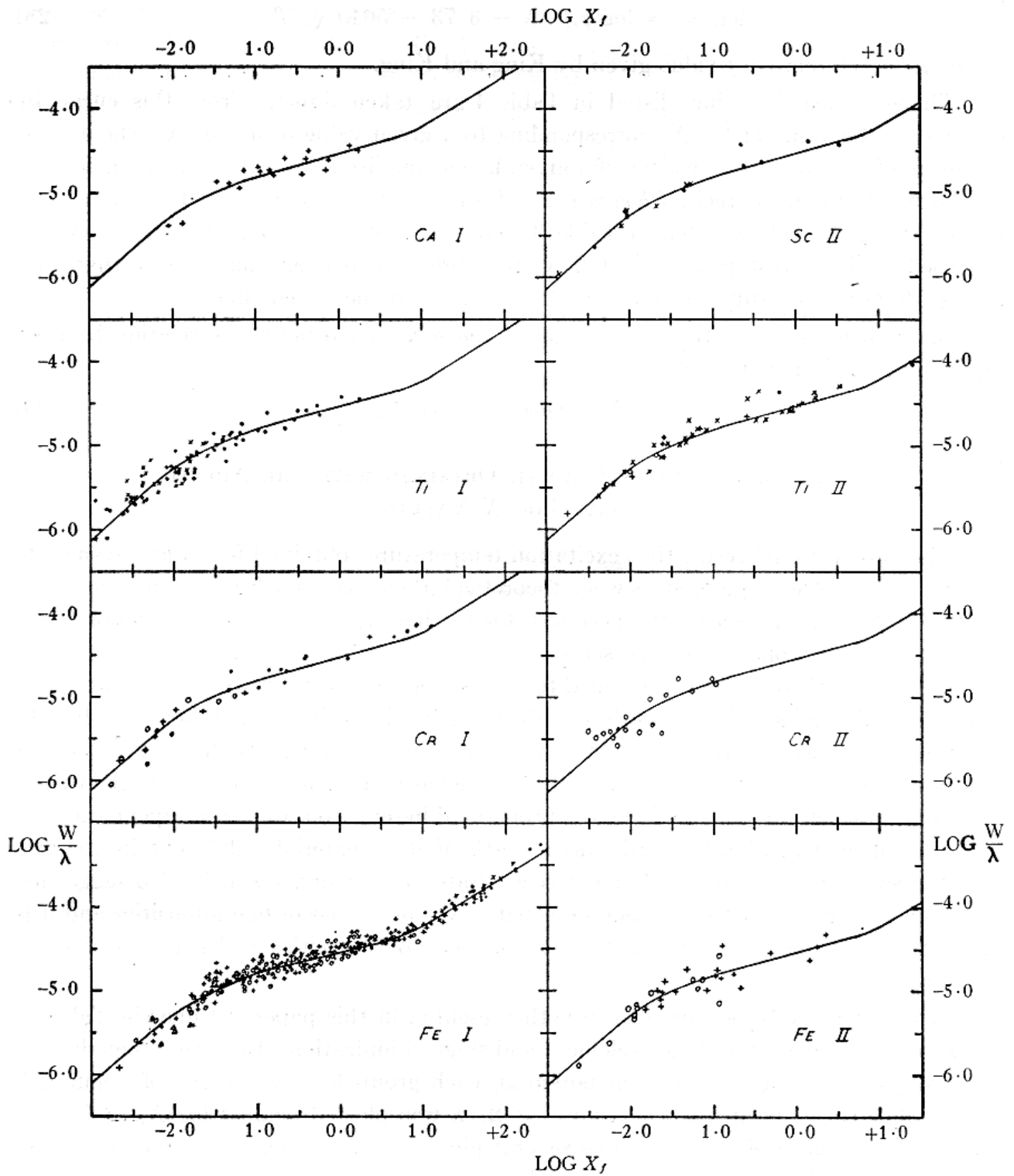


FIG. 11. Solar Curve of Growth Based on Victoria Equivalent-Width Measures and  $\log X_f$ -Values.

The observations for both neutral and ionized atoms fit the same curve and the scatter about the curve indicates to some extent the uncertainty of the measures. In Figs. 11-14 the  $\log W/\lambda$ -scale has been reduced to absolute units by adding  $-6.0$  to the values given in Tables 3 and 4.

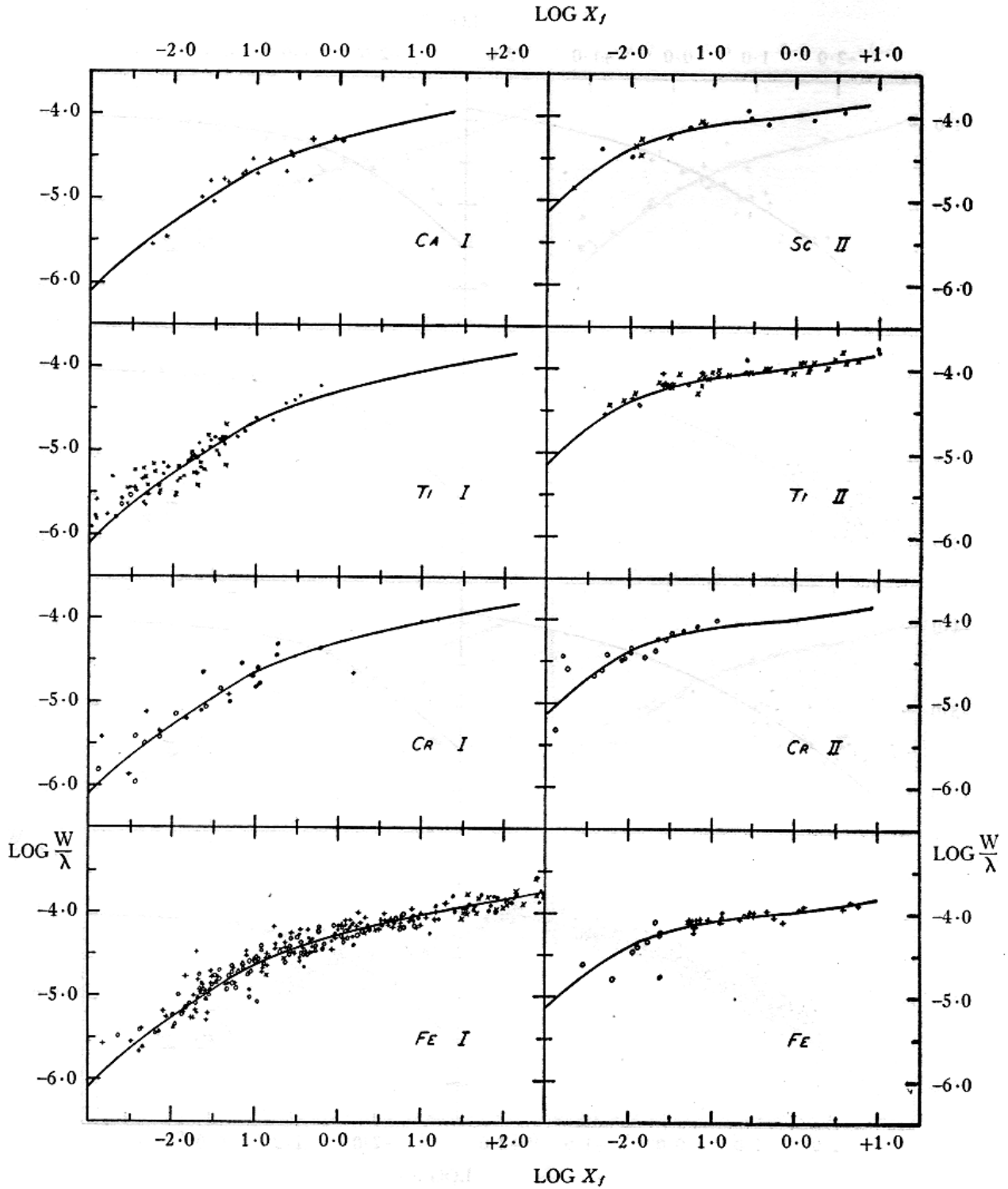


FIG. 12. Empirical Curves of Growth for  $\gamma$  Cygni.

Plots for each excitation potential have been shifted to give the best fit on the adopted mean curve, which is shown as a solid line; each symbol represents a different excitation potential. Note that the shape of the curve for neutral atoms is different from that for ionized atoms. The lower right diagram is for Fe II.

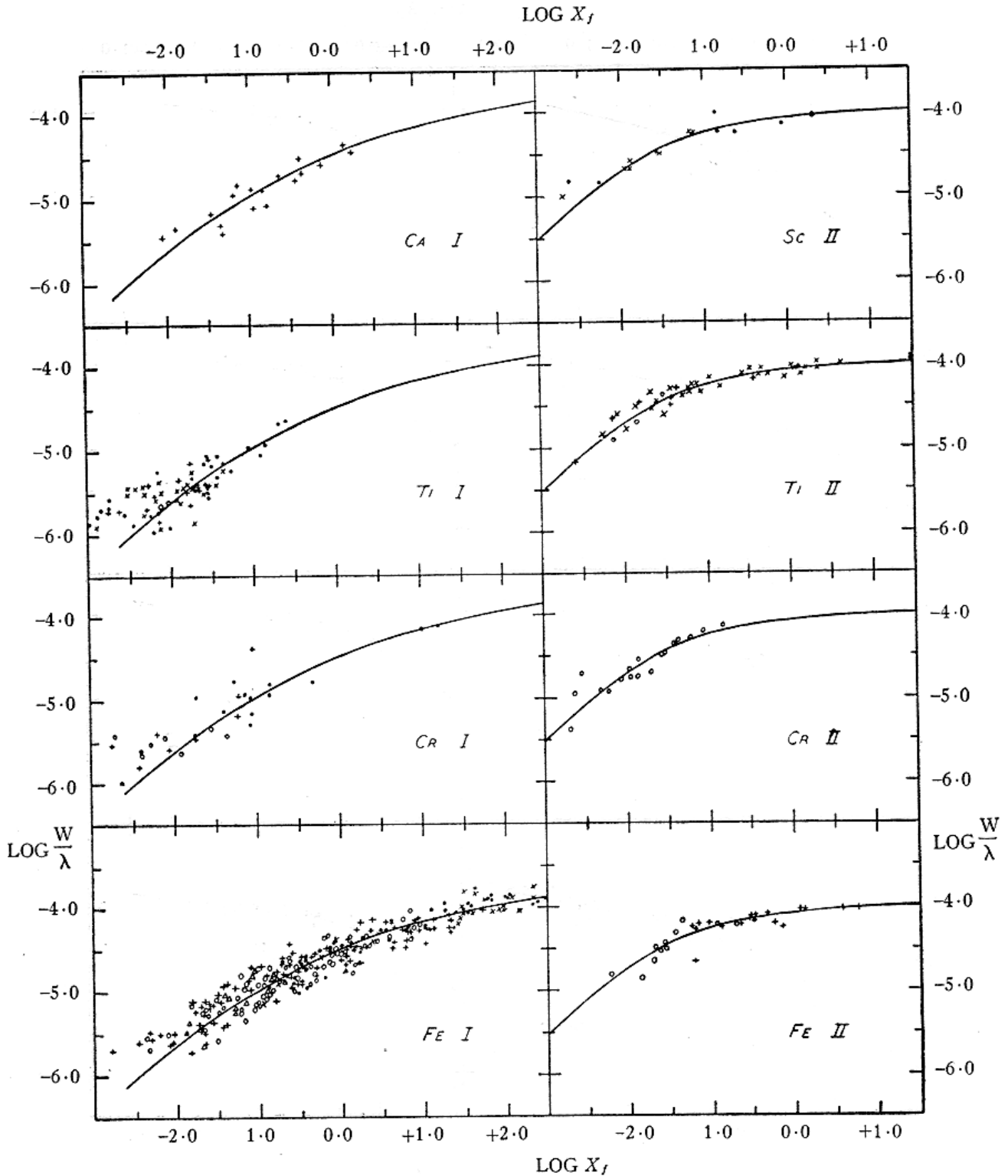


FIG. 13. Empirical Curves of Growth for  $\alpha$  Persei.

The plots of the observations for representative atoms have been fitted on the adopted mean curve which is shown as a solid line. One curve has been adopted for all neutral atoms and a different curve has been adopted for ionized atoms. The plot for each excitation potential has been treated separately to give the best fit on the curve. The large scatter shown by the Ti I lines is a result of the weakness of the lines, many of which are barely visible.

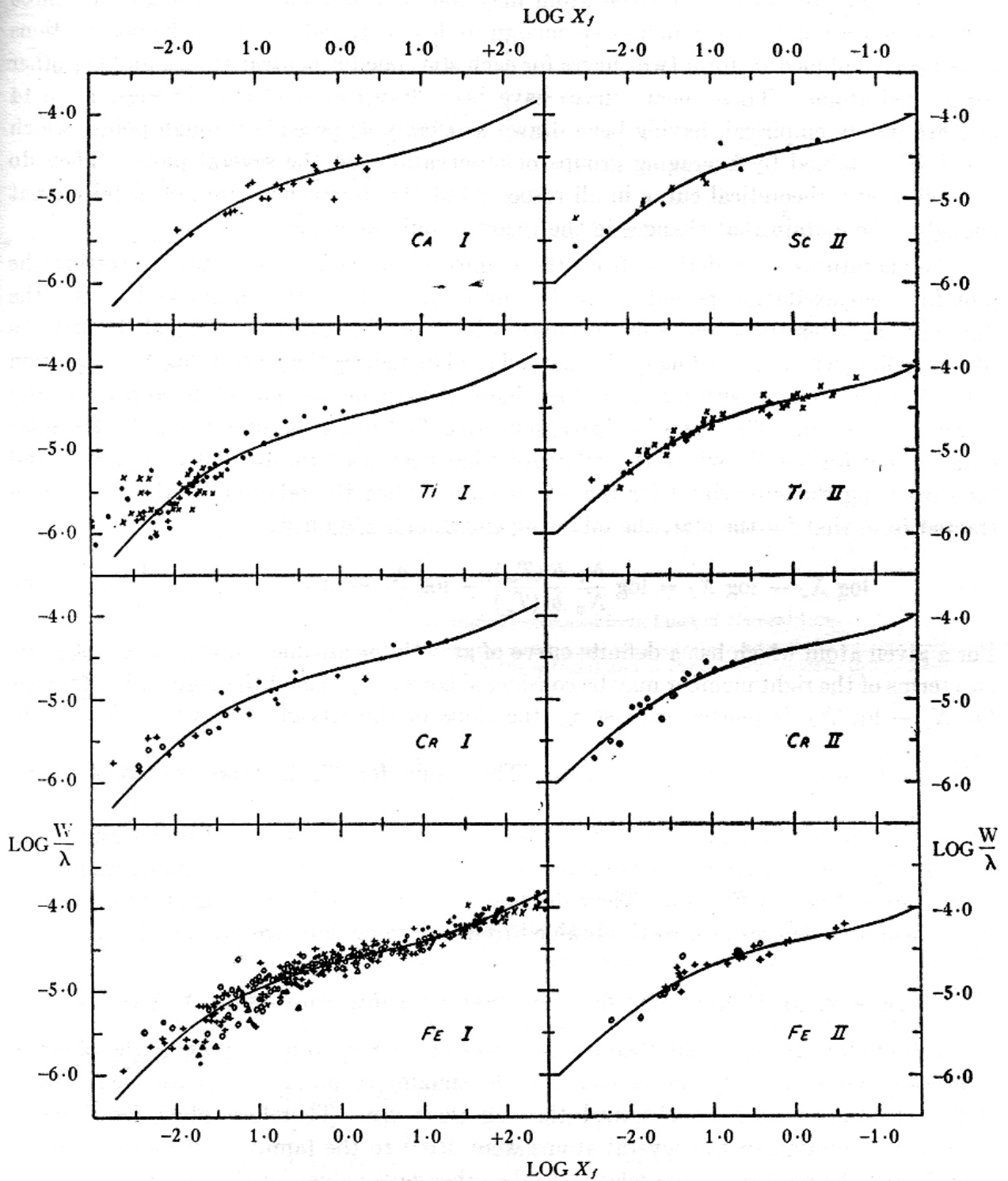


FIG. 14. Empirical Curves of Growth for  $\alpha$  Canis Minoris.

The observations for representative neutral and ionized atoms have been superposed on the adopted mean curve which is shown as a solid line. Plots for each excitation potential, indicated by different symbols, have been fitted separately to the appropriate curve for neutral or ionized atoms. The scatter of the observations for Ti I and Fe I seems rather large but the lines are very narrow and weak lines are seriously affected by plate grain.

values were obtained, and that for integrated sunlight. Although it is possible that different lines produced by a given atom may follow a different curve of growth, these observations are not usually definitive enough to detect it, and therefore the observations have been combined to form two curves for each star, one for neutral atoms, and the other for ionized atoms. These mean curves have been drawn as solid lines in Figs. 11 to 14 and are purely empirical, having been drawn as closely as possible through points which had been obtained by averaging groups of observations on the several plots. They do not follow any theoretical curve in all respects but the divergences are not usually great enough to be certain that changes in the theory should be made.

Temperatures were derived from the empirical curves for each star by setting the plot for each excitation potential on the curve adopted for that atom and noting the difference between the abscissa of the curve, which may be called  $\log X_*$ , and that for the plotted points which, according to the method used in making the plots, is  $\log X_f$ . Equation (21) gives the relation between  $X_*$  and  $f$ -values; it may be considered to apply for any star or for the sun. This equation is written twice, first using the subscript  $\odot$  for the solar data (except for  $\log X_f$ , where the subscript  $f$  has been used throughout this paper), and then inserting the subscript  $*$  for the stellar data; when the relation for the sun is subtracted from that for the star, the following equation is obtained:

$$\log X_* - \log X_f = \log \frac{N_*}{N_\odot} \frac{b(T_\odot)}{b(T_*)} - \log \frac{v_*}{v_\odot} - 5040 \chi_i \left( \frac{1}{T_*} - \frac{1}{T_\odot} \right). \quad (30)$$

For a given atom which has a definite curve of growth (as assumed in this paper) the first two terms of the right member may be considered constant; then if the observed difference,  $\log X_* - \log X_f$ , is plotted against  $\chi_i$ , the slope of the straight line which defines the points best is given by  $5040 \left( \frac{1}{T_*} - \frac{1}{T_\odot} \right)$ . The value for  $T_\odot$  is taken as  $4550^\circ \text{K}$ . for

Ti I,  $4850^\circ \text{K}$ . for Fe I and  $4700^\circ \text{K}$ . for all other atoms, as suggested previously. The results for representative atoms are given in Table 12 and are shown diagrammatically for neutral iron atoms in Fig. 15. Their discussion is postponed until temperatures derived from theoretical curves of growth obtained from the same data are presented.

#### THEORETICAL CURVES OF GROWTH DERIVED FROM SOLAR $\log X_f$ -VALUES

Although it appears that theoretical curves of growth do not represent the observations completely, nevertheless a considerable amount of useful information concerning stellar atmospheres can be obtained through their use. Therefore plots for different excitation potentials of the several atoms were fitted to the family of theoretical curves (Fig. 7) and the position of one relative to the other gave values for the turbulent velocity,  $v$ , and the damping factor,  $\Gamma/v$ . The average values for each atom for which positive results could be obtained are listed in Table 11, together with the adopted values for the curves of growth of neutral and ionized atoms in each star. It is seen that reasonably accordant results are obtained—the mean values adopted for each curve are not greatly different from those found for each atom. As described elsewhere<sup>142</sup>, neutral iron lines

<sup>142</sup> *J. R. A. S., Can.*, **41**, 49, 1947.

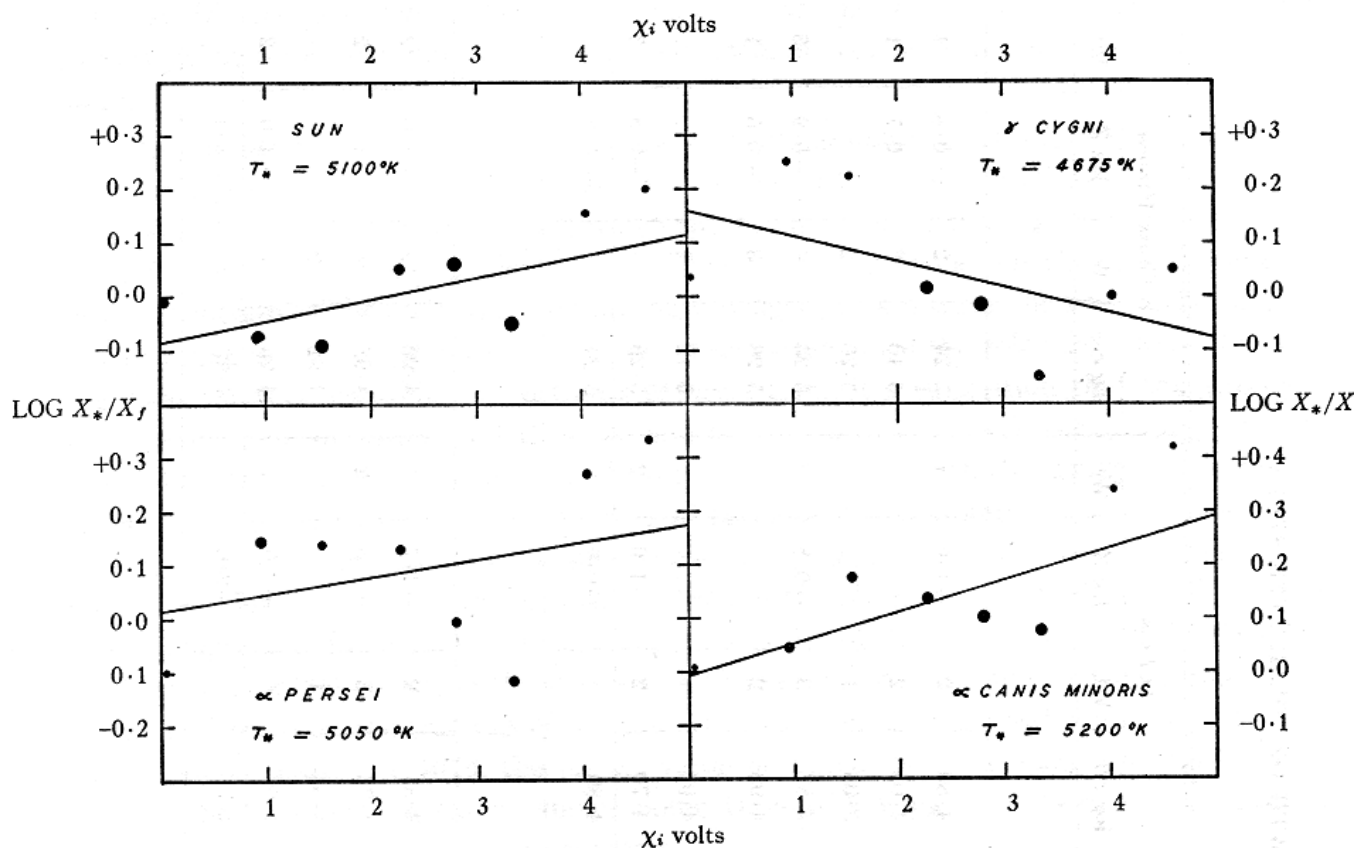


FIG. 15. Excitation Temperatures Determined from Lines of Neutral Iron.

Plots for each excitation potential were fitted to the mean curve for neutral atoms and the relative shifts of the abscissae gave  $X_*/X_f$ . The large scatter, particularly for  $\gamma$  Cygni and  $\alpha$  Persei may indicate that a single mean curve cannot be chosen to represent all the observations.

showed some variation in the turbulent velocity with excitation potential, but this effect could not be detected with any certainty for other atoms because so few lines were available for study.

The values adopted for  $v$  and  $\Gamma/v$  which are listed in Table 11 show clearly that ionized atoms behave in a manner different from neutral atoms when studied in relation to curve-of-growth phenomena, except in the case of the sun. For the sun, it was assumed that neutral and ionized atoms gave the same curve of growth when the  $\log X_f$ -values were derived because there were not sufficient  $f$ -values available for ionized atoms to detect any differences. When  $\log c/v$  is compared for neutral and ionized atoms, there is a difference for each star which is of the same order (about 0.2) in each case; this would appear to be real as the individual data for neutral atoms are almost all below the lowest values for the ionized atoms; the probable error of  $\log c/v$  is about 0.05 when determined from the values given in Table 11. (In Table 11 it will be found that the adopted values for the constants are sometimes slightly different from the means of the data given for the several atoms. This is because independent preliminary curves were drawn and these were given some weight in the determination of the adopted constants.) In addition to the difference in turbulent velocities between neutral and ionized atoms, these results suggest that there is a real difference from star to star. As it is known that the sun and

TABLE II. CONSTANTS FOR CURVES OF GROWTH OF SOLAR-TYPE STARS  
(1946 DATA)

Atom	Sun			$\gamma$ Cygni			$\alpha$ Persei			$\alpha$ Canis Minoris			
	log c/v	Wt.	log Z	log c/v	Wt.	log Z	log c/v	Wt.	log Z	log c/v	Wt.	log Z	Wt.
Neutral Atoms													
Ca I.....	5.18	2	-0.6	4.83	2	.....	4.89	2	-1.0	5.24	2	-0.8	1
Ti I.....	5.20	3	-0.6	4.76	1	.....	4.90	2	.....	5.10	3	-0.7	1
Cr I.....	5.15	2	-0.6	4.79	1	.....	5.05	1	.....	5.20	2	.....	.....
Fe I.....	5.18	4	-0.6	4.77	3	-1.1	4.87	3	-0.8	5.25	4	-0.9	3
Ni I.....	5.08	2	-0.6	4.82	2	.....	4.98	2	.....	5.26	3	-0.5	1
<i>f</i> -values													
Ti I.....	5.20	2	-0.7	4.82	2	.....	4.97	1	.....	5.12	2	.....	.....
Fe I.....	5.20	2	-0.5	4.65	3	-1.2	4.70	2	-1.0	5.20	4	-0.8	3
Adopted.....	5.19		-0.6	4.77		-1.1	4.89		-0.9	5.24		-0.8	
Ionized Atoms													
Sc II.....	5.21	2	-0.7	4.65	2	-2.2	4.81	2	-1.7	4.93	2	-1.0	2
Ti II.....	5.20	3	-0.6	4.65	3	-2.0	4.73	3	-1.8	4.98	4	-1.0	2
Cr II.....	5.17	2	.....	4.58	1	.....	4.54	1	.....	4.92	2	.....	.....
Fe II.....	5.19	3	-0.7	4.58	2	-2.2	4.68	3	-2.0	4.96	3	-1.0	2
Adopted.....	5.19		-0.6	4.62		-2.1	4.71		-2.0	4.97		-1.0	

$\alpha$  *Canis Minoris* are dwarf stars and that  $\gamma$  *Cygni* and  $\alpha$  *Persei* are supergiants, this investigation would indicate that turbulent velocities may be lower in dwarf than in giant stars.

Results for the damping constant,  $\log Z$ , while apparently giving a higher value of  $\Gamma/\nu$  for neutral atoms than for ionized atoms, cannot be considered as definitive since there are very few lines in these stars which show real evidence of wings to prove that they lie on the damping portion of the curve. There is no question about the strong iron lines in the spectrum of the sun; they are strongly winged, as are those for a few other atoms, but no conclusions can be drawn from this observation since the solar data were taken as the basis for this research. In  $\alpha$  *Canis Minoris* there is a suggestion that the strongest lines have traces of wings, and that the end of the curve of growth is beginning to turn upwards, but the agreement between the observational data with the family of theoretical curves is none too good—part of this lack of agreement undoubtedly arises from the fact that it was necessary to adopt a solar curve of growth which also did not follow the theoretical data when a curve was drawn through the observational material. Profiles of a few of the lines of neutral iron best suited for a study of the wings are shown in Plate IV. In this region  $\lambda$  3860 is one of the strongest iron lines which is not in the wing of one of the hydrogen lines, and the tracings of  $\gamma$  *Cygni* and  $\alpha$  *Persei* show no real evidence of a wing. On the other hand,  $\lambda$  4046, the  $\log X_f$ -value of which is of the same order as  $\lambda$  3860 though the  $f$ -value is greater, shows some trace of a wing in  $\gamma$  *Cygni*; other lines of the same multiplet, however, are narrower.

In spite of this difficulty, some estimate of the damping factor can be made from the length of the transition portion of the curve of growth. If the values of  $\log Z$  were less negative than those given in Table 11, the curves would have begun to rise above the flat portion. The values adopted may be considered as maximum estimates in each case, and it is believed, therefore, that there is evidence that the damping constant is greater for neutral than for ionized atoms.

Excitation temperatures have been determined from the theoretical curves of growth by applying equation (30) and the same method as for the empirical curves. Table 12 gives temperatures determined from both empirical and theoretical curves for all atoms where there were sufficient observations available to place any reliance on the results. The data for neutral and ionized atoms have been separated for each star; weighted mean values are listed at the end of each section and the adopted temperature for each star—the mean of all these determinations—is given at the end of the table. As the quantity  $\theta = 5040/T$  is the value which is determined directly from the plots between  $\log X_i/X_f$  and  $\chi_i$ , the weighted means have been calculated from the  $\theta$ -values and then have been transformed into the temperatures which are given in the Table. The probable errors of these temperatures have been calculated for Ti I and Fe I; when the probable error of the solar temperature is included, these values range from 200 to 400° K. It would seem that the probable error of the adopted temperature for each star is about 300° K.

A study of Table 12 shows that the same temperatures are obtained from these data whether empirical or theoretical curves are employed in the determination. The values obtained from the laboratory  $f$ -values of Ti I and Fe I are somewhat higher than those where the  $\log X_f$ -values were employed. This difference may be due to the fact that

TABLE 12. EXCITATION TEMPERATURES OF SOLAR-TYPE STARS

(1946 DATA)

Atom	Sun				$\gamma$ Cygni				$\alpha$ Persei				$\alpha$ Canis Minoris			
	Emp.	Wt.	Theor.	Wt.	Emp.	Wt.	Theor.	Wt.	Emp.	Wt.	Theor.	Wt.	Emp.	Wt.	Theor.	Wt.
Neutral Atoms																
	° K.		° K.		° K.		° K.		° K.		° K.		° K.		° K.	
Na I	4650	1	4325	1	4775	1	4750	1	4425	1	4175	1	4900	1	5125	1
Mg I	5200	1	4775	1	4575	1	4525	1	5350	1	5275	1	5025	1	5175	1
Si I	5075	—	4775	—	4850	—	4975	—	5800	—	5425	—	5175	—	5175	—
Ca I	4825	2	4500	2	4150	1	4700	1	5150	1	5175	1	4775	2	5025	1
Ti I	4550	6	4675	6	5050	5	5025	4	5775	3	6100	3	5175	2	5250	3
V I	5550	1	5400	—	5775	—	5175	—	6325	—	5075	—	6425	—	6125	—
Cr I	4550	3	4600	1	4725	3	4825	2	4900	2	5025	1	4625	2	4600	1
Mn I	5075	2	4850	2	4675	2	4625	2	4550	2	4500	1	4575	2	4400	2
Fe I	5100	15	5025	13	4675	13	4900	11	5050	10	5350	9	5200	9	5125	11
Ni I	4550	3	4625	4	4300	3	4375	3	4625	3	4525	3	4700	2	4825	3
<i>f</i> -values																
Ti I	5175	2	5050	2	6000	2	6400	2	6700	1	7150	1	5200	1	5050	2
Fe I	5025	3	5175	2	5075	2	5200	1	5825	2	5875	1	5425	2	5150	2
Mean . . . .	4900	39	4825	34	4775	33	4900	28	5100	26	5250	22	5000	24	5000	27
Mean Neutral.	4875				4825				5175				5000			
Ionized Atoms																
Sc II	4750	1	5300	1	4775	—	7525	—	7775	—	8375	—	8450	—	10600	—
Ti II	4925	4	4875	3	5500	3	5550	3	4400	4	5100	3	5075	3	5050	3
Cr II	3975	—	4025	—	8675	—	11850	—	6475	—	6675	—	5175	—	4725	—
Fe II	4750	2	4800	2	3425	1	3875	1	4425	2	4725	1	4950	2	4950	1
Mean	4850	7	4900	6	4775	4	4925	4	4425	6	5000	4	5025	5	5025	4
Mean Ionized .	4875				4850				4700				5025			
Mean, Neutral + Ionized Atoms	4875				4825				5100				5000			

There are fewer lines for which *f*-values are available and that they arise from low levels of excitation. It could be inferred from these results that the same curves of growth are not applicable to lines of high excitation—this is the result that has been studied elsewhere<sup>142</sup> for lines of neutral iron—but even if that were the case, the temperatures would not be greatly different. In any event, such an effect is not large, and for most atoms it is impossible to do better than to adopt a mean curve of growth and obtain the best results possible from it.

The results for the neutral atoms have been given greater weight than those for the ionized atoms not only because there are more lines available, but, in most cases, there are more lines which occur on the Doppler or damping portions of the curve of growth where differences in  $\log X_0$  between star and sun can be detected—since this difference is the quantity which determines the temperature. For the giant stars particularly, the lines of the ionized atoms are strong and lie on the flat transition portion of the curve. Therefore the temperature is very poorly determined and, indeed, it is surprising that the values given in Table 12 agree as well as they do and that the mean values are so nearly the same as those for the neutral atoms.

Since the temperatures determined for neutral and ionized atoms differ by less than the probable errors, a weighted mean value has been adopted as the excitation temperature for each star.

#### DISCUSSION OF RESULTS AND COMPARISONS WITH OTHER OBSERVERS

In Table 13 are compiled most of the available results, for the stars studied in this paper, on turbulent velocities, damping factors and excitation temperatures; it includes the results obtained by the author in 1942 when the same observations were studied using theoretical intensities. As early investigations were not sufficiently detailed to show differences between neutral and ionized atoms, it is not easy to compare the results but it is seen that, when this difficulty is considered, the differences between observers are not unduly large.

#### TURBULENT VELOCITIES:

For the sun, the lines are quite sharp and studies of line profiles by Allen<sup>143</sup> and by ten Bruggencate<sup>144</sup> indicate that the turbulent velocity is not more than 1.8 km/sec. The results summarized in Table 13 may be taken to agree with this conclusion. Curves of growth obtained at Harvard Observatory<sup>145</sup> have been taken to indicate that the velocity may be considered as purely thermal, with temperatures of 5740° K. and 5400° K., respectively. The lines in  $\alpha$  *Canis Minoris* are even sharper in appearance than those of the sun and it would be expected that the turbulent velocities should be small. The differences in the curves of growth for neutral and ionized atoms suggest that if they can be interpreted in terms of real velocities it might be possible to check this result by measurements of the shape of line profiles for neutral and ionized atoms.

For the stars,  $\gamma$  *Cygni*,  $\alpha$  *Persei* and  $\alpha$  *Canis Minoris* it would appear that the turbulent velocities are different for neutral and ionized atoms. As noted in a previous *Contribution*<sup>146</sup>, observations of line intensities in the spectrum of  $\alpha$  *Persei* suggest that the velocity may vary from atom to atom, whether it be neutral or ionized. If this result is verified by later investigations it seems difficult to escape the conclusion that there is a definite stratification in the atmospheres of these stars. In view of the appearance of solar flash spectra and the inferred great extension of the atmospheres of giant stars, such a suggestion does not appear unreasonable. However, refinements in the theory may suggest other interpretations of this result.

<sup>143</sup> *Ap. J.*, 85, 165, 1937.

<sup>144</sup> *Z. f. Ap.*, 18, 316, 1939.

<sup>145</sup> Menzel, D. H., *Ap. J.*, 84, 462, 1936; Rubenstein, Pearl J., *Ap. J.*, 92, 114, 1940.

<sup>146</sup> *J. R. A. S., Can.*, 40, 183, 1946.

TABLE 13. CONSTANTS DETERMINED FROM CURVES OF GROWTH OF SOLAR-TYPE STARS

## (a) Results of the Present Investigation

	Sun <i>g, f</i> -curve	Sun		$\gamma$ Cygni		$\alpha$ Persei		$\alpha$ Canis Minoris	
		Neutral Atoms	Ionized Atoms	Neutral Atoms	Ionized Atoms	Neutral Atoms	Ionized Atoms	Neutral Atoms	Ionized Atoms
$v_*$ km/sec.....	1.6	2.0	2.0	5.1	5.8	3.9	5.9	0.7	3.2
$v_T$ km/sec.....	0.9	1.5	1.5	5.0	5.6	3.7	5.7	1.2	3.0
$\Gamma/\nu \times 10^6$ .....	2.6	1.6	1.6	1.3	0.15	1.6	0.20	0.9	1.1
$T^\circ$ K.....	4700	4875	4875	4825	4825	5100	5100	5000	5000

## (b) Results of Earlier Investigations

Author	Sun				$\gamma$ Cygni		
	Menzel Baker and Goldberg <sup>1</sup>	Rubenstein <sup>2</sup>	Wright <sup>3</sup>	Wright <sup>4</sup>	Wright <sup>3</sup>	Bailey <sup>5</sup>	Sahade and Cesco <sup>6</sup>
Date	1938	1940	1942	1943	1942	1942	1946
$v_*$ km/sec.....	1.4	1.34	2.1	1.6	6.7	6.9	7.6
$\Gamma/\nu \times 10^6$ .....	1.52	1.7	3.5	2.6	3.5	.....	.....
$T^\circ$ K.....	4400	5400	4600	4700	5350	5600	4600

Author	$\alpha$ Persei					$\alpha$ Canis Minoris	
	Struve and Elvey <sup>7</sup>	Dunham <sup>8</sup>	Wright <sup>3</sup>	Steel <sup>9</sup>	Wright <sup>10</sup>		Wright <sup>3</sup>
					Neutral Atoms	Ionized Atoms	
Date	1934	1934	1942	1945	1946		1942
$v_*$ km/sec.....	7	5	6.0	3.7	4.5	7.2	2.6
$\Gamma/\nu \times 10^6$ .....	.....	.....	5.2	1.2	1.5	0.1	3.0
$T^\circ$ K.....	.....	.....	6000	4400	5075	5350	5500

<sup>1</sup> *Ap. J.*, 87, 81, 1938.<sup>2</sup> *Ap. J.*, 92, 114, 1940.<sup>3</sup> *This Paper*, p. 71.<sup>4</sup> *Ap. J.*, 99, 249, 1944.<sup>5</sup> Thesis, Dept. of Physics, U. of Arizona, 1942.<sup>6</sup> *Ap. J.*, 104, 133, 1946.<sup>7</sup> *Ap. J.*, 79, 409, 1934.<sup>8</sup> *Mt. W. An. Rep.*, p. 149, 1933-34.<sup>9</sup> *Ap. J.*, 102, 43, 1945.<sup>10</sup> *J. R. A. S. Can.*, 40, 183, 1946.

## DAMPING FACTORS

As noted in the introduction, the damping factors derived from stellar data are almost always greater than the classical value which, assuming a mean wave-length of 5000 Å., would give  $\Gamma/\nu = 1.47 \times 10^{-7}$ . The data presented in Table 13 suggest that it is about ten times the classical value for the dwarfs and for neutral atoms of the giant stars, but it is about equal to the classical value of the radiation damping constant for ionized atoms of the giants. Unsöld<sup>126</sup> has suggested that the damping constant derived from curves of growth is the sum of the effects of radiation damping and collisional damping, and also suggested that this value should be greater in the dwarf stars where the pressure is greater than in the giant stars of lower pressure. This prediction seems to hold for the sun and for  $\alpha$  *Canis Minoris*, and it seems very unlikely that the damping constant is greater than the values given in Table 13 for the ionized atoms of the giant stars if the elementary theory of the curve of growth represents, even remotely, conditions in these atmospheres. It is quite possible that the damping portion of the curve has not been reached for the neutral atoms of these stars, in which case the constant should be more nearly equal to that assigned to the ionized atoms. This point is difficult to settle since the curves of Figs. 12 and 13 do not prove conclusively that the strongest lines at the right side of the curves depart from the flat transition portion of the curve and are in the damping region, and since the only strong lines of neutral iron which have not been included in this study are in and around the Balmer continuum where it is difficult to make accurate measurements of line intensities in these stars.

In the above discussion it might seem that the sun and  $\alpha$  *Canis Minoris* represent typical dwarf stars and that the turbulent velocities and damping factors (at least for the ionized atoms) are quite different from the giant stars, as represented by  $\gamma$  *Cygni* and  $\alpha$  *Persei*. It should be mentioned, however, that  $\alpha$  *Carinae*, which was studied by Greenstein<sup>147</sup>, is undoubtedly a giant star, yet the turbulent velocity and damping factor are very similar to those found for the dwarfs above. Therefore, it would appear that the results found in this paper should not be generalized to include all dwarfs and giants of the same spectral classes.

## EXCITATION TEMPERATURES

In Table 14 are listed other determinations of the excitation temperature of the solar reversing layer for several atoms and molecules. Of these values, those derived using  $gf$ -values for atomic lines and theoretical intensities for molecular bands should probably be given greatest weight. The value given by Miss Rubenstein was obtained from the velocity determined from the curve of growth and therefore is not strictly an excitation temperature; and the values found by Shane and Prouse were derived from central intensities and line profiles, which also give temperatures based on the Doppler broadening of the line. From this table it appears that there may be a real variation in excitation temperature among the atoms and molecules in the solar reversing layer, and, indeed, Richardson and Miss Adam have observed a level effect among lines of the same molecule which would confirm this conclusion.

---

<sup>147</sup> *Ap. J.*, 95, 161, 1942.

TABLE 14. EXCITATION TEMPERATURES OF THE SOLAR REVERSING LAYER

Author	Source	Method	Temperature ° K.	Reference
Menzel, Baker and Goldberg..	Fe I Ti I	Theor. Int. Theor. Int.	4150 ± 50 4400 ± 100	<i>Ap. J.</i> , 87, 81, 1938
King.....	Ti I	$g_i f$ -values	4400 ± 100	<i>Ap. J.</i> , 87, 40, 1938
ten Bruggencate and von Klüber	Ti I Fe I	Theor. Int. and $g_i f$ -values	5040	<i>Z. f. Ap.</i> , 18, 284, 1939
Rubenstein.....	Fe I	Theor. Int.	5400 ± 1300	<i>Ap. J.</i> , 92, 114, 1940
King.....	Fe I	$g_i f$ -values	4400	<i>Ap. J.</i> , 95, 82, 1942
Wright.....	Ti I Fe I	$g_i f$ -values $g_i f$ -values	4550 ± 125 4900 ± 125	<i>Ap. J.</i> , 99, 249, 1944
Prouse.....	Ti I	Central Intensities	4300	<i>Ap. J.</i> , 95, 322, 1942
Shane.....	Na I	Profiles	5700	<i>Lick O. B.</i> , 19, 119, 1941
Richardson.....	CH	Theor. Int. Bands	5080 ± 120	<i>Tr. I. A. Un.</i> 4, 55, 1932
Richardson.....	C <sub>2</sub>	Theor. Int. Bands	5300 ± 400	<i>Ap. J.</i> , 73, 216, 1931
Adam.....	C <sub>2</sub>	Theor. Int. Bands	4550	<i>M. N.</i> , 98, 544, 1938
Birge.....	CN	Theor. Int. Bands	4000 ± 500	<i>Ap. J.</i> , 55, 273, 1922
Roach.....	CN OH	Theor. Int. Bands Theor. Int. Bands	5630 ± 500 4640	<i>Ap. J.</i> , 89, 99, 1939
Blitzer.....	CN	Theor. Int. Bands	4490 ± 100	<i>Ap. J.</i> , 91, 421, 1940

The stellar excitation temperatures given in Table 13 are quite similar to that of the sun. Although some differences from one atom to another are observable in Table 12, they are too small or the temperatures are too poorly determined to be sure that the effect is real. Fortunately the shape of the curve of growth does not depend greatly on the temperature which is adopted, for, especially in the case of the giant stars with their long, flat transition portions of the curve, the temperature is almost indeterminate.

In view of the uncertainties in the excitation temperatures derived for these stars, a full discussion of possible differences does not seem to be warranted. However, two further points should be mentioned:

All determinations of excitation temperature have indicated that it is lower than the effective temperature of a given star. For comparison purposes, the excitation temperatures studied in this paper and the effective temperatures suggested for these stars by Kuiper<sup>148</sup> have been collected in Table 15; temperatures obtained from Ti I  $f$ -values have been omitted since the lines are weak and little reliability can be placed on the results. It should not be considered surprising that the excitation temperature is below the effective temperature since the effective temperature can be related to the local

<sup>148</sup> *Ap. J.*, 88, 429, 1938.

TABLE 15. TEMPERATURES OF SOLAR-TYPE STARS

Star	Sun	$\gamma$ Cygni	$\alpha$ Persei	$\alpha$ Canis Minoris
Spectral Type.....	dG2	cF7	cF4	dF3
Effective Temperature.....	5725 ° K.	5500 ° K.	6325 ° K.	6725 ° K.
Temperature, $\tau = 0.3$ .....	5275	5075	5850	6200
Excitation Temperature, Theoretical Intensities, 1942.....	4600	5350	6000	5500
$f$ -values, 1946.....	5100	5150	5850	5300
log $X_f$ -values, 1946.....	4875	4825	5100	5000

temperature in a stellar atmosphere at optical depth,  $\tau = 0.6^{149}$  whereas the temperature of the level at which the absorption lines originate, which has been taken by Strömgen<sup>150</sup> as  $\tau = 0.3$ , is appreciably lower. The relation between temperature and optical depth used by Strömgen is\*

$$T_{\tau}^4 = T_e^4 \left( \frac{1}{2} + \frac{3}{4} \tau \right)$$

and this value for  $\tau = 0.3$  has been included in Table 15. It is seen that the excitation temperatures derived from  $f$ -values (1946) or from theoretical intensities (1942) are usually closer to those calculated for  $\tau = 0.3$  than the temperatures determined from the solar log  $X_f$ -values.

This result may be related to a discussion by Pannekoek and van Albada<sup>151</sup> which was received after the present calculations had been completed. They noted that when stellar excitation temperatures were determined from empirical curves of growth based on solar intensities (similar to the log  $X_f$ -values), the results differed very little from the excitation temperature of the sun. They explain this effect as follows: Lines of a given atom arising from low levels of excitation are usually stronger than those arising from high levels. If the temperature of the star is considerably higher than that of the sun, there will be a corresponding increase in the strength of the high excitation lines according to the Boltzmann formula. However, this increase has already been incorporated in the empirical curve of growth. Therefore the temperature difference is reflected very little in the excitation temperature of the star.

This explanation may not be complete since the solar log  $X_f$ -values may be considered as solar log  $gf$ -values with the Boltzmann factor for the temperature of the sun included; therefore they should be proportional to the number of atoms producing the line and, except for effects of stratification in the atmosphere and differences in the stellar absorption coefficient, which should also be present when laboratory  $f$ -values are used, the temperatures derived should be comparable. Nevertheless some effect of

<sup>149</sup> See e.g. Chandrasekhar, S. and G. Münch, *Ap. J.*, **104**, 447, 1946.

<sup>150</sup> *P. Med. Kobenhavs O.*, No. 138, 1944.

<sup>151</sup> *P. A. Inst.*, Amsterdam, **6**, Pt. 2, 1946.

\* The original derivation of this formula was given by K. Schwarzschild (*Göttinger Nach.*, p. 41, 1906).

this nature seems to be present for there is a smaller variation in the excitation temperatures for the  $\log X_f$ -values than for theoretical intensities or  $f$ -values and it is less than the differences which might be suggested by the effective temperatures. This difference is particularly apparent for *Sirius* and  $\gamma$  *Geminorum*; for these stars Aller<sup>152</sup> found that the excitation temperatures derived from  $\log X_0$ -values based on a solar curve of growth are only 6000° K. whereas the effective temperatures are 10,000° K.

---

<sup>152</sup> *Ap. J.*, 96, 321, 1942.

## SECTION IV. THE COMPOSITION OF STELLAR ATMOSPHERES

In the previous section, the excitation temperature,  $T$ , was obtained for each of the four stars, the sun,  $\gamma$  *Cygni*,  $\alpha$  *Persei*, and  $\alpha$  *Canis Minoris*, from the observational data by means of equation (25). The second unknown,  $L$ , in this equation was determined at the same time and will now be used to calculate  $N_a$ , the number of atoms in any observed stage of ionization of an element above one square centimetre of the photosphere. By equation (26)

$$L = \log \left( \frac{1}{3} \frac{\pi \epsilon^2 c}{\sqrt{\pi} R m c} \frac{N_a}{v b(T)} \varphi \right)$$

which is constant for each transition array of an element. On the substitution of numerical values in the above equation, it is found that

$$\log N_a = 17.82 + L - \log \frac{c}{v} + \log b(T) - \log \varphi \quad (31)$$

In this equation, all but one term of the right member is known or can be calculated.  $\log c/v$  has been determined from the curve of growth for each star; and  $\log b(T)$  may be calculated from equation (22) with the aid of the adopted excitation temperatures and the known energy levels for each atom.  $\varphi$  is difficult to determine for most atoms; it is given by the equation

$$\varphi = \frac{\rho}{4l^2 - 1} \quad (32)$$

where  $\rho$  is the radial quantum integral and  $l$  is the larger azimuthal quantum number of the jumping electron in the transition array. According to Menzel<sup>153</sup>,  $\varphi$  is nearly equal to unity for first members of a series, but smaller values are to be expected for high members of a series. As a first approximation, therefore,  $\varphi$  may be set equal to unity since the complicated wave-mechanical calculations and the numerous laboratory experiments needed to determine  $\varphi$  have been carried out for very few atoms. Goldberg<sup>154</sup> has derived an approximate formula for  $\varphi$  based on Slater's study of wave functions and atomic shielding constants<sup>155</sup> and he has kindly communicated it to the writer for use in the final calculations. These values are very approximate for most elements but it is believed that it is better to use them than to adopt the even poorer approximation,  $\varphi = 1$ .

Before considering the observational results, the remainder of the theory needed to determine  $N$ , the total number of atoms of a given element above one square centimetre of the photosphere, will be presented.

Having determined  $\log N_a$  from equation (31), the mean electron pressure,  $P_e$ , may be calculated for elements for which both neutral and ionized atoms have been studied. This comes directly from Saha's ionization equation:

$$\log P_e = \log \frac{2 b_1}{b_0} + \frac{5}{2} \log T - \log \frac{N_1}{N_0} - \frac{5040}{T} \chi_0 - 0.48 \quad (33)$$

where  $b_1$  and  $b_0$  are the partition functions of the ionized and neutral atoms at temperature  $T$ ;

<sup>153</sup> *Pop. A.*, 47, 66, 1939.

<sup>154</sup> Unpublished.

<sup>155</sup> *Phys. Rev.*, 36, 57, 1930.

$N_1$  and  $N_0$  are the observed number of atoms in these stages of ionization and  $\chi_0$  is the ionization potential of the neutral atom.

The numerical value of the constant reduces the units of  $P_e$  to dynes/cm<sup>2</sup>.

A considerable variation in  $P_e$  as determined from data for different elements is usually found. The variation may be real in some cases, but in this paper, a mean value has been adopted for each star.

The level of ionization of a stellar atmosphere,  $\bar{\chi}$ —which was defined by Russell<sup>156</sup> as the ionization potential of an element for which the number of singly ionized atoms would just equal the number of neutral atoms—is found from the equation

$$\bar{\chi} \frac{5040}{T} = \frac{5}{2} \log T - 0.48 - \log P_e \quad (34)$$

As Unsöld<sup>157</sup> has pointed out,  $P_e$  varies rapidly with  $T$ ;  $\bar{\chi}$ , on the other hand, remains very stable and its determination should probably prove a good indication of the ionization in any given stellar atmosphere.

After  $\bar{\chi}$  has been evaluated, the ratio of the number of atoms in the ionized and neutral states can then be calculated for any element from

$$\log \frac{N_1}{N_0} = (\bar{\chi} - \chi_0) \frac{5040}{T} + \log \frac{2 b_1}{b_0} \quad (35)$$

If second ionization is appreciable,  $\log N_2/N_1$  may be calculated by replacing the subscripts 1 and 0 in equation (35) by 2 and 1, respectively. As second ionization is very small in the stellar atmospheres studied in this paper,  $N_2$  may usually be neglected and no further stages of ionization need be considered.

Then  $N$ , the total number of atoms above one square centimetre of the photosphere, is given by

$$N = N_0 + N_1 + N_2 \quad (36)$$

where  $N_2$  is very small.

#### THE 1942 DETERMINATION OF THE ABUNDANCE OF ELEMENTS IN THE ATMOSPHERES OF SOLAR-TYPE STARS

In the 1942 derivation of the number of atoms in stellar atmospheres, the methods described above were used. Although values of  $L$  had been calculated for all transition arrays when the excitation temperatures were being determined, they were very uncertain in many cases where few lines were available. Accordingly a new  $L$  was calculated for each array by means of equation (26) with the observed values of  $Y$  and the value of  $T$  adopted for each star. Where several transition arrays were studied for a given element, the mean value of  $L$  was obtained from a consideration of the relative weights of the  $Y$ 's. The corresponding values derived from the  $g_f$ -values of Ti I and Fe I were also included in these results by relating the laboratory values to the theoretical intensities as described in the Appendix.

<sup>156</sup> *Ap. J.*, **70**, 11, 1929.

<sup>157</sup> *Physik der Sternatmosphären*, p. 345. Springer, Berlin, 1938.

In Table 16 mean values of  $L$  and  $\log N_a$  for each star have been listed for the atoms included in Table 3. In the second column,  $\log b(T)$  has been calculated for  $T = 5350^\circ \text{K.}$ ; in most cases it does not vary appreciably over the range in temperature adopted for these stars but, for a few atoms, there is some change and the more accurate value has been used in the calculation of  $\log N_a$ . In this subsection it has been assumed that  $\varphi = 1$  in all cases.

TABLE 16. ABUNDANCES OF ATOMS IN SOLAR-TYPE STARS

(1942 DATA)

Atom	$\log b(T)$	Sun		$\gamma$ Cygni		$\alpha$ Persei		$\alpha$ Canis Minoris	
		$L$	$\log N_a$	$L$	$\log N_a$	$L$	$\log N_a$	$L$	$\log N_a$
C I	0.97	7.06	20.68	6.47	20.61	5.56	19.66	6.28	20.02
Na I	0.32	2.52	15.48	1.72	15.21	1.40	14.85	1.91	15.00
Mg I	0.00	5.88	18.54	4.18	17.35	3.33	16.49	4.70	17.47
Mg II	0.30	8.02	20.98	6.49	19.96	5.63	19.05	6.60	19.67
Al I	0.78	2.37	15.81	1.52	15.47	0.95	14.85	1.70	15.25
Si I	1.00	5.19	18.84	3.95	18.12	3.36	17.49	4.41	18.18
Si II	0.78	8.17	21.61	7.60	21.55	6.95	20.85	7.32	20.87
Ca I	0.08	3.23	15.93	1.84	15.09	1.27	14.54	2.24	15.13
Sc I	1.10	-0.17	13.55	-0.74	13.53	-1.01	13.25	-0.70	13.18
Sc II	1.38	0.50	14.51	0.93	15.47	0.30	14.82	0.46	14.61
Ti I	1.52	0.97	15.09	0.22	14.91	-0.14	14.54	0.25	14.55
Ti II	1.78	1.82	16.23	2.57	17.52	1.80	16.72	1.76	16.31
V I	1.71	0.28	14.61	-0.45	14.43	-0.78	14.08	-0.35	14.14
Cr I	1.04	2.06	15.71	1.27	15.48	0.82	15.03	1.54	15.36
Mn I	0.81	3.44	16.90	1.90	15.88	1.37	15.33	2.13	15.72
Fe I	1.49	4.32	18.44	3.05	17.71	2.54	17.18	3.30	17.57
Co I	1.60	2.17	16.40	1.14	15.91	0.64	15.39	1.18	15.56
Ni I	1.55	3.71	17.90	2.65	17.37	1.70	16.38	2.60	16.92
Zn I	0.00	4.31	16.97	3.13	16.30	2.32	15.44	3.38	16.15
Sr I	0.11	-1.15	11.59	-1.43	11.86	-1.75	11.54	-1.30	11.61
Sr II	0.34	2.22	15.20	2.24	15.75	2.12	15.61	2.20	15.32
Y II	1.23	-0.39	13.46	0.46	14.86	-0.14	14.25	-0.38	13.63
Zr II	1.74	-0.62	13.74	-0.37	14.54	-1.11	13.78	-0.89	13.63
Ba II	0.67	1.14	14.43	1.39	15.23	0.79	14.63	0.94	14.39
La II	1.57	-1.68	12.51	-1.32	13.42	-1.82	12.89	-1.47	12.87

The required observational data for the determination of the electron pressures,  $N_1$  and  $N_0$ , are available for five elements listed in Table 16—Mg, Si, Sc, Ti and Sr. The values of  $\log P_e$  for each element have been tabulated in Table 17 and the weighted mean value for each star has been determined. Greatest weight in these calculations was given to the titanium lines because  $N_a$  was well determined for atoms in both neutral and ionized states.

At the end of Table 17 the quantities which determine conditions in stellar atmospheres are listed:  $P_e$  as noted above;  $\bar{\chi}$ , the level of ionization calculated from equation (34); and  $T$ , the excitation temperature adopted from the curve-of-growth data which seemed best at that time.

TABLE 17. ELECTRON PRESSURES AND MEAN LEVEL OF IONIZATION

(1942 DATA)

Element	Sun		$\gamma$ Cygni		$\alpha$ Persei		$\alpha$ Canis Minoris	
	log $P_e$	Wt.	log $P_e$	Wt.	log $P_e$	Wt.	log $P_e$	Wt.
Mg.....	-1.45	1	-0.37	1	+0.56	1	+0.29	1
Si.....	-2.84	1	-2.20	1	-1.16	1	-1.19	1
Sc.....	+1.16	1	+1.26	1	+2.43	1	+1.99	1
Ti.....	+0.71	5	+0.35	5	+1.60	5	+1.42	5
Sr.....	-0.54	1	+0.13	1	+0.63	1	+0.48	1
log $P_e$ .....	-0.01		+0.06		+1.16		+0.96	
$P_e$ dynes/cm. <sup>2</sup> .....	1.0		1.2		14.5		9.0	
$T^\circ$ K.,.....	4600		5350		6000		5500	
$\bar{\chi}$ volts.....	8.0		9.3		9.3		8.6	

The total numbers of atoms,  $N$ , for the elements listed in Table 3 are given in Table 18. In all cases the value of  $\log N$  is the sum of the values for neutral and singly ionized atoms; only in the case of barium does second ionization account for more than one per cent of the total number of atoms and this number is negligible compared with other uncertainties in the calculations.  $\log N_1/N_0$  is also tabulated for each element in Table 18 in order to show how differences in temperature and pressure produce large differences in the relative numbers of neutral and ionized atoms in the atmosphere.

Although the temperatures and pressures which were adopted in 1942 are quite different from those which seem most reliable now, the total number of atoms obtained for each star usually agrees, within the probable error of the determination, with that calculated in 1946. Major factors in the decision to continue this study of line intensities were the facts that (1) the excitation temperatures seemed to be higher for giant stars than for dwarfs—which did not agree with the trend found for the effective temperatures—and (2) the pressures were greater for giants than for dwarfs—which also did not agree with the information obtained from other sources.

#### THE 1946 DETERMINATION OF STELLAR ABUNDANCES

##### *The Solar Atmosphere*

Data obtained from high-dispersion spectrograms taken at the centre of the solar disk have been used in Section III as the basis for the determination of curves of growth, turbulent velocities and excitation temperatures of solar-type stars. These observations can also be used to derive the number of atoms above the photosphere for elements having absorption lines in the region of the spectrum studied in this paper.

In the present investigation, both the empirical curve of growth derived from the  $f$ -values of neutral iron and titanium and the theoretical curve most nearly representing

TABLE 18. THE COMPOSITION OF SOLAR-TYPE STELLAR ATMOSPHERES

(1942 DATA)

	Sun (Russell)		Sun dG2		$\gamma$ Cygni cF7		$\alpha$ Persei cF4		$\alpha$ Canis Minoris dF3	
$T$ ° K. $P$ , bar	5040 3.1		4600 1.0		5350 1.2		6000 14.5		5500 9.0	
Element	$\log \frac{N_1}{N_0}$	$\log N$	$\log \frac{N_1}{N_0}$	$\log N$						
C.....	-3.0	19.2:	-3.4	20.7:	-1.7	20.6:	-1.5	19.7:	-2.3	20.0:
Na.....	3.2	19.0	3.1	18.6	3.9	19.1	3.5	18.3	3.2	18.2
Mg.....	0.7	19.6	1.0	19.9	2.2	19.6	2.0	18.6	1.5	19.1
Al.....	1.8	18.2	1.7	17.5:	2.7	18.1:	2.3	17.2:	2.0	17.2:
Si.....	0.0	19.1	-0.1	19.9	1.2	20.0	1.0	19.2	0.5	19.4
Ca.....	2.1	18.5	2.7	18.6	3.6	18.7	3.2	17.8	2.9	18.0
Sc.....	1.7	15.4	2.1	14.6	3.1	15.5	2.8	14.9	2.5	14.7
Ti.....	1.6	17.0	1.9	16.8	2.9	17.7	2.6	17.0	2.2	16.6
V.....	3.1	16.8	1.6	16.2	2.6	17.1	2.4	16.4	2.0	16.1
Cr.....	1.3	17.5	1.5	17.2	2.5	18.0	2.3	17.3	1.9	17.2
Mn.....	0.7	17.7	1.0	18.0	2.2	18.0	2.0	17.3	1.5	17.2
Fe.....	0.4	19.0	0.6	19.2	1.8	19.6	1.7	18.9	1.2	18.8
Co.....	0.3	17.4	0.2	16.8:	1.4	17.3:	1.2	16.6:	0.8	16.4:
Ni.....	0.0	17.8	0.2	18.3	1.4	18.8	1.3	17.7	0.8	17.8
Zn.....	-1.1	16.7	-0.9	17.0	0.5	16.9	0.5	16.1	-0.1	16.4
Sr.....	2.7	15.1	3.1	15.1	4.0	15.8	3.5	15.5	3.2	15.2
Y.....	1.8	14.4	2.0	13.5	3.0	14.9	2.7	14.2	2.3	13.6
Zr.....	1.6	14.3	1.6	13.8	2.7	14.5	2.4	13.8	2.0	13.6
Ba.....	3.5	15.1	3.6	14.4	4.4	15.5	3.9	14.9	3.6	14.5
La.....	2.5	13.6	3.1	12.5	4.0	13.4	3.6	12.9	3.3	12.9

these observations were used; differences between these curves are unimportant relative to uncertainties in other quantities which are used in these calculations; e.g. it is not certain that the same temperature and pressure should be used for all atoms in the atmosphere, and the calculation of  $\varphi$ -values is only approximate. Therefore, while the required data have been determined for each curve separately, average values have been used throughout the remainder of this section. The relation between  $\log X_i$  and  $\log X_0$  is given by equation (29).

For each element, the transition arrays listed by number in Table 3 and also others containing lines which are included in Table 4 were studied in more detail. Theoretical intensities were calculated for all lines in these arrays which had been measured by Allen<sup>158</sup> or which the author had measured in the Utrecht *Photometric Atlas*<sup>159</sup>. A temperature of 4700° K. was assumed for all lines (since the results are to be used for a study of stellar atmospheres and a single temperature has been adopted for each star). Then for the lines in each transition array,  $\log W/\lambda$  was plotted against

$$\log S s/\Sigma s - \frac{5040}{T} \chi_i .$$

<sup>158</sup> *Mem. Comm. Sol. O.*, Canberra, 1, No. 5, 1934; 2, No. 6, 1938.

<sup>159</sup> Minnaert, M., G. F. W. Mulders and J. Houtgast, Schnabel, Kampert and Helm, Amsterdam, 1940.

This plot was fitted to the solar curve of growth and the difference between the abscissae at any point gave a value of  $L$ , i.e.

$$\log X_0 - (\log S s / \Sigma s - \frac{5040}{T} \chi_i) = L$$

according to equation (25).

Goldberg's formula<sup>154</sup> was used to calculate  $\varphi$  for all transition arrays and thus a value of  $\log N_a$  could be determined from equation (31) by inserting the value 5.29 for  $\log c/v$  and the correct value of  $\log b(T)$  for a temperature of 4700° K. As a value of  $\log N_a$  is required for each atom in the study of the stellar atmospheres, the mean value of  $(L - \log \varphi)$  was found for each array and the weighted mean value obtained for the atoms of each element. Values of  $(L - \log \varphi)$  for the sun are listed in Table 19 for all transition arrays which have been studied in this paper, including those for which numbers

TABLE 19. VALUES OF  $L - \log \varphi$  FOR ATOMS IN THE SOLAR ATMOSPHERE

No.	Atom	Transition Array	$L - \log \varphi$	Wt.	No.	Atom	Transition Array	$L - \log \varphi$	Wt.
1	C I	2p 3s — 2p 4p	7.33	2	33	Ti I	3d <sup>2</sup> 4s4p— 3d <sup>2</sup> 4s5s	2.34	5
2	Na I	3s — 3p	3.02	2	35		3d <sup>2</sup> 4p — 3d <sup>2</sup> 4d	2.29	2
3		3p — 5s	2.97	2	36	Ti II	3d <sup>2</sup> — 3d <sup>2</sup> 4p	2.58	5
4		3p — 4d	3.62	1	37		3d <sup>2</sup> 4s — 3d <sup>2</sup> 4p	2.85	2
5		3p — 6d	2.96	2	38	V I	3d <sup>4</sup> s — 3d <sup>4</sup> 4p	0.41	7
6	Mg I	3s 3p — 3s 4s	7.66	2	39	V II	3d <sup>4</sup> — 3d <sup>4</sup> 4p	2.34	3
7		3s 3p — 3s 5s	7.39	1	40	Cr I	3d <sup>4</sup> s — 3d <sup>4</sup> 4p	2.36	2
9		3s 3p — 3s 6s	6.99	1	41		3d <sup>4</sup> s <sup>2</sup> — 3d <sup>4</sup> s4p	1.92	5
10		3s 3p — 3s 5d	8.80	1	42		3d <sup>4</sup> 4p — 3d <sup>4</sup> 4d	3.76	2
11		3s 3p — 3s 7d	.....	—	43		3d <sup>4</sup> s — 3d <sup>4</sup> s4p	2.45	1
6a		3s 3p — 3s 3d	7.85	2	44		3d <sup>4</sup> s4p— 3d <sup>4</sup> s5s	4.07	6
8		3s 3p — 3s 4d	8.13	1	45	Cr II	3d <sup>5</sup> — 3d <sup>4</sup> 4p	4.73	3
11a		3s 3p — 3s 9d	.....	—	46	Mn I	3d <sup>5</sup> 4s <sup>2</sup> — 3d <sup>5</sup> 4s4p	2.09	1
12	Mg II	3d — 4f	9.61	1	47		3d <sup>4</sup> s — 3d <sup>4</sup> 4p	3.78	6
13	Al I	4s — 5p	1.94	2	48		3d <sup>5</sup> 4s4p— 3d <sup>5</sup> 4s5s	4.79	3
13a		3p — 4s	5.02	2	49	Fe I	3d <sup>7</sup> 4s — 3d <sup>7</sup> 4p	4.60	8
14	Si I	4s — 5p	4.73	2	50		3d <sup>6</sup> 4s4p— 3d <sup>6</sup> 4s5s	6.30	8
14a		3p <sup>2</sup> — 3p 4s	7.29	1	52	Co I	3d <sup>7</sup> 4s4p— 3d <sup>7</sup> 4s5s	4.06	3
15	Si II	4s — 4p	7.39	1	52a		3d <sup>8</sup> 4s — 3d <sup>8</sup> 4p	2.21	1
16	Ca I	4s <sup>2</sup> — 4s 4p	3.45	1	54	Ni I	3d <sup>8</sup> 4s4p— 3d <sup>8</sup> 4s5s	5.61	5
17		4s 4p — 4p <sup>2</sup>	3.74	3	55		3d <sup>8</sup> 4s — 3d <sup>8</sup> 4p	4.27	4
18		4s 4p — 4s 5s	4.42	1	56a	Cu I	3d <sup>10</sup> 4p — 3d <sup>10</sup> 4d	4.99	1
19		4s 4p — 4s 4d	4.50	3	57	Zn I	4s 4p — 4s 5s	6.42	1
20		4s 3d — 3d 4p	3.56	4	58		4s 4p — 4s 4d	6.82	1
21		4s 3d — 4s 5p	2.76	3	59	Sr I	5s <sup>2</sup> — 5s 5p	-0.60	1
22		4s 3d — 4s 4f	3.03	2	60	Sr II	5s — 5p	2.25	1
23		4s 3d — 4s 5f	3.23	1	61	Y II	4d <sup>2</sup> — 4d 5p	0.31	4
24		4s 3d — 4s 6f	2.86	1	61a		4d 5s — 4d 5p	0.45	2
25		4s 4p — 4s 6s	4.19	2	62	Zr II	4d <sup>2</sup> 5s — 4d <sup>2</sup> 5p	0.16	1
26		4s 4p — 4s 6d	3.78	1	63		3d <sup>3</sup> — 3d <sup>2</sup> 5p	1.17	2
26a	Ca II	4s — 4p	5.34	1	64	Ba II	5p <sup>6</sup> 6s — 5p <sup>6</sup> 6p	1.53	1
27	Sc I	3d <sup>2</sup> 4s — 3d <sup>2</sup> 4p	-0.07	2	65		5p <sup>6</sup> 5d — 5p <sup>6</sup> 5p	0.78	1
28	Sc II	3d 4s — 3d 4p	1.88	1	66	La II	5d <sup>2</sup> — 4f 5d	-1.33	1
29		3d <sup>2</sup> — 3d 4p	1.17	4	67		5d <sup>2</sup> — 5d 6p	-1.01	1
30	Ti I	3d <sup>2</sup> 4s <sup>2</sup> — 3d <sup>2</sup> 4s4p	0.83	5	68		5d 6s — 5d 6p	-0.25	2
31		3d <sup>3</sup> 4s — 3d <sup>3</sup> 4p	1.52	9	69		5d 6p — 5d 6d	3.86	1
32		3d <sup>3</sup> 4s — 3d <sup>2</sup> 4s4p	1.88	4					

are given in Table 3 and additional arrays which contain lines listed in Table 4. The weight of each determination is based on the number of lines available and the fit of the observations on the curve of growth. In view of the large differences between transition arrays of the same atom, even in cases where  $L$  should be well-determined, it seems probable that many of the  $\varphi$ -values will be changed when more detailed knowledge concerning the radial quantum integral is available. In the meantime it seems better to use the weighted mean values for each atom rather than assume that  $\varphi = 1$  in all cases.

The results of these calculations for  $\log N_a$  are listed in Table 22, column 2. It is seen that data for both neutral and ionized atoms are available for Mg, Si, Ca, Sc, Ti, V, Cr and Sr and, therefore, for these elements, mean electron pressures may be determined from Saha's ionization equation (33). The temperature to be used here is very important since it enters to the  $5/2$ -power. General considerations would suggest that the same temperature should be used for all studies based on curve-of-growth data, and therefore the excitation temperature should be retained. However, different values are obtained for different atoms ( $4550^\circ$  K. for Ti I,  $4850^\circ$  K. for Fe I and, very recently<sup>160</sup>,  $5400^\circ$  K. for V I). As some mean value must be adopted for the present discussion, calculations have been carried out for the adopted excitation temperature,  $4700^\circ$  K., and also for  $T = 5275^\circ$  K. which is the value corresponding to the level  $\tau = 0.3$  in the solar atmosphere as suggested by Strömgren<sup>160</sup>. Thus if future work should indicate the use of a different temperature, the trend of the electron pressure and level of ionization will be evident.

The electron pressures derived for each temperature for the eight elements are listed in Table 20. Weights have been assigned according to the estimated value of the deter-

TABLE 20. ELECTRON PRESSURES IN THE SOLAR ATMOSPHERE

Atom	Ionization Potential, $\chi$ volts	Electron Pressure, $P_e$ dynes/cm. <sup>2</sup>		
		$T = 4700^\circ$ K.	$T = 5275^\circ$ K.	Wt.
Mg.....	7.61	0.10	1.1	—
Si.....	8.11	0.031	0.36	—
Ca.....	6.09	5.5	36.0	1
Sc.....	6.7	2.8	22.0	1
Ti.....	6.81	5.1	41.0	3
V.....	6.71	0.76	6.1	2
Cr.....	6.74	1.20	8.4	2
Sr.....	5.67	1.18	6.6	1
Adopted Value.....		2.14	15.7	

mination, and depend on the number of lines, their fit on the curve of growth and their excitation potentials. At the suggestion of Dr. Menzel, no weight has been given to the results for Mg and Si because the few measurable lines in the region studied arise from levels of high excitation potential ( $\sim 8$  volts) and a small change in the temperature adopted would change  $\log N_a$  and hence  $P_e$  considerably. The lines of ionized calcium

<sup>160</sup> King, R. B. and K. O. Wright, *Mt. Wilson Cont.*, No. 736; *Ap. J.*, **106**, 224, 1947.

are so strong that the curve of growth must be extrapolated considerably; the lines of neutral scandium and strontium are weak; therefore low weight must be attached to the electron pressures derived for these elements. The adopted pressure has been calculated from the weighted mean value of the logarithm. The change from 2.1 dynes/cm<sup>2</sup> at 4700° K. to 16 dynes/cm<sup>2</sup> at 5275° K. indicates the extreme sensitivity of electron pressure to temperature; a test calculation for the effective temperature,  $T = 5725^\circ$  K., gave a value of 62 dynes/cm<sup>2</sup> for the same data.

The range in the electron pressures found for the several elements is somewhat greater than might be expected for a homogeneous atmosphere. However, the uncertainties in the  $\varphi$ -values and the possible real differences in temperature, combined with the high excitation potentials for lines of Mg II and Si II, make the reality of these differences difficult to test. If the data for Mg and Si were given weight 1, the calculated probable error of  $\log P_e$  would be 0.3; with the adopted weights it is 0.1. Therefore although the differences are definitely greater than the probable errors and there may be a real variation in electron pressure (and thus atmospheric level at which the lines arise) for the several elements, no positive conclusions can be drawn and a mean value has been adopted in the derivation of abundances of the elements.

The level of ionization of the solar atmosphere has been calculated from equation (34) for the adopted electron pressures. It is 7.81 volts for  $T = 4700^\circ$  K and 7.99 volts for  $T = 5275^\circ$  K.

The ratio of the number of ionized atoms to the number of neutral atoms for each element is given by equation (35) and the values of  $\log N_1/N_0$  are tabulated in Table 21. In all cases the total number of atoms is effectively the sum of the numbers of neutral and ionized atoms and  $\log N$  is given in the same table. For barium, the element most likely to have atoms in the second stage of ionization,  $N_2$  is only 0.2 per cent of  $N_1$  and it may be neglected in these calculations.

These results for the number of atoms above the photosphere in the sun may be compared with other similar analyses, the results of which are included in Table 21. Russell<sup>156</sup> based his investigation on his calibration of Rowland's solar intensities; since he did not use the curve of growth, it must be considered a first approximation. The values listed here have been reduced by a constant, 1.0, as suggested by Unsöld<sup>157</sup> to allow for the observed result that the astrophysical value of the damping constant is about ten times the classical value. Menzel and his collaborators at Harvard Observatory<sup>161</sup> used a curve of growth based on Allen's equivalent widths<sup>158</sup> and theoretical line intensities. As the method is essentially the same as that used in the present investigation, any differences would seem to arise from the use of different lines arising from other transition arrays, and the relative weights assigned to lines of neutral and ionized atoms of the same element. They do not give information concerning the temperature or pressure adopted but, as the two temperatures studied in this paper indicate, these values do not change the observed total number of atoms of a given element greatly. Therefore the differences between the two sets of data may be taken as some indication of the probable error of the determinations; calculations show that it is about 0.5 in  $\log N$ .

<sup>161</sup> Goldberg, L. and L. H. Aller, *Atoms, Stars and Nebulae*, p. 114, Blakiston, Philadelphia, 1943.

TABLE 21. THE NUMBER OF ATOMS IN THE SOLAR ATMOSPHERE

Atom	Log N				
	Russell	Menzel	Strömngren	Wright	
$T \text{ }^\circ \text{K} \dots\dots\dots$	5600			4700	5275
$P, \text{ dynes/cm.}^2 \dots\dots\dots$	18			2.1	15.7
volts.....	8.48			7.81	7.99
H.....	23.3::	23.9	23.4		
He.....		23.2			
C.....	19.2	19.4		19.8	19.8
N.....	19.4?	19.9			
O.....	20.8	20.6			
Na.....	19.0	18.4	18.0	17.8	17.6
Mg.....	19.6	20.4	19.0	20.3	20.4
Al.....	18.2	18.4	18.0	17.3	17.2
Si.....	19.1	19.8	19.0	18.6	18.8
S.....	17.5:	19.3			
K.....	18.6:	16.7			
Ca.....	18.5	18.5	17.8	17.6	17.5
Sc.....	15.4			14.2	14.2
Ti.....	17.0	16.6		16.2	16.2
V.....	16.8	16.1		15.2	15.2
Cr.....	17.5	16.8		17.0	16.9
Mn.....	17.7	17.0		17.1	17.2
Fe.....	19.0	18.8	19.0	19.0	19.1
Co.....	17.4	16.6		17.1	17.2
Ni.....	17.8	18.3		18.4	18.5
Cu.....	16.8	16.3		17.2	17.3
Zn.....	16.7	17.4		18.2	18.2
Sr.....	15.1			14.0	13.9
Y.....	14.4			13.1	13.1
Zr.....	14.3			14.0	14.0
Ba.....	15.1			13.3	13.3
La.....	13.6			12.3	12.3

Strömngren's model for the solar atmosphere<sup>162</sup> was based on the relative abundances of the metals found for meteorites by Goldschmidt<sup>163</sup> and the logarithm of the ratio of hydrogen to all the metals was found to be 3.9. In order to make Strömngren's values comparable, it was assumed that the number of atoms of iron are the same as for other analyses included in Table 21.

*The Atmospheres of Solar-Type Stars*

When the number of atoms in a given stage of ionization has been found for the sun, the number of atoms in a stellar atmosphere can be determined by comparing the stellar plots of  $\log W/\lambda$  against  $\log X_f$  with the adopted theoretical curve of growth for the star. When the observational plot is set on the theoretical curve in the position of best fit, the relative shift along the  $\log X_0$ -axis gives a value of  $\log X_*/X_f$ . But, from equation (30),

$$\log \frac{N_*}{N_\odot} = \log \frac{X_*}{X_f} + \log \frac{b(T_*)}{b(T_\odot)} + \log \frac{v_*}{v_\odot} + 5040 \chi_i \left( \frac{1}{T_*} - \frac{1}{T_\odot} \right). \quad (37)$$

<sup>162</sup> *Festschrift für Elis Strömngren*, p. 218, Munksgaard, Copenhagen, 1940.

<sup>163</sup> *Norske Vid. Ac.*, Oslo, No. 4, 1937.

Of the remaining quantities in the right member,  $T_*$  and  $T_\odot$  are the excitation temperatures determined in Section III and the values given in Table 12 have been adopted here; therefore  $b(T_*)$  and  $b(T_\odot)$  can be calculated for any atom.  $v_*$  and  $v_\odot$  are known from the fit of the observations on the family of theoretical curves and these values are given in Table 13. Therefore  $\log N_*/N_\odot$  can be determined.

In practice,  $\log X_*/X_f$  was determined, for atoms with numerous lines, for each value of the excitation potential when the excitation temperatures were derived. For such cases, a mean value of  $\log N_*/N_\odot$  is obtained by inserting the original value of  $\log X_*/X_f$  and the adopted temperatures in equation (37) for each excitation potential and taking a weighted mean of the sum. For other atoms, new plots of  $\log W/\lambda$  against

$$\log X_f - 5040 \chi_i (1/T_* - 1/T_\odot)$$

were made and the relative positions of the abscissae of this plot and the theoretical curve when the best fit was obtained were used to determine  $\log N_*/N_\odot$ . For atoms with only one or two lines, the value of  $\log X_*$  corresponding to a given  $\log W/\lambda$  taken from the proper curve of growth was combined with the  $\log X_f$ -value for the same line to obtain a value of  $\log N_*/N_\odot$ .

Thus values of  $\log N_*/N_\odot$  were obtained for all atoms represented in Tables 3 and 4. As  $\log N_\odot$  had been found for most of these atoms in the previous sub-section,  $\log N_*$  was obtainable immediately. Table 22 gives the values of  $\log N_*$  for each atom for the four stars, and also includes  $\log N_\odot$  and  $\log N_*/N_\odot$  as determined above. In the case of Fe II and Ni II, where no theoretical intensities are available and hence an observational  $\log N_\odot$  could not be found, the mean electron pressure was assumed; the two values correspond to the solar  $\log N_\odot$  found for  $P_e = 2.1$  dynes/cm<sup>2</sup> and  $T = 4700^\circ$  K., and  $P_e = 15.7$  dynes/cm<sup>2</sup> and  $T = 5275^\circ$  K., respectively. In all other cases  $\log N_*$  has been taken from the observed  $\log N_\odot$  listed in the table.

Electron pressures were calculated for these stellar atmospheres by combining the data for neutral and ionized atoms of elements where observations of both states could be made. Saha's equation (33) was used to determine electron pressures for the elements Mg, Si, Ca, Sc, Ti, V, Cr, and Sr and these values are listed in Table 23 in the first column under each star. The weight of each determination was selected as before with no weight given the data for Mg and Si; the relative weights are approximately the same as for the sun, but each value is less well-determined either because fewer lines were available or because the lines of the ionized atoms lay on the flat portion of the curve of growth. As noted in the previous sub-section, the calculations have been made for both the excitation temperature and that corresponding to the level where  $\tau = 0.3$  for each star.

In Table 23 the second column under each star gives an adjusted value of  $\log P_e$  for the above elements and also for Fe and Ni. Instead of using the observed values of  $\log N_1$  (or  $\log N_0$ ) for the sun for a given element, it was assumed that the average electron pressure was correct (2.1 or 15.7 dynes/cm<sup>2</sup>) and  $\log N_0$  (or  $\log N_1$ ) was calculated for this value. The adjusted value for each stage of ionization in the sun was obtained by giving observed and calculated values weights inversely proportional to those listed in Table 22, column 3. The listed differences,  $\log N_*/N_\odot$ , were then applied for each star and the calculations carried through as before. As might be expected, this average value

TABLE 22. NUMBER OF ATOMS IN A GIVEN STAGE OF IONIZATION IN STELLAR ATMOSPHERES

Atom	Sun	Sun			$\gamma$ Cygni			$\alpha$ Persei			$\alpha$ Canis Minoris		
	<i>g,f</i> -curve log $N_{\odot}$	log $\frac{N^*}{N_{\odot}}$	log $N^*$	Wt.									
C I	19.79	-0.66	19.13	1	0.42	20.21	3	-0.20	19.59	3	-0.32	19.47	2
Na I	14.88	0.09	14.97	8	0.24	15.12	6	-0.14	14.74	6	-0.06	14.82	6
Mg I	19.29	-0.12	19.17	9	-0.63	18.66	6	-1.24	18.05	7	-0.49	18.80	8
Mg II	21.41	-0.13	21.28	1	0.32	21.73	1	0.00	21.41	1	0.02	21.43	1
Al I	15.76	0.02	15.78	4	0.08	15.84	4	-0.58	15.18	5	-0.31	15.45	4
Si I	18.07	0.00	18.07	5	-0.15	17.92	4	-0.50	17.57	4	-0.24	17.83	4
Si II	19.67	0.11	19.78	4	0.74	20.41	4	0.66	20.33	3	0.22	19.89	3
Ca I	15.16	0.00	15.16	16	-0.38	14.78	14	-0.74	14.42	12	-0.32	14.84	14
Ca II	17.18	0.18	17.36	2	1.54	18.72	2	1.48	18.66	2	0.37	17.55	2
Sc I	12.49	0.04	12.53	1	0.10	12.59	1	-0.16	12.33	1	-0.20	12.29	1
Sc II	14.16	-0.08	14.08	11	1.01	15.17	6	0.53	14.69	6	-0.13	14.03	6
Ti I	14.64	-0.06	14.58	42	-0.24	14.40	28	-0.68	13.96	17	-0.54	14.10	16
Ti II	15.91	-0.10	15.81	23	1.14	17.05	22	0.70	16.61	21	-0.03	15.88	20
V I	13.59	-0.12	13.47	8	0.02	13.61	5	-0.26	13.33	5	-0.43	13.16	6
V II	15.47	0.00	15.47	3	1.14	16.61	3	0.46	15.93	2	-0.05	15.42	3
Cr I	15.63	-0.04	15.49	16	-0.28	15.25	17	-0.73	14.80	9	-0.48	15.05	14
Cr II	17.07	-0.16	16.91	9	0.84	17.91	6	0.39	17.46	7	-0.04	17.03	9
Mn I	16.20	0.01	16.21	13	-0.44	15.76	12	-0.86	15.34	10	-0.48	15.72	12
Fe I	18.42	-0.06	18.36	95	-0.22	18.20	80	-0.68	17.74	64	-0.36	18.06	70
Fe II	{ 18.85 18.85 19.02	-0.24	18.61 18.78	16	1.15	20.00 20.17	12	0.71	19.56 19.73	13	0.00	18.85 19.02	16
Co I	16.69	0.00	16.69	6	-0.28	16.41	6	-0.56	16.13	7	-0.23	16.46	6
Ni I	18.05	-0.12	17.93	24	-0.26	17.79	20	-0.80	17.25	17	-0.42	17.63	17
Ni II	{ 18.10 18.25	-0.06	18.04 18.19	1	1.26	19.36 19.51	2	1.16	19.26 19.41	2	0.13	18.23 18.38	2
Cu I	16.86	0.71	17.57	1	0.12	16.98	1	-0.57	16.29	1	0.08	16.94	1
Zn I	18.12	-0.07	18.05	3	-0.02	18.10	3	-0.66	17.46	3	-0.07	18.05	3
Sr I	10.97	-0.22	10.75	1	-0.10	10.87	1	-0.52	10.45	1	-0.30	10.67	1
Sr II	14.08	-0.08	14.00	2	0.60	14.68	2	1.19	15.27	2	-0.02	14.06	2
Y II	13.06	0.06	13.12	6	1.58	14.64	6	1.10	14.16	6	0.28	13.34	7
Zr II	14.03	-0.14	13.89	3	1.04	15.07	4	0.38	14.41	3	-0.19	14.84	4
Ba II	13.29	0.12	13.41	5	0.96	14.25	5	0.66	13.95	5	-0.02	13.27	5
La II	12.33	-0.02	12.31	3	1.00	13.33	4	0.52	12.85	4	-0.20	12.13	3
Ce II		0.54			0.75			0.08			-0.50		
Nd II		-0.33			1.00			0.68			0.14		
Sm II		-0.17									-1.04		
Eu II					1.52			0.98			0.50		
Gd II		0.72			0.06			-0.02			-0.36		

TABLE 23. ELECTRON PRESSURES IN THE ATMOSPHERES OF SOLAR-TYPE STARS

Element	log $P_e$											
	Calculated for Excitation Temperatures						Calculated for Temperatures at Level $\tau = 0.3$					
	Sun			$\gamma$ Cygni			$\alpha$ Persei			$\alpha$ Canis Minoris		
	Obs.	Adj.	Wt.	Obs.	Adj.	Wt.	Obs.	Adj.	Wt.	Obs.	Adj.	Wt.
Mg.....	1.35	0.66	.....	2.32	1.63	.....	2.52	1.82	.....	1.62	0.40	.....
Si.....	2.72	0.56	.....	3.87	1.71	.....	2.10	1.94	.....	2.64	0.48	.....
Ca.....	0.81	0.40	1	1.02	2.60	1	1.10	2.69	0.50	0.10	1	.....
Sc.....	0.84	0.74	1	1.74	1.64	1	0.39	0.29	0.87	0.77	1	.....
Ti.....	1.04	0.66	1	1.55	1.17	3	1.98	1.60	0.71	0.33	3	.....
V.....	0.04	0.49	1	2.98	1.43	1	1.81	0.26	0.01	0.46	1	.....
Cr.....	0.48	0.73	2	1.18	1.43	2	1.61	1.86	0.15	0.40	2	.....
Fe.....	.....	0.84	3	.....	1.22	3	.....	1.69	.....	0.56	3	.....
Ni.....	.....	0.59	1	.....	1.06	1	.....	1.11	.....	0.36	1	.....
Sr.....	0.17	0.44	1	1.56	1.83	1	2.91	1.18	0.22	0.51	1	.....
Mean.....	0.66	0.66		1.37	1.28		1.71	1.62	0.45	0.44		
Adopted.....	0.66			1.32			1.67		0.44			
$P_e$ dynes/cm. <sup>2</sup> .....	4.57			0.21			0.46		2.77			

of  $\log P_e$  obtained for each star is very nearly the same as that obtained by the first method, but it is frequently quite different for individual elements. This difference is greatest for Mg and Si because, in the sun, the electron pressures obtained for these elements are considerably less than the average, and the difference is reflected in the results obtained for the stars. The electron pressures adopted for each star are derived from the mean values of the logarithms and equal weight has been given to the observed and adjusted results.

At the end of Table 23 are listed the level of ionization found for the adopted electron pressure and also the temperatures used in their determination. It is seen again how very sensitive the electron pressure is to relatively small changes in temperatures. However, the general trend remains the same for either the excitation temperature or that for  $\tau = 0.3$ : the pressures in the atmospheres of the giant stars are less than those in the dwarfs and the levels of ionization are greater.

In Table 24,  $\log N$  and  $\log N_1/N_0$  are given only for the temperatures at the level  $\tau = 0.3$ . The results agree with those calculated for the adopted excitation temperatures within 0.2 in almost all cases and the uncertainties in  $\log N$  are believed to be about 0.5. In this study of solar-type stars 99 per cent or more of the atoms are in the neutral and singly ionized stages but the numbers of doubly ionized atoms were calculated for Sr, Ba and La and, where necessary, these values have been included in the final results. It is seen that for the elements studied here only carbon has a greater number of neutral than ionized atoms for all stars; the reason is that its ionization potential of 11.2 volts is

TABLE 24. NUMBER OF ATOMS IN SOLAR-TYPE STARS ABOVE LEVEL  $\tau = 0.3$

Element	Sun ( <i>g-f</i> -curve)		Sun		$\gamma$ Cygni		$\alpha$ Persei		$\alpha$ Canis Minoris	
	$\log N$	$\log N_1/N_0$	$\log N$	$\log N_1/N_0$	$\log N$	$\log N_1/N_0$	$\log N$	$\log N_1/N_0$	$\log N$	$\log N_1/N_0$
C.....	19.79	-2.96	19.13	-3.00	20.22	-1.90	19.62	-1.24	19.48	-1.94
Na.....	17.60	2.72	17.64	2.67	19.13	4.01	18.62	3.88	17.72	2.88
Mg.....	20.38	0.96	20.24	0.92	20.77	2.15	20.41	2.36	20.36	1.48
Al.....	17.23	1.46	17.21	1.41	18.55	2.71	17.88	2.70	17.20	1.74
Si.....	18.76	-0.03	18.82	-0.08	19.36	1.15	19.27	1.40	18.84	0.54
Ca.....	17.52	2.39	17.57	2.34	18.72	3.63	18.53	3.61	17.72	2.63
Sc.....	14.21	1.81	14.16	1.76	15.36	3.03	15.06	3.10	14.25	2.17
Ti.....	16.20	1.69	16.10	1.64	17.26	2.91	16.89	2.99	16.15	2.06
V.....	15.19	1.47	15.10	1.43	16.37	2.69	16.46	2.78	15.20	1.86
Cr.....	16.86	1.27	16.72	1.23	17.72	2.48	17.37	2.60	16.86	1.69
Mn.....	17.19	0.94	17.16	0.90	17.90	2.14	17.68	2.32	17.21	1.43
Fe.....	19.12	0.60	18.94	0.53	20.08	1.78	19.76	2.01	19.18	1.13
Co.....	17.19	0.35	17.15	0.31	17.92	1.52	17.91	1.77	17.45	0.91
Ni.....	18.46	0.22	18.36	0.18	19.37	1.40	19.17	1.63	18.48	0.77
Cu.....	17.28	0.21	17.95	0.16	18.39	1.39	17.92	1.59	17.77	0.69
Zn.....	18.20	-0.70	18.12	-0.75	18.66	0.42	18.38	0.86	18.39	0.05
Sr.....	13.90	2.74	13.72	2.69	14.80	4.02	14.88	3.92	13.92	2.92
Y.....	13.07	1.82	13.12	1.78	14.64	3.05	14.18	3.11	13.40	2.16
Zr.....	14.04	1.46	13.90	1.41	15.07	2.67	14.43	2.79	13.89	1.87
Ba.....	13.29	2.78	13.40	2.73	14.28	4.04	14.06	3.97	13.33	3.01
La.....	12.33	2.79	12.30	2.75	13.33	4.05	12.87	4.00	12.17	3.02

greater than the level of ionization in these atmospheres. For silicon and zinc there are more neutral than ionized atoms in the sun, but for the other stars this ratio is reversed.

A comparison of the values of  $\log N$  found from the Victoria observations of solar lines and the higher-dispersion studies of equivalent widths shows very satisfactory agreement. Only for carbon and for copper are the differences large and in each case the Victoria results are based on only one or two lines. In order to use homogeneous data, the Victoria data are compared with those for the stars.

It is seen that there are about ten times as many atoms of the elements studied above the level  $\tau = 0.3$  in  $\gamma$  *Cygni* as in the sun and five times as many for  $\alpha$  *Persei*; the numbers are nearly equal for  $\alpha$  *Canis Minoris* and the sun. This indicates that the giant atmospheres are considerably more extensive than the dwarfs.

To test the uniformity of these atmospheres, the above ratios were assumed to hold for all elements and the differences between the expected values and those observed were noted. If the uncertainty of  $\log N$  is taken to be 0.5, as indicated by the difference between Menzel's data for the sun and those of the present study, no exceptional differences can be detected. However, these data are homogeneous, since systematic errors, such as the use of different  $\varphi$ -values, etc. do not occur and therefore 0.3 may be a more appropriate value for the uncertainty. On this basis, the relative composition of the sun and  $\alpha$  *Canis Minoris* may be considered identical for the elements studied in this paper and no significant differences can be detected between the results for  $\gamma$  *Cygni* and  $\alpha$  *Persei*. However, it seems that sodium and yttrium may be more abundant in the giant stars than in the dwarfs and magnesium and silicon may be less abundant. But the latter two elements are precisely those for which the electron pressures do not agree with the results for other elements and these differences may be a reflection of this discrepancy. Differences of the order of the probable errors are also observed for copper and zinc between the sun and  $\gamma$  *Cygni* and  $\alpha$  *Persei*, as well as for vanadium in the case of  $\alpha$  *Persei*, but the relatively few lines studied and their low intensities, particularly in the case of vanadium, prevent any conclusions being drawn from these results.

#### GENERAL REMARKS ON STELLAR ATMOSPHERES AND COMPARISON WITH OTHER OBSERVERS

The study of stellar atmospheres must be considered still in its preliminary stages in spite of the extensive literature, mentioned in the introduction, which has accumulated up to the present time. The results presented in this paper cannot be classed as definitive, though it is believed that the errors are not excessive; improved observational material and more accurate theoretical data may well change the values somewhat. The studies of Strömberg "On the Chemical Composition of the Solar Atmosphere"<sup>162</sup> and his "Tables of Model Stellar Atmospheres"<sup>164</sup> indicate the probable direction of future lines of inquiry. In a real star there is almost certainly no single radiating surface with an absorbing atmosphere above it, such as is postulated in the Schuster-Schwarzschild model, and hence the continuous and atomic absorption coefficients are intimately related. Although there may not be sharply-defined layers of absorbing atoms in the stars, studies of solar flash spectra indicate positive differences in temperature and pressure between the top and the

<sup>164</sup> *P. Med. Kobenhavns O.*, No. 138, 1944.

bottom of the chromosphere, and it seems probable that in the extensive atmospheres of giant stars, similar effects must be present. Such possible variations have not yet been studied in full detail. Strömngren examines the variation of the absorption coefficients with temperature and optical depth in the atmosphere and, for certain specified conditions, is able to calculate the theoretical shape (and, therefore, the equivalent width) of the principal absorption lines of different elements.

In the present study the atmosphere of each star is assumed to be at a constant temperature and pressure—though it has been necessary to adopt different curves of growth for neutral and ionized atoms. Since these curves have been fitted separately to theoretical curves, the abscissae do not necessarily have the same origin and hence it is possible that systematic differences in  $N$  between neutral and ionized atoms may have been introduced; such an error would appear directly in the electron pressure since the calculation involves the ratio of neutral to ionized atoms. However, in the 1942 study of these observations, the same curves of growth were used for both neutral and ionized atoms for each star and it was found that electron pressures for giants were approximately the same as those for dwarfs of the comparable spectral class (see Table 17). On the other hand, electron pressures determined during the present analysis from the two sets of temperatures are quite different. For the adopted excitation temperatures, which are open to some suspicion since they do not differ markedly from that of the sun, pressures in the giant stars are very nearly equal and approximately one-tenth those of the dwarfs. For the temperatures adopted for the level  $\tau = 0.3$ , the pressures in the giant stars are about one-twentieth those of the dwarf stars of similar spectral class but there is a progression suggesting that the electron pressure increases with earlier spectral type. Although it cannot be considered proven that the latter values are more correct, it is felt that such a progression might be expected and these results are considered the best of the present investigation.

Observational data on pressures are available for very few other stars. The principal observational results known to the writer are listed in Table 25. Many of the published results have been given in terms of the solar electron pressure but, for comparison purposes, they have been reduced to dynes/cm.<sup>2</sup> by assuming that the value for the sun is 16 dynes/cm.<sup>2</sup>

In their preliminary analysis of the atmospheres of bright stars, Adams and Russell made estimates of the relative strengths of lines in the stars and in the sun on the Rowland intensity scale. The temperatures they derived were very similar to the adopted effective temperatures, although they found some evidence of a departure from thermodynamic equilibrium. They also found that there was a great range in the electron pressure obtained not only for different stars but also from one element to another in the same star; a factor of  $10^{10}$  between  $\alpha$  Orionis and  $\alpha$  Canis Majoris appeared from their observations. Part of this large range appears to be due to the extended scale of their intensity estimates but it is not completely explained yet. Miss van Dijke studied high-dispersion spectra of  $\alpha$  Bootis (gK2) and 70 Ophiuchi A (K0) as typical K-type giant and dwarf stars and found  $\log (P_{e^*}/P_{e\odot}) = -3.74$  and  $-1.10$ , for temperatures of  $3160^\circ$  K. and  $4150^\circ$  K., respectively. Pannekoek and van Albada applied differential corrections to the curve-of-growth phenomena which had been studied in a manner similar to that of the

TABLE 25. ELECTRON PRESSURES IN STELLAR ATMOSPHERES

Star	Spectral Type	Electron Pressure dynes/cm. <sup>2</sup>	Reference	Star	Spectral Type	Electron Pressure dynes/cm. <sup>2</sup>	Reference
$\alpha$ Orionis.....	cM2	$5.1 \times 10^{-7}$	1				
$\alpha$ Scorpii.....	cM1	$1.3 \times 10^{-6}$	1				
$\alpha$ Bootis.....	gK0	0.004 0.003	1 2	70 Ophiuchi A...	dK0	1.2	2
$\pi$ Cephei.....	G5	3.5	3	Sun.....	dG2	18 46 17 31	4 5 6 12
$\alpha$ Aurigae.....	G0	3.4 0.05	12 1				
$\gamma$ Cygni.....	cF8	0.5	6				
$\delta$ Cephei.....	cF5	1.2 2.0	3 1	$\theta$ Cygni.....	F5	12	3
$\alpha$ Persei.....	cF4	7.4 4.2	7 6	$\alpha$ Canis Minoris	dF3	160 86	1 6
$\alpha$ Carinae.....	gF0	10	8				
	$\alpha$ Canis Majoris.....		dA2	950 120	1 9		
	$\gamma$ Geminorum.....		dA2	120	9		
	$\tau$ Scorpii.....		dB0	1200	10		
	$\phi^1$ Orionis.....		B0	630	13		
	10 Lacertae.....		O8.5	630	11		

<sup>1</sup> Adams and Russell, *Ap. J.*, **68**, 9, 1928.<sup>2</sup> Suzanne E. A. van Dijke, *Ap. J.*, **104**, 27, 1946.<sup>3</sup> Pannekoek and van Albada, *P. Amst. Inst.*, No. 6, Pt. 2, 1946.<sup>4</sup> A. Unsöld, *Physik der Sternatmosphären*, p. 345, Springer, Berlin, 1938.<sup>5</sup> H. N. Russell, *Ap. J.*, **78**, 277, 1933.<sup>6</sup> *This Paper.*<sup>7</sup> Helen R. Steel, *Ap. J.*, **102**, 43, 1945.<sup>8</sup> J. L. Greenstein, *Ap. J.*, **95**, 161, 1942.<sup>9</sup> L. H. Aller, *Ap. J.*, **96**, 321, 1942.<sup>10</sup> A. Unsöld, *Z. f. Ap.*, **21**, 22, 1941.<sup>11</sup> L. H. Aller, *Ap. J.*, **104**, 347, 1946.<sup>12</sup> J. A. Milne, *Phil. Trans. A.*, **228**, 421, 1929.<sup>13</sup> L. H. Aller, *Introduction to Astrophysics*, p. VIII-33 Indiana Univ., 1947.

present investigation, and, assuming a solar electron pressure of 7.6 dynes/cm<sup>2</sup>., obtained electron pressures of 0.58, 5.6 and 1.7 for  $\delta$  *Cephei*,  $\theta$  *Cygni* and  $\pi$  *Cephei*, for adopted temperatures of 5225°, 5325° and 4725° K., respectively. Unsöld adopted an electron pressure of 16 dynes/cm<sup>2</sup>. for a temperature of 5600° K. as the best value which could be obtained from Russell's analysis of the Rowland intensities for the sun, although Russell finally adopted a value of 46 dynes/cm<sup>2</sup>. for a temperature of 5740° K. Allen obtained the value of 14 dynes/cm<sup>2</sup>. from a study of the Stark broadening of Fe I lines in the solar spectrum.

In her study of  $\alpha$  *Persei*, Miss Steel found that the electron pressures seemed to vary with the element considered and that they were very sensitive to the adopted temperature; therefore, basing her argument on the number of electrons in the atmosphere and using a temperature of 6600° K., she derived a pressure of 4.7 dynes/cm<sup>2</sup>. for the electron pressure at the base of the photosphere. The same method for the sun gives a value of about 40 dynes/cm<sup>2</sup>. at  $T = 5000^\circ$  K. Greenstein's value of  $\log P_e = 1.0$  for  $\alpha$  *Carinae* was obtained from a study of ionization equilibria and he adopted a temperature of 7300° for the ionization temperature. Aller found that the atmospheres of *Sirius* and  $\gamma$  *Geminorum* were very similar and obtained electron pressures of 120 dynes/cm<sup>2</sup>. from the profiles of the hydrogen lines; this agreed approximately with the values obtained for other elements with an adopted ionization temperature of 8700° K.

Unsöld made a very complete study of curve-of-growth phenomena for  $\tau$  *Scorpii* and derived a mean temperature of 28,150° and  $\log P_e = 3.07$ . Aller applied the same methods in his studies of 10 *Lacertae* and  $\phi^1$  *Orionis*, and found  $\log P_e = 2.80$  for temperatures of 29,600° and 25,600° K., respectively.

The results given in Table 25 suggest that an observational scale of electron pressures is now being established throughout the range of stellar spectra which should prove of great importance in the analysis of stellar atmospheres. Although the above data must be considered tentative, the general trend is clear. Electron pressures are very low in late-type stars, less than 10<sup>-3</sup> dynes/cm<sup>2</sup>., and increase steadily with earlier spectral type to values of 1000 or more dynes/cm<sup>2</sup>. For that portion of the spectral sequence where the spectra may be separated readily according to luminosity criteria, there seems little doubt that the electron pressures are from ten to 100 times less in the giants than in the dwarfs.

In earlier work, Fowler and Milne<sup>165</sup> developed the theory of ionization in stellar atmospheres and, by means of their method of intensity-maxima—whereby the maximum intensity of lines of a given atom were studied with reference to their position in the spectral sequence—were able to derive temperatures and electron pressures. However, they assumed that a mean electron pressure of 130 dynes/cm<sup>2</sup>. could be used throughout the range of stellar spectra and derived their scale of ionization temperatures from that point. In later work, Milne<sup>166</sup> developed the theory further and, from the maximum of the zinc triplet, 1 <sup>3</sup>P — 1 <sup>3</sup>S, derived an electron pressure of 31 dynes/cm<sup>2</sup>. for the sun and 3.4 dynes/cm<sup>2</sup>. for *Capella*, for temperatures of 5740° and 5200° K., respectively.

<sup>165</sup> *M. N.*, **83**, 403, 1923.

<sup>166</sup> *Phil. Tr., A.*, **228**, 421, 1929.

## CONCLUSION

In the future the theory of line intensities in stellar spectra will undoubtedly be improved greatly but its present position is by no means entirely satisfactory. Houtgast<sup>172</sup> studied the variation in the shapes of Fraunhofer lines from centre to limb over the solar disk and came to the conclusion that they must be produced by non-coherent scattering processes. This would require a complete revision of the theory employed in this paper, though Spitzer<sup>173</sup>, in a brief discussion of non-coherent scattering, concludes that in spite of this radical modification, the shape of the curve of growth would not be changed greatly. On the other hand, Redman<sup>174</sup> advises theoretical astrophysicists to make further trials of the theory of coherent scattering before abandoning it.

The discussion of the results of this and other papers indicates that a good beginning has been made in the study of stellar atmospheres by means of curve-of-growth phenomena. Numerous difficulties and uncertainties remain to be overcome. There is a great need for many more accurate intensities of lines in the spectra of representative stars but the demand for laboratory measurements is equally pressing in order that the true course of the curve of growth may be traced for many atoms. This would also enable more accurate excitation temperatures to be derived in order to determine their relation to the effective and ionization temperatures. The ionization temperature is difficult to obtain but until it is known, the mean electron pressure and its possible variation from element to element will remain uncertain.

Fortunately the work of Strömberg<sup>164</sup> and Pannekoek and van Albada<sup>175</sup> has indicated that when the observations become sufficiently precise, the necessary theory may become available. Thus by combining the information obtained from a study of curve-of-growth phenomena with that gained from the investigation of the true shapes of spectral lines it may be possible to extend our knowledge concerning the physics and chemistry of stellar atmospheres.

Finally the writer would like to record his appreciation of the great interest which the late Dr. H. D. Curtis, Director of the Observatories of the University of Michigan, showed in the progress of the work. He would also like to express his gratitude to Dr. R. M. Petrie who suggested the original problem at the University of Michigan and to other members of the staff at this Observatory who have always been ready with advice and assistance. The dissertation was read by a number of astronomers to all of whom, but particularly to Professor D. H. Menzel of Harvard Observatory, grateful acknowledgment for friendly advice and criticism is now made. More recently, information useful at several points throughout the analysis has been generously given by Miss Helen R. Steel and Messrs. L. H. Aller, Leo Goldberg, and William Petrie.

<sup>172</sup> *Diss.*, Utrecht, 1942.

<sup>173</sup> *Ap. J.*, **99**, 1, 1944.

<sup>174</sup> *M. N.*, **104**, 99, 1944.

<sup>175</sup> *P. A. Inst.*, Amsterdam, No. 6, Pt. 2, 1946.

DOMINION ASTROPHYSICAL OBSERVATORY,  
VICTORIA, B.C.

June, 1947.

## CONCLUSION

In the future the theory of line intensities in stellar spectra will undoubtedly be improved greatly but its present position is by no means entirely satisfactory. Houtgast<sup>172</sup> studied the variation in the shapes of Fraunhofer lines from centre to limb over the solar disk and came to the conclusion that they must be produced by non-coherent scattering processes. This would require a complete revision of the theory employed in this paper, though Spitzer<sup>173</sup>, in a brief discussion of non-coherent scattering, concludes that in spite of this radical modification, the shape of the curve of growth would not be changed greatly. On the other hand, Redman<sup>174</sup> advises theoretical astrophysicists to make further trials of the theory of coherent scattering before abandoning it.

The discussion of the results of this and other papers indicates that a good beginning has been made in the study of stellar atmospheres by means of curve-of-growth phenomena. Numerous difficulties and uncertainties remain to be overcome. There is a great need for many more accurate intensities of lines in the spectra of representative stars but the demand for laboratory measurements is equally pressing in order that the true course of the curve of growth may be traced for many atoms. This would also enable more accurate excitation temperatures to be derived in order to determine their relation to the effective and ionization temperatures. The ionization temperature is difficult to obtain but until it is known, the mean electron pressure and its possible variation from element to element will remain uncertain.

Fortunately the work of Strömngren<sup>164</sup> and Pannekoek and van Albada<sup>175</sup> has indicated that when the observations become sufficiently precise, the necessary theory may become available. Thus by combining the information obtained from a study of curve-of-growth phenomena with that gained from the investigation of the true shapes of spectral lines it may be possible to extend our knowledge concerning the physics and chemistry of stellar atmospheres.

Finally the writer would like to record his appreciation of the great interest which the late Dr. H. D. Curtis, Director of the Observatories of the University of Michigan, showed in the progress of the work. He would also like to express his gratitude to Dr. R. M. Petrie who suggested the original problem at the University of Michigan and to other members of the staff at this Observatory who have always been ready with advice and assistance. The dissertation was read by a number of astronomers to all of whom, but particularly to Professor D. H. Menzel of Harvard Observatory, grateful acknowledgment for friendly advice and criticism is now made. More recently, information useful at several points throughout the analysis has been generously given by Miss Helen R. Steel and Messrs. L. H. Aller, Leo Goldberg, and William Petrie.

<sup>172</sup> *Diss.*, Utrecht, 1942.

<sup>173</sup> *Ap. J.*, **99**, 1, 1944.

<sup>174</sup> *M. N.*, **104**, 99, 1944.

<sup>175</sup> *P. A. Inst.*, Amsterdam, No. 6, Pt. 2, 1946.

DOMINION ASTROPHYSICAL OBSERVATORY,

VICTORIA, B.C.

June, 1947.

## APPENDIX. A COMPARISON OF LABORATORY AND THEORETICAL LINE INTENSITIES

The presence of numerous intercombination lines in the spectra of complex atoms is evidence that the elementary character of the electron transitions assumed in LS coupling does not truly represent conditions within these atoms. Other mechanisms of electron coupling have been suggested but uncertainties concerning the structure of the atom and the labour involved in the long computations have delayed the calculation of theoretical intensities for JJ and "intermediate" coupling. However, the application of the J-file sum rule by Menzel, Baker, and Goldberg<sup>176</sup> to the spectrum of neutral titanium led to improved theoretical intensities which were used to calculate the excitation temperature of the solar reversing layer.

Another method of improving theoretical line intensities is by comparing the LS intensity of a line with the corresponding laboratory  $g,f$ -value. The latter have been determined by R. B. King and A. S. King<sup>177</sup> for low-level lines of Ti I and Fe I and such a comparison is shown in Fig. 16.  $\log S_s/\Sigma s$  has been plotted against  $\log \left( g,f \frac{\lambda}{5000} \right)$  for

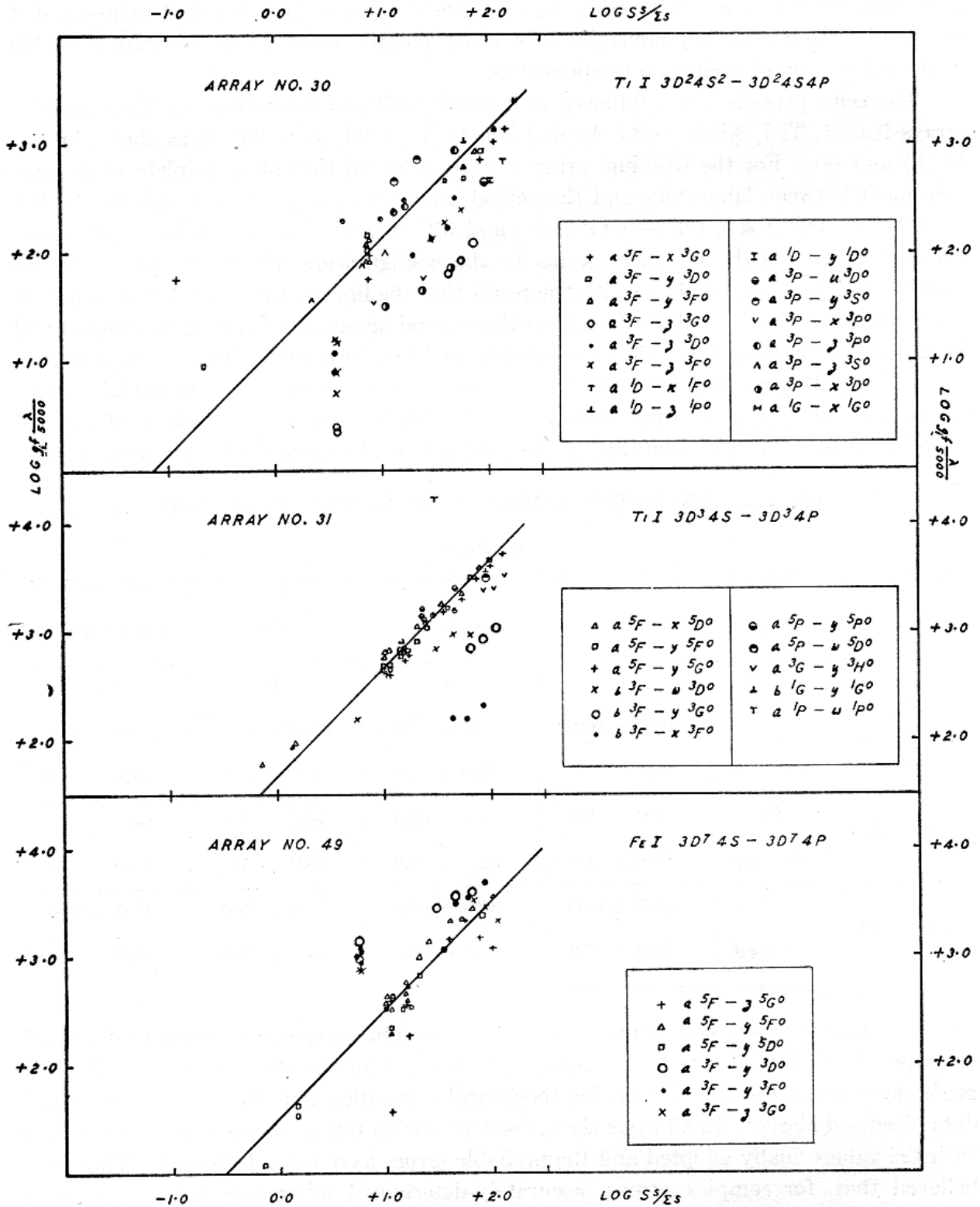
the available transition arrays; the diagrams include all lines for which the  $g,f$ -values have been determined whether stellar equivalent widths have been measured or not. As the laboratory values are believed to be accurate within ten per cent, the large deviations from a one-to-one correspondence in each case are most probably due to the failure of LS coupling to predict the relative intensities. For each transition array a straight line at an angle of  $45^\circ$  has been drawn on the diagram to show how the points would lie if the agreement were exact; it has been determined by least squares from all points lying within about 0.2 units of the final position. Lines belonging to each multiplet have been marked according to the designation listed on the diagrams and it is seen that, in nearly all cases, lines within a multiplet follow the simple intensity rules fairly well.

Fig. 16 (a) shows the relation between theoretical and laboratory intensities for Array No. 30, Ti I,  $3d^2 4s^2 - 3d^2 4s 4p$ . For this transition array it is seen that the relative multiplet strengths,  $S$ , are not accurately determined by Shortley's intensity rules.<sup>178</sup> The scatter is much greater than that of other transition arrays and may be due in part to uncertainties in the fractional parentage of transitions arising from jumps of the  $s^2$  electrons. The overlapping of terms in the titanium spectrum near  $\chi_i = 3$  volts is serious and undoubtedly some interaction between the different configurations results; this may contribute to the weakness of the lines in the multiplets  $a^3F - z^3F^\circ$  ( $\times$ ),  $a^3F - z^3D^\circ$  ( $\bullet$ ) and  $a^3F - z^3G^\circ$  ( $\circ$ ). Although it is difficult to evaluate the precise effect of these perturbations, an empirical correction can be applied to the theoretical multiplet intensity to reduce it to the observed correlation between theoretical and laboratory intensities. For this purpose, all lines within a single multiplet were assumed to follow the LS intensities and this one-to-one relation with the laboratory intensities was determined by the method of least squares. Then for each multiplet the correction to the calculated  $S$ -value was determined as the shift along the  $\log S_s/\Sigma s$ -axis required to

<sup>176</sup> *Ap. J.*, **87**, 81, 1938.

<sup>177</sup> *Ap. J.*, **87**, 24, 1938.

<sup>178</sup> *Pr. Ac. Sc.*, Washington, **20**, 591, 1934.



bring the straight line determined above into coincidence with that determined for the whole transition array as shown by the  $45^\circ$  line on the diagram. Thus multiplet intensities were obtained which are believed to be more reliable than the calculated values and it was possible to include numerous lines, for which no laboratory intensities were available in the calculation of excitation temperatures.

The same procedure was followed to improve multiplet intensities for the transition arrays No. 31, Ti I,  $3d^3 4s - 3d^3 4p$  and No. 49, Fe I,  $3d^7 4s - 3d^7 4p$  as shown in Fig. 16 (b) and (c). For the titanium array it may be noted that all multiplets show good agreement between laboratory and theoretical intensities except those based on the  $b^3F$  term,  $b^3F - x^3F^\circ$  (●),  $b^3F - y^3G^\circ$  (○) and  $b^3F - w^3D^\circ$  (×). Menzel, Baker, and Goldberg have noted that these terms in the configuration  $3d^3 4p$  are perturbed by neighbouring terms of  $3d^2 4s 4p$  with the result that the lines in the array  $3d^3 4s - 3d^3 4p$  are weakened unduly. For the iron lines the general agreement between theoretical and laboratory intensities is fair. Of the multiplets used to determine excitation temperatures, only  $a^3F - y^3F^\circ$  (●) and  $a^3F - z^3G^\circ$  (×) contain lines for which there are laboratory intensities and it appears that, within these multiplets, there is a failure of the LS intensities; therefore the laboratory values, reduced to the theoretical scale, were used.

TABLE 26. EXCITATION TEMPERATURES OF SOLAR-TYPE STARS

(1942 DATA)

Atom	Array No.	Intensity	Sun	$\gamma$ Cygni	$\alpha$ Persei	$\alpha$ Canis Minoris
			° K.	° K.	° K.	° K.
Ti I	30	LS	10500 ± 2000	11500 ± 2500	12000 ± 5000	13000 ± 5000
		LS + $g:f$	4700 ± 750	4650 ± 850	4550 ± 1250	4950 ± 1150
Ti I	31	LS	5800 ± 850	6900 ± 1000	7600 ± 800	6350 ± 600
		LS + $g:f$	5050 ± 300	5650 ± 350	7300 ± 750	5500 ± 350
Fe I	49	LS	4150 ± 1000	3300 ± 1000	3050 ± 900	4000 ± 1200
		LS + $g:f$	5350 ± 450	3850 ± 350	3550 ± 300	4950 ± 450

Excitation temperatures were determined for these three transition arrays as discussed on page 73. Table 26 lists the temperatures obtained for the stars together with their probable errors as calculated from the theoretical intensities and also from the improved data discussed above. In all cases the revised excitation temperatures agree more closely with the values finally adopted and the probable errors have been decreased. Thus it is believed that, for complex atoms, accurately-determined laboratory intensities are a considerable improvement over theoretical intensities calculated from the sum rules for LS coupling.

